Book of Abstracts

EPDIC 11

Book of Abstracts: EPDIC 11

Published September 2008, ISBN 83-89585-22-7

Disclaimer

Printed in Poland
Revision: 142.2.12, 2008-09-04 15:30 GMT

Table of Contents

Symposia

Plenary session

Programme

Friday, 19 September

EPDIC - E-MRS Joint Session
Friday morning, 19 September, 9:00
Univ. of Tech. Main Building
Chair: Andrzej Mycielski (EMRS), Bogdan Palosz (EPDIC)

9:00 Invited oral

Synthesis and applications for catalysis of carbon and carbides nanostructures

Marc J. Ledoux

European Laboratory for Catalysis and Surface Sciences, ELCASS (CNRS-ULP), 25 rue Becquerel, Strasbourg 67087, France

e-mail: ledoux@ecpm.u-strasbg.fr

Development of new supports for catalytic active phases is one of the most important research fields in heterogeneous catalysis, for use in many gas-phase and liquid-phase reactions.
Since the discovery of carbon nanotube, an increasing interest has been devoted to the preparation of new one-dimensional (1D) nanostructured materials such as nanowires or nanotubes – initiated from sp2 carbon and rapidly extended to oxides – for fundamental studies as well as for a wide range of applications. The field of catalysis also benefits from this (nano)material approach, and carbon nanotubes and nanofibers as well as high surface area silicon carbide (b-SiC) nanotubes obtained by a Shape Memory Synthesis process, used as catalytic active phase supports led to significant breakthroughs with interesting catalytic behaviors, due to their peculiar 1D morphology.
However, severe drawbacks are inherent to the use of fluffy 1D nanostructures, including an almost impossible recovery of the catalysts in liquid-phase medium, huge pressure drops and moving bed phenomena in fixed-bed reactors, and a health impact during handling. Therefore the macronisation of 1D catalysts is of great interest.
This talk details the synthesis, characterization and catalytic use of 1D carbon and b-SiC nanostructures, and focuses on the approach for designing safe and efficient macronized 1D carbon and b-SiC nanostuctures. A wide panel of environmental and energy impact target reactions is taken as key-reactions for highlighting the interest of using 1D carbon and b-SiC nanostructures as catalyst supports, in order to target new conversion and selectivity patterns. Supported by the development of a new electron tomography tool (3D microscopy) for getting more insight on the active phase location inside/outside of a nano-tube shaped support, the nanoreactor concept is pointed out, in which each carbon or b-SiC nanotube, either as fluffy or macronized material can be considered as a single nanoscale reactor.

9:45 Invited oral

Negative thermal epansion materials

John S. Evans

Department of Chemistry, University of Durham, Science Labs, South Road, Durham DH1-3LE, United Kingdom

e-mail: john.evans@durham.ac.uk

We've an on-going interest in materials that show the unusual property of "Negative Thermal Expansion" and contract in volume on heating. Much of this was stimulated by ZrW_2O_8, which contracts isotropically and continually over a temperature range of 2 to 1050 K with a coefficient of thermal expansion of alpha = -9 x 10^{-6} K^{-1}. In addition to this behaviour this and related materials show oxide ion mobility at remarkably low temperatures. Other materials such as $Ag_3Co(CN)_6$ show a remarkable "colossal" negative thermal expansion, with alpha = -130 x 10^{-6} K^{-1} in one direction. The observation of NTE behaviour is often intimately related to phase transitions in materials and in many cases these can lead to structures with a remarkable degree of complexity which present a considerable challenge for powder diffraction methods. A full understanding the synthesis and properties of such materials requires application of a range of complementary techniques such as diffraction, total scattering and multi-nuclear solid state NMR. In this presentation I'll discuss recent advances in our understanding of these materials and highlight in particular the information available from powder methods. I'll also use the presentation to highlight methods for analysis of diffraction data such as "parametric" Rietveld refinement which can allow the extraction of "unusual" information from powder diffraction data such as temperatures or activation energies for processes in the solid state.

EPDIC Award for Young Scientist
Friday evening, 19 September, 18:00
Lecture Hall I
Chair: Paolo Scardi, Bogdan Palosz

18:00 Invited oral

The crystallography of flexibility: using powder diffraction to study local structure and dynamics in framework materials

Andrew L. Goodwin

University of Cambridge, Department of Earth Sciences, Downing Street, Cambridge, Cambridge CB23EQ, United Kingdom

e-mail: alg44@cam.ac.uk

Flexible framework materials – compounds whose underlying crystal structures allow local distortions at very low energy costs – often exhibit a range of interesting physical properties: examples include negative thermal expansion, amorphisation under pressure, and the existence of nano-sized polar domains in relaxor ferroelectrics. Understanding these effects involves understanding the local environment of atoms, how this differs from the time-average environment, and how the atoms move in the process. These are concepts that are heavily disguised, if not inaccessible, in “conventional” average

structure analysis, and yet key to a number of important problems in materials science.
This talk will discuss some recent developments in the use of powder diffraction techniques (principally neutron and x-ray "total" scattering) to probe local structure and dynamics in framework materials. The emphasis is twofold: (i) on producing large and realistic supercell descriptions of atomic structure, and (ii) on developing methods of extracting useful information from these atomistic configurations, such as domain size and structure, vibrational energies, and displacement correlation functions. Reference will be made to a number of recent case-studies, including colossal positive and negative thermal expansion in $Ag_3[Co(CN)_6]$ [1], dynamic instabilities and polar nano regions in $SrSnO_3$ [2], and the determination of vibrational energies in MgO [3] and $SrTiO_3$ [4].
[1] A L Goodwin, M Calleja, M J Conterio, M T Dove, J S O Evans, D A Keen, L Peters and M G Tucker, *Science***319**, 794 (2008).
[2] A L Goodwin, S A T Redfern, M T Dove, D A Keen and M G Tucker, *Phys. Rev. B***76**, 174114 (2007).
[3] A L Goodwin, M G Tucker, M T Dove and D A Keen, *Phys. Rev. Lett.***93**, 075502 (2004).
[4] A L Goodwin, M G Tucker, E R Cope, M T Dove and D A Keen, *Phys. Rev. B***72**, 214304 (2005).

Saturday, 20 September

Plenary lecture 1
Saturday morning, 20 September, 8:30
Lecture Hall I
Chair: Lucas Palatinus

8:30 Invited oral

Charge flipping in powder diffraction

Gábor Oszlányi, András Sütő

Hungarian Academy of Sciences, Research Institute for Solid State Physics and Optics (SZFKI), Konkoly Thege M. út 29-33, Budapest H-1121, Hungary

e-mail: go@szfki.hu

Charge flipping is a recently discovered algorithm of ab initio structure determination that is easy to implement and adapt to various tasks. It is essentially an iterative Fourier cycle that modifies the calculated electron density and structure factors in the appropriate half-cycles. The modifications have two different roles: they either act as constraints or as (weak) perturbations. Constraints are needed to limit the size of the search space, while perturbations are needed to avoid stagnation. The name-giving step of charge flipping is a good example of a fine balance, changing the sign of electron density below a small positive threshold simultaneously forces the constraint of positivity and introduces high-frequency, orthogonal perturbations. The basic algorithm has several attractive properties: it solves the structure without utilizing atom types, chemical composition or any information on the space group symmetry.

The crystallographic community has already found that charge flipping works well in practice: structure solution examples of small molecules, modulated crystals, quasicrystals, and of powder diffraction data have all been reported (see [1] for references). Many variants of the basic algorithm exist, which usually add more constraints and add/remove some perturbations. Any improvement developed for single crystal data is likely to work for powder data, although the limit of structure size/complexity that can be solved is naturally smaller. The only extension required by powder charge flipping is the need to repartition the calculated intensity of overlapping reflections. At least three different approaches have been tested, the one that worked most efficiently does repartitioning in an auxiliary cycle where histogram matching is also performed. Our experience confirms that such an auxiliary cycle is useful and can easily be extended to contain a variety of other actions. The efficiency strongly depends on small details. As a general rule, structure solution of powder data requires more constraints and less perturbation, and between subsequent interventions one must allow a reasonable period of pure charge flipping.

There are two remaining problems that require further investigation. While missing data at high resolution is a general problem of any *ab initio* method, problems with the utilization of symmetry is specific to charge flipping. Most space groups fix the origin and the structure can emerge only at a single position. Charge flipping that works in P1 allows continuous phase changes and therefore, the structure can emerge at the continuum of shifted positions. This is such a big an advantage that it prevented us from the efficient use of symmetry information. At present we are trying to combine the best of both approaches, and prescribe only partial symmetry.

[1] G. Oszlányi & A. Sütő, *Acta Cryst.* A **64**, 123-134 (2008)

Plenary lecture 2
Saturday afternoon, 20 September, 13:00
Lecture Hall I
Chair: Hartmut Fuess

13:00 Invited oral

Advances in structure solution from powder diffraction Data: EXPO2008

Carmelo Giacovazzo, Angela Altomare, Gaetano Campi, Cuocci Corrado, Moliterni Anna Grazia, Rizzi Rosanna

CNR-Istituto di Cristallografia (IC), via Amendola 122/O, Bari 70126, Italy

e-mail: carmelo.giacovazzo@ic.cnr.it

The various steps necessary for crystal structure determination from powder data are the following: a) unit cell indexation; b) space group determination; c) crystal structure determination; d) crystal structure refinement by least squares-Rietveld refinement techniques. In the last years strong advances in the methods allowed to solve crystal structures of size forbidden for old techniques. Also the accuracy of the final molecular models improved. EXPO2008 contains various advances with respect to the previous release. They concern:

a) the unit cell indexation. The search has been made more efficient and exhaustive.

b) The space group determination. The use of the joint probability distribution method has been made more efficient by combining it with the automatic control of the experimental pattern.

c) Crystal structure determination. A recent theory aiming at reducing the effects of the limited resolution (so important when powder data arise from organic samples) in the electron density maps has been implemented in EXPO2008. The capacity of EXPO2008 of solving organic crystal structures from powder data, even at non-atomic resolution and via laboratory diffractometer data, reached now a new powerful standard.

In case in which the molecular geometry is known, EXPO2008 customers may use a robust simulated annealing algorithm.

EPDIC Award for Distinguished Scientist

Saturday evening, 20 September, 18:30
Lecture Hall I
Chair: Jordi Rius, Bogdan Palosz

18:30 Invited oral

Powder Diffraction Data Analysis with FullProf. Past, Present and Future

Juan Rodriguez-Carvajal

Institut Laue Langevin (ILL), Avenue des martyrs, Grenoble 38042, France

e-mail: rodriguez-carvajal@ill.fr

The seminal papers from Hugo Rietveld [1-2] provoked long time ago a wealth of excitement on people using powder diffraction. From those times to now the advancement on data treatment of powder data has been huge. Presently the number of computing tools able to treat powder diffraction data to different levels of complexity is enormous. Among them, the FullProf Suite is one of the most largely used in the solid state physics and chemistry community.
I started to use the Rietveld method in 1980 and the programs I used for my training were the DBW program (sent to me by Ray Young after the publication of his paper [3]) for X-ray diffraction and the program from Alan Hewat at ILL (translation and enhancement of the original Algol program written by Hugo Rietveld) for neutron diffraction. At that moment in Spain nobody believed in the Rietveld method. However, I needed it for pursuing my PhD work on perovskites at the University of Barcelona and I learn plenty of things for working in condensed matter physics and chemistry. My original training was completely different: theoretical physics, group theory, general relativity but not solid state theory! I had to enter into the details of the Rietveld method in order to understand what I was doing and to correct bugs and improve the original programs. This was done progressively during the eighties in Barcelona and Grenoble. I moved to the ILL in 1988 after implementing the STRAP system for data treatment of neutron diffraction patterns as a function of temperature [4]. I started then to implement the analysis of incommensurate magnetic structures and new ideas, as the nowadays called the Le Bail method [5], in my strongly modified personal version of the DBW program. All this computing development was done because I needed it for my personal scientific work. A summary of the methods I implemented up to 1992 was published in 1993 [6].
In this talk I will present the genesis and evolution of the FullProf Suite and I will describe in some detail the features of the present programs as well as the current developments and future improvements.

1.Line Profiles of Neutron Powder-diffraction Peaks for Structure Refinement. H.M. Rietveld (1967), Acta Cryst. 22,151-152
2. A Profile Refinement Method for Nuclear and Magnetic Structures. H.M. Rietveld (1969), J. Appl. Cryst. 2, 65-71
3.New Computer Program for Rietveld Analysis of X-Ray Powder Diffraction Patterns. D. B. Wiles and R. A. Young (1981), J. Appl. Cryst. 14, 149-151.
4. STRAP: A System for Time-Resolved Data Analysis (Powder Diffraction Data). A Simple Tutorial by J. Rodríguez, M. Anne and J. Pannetier, ILL Internal Report 87RO14T, pp 1-87, December 1987.
5. Ab-initio structure determination of LiSbWO6 by X-ray powder diffraction. A. Le Bail, H. Duroy and J.L. Fourquet (1988), Mater. Res. Bull. 23, 447-452
6. Recent Advances in Magnetic Structure Determination by Neutron Powder Diffraction. J. Rodríguez-Carvajal (1993), Physica B, 192, 55-69

Sunday, 21 September

Plenary lecture 3

Sunday morning, 21 September, 8:30
Lecture Hall I
Chair: Davor Balzar

8:30 Invited oral

Characterization of proteins by powder diffraction

Robert Von Dreele

Argonne National Laboratory (ANL), 9700 South Cass Avenue, Argonne, IL 60439, United States

e-mail: vondreele@anl.gov

A simulation of a protein powder diffraction pattern was stunning in the apparent amount of information that was seen. A subsequent experiment on metmyoglobin gave a powder diffraction pattern that showed very little sample broadening; the peak widths were essentially limited by the instrument resolution. The challenge is to make use of this in protein structure analysis. This talk will recall some of those early experiments and data analyses as well as an overview of current progress and future possibilities.

Supported by US DOE/OS/BES under Contract No. DE-AC-02-06CH11357.

Plenary lecture 4

Sunday afternoon, 21 September, 13:00
Lecture Hall I
Chair: Hideo Toraya

13:00 Invited oral

Past and present of Line Profile Analysis: an outlook on its practice in the future

Rob Delhez[1], Arnold C. Vermeulen[2]

1. *Delft University of Technology, Department of Materials Science and Engineering, Mekelweg 2, Delft 2628CD, Netherlands*
2. *PANalytical, Lelyweg 1, Almelo 7600AA, Netherlands*

e-mail: r.delhez@tudelft.nl

Line Profile Analysis is not difficult, but it is complicated. Because it is not difficult it is tempting to think that it is simple and easy to apply, whereas one should be careful because it is complicated matter. Therefore experts in the field exist and it is to be regretted sincerely that their expertise and experience is not yet translated into algorithms - which is a complicated and time consuming task if possible at all. Diffraction-line broadening is determined by (a) contributions from the instrument ("instrumental aberrations"), (b) by the spectral distribution of the radiation used, and (c) the microstructure of the specimen, i.e. small crystallite size and lattice strains caused by lattice defects, e.g. dislocations, small inclusions or precipitates, stacking and twin faults. Although it is known for half a century that some of these microstructural phenomena do not only influence diffraction-line breadth and shape, but also diffraction-line positions, it is only rather recent that their influence is taken into account more commonly in structure determination, and in particular in structure determination from powder diffraction patterns. Examples of such causes of peak shifts are stacking and twin faults as well as macrostresses (residual stresses). Just reviewing the literature on the analysis of diffraction-line broadening does not lead to better understanding or to new insights and it does not help non-experts to understand and apply these methods. Therefore it will be tried to reconstruct the Evolutionary Tree of Diffraction-Line Broadening Analysis Methods with the main intention to order its present scientific basics and possibilities along with its methods / techniques. In addition some examples will be given of the relations of line-broadening analyses with other branches of diffraction analysis and with fields of application such as materials science, crystal structure determination, microstructure determination, residual stress determination, and texture determination. In today's practice simple procedures that are easy to apply (e.g. Williamson Hall plots) are used widely and frequently to determine whether the observed broadening of diffraction lines is generated by the presence of finite crystallite dimensions and/or by lattice strains on a nanometer scale. In this respect they are an obligatory "instrument" and truely helpful. But it is amazing that they are applied often without justification for the (semi)quantitative analysis of crystallite sizes and their distribution and the various types of lattice defect that cause lattice strain (size-strain analysis). The increase in power of PC's makes the use of more dedicated and complicated methods of diffraction-line broadening analysis less prohibitive, but the very detailed, complicated, and often unknown crystal-structure dependence of the lattice defects prevent the writing of straightforward, generally applicable computer programs: software becomes the bottleneck. Several examples will be given of cases of misuse as well as correct use and of probable future practical applications. The main conclusion will be that there is a need for a joint, international effort: (i) to identify the implications of diffraction-line profile analysis for other diffraction analyses like crystal-structure determination, in particular from powder data, (ii) to develop algorithms for these implications, and (iii) implement these algorithms in software.

Monday, 22 September

Plenary lecture 5

Monday morning, 22 September, 8:30
Lecture Hall I
Chair: Gilberto Artioli

8:30 Invited oral

X-ray powder diffraction on Mars

David L. Bish[1], David F. Blake[2], Philippe Sarrazin[3], David T. Vaniman[4], Steve J. Chipera[5]

1. *Indiana University, 1001 E. 10th St., Bloomington 47405, United States* **2.** *NASA Ames Research Center, Moffett Field, CA 94053, United States* **3.** *InXitu, 2551 Casey Ave. Suite A, Mountain View 94043, United States* **4.** *Los Alamos National Laboratory (LANL), Los Alamos, NM 87545, United States* **5.** *Chesapeake Energy Corp, 6100 N. Western Ave., Oklahoma City 73118, United States*

e-mail: bish@indiana.edu

Minerals generally form under specific sets of conditions reflective of equilibrium. Therefore, the details of a mineral assemblage (i.e., rocks) can often be used to infer rock formation conditions and the history of mineral formation and alteration. For this reason, since the late 19th century when scientists believed that Mars surface was covered by *canali*, mankind has sought to learn the mineralogical makeup of planetary bodies. Virtually all of our knowledge of Earth's neighbors (apart from our Moon and Mars) has been obtained remotely via spectroscopic or photographic methods. Not unlike Percival Lowell, who suggested in 1895 that martian canals had been constructed by an intelligent race tapping melting polar ice for water to irrigate equatorial crops, understanding the mineralogy of other planetary bodies has often required imagination. Although considerable chemical and spectroscopic data exist for the surface of Mars, these do not provide unambiguous mineralogic information, thereby generating considerable speculation about the mineralogy of the martian surface. Orbital data show the widespread occurrence of common basaltic or andesitic minerals, but it has proven more difficult to unravel Mars' alteration mineralogy. Spectroscopic and chemical data obtained by the martian landers have provided tantalizing suggestions of a secondary minerals, such as phyllosilicates (e.g., clay minerals) and evaporite minerals, but there are few relatively unambiguous mineralogical identifications, including jarosite, $KFe_3(SO_4)_2(OH)_6$ (based on Mössbauer spectroscopy), gypsum, and a variety of less well-constrained sulfates and silicates. CheMin is a miniature XRD/XRF instrument designed for mineralogical analyses on extraterrestrial bodies (e.g., planets, moons, asteroids and cometary nuclei). CheMin uses a Co X-ray source in transmission mode with a 2-D CCD detector, operating in single-photon counting mode, capable of spatial and energy resolution of X-ray photons. Sample preparation requires only crushing to <150 μm by virtue of its sonic

vibration sample movement technique applied during analysis for enhanced particle statistics. A 2-D image of fluorescent and diffracted photons is obtained on the CCD, and imaging only the characteristic Co Kα photons produces Laue rings. Circumferential integration of the rings produces a conventional diffraction pattern. The instrument has been lab and field tested and was used to obtain *in situ* XRD and XRF analyses in Death Valley, Rio Tinto, Spain, the Arctic, and the Antarctic. The mineralogy of rock and soil samples is easily identified in the field, with analysis times as short as 5 min, and data were analyzed on-site, including Rietveld refinements to compute the quantitative compositions of mineral mixtures. *In situ* analysis largely eliminates the concern with changes in sample mineralogy after field sampling, either by hydration/dehydration or mineral-mineral reactions. CheMin is scheduled to fly on the 2009 NASA Mars Science Laboratory landed mission to Mars, where it will perform mineralogical and elemental analyses of rocks, sediments, and regoliths to provide the first definitive mineralogical data for Mars, including assessing the possible role of water in mineral formation and searching for indicators of past habitable environments.

Plenary lecture 6

Monday afternoon, 22 September, 13:00
Lecture Hall I
Chair: Anton Meden

13:00 Invited oral

Characterization of Metal Hydrides by Powder Diffraction

Radovan Cerny

University of Geneva, 24 quai Ernest-Ansermet, Geneva 1211, Switzerland

e-mail: Radovan.Cerny@cryst.unige.ch

The methods of structural characterization of metal hydrides are reviewed (see also [1]). The existing difficulties and problems are outlined and possible solutions presented. It is shown that powder diffraction is essential component of metal hydrides research where the structural characterization is currently undertaken by X-ray and neutron diffraction. In the case of light metal hydrides like borohydrides of light alkaline metals/earths X-ray diffraction alone can provide the structural parameters with sufficient accuracy. A crystallographer analyzing metal hydrides has to face numerous crystallographic challenges which include complex structures, superstructures, pseudo-symmetries, twinning, chemical and positional disorder, structural solution from low quality data (powder patterns), joint use of several data sets, resonant scattering and fast in-situ data collection.

Direct space approach is currently the powder diffraction method mostly used in metal hydride research for its simplicity of use, ability to work with powder patterns of low quality (broad peaks), easy way to treat the occupation disorder on hydrogen sites and active use of simple geometrical constraints. Crystal structures containing as many as 55 independent atoms (including hydrogen) have been fully characterized using powder diffraction. This is of great importance, because rapid collection of powder data thanks to modern synchrotron and neutron time-of-flight sources opens the possibility for fast *in-situ* studies, mapping of phase transitions induced by the temperature, pressure, hydrogen content, and chemical reactions. The progress in structural characterization of metal hydrides goes hand in hand with the progress in the powder diffraction methodology.

[1] Černý R.; *Z. Kristallogr.* (2008), in preparation

Microsymposium 1

Programme

Saturday, 20 September

Structure determination by reciprocal space methods
Saturday morning, 20 September, 10:00
Lecture Hall I
Chair: Wieslaw Lasocha

10:05 Oral

Resolution bias correction and crystal structure solution from powder data

Carmelo Giacovazzo, Angela Altomare, Gaetano Campi, Cuocci Corrado, Moliterni Anna Grazia, Rizzi Rosanna

CNR-Istituto di Cristallografia (IC), via Amendola 122/O, Bari 70126, Italy

e-mail: carmelo.giacovazzo@ic.cnr.it

Diffraction experiments provide intensities up to a limited resolution: as a consequence, always the Fourier syntheses show series termination errors. The worse the resolution, the worse is the Fourier representation of the electron density: peaks are misplaced and deformed, positive and negative ripples are present. An algorithm has been settled which is able to reduce the resolution bias by relocating the peaks in more correct positions and by modifying the peak profile to better fit the real atomic electron densities.
We have applied the procedure to several test structures for which only powder data are available. Organic as well as metallorganic structures have been considered, with experimental data at non-atomic resolution. The electron density maps provided by Direct Methods, affected by series termination errors, by phase errors and by inaccuracy of the structure factor magnitudes, were submitted to the new algorithm. In spite of the above difficulties the new algorithm succeeded in several cases which could not be solved without the resolution bias correction.

10:30 Oral

Structure solution from powders by charge flipping combined with histogram matching

Lukas Palatinus[1], Christian Baerlocher[2]

1. *Ecole Polytechnique Federale de Lausanne (EPFL), Ecublens, Lausanne 1015, Switzerland* **2.** *ETH Zürich (ETHZ), Wolfgang-Pauli-Strasse 10, Zürich 8093, Switzerland*

e-mail: palat@fzu.cz

Charge flipping is an increasingly popular structure solution method based on an iterative application of constraints in both direct and reciprocal space. The output of the structure-solution process is a scattering density in the unit cell of the crystal. It is very successful, if good-quality single-crystal diffraction data are available. The intrinsic problem of the structure solution from powder diffraction data is the reflection overlap, as a result of which the intensities of individual reflections can be extracted only approximately. Consequently, the scattering density obtained with these approximate intensities is often of mediocre quality, even if the phases are known. This problem can be circumvented by combining the basic charge-flipping algorithm with a histogram matching procedure. The histogram of a structure can be satisfactorily estimated from the chemical composition only, without the knowledge of the crystal structure, and as such provides additional external information. Modifying an intermediate electron density to fit the expected histogram results in a change of its Fourier spectrum, and this improved spectrum can be used to repartition the intensities of the overlapped reflections.

The method has been applied to extracted intensities of several powder data sets [1], where the overlap was determined based on the angular separation of the reflections in the pattern, and the overlapped reflections were repartitioned according to the intensity ratios of the histogram-matched density. Although the method works well, it is clearly not exploiting all the information contained in the diffraction pattern, because the distribution of the intensities within one overlap group is not used in the process. Therefore a method was generalized to use the full powder diffraction pattern during the histogram-matching procedure.

The charge flipping combined with histogram matching is a powerful method especially in cases of large unit cells with strong systematic overlap. On the other hand, it is limited by the requirement of atomic-resolution data, i.e. effective resolution of about dmin=1.2 or better. That means that for structures with larger unit cells very good experimental data is required, usually data obtained with synchrotron radiation.

[1] Baerlocher, Ch., McCusker, L. B. and Palatinus, L. (2007), Z. Kristallogr. 222, 47-53

10:55 Oral

Advances of the constrained S-FFT direct phasing method to powder diffraction data

Jordi Rius

Institut de Ciencia de Materials (ICMAB) - CSIC (ICMAB), Campus de la UAB, Barcelona 080193, Spain

e-mail: jordi.rius@icmab.es

Since its discovery, the direct methods origin-free modulus sum function S [Rius (1993) Acta Cryst. A49, 406-409] has been used for solving some complex crystal structures from powder X-ray diffraction data. In these applications, phase refinement was normally carried out by maximising function S with a modified tangent formula. However, further progress in the powder diffraction field was hampered by the complexity of combining the tangent formula refinement that makes explicit use of triple-phase sums, with the introduction of constraints in real space necessary to counterbalance the information loss produced by peak overlap in powder diffraction. In this connection the recently developed S-FFT phasing algorithm that maximises S by means of the FFT algorithm (thereby considering the triple-phase sums implicitly [Rius, Crespi, Torrelles (2007) Acta Cryst A63, 131-134]) is considerably simpler, completely general

and can represent a source of progress in powder diffraction. It will be shown how the application of the S-FFT algorithm according to the SnB philosophy can treat powder diffraction data more effectively due to the easy introduction of real-space constraints. This has been implemented in the new version of the direct methods program XLENS (Rius, 2008) distributed through the Fullprof suite of programs (Rodríguez-Carvajal, 2008).

11:20 Oral

Solving zeolite structures from powder data using maximum entropy with density building functions and histogram matching

Chris J. Gilmore[1], Douglas L. Dorset[2]

1. *University of Glasgow, University Gardens, Glasgow G12-8QW, United Kingdom* **2.** *Advanced Characterization, ExxonMobil, 1545 Route 22 East, Annandale NJ08801, United States*

e-mail: chris@chem.gla.ac.uk

Recently we have applied techniques that use density building functions and density histogram matching methods coupled with entropy maximisation and likelihood analysis to solve a number of structures *ab initio* using electron diffraction data in 2- and 3-dimensions at resolutions that are often around 2A. [1]. The same methodology can be used very effectively with powder diffraction data:

1. A low resolution structure is generated using non-overlapped low resolution structure factors combined with the origin defining rules of direct methods.
2. New reflections are given permuted phase angles (and intensities if overlapped) and analysed using density building functions [2].
3. The optimal phase sets are subjected to entropy maximisation [3].
4. Likelihood and density histogram matching are used to select the optimal phase set.

The method is very simple to use, works automatically and is very effective at low resolution (ca. 2A) where traditional reciprocal methods can struggle. Inn these cases it gives excellent molecular envelopes that can be used by the FOCUS software [4].

Applications to a number of varied zeolite systems will be presented including EMM-3, EMM-8, ECR-40, DOH, MCM-70 and some unsolved structures. A typical envelope for DOH [5] is shown below.

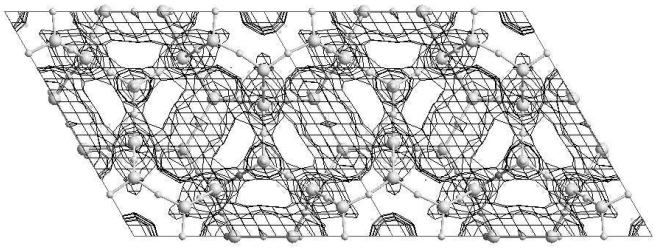

Figure: Envelope for DOH using laboratory data.

The use successful of charge flipping algorithms [6] with some of this data will also be discussed.

[1] Dorset, D.L., Dong, W. & Gilmore, C.J. *Acta Cryst.* (2008). **A64**, 284-294; 295-302.

[2] Gilmore, C.J., Bricogne, G & Bannister, C. (1990). *Acta Cryst.***A46,** 297-308.

[3] Bricogne, G & Gilmore, C.J. (1990). *Acta Cryst.***A46**, 284-297.

[4] Grosse-Kunstleve, R.W., McCusker, L.B. & Baerlocher, Ch. (1999). *J. Appl. Cryst.***32**, 536-542.

[5] Gerke, H. & Gies, H (1984) 166, 11-22.

[6] Oszlanyi, G & Suto, A (2004). *Acta Cryst***A60**, 134-141.

11:40 Oral

Powder Shake-and-Bake method

Hongliang Xu, Charles M. Weeks, Robert H. Blessing

Hauptman-Woodward Institute (HWI), 700 Ellicott Street, Buffalo 14203, United States State University of New York, Department of Structural Biology (UB), Buffalo 14203, United States

e-mail: xu@hwi.buffalo.edu

Over the past decade, structure determination from powder diffraction data has been widely and successfully used to determine structures of many organic, inorganic and organometallic compounds. Nevertheless, *ab initio* structure solution from powder data is still a challenge in many cases, due to the inevitable overlap of Bragg reflections resulting from the collapse of the three dimensions of reciprocal space onto the single dimension of a powder diffraction pattern. To develop the full capacity of structure determination from powder diffraction data, new methods, including the direct-methods approach, have to address the correct handling of multiply overlapped reflections.

The dual-space-based *Shake-and-Bake* procedure is one of the most successful direct methods for phasing single crystal diffraction data. A new method, termed Powder *Shake-and-Bake* and implemented in the computer program P-*SnB*, incorporates *extracted* and *overlapped* reflections in the *Shake-and-Bake* procedure. It performs in each *SnB* cycle (i) an overlapped-reflection partition (*via* partial structural information from the previous cycle), (ii) a reciprocal-space phase refinement (*via* the reduction of the values of a statistical minimal function), and (iii) a real-space density modification (*via* peak picking).

The detailed Powder *Shake-and-Bake* algorithmic development and implementation, and the successful P-*SnB* applications with experimental powder diffraction data will be discussed.

This research was supported by NIH grant GM072023.

Microsymposium 2

Programme

Saturday, 20 September

Thin films, coating and surfaces
Saturday morning, 20 September, 10:00
Lecture Hall II
Chair: Radomir Kuzel, Jordi Rius

10:00 Oral

On grain growth and residual stress in thin metal films

Yener Kuru, Udo S. Welzel, Markus Wohlschlögel, Eric J. Mittemeijer

Max Planck Institute for Metals Research (MPI-MF), Heisenbergstrasse 3, Stuttgart 70569, Germany

e-mail: u.welzel@mf.mpg.de

Changes in residual stress, crystallite size, microstrain and texture of 50 nm thick sputter-deposited polycrystalline Cu and Ni thin films with temperature have been investigated employing in-situ X-ray diffraction measurements in a temperature range between 25°C and 250°C. Stress determinations were performed by analyzing the X-ray diffraction data according to the $\sin^2\psi$-method on the basis of the crystallite group variant. It has been found that grain growth in both layers is accompanied by the emergence of a considerable tensile stress component parallel to the surface. The stress evolutions in the layers were correlated with the changes of their coherently diffracting domain sizes and microstrains with temperature. The advantages of additional measurements at temperatures below ambient temperature to distinguish the thermal stresses from effects of stress relaxation and emerging secondary stresses, arising from thermally activated processes (such as grain growth) are emphasized.
The obtained results on grain growth and stress evolution are discussed in the light of different grain growth models. The excess volume in grain boundaries has been determined from the evolution of the residual stress and crystallite size with temperature.

10:30 Oral

X-ray studies in radiation physics: New data on bulk effects of the ion-plasma surface treatment

Yuriy Perlovich, Margarita Isaenkova, Olga Krymskaya, Maxim Grekhov, Valeriy Polskiy

Moscow Engineering Physics Institute (MEPhI), Kashirskoe shosse, Moscow 115409, Russian Federation

e-mail: yuperl@mail.ru

It is meant usually that the main mechanisms of radiation physics are well-known already and new experimental facts of fundamental importance are rather improbable. In particular, the ion-plasma surface treatment of metal materials is wide-spread in industrial technologies and its effects on structure features of irradiated products are believed to be restricted by the surface layer of ion braking, having a thickness up to ~15 nm by ion energies of several KeV. Meantime, the layer-by-layer X-ray study has shown that irradiation of metal materials by low-energy ions is accompanied by the long-range effect, consisting in distinct texture and structure changes at the depth, exceeding, at least, by 10^4-10^5 times the thickness of the layer, where all ions prove to be stopped.

Texture and structure changes in bulk of tubes from Zr-based alloys for nuclear reactors under the ion-plasma treatment by regimes, differing in the density of plasmic flow energy, were compared by methods of X-ray diffractometry. The systematic layer-by-layer X-ray study of treated tubes reveals distinguishing features of gradient structures, formed by the ion-plasma irradiation. Heating and the following cooling of the surface layer are accompanied by development of various processes, including melting, crystallization, amorphization, quenching, phase transformations. Ion irradiation exerts influence of two kinds on the substructure of tubes: it produces new defects in the recrystallized matrix, causing distortion of its crystalline lattice, and results in substructure perfection of cold-rolled tubes. Therefore, the character of structure changes, observed in bulk of treated tubes, depends on their initial condition (cold-rolled or recrystallized). The ion-plasma treatment of the deformed tube is accompanied by perfection of its substructure, as opposed to the case of the recrystallized tube. Positions and thickness of layers, characterized by domination of that or another processes, are seen by analysis of obtained X-ray data.

There are two effects, indicating to operation of the mechanism of shock waves, arising by ion retardation. The first effect consists in strengthening of the axial texture component over the whole thickness of tube's wall (0.7 mm), the second effect – in suppression of the first one due to melting of the surface layer or in the tube from the Zr-based alloy, containing the fine-dyspersated intermetallic phase at the initial stage of precipitation. In both cases weakening and/or scattering of shock waves takes place, so that the layer of noticeable irradiation effects becomes thinner. The distorted crystalline lattice of the deformed tube suppresses the shock waves, produced by ions, by analogy with the effect of melted layer.

10:55 Oral

Investigating interdiffusion in Cu/Ni multilayers from x-ray diffraction and kinetic simulation

FengJu Gao[1,2,3], Mohamed-Cherif Benoudia[1,2], Jean-Marc Roussel[1,2], Stephane Labat[1,2], Olivier Thomas[1,2], Dezső L. Beke[4], Gábor Langer[4], Miklós Kis Varga[4]

1. *Aix-Marseille Université, Institut Matériaux Microélectronique Nanosciences de Provence, Marseille 13397, France* **2.** *CNRS, Faculté des Sciences et Techniques, Campus de St Jérome, Marseille 13397, France* **3.** *Department of Materials Science and Engineering, Beijing Normal University, Avenue Xinjiekouwai 19, Beijing 100875, China* **4.** *Department of Solid State Physics, L. Kossuth University, Debrecen H-4010, Hungary*

e-mail: fengju.gao-inv@univ-cezanne.fr

Epitaxial Cu/Ni multilayers are model systems for investigating the early stages (at the nm scale) of interdiffusion and mechanical stress.

In this work we present a method that combines both atomistic simulations of the interdiffusion and x-ray diffraction experiments in this system. The aim of this approach is mainly to confirm (or not) the non-fickian interdiffusion mode that is expected in Cu/Ni multilayers. Indeed, due to the large asymmetry of the atomic mobility (Ni atoms diffuse faster in Cu regions than Cu atoms do in Ni ones), a layer-by-layer mode should be observed experimentally [1].

First, by using a one dimensional mean-field diffusion model, we report our simulation results for two extreme cases of diffusion asymmetry: the Fickian mode where the diffusion coefficient is constant (no asymmetry) and the layer-by-layer mode resulting from a strong concentration dependence of the diffusion coefficient. The theoretical angular shift of the spectra and the evolution of peak intensities are calculated for the two different kinetics. Signatures of the layer-by-layer mode are discussed.

Then, the x-ray diffraction experimental results are presented. The samples [Cu3.375 nm /Ni2.25nm] × 25 and [Cu3.521nm/Ni3.521nm] × 25 are made by magnetron sputtering on the MgO substrate and annealed at about 380°C for different time. The resulting experimental data show important trends. The multilayers are coherent and remain so after annealing. From the out of plane scans, we observed a significant change of the relative values of the peak intensity.

From these experimental evolutions of the peak intensities and with the help of our simulations, we attempt to identify the interdiffusion modes that take place in the CuNi multilayers.

Reference: [1] J. M. Roussel, P. Bellon, Phys. Rev. B 73, 085403 (2006).

11:20 Oral

Thickness dependence of crystallization of amorphous and nanocrystalline magnetron deposited TiO_2 thin films

Lea Nichtova[1], Radomír Kužel[1], Zdenek Matej[1], Jan Šícha[2], Jindrich Musil[2]

1. *Charles University, Faculty of Mathematics and Physics, Ke Karlovu 3, Prague 12116, Czech Republic* **2.** *University of West Bohemia, Univerzitní 22, Pilsen 30614, Czech Republic*

e-mail: nichtova@gmail.com

Titanium dioxide films have many remarkable properties, for example photocatalytic activity and hydrophilicity. However, these properties depend significantly on the crystallinity, phase composition and microstructure of the films. In this study, crystallization of amorphous films with different thickness (50−2000 nm) deposited on glass and silicon substrates was investigated by in-situ isochronal and isothermal annealing at different temperatures and compared with the post-annealing of both amorphous and nanocrystalline films.

The X'Pert Pro diffractometer with MRI high-temperature chamber and parallel beam geometry with Goebel mirror, for texture and stress measurements, the Eulerian cradle and polycapillary were used, respectively.

In-situ measurements were performed at slightly lower temperatures (180 ºC, 220 ºC) than the crystallization temperatures previously found on the post-annealed samples and time dependences of selected XRD profiles were investigated. It was found, that the process can well be described by the modified Avrami equation that is applied to integrated intensities of the diffraction peaks, $I = 1\text{-}\exp[-b(t - t_0)n)]$, where the exponent n was in the range 2−2.5 and slightly increasing with the film thickness. This may indicate two dimensional character of the crystallite growth. The initial time t_0 of crystallization (non-zero intensity) increases nearly exponentially with the decreasing thickness while the slope b increases significantly for thicker films. Typical time necessary for the crystallization of the whole film volume varied from several hours for thicker layers to about ten days for the thinnest films, for the mentioned temperatures. Fast crystallization of the order of minutes appeared at 230 ºC for thicker films and were higher (290 ºC) for the thin films with the thickness below 100 nm. This confirmed the results obtained on post-annealed films. Weak texture was changing during the crystallization. At the beginning, the crystallites with the (00l) orientation were developed. However, after complete crystallization, the texture was weak except the very thin films (below 100 nm). Significant shifts of diffraction peaks with the temperature were observed and tensile residual stresses were confirmed by the $\sin^2\psi$ method for different diffraction peaks. They decrease with the increasing film thickness. Line profile analysis indicated the growth of relatively large crystallites (100 nm) already at the beginning of crystallization unlike the films which were deposited as nanocrystalline with the crystallite size of 5-10 nm which remained nanocrystalline to relatively high temperatures (600 ºC).

The work is supported by the Grant Agency of the Czech Republic (no. 106/06/0327).

11:40 Oral

In-line accurate monitoring of pseudomorphic SiGe layers

Emmanuel S. Nolot, Jean-Michel Hartmann, Christophe Licitra, Denis Rouchon, Denis Renaud

CEA-LETI-MINATEC (MINATEC), 17 rue des Martyrs, Grenoble 38054, France

e-mail: emmanuel.nolot@cea.fr

X-ray metrology techniques are quickly moving from characterization laboratories to semiconductor fabrication lines. They are now used to monitor Front End of the Line (FEOL) and Back End of the Line (BEOL) processes for the development of sub-45 nm technology nodes. Owing to their ability to determine thickness and elemental composition of thin films, as well as physical (crystallographic texture, density, porosity, roughness) and chemical (chemical bonding) properties of thin films and surfaces, they are more and more considered as at-line reference techniques, used to build calibration curves for other techniques (spectroscopic ellipsometry, etc) dedicated to fast in-line metrology on product wafers.

Bandgap engineering by controlling either the strain or the Ge content significantly improves the performances of Si-based devices such as high performance Metal Oxide Semiconductor Field Effect Transitors (MOSFETs) etc. To meet the need of in-line accurate characterization of thin pseudomorphic SiGe layers, we used the following procedure.

First, a set of SiGe layers with Ge contents in the 5 to 55% range

were grown by Reduced Pressure Chemical Vapor Deposition (RP-CVD) on Si(001) substrates. In order to get smooth, pseudomorphic SiGe layers, both process temperature (550-750°C) and SiGe layer thickness (20-60 nm range) were decreased as the Ge content increased. Secondly, conventional ω-2θ scans around the (004) diffraction orders were performed on each samples (figure 1) using a Panalytical X'Pert high resolution diffractometer in order to precisely gain access to the Ge content. Then, SiGe layer thickness was determined by X-Ray reflectometry (XRR) with a convergent beam Jordan Valley JVX5200 tool. High-precision Variable Angle Spectroscopic Ellipsometry was then performed on a Woollam M2000 rotating compensator ellipsometer in the 190-1700 nm wavelength range. The SiGe dielectric function was calculated for each Ge contents, using XRR thickness as a reference. Based on these data, an alloy model (figure 2) was built and finally implemented on fast in-line ellipsometers for accurate determination of Ge content (in the 0-55% range) and thickness of pseudomorphic SiGe layers grown on 200 mm or 300 mm product wafers.

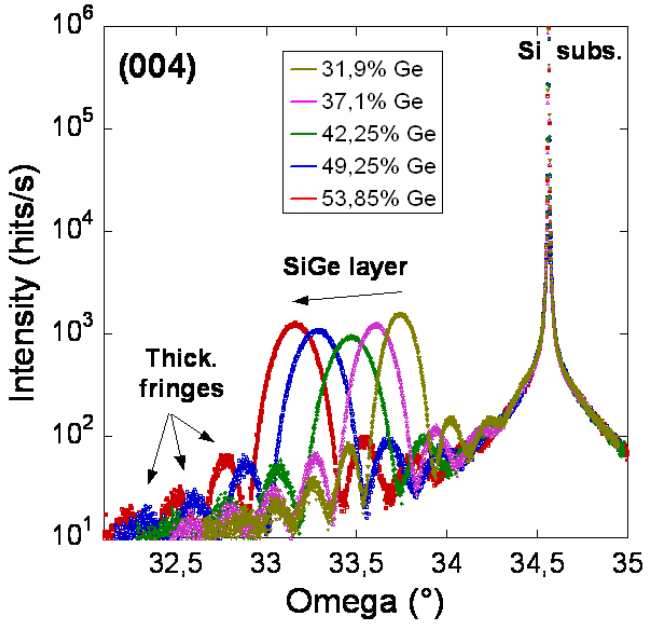

Figure1: ω-2θ scans around the (004) diffraction orders for pseudomorphic SiGe layers in the 31.9% to 53.85% Ge content.

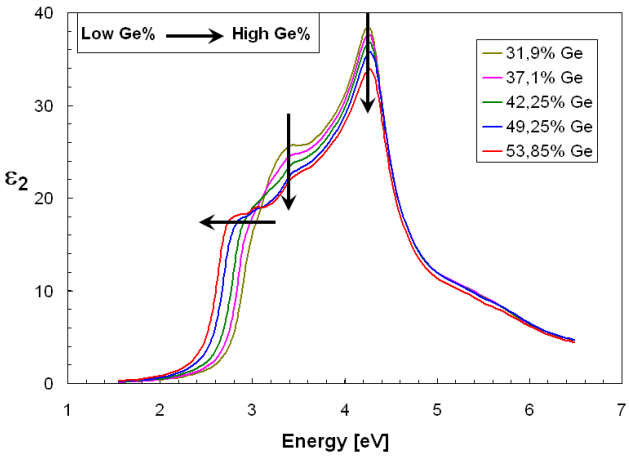

Figure2: Evolution of the imaginary part of the dielectric function of pseudomorphic SiGe layers in the 31.9% to 53.85% Ge content.

Microsymposium 3

Programme

Saturday, 20 September

Structure determination by direct space methods
Saturday afternoon, 20 September, 16:30
Lecture Hall I
Chair: Kenneth D.M. Harris

16:30 Oral

Overcoming poor particle statistics - low temperature structure of succinonitrile using a combination of simulated annealing and quantum optimization

Pamela S. Whitfield, Yvon Le Page, Ali Abouimrane, Isobel J. Davidson

Institute for Chemical Process and Environmental Technology National Research Council of Canada, Ottawa ONK1A06, Canada

e-mail: pamela.whitfield@nrc.gc.ca

Succinonitrile at room temperature forms what is known as a plastic-crystal phase with positional ordering but rotational disorder yielding an I-centred cubic lattice. There is a phase transition on cooling at around 218K to an ordered crystalline phase which currently has an unknown crystal structure. Given that samples are normally mounted around room temperature, the morphology and properties of the plastic crystal phase become important for the quality of the sample. The plastic and 'sticky' nature of the succinonitrile makes producing a good powder almost impossible. Injecting the molten succinonitrile inside a capillary is the most practical way to mount a sample of succinonitrile, but its tendency towards dendritic and direction crystal growth may be problematic. The sample is likely to be prone to both preferential orientation and poor particle statistics, neither of which is conducive to lab-based structure solution techniques. This may explain why the low temperature structure of a very common laboratory chemical has not been solved previously.

Data were taken from a capillary sample of succinonitrile at 173K using a Vantec PSD detector with a focussing primary mirror. After indexing using TOPAS, the structure solution was attempted using simulated annealing. Constraints were used to prevent errors in the relative intensities forcing the structure away from a chemically reasonable conformation. Succinonitrile can adopt the cis-, trans- or gauche- conformations. The SA was set up with a z-matrix rigid body such that the conformation of succinonitrile was randomly selected for each cycle before minimization with limited freedom in the torsion angle such that it had to remain in the selected conformation. A constrained March-Dollase correction was also included in the SA to help account for orientation.
Quantum optimization was used to minimize the energy of the resultant succinonitrile structure before refining the energy-optimized structure as a rigid-body against the experimental data. Analysis of the spherical harmonic orientation coefficients from the final refinement confirm moderate texture with an orientation that can be rationalized in terms of the expected temperature gradients in the capillary on cooling. The structure is monoclinic in $P2_1/a$ with a = 9.160(1), b =8.6085(9), c = 5.8568(4) Å and ß = 79.652(4)º with Z = 4. The succinonitrile is present solely in the gauche conformation. Although the data quality limits the residual that may be achieved in the final fit, the resulting structure is consistent with available literature spectroscopy results.

16:50 Oral

Powders and 'peer-pressure': Pitfalls and progress

Maryjane Tremayne, Samantha Y. Chong, Duncan Bell, Adam Cowell

School of Chemistry, University of Birmingham, Edgbaston, Birmingham B152TT, United Kingdom

e-mail: m.tremayne@bham.ac.uk

An important factor in the increasing number of crystal structures determined by PXRD is the development of direct space structure solution techniques [1], in which a range of predicted structural models are compared with the experimental powder data using a global optimisation technique to locate the best crystal structure solution. A number of optimisation algorithms have been applied to this problem, but our work has focussed recently on the development of the Cultural Differential Evolution (CDE) technique [2,3]. This approach combines the traditional biological dictates of mating, mutation and natural selection in the Differential Evolution method (DE) [4,5], a relatively new algorithm that follows similar principles to conventional genetic algorithms, with an approach that models human social behaviour or cultural selection.

We will present the progress that we have made in the development of the CDE algorithm in which 'cultural' behaviour or 'peer pressure' – in this case, the distribution in values of structural parameters in each generation – is used to guide and enhance the DE process. This approach uses social factors to guide and speed-up evolution but natural biological selection to drive the optimisation process. By optimisation of search control parameters such as population size, mutation rate and the degree of cultural pruning, we will demonstrate significant improvement in efficiency of our structure solution calculation in all test cases, over the DE method alone. The advantages of cultural pruning when using relatively large population sizes with relatively high population diversity will also be presented.

Although the main focus of this presentation will be on the development and the improvements in efficiency of the CDE approach, potential pitfalls in the direct space structure solution process using any form of optimisation technique, will also be discussed. Examples will include the effects of preferred orientation on the location of the global structure solution and refinement minima [6], and limitations that should be considered when defining structural models for use in direct-space structure solution approaches.

[1] M. Tremayne (2004), M., Phil. Trans. R. Soc. Lond. A, 362, 2691.
[2] S.Y. Chong, M. Tremayne (2006), Chem. Comm., 4078.
[3] A. P. Engelbrecht (2002), in Computational Intelligence: An Introduction, John Wiley & Sons, Chichester, p171.

[4] K.V. Price (1999), in New Ideas in Optimization (ed: Corne, D.; Dorigo, M.; Glover, F.), McGraw-Hill, London.
[5] M. Tremayne, C.C. Seaton, C. Glidewell (2002), Acta. Cryst., B58, 823.
[6] S.Y. Chong, C.C. Seaton, B.M. Kariuki, M. Tremayne (2006), Acta Cryst., B62, 862.

17:10 Oral

Large-scale distributed computing for accelerated structure determination

Kenneth Shankland[1], Thomas Griffin[1], Jacco Van de Streek[3], Norman Shankland[2], Alastair J. Florence[2], William David[1]

1. *Rutherford Appleton Laboratory (RAL), Chilton, Didcot, Oxon OX11 0QX, United Kingdom* **2.** *University of Strathclyde, Strathclyde Institute for Pharmacy and Biomedical Sciences, 27 Taylor Street, Glasgow G40NR, United Kingdom* **3.** *Cambridge Crystallographic Data Centre (CCDC), Cambridge CB21EZ, United Kingdom*

e-mail: k.shankland@rl.ac.uk

Improvements in SDPD methodology have meant that ever more complex structures are being tackled using direct space methods. As a very general rule of thumb, the more complex the structure, the more difficult it is to locate the global minimum in the direct space search. This difficulty can, to some extent, be circumvented by running many instances of the search; for stochastic search methods such as simulated annealing, each instance can be run independently of any other. Such search problems are therefore ideally suited to disposition on a distributed grid-type system that makes use of existing compute resources on a network. At the Rutherford Appleton Laboratory, we have adapted the *DASH* structure determination code to run on a Univa UD *GridMP* system in order to distribute simulated annealing runs across hundreds of computer simultaneously with excellent scaling.

We will illustrate the use of this approach with some challenging Z'=4 structures and show how the approach usually means 'better' results rather than simply 'faster', even when faster equates to more than *two orders of magnitude* when compared to execution on a single computer. The principles outlined are equally well applicable to other global-optimisation based structure determination codes and to other grid-type systems, such as the widely used and freely available *CONDOR* system.

17:30 Oral

Crystal structure determination of two organic yellow azo pigments from X-ray powder diffraction data

Svetlana N. Ivashevskaya[1,2], Jacco Van de Streek[1], Martin U. Schmidt[1]

1. *Institut für Anorganische und Analytische Chemie, Johann Wolfgang Goethe-Universität, Max-von-Laue-Strasse 7, Frankfurt am Main 60438, Germany* **2.** *Institute of Geology Karelian Research Centre Russian Academy of Sciences, Pushkinskaya, 11, Petrozavodsk 185910, Russian Federation*

e-mail: ivashevskaja@yahoo.com

The crystal structures of two industrially produced yellow organic azo pigments were determined from X-ray powder diffraction data.

Powder patterns were recorded on a STOE-STADI-P-diffractometer equipped with a curved Ge(111) monochromator using CuK_{a1}-radiation in transmission mode.Powder patterns were indexed using the program *DICVOL91* [1] with triclinic unit cells. The structure solution from powder data was difficult because from the crystal symmetries it was obvious that the asymmetric unit contained one organic anion and one Ca cation, with the anion in general position; but it was not known if the Ca ions are situated on general or special positions (inversion centre). Furthermore the number of water molecules per unit cell was not known.

These difficulties were overcome by using combination of direct space methods and Rietveld refinement for structure solution. The crystal structures were solved in an iterative approach using a combination of simulated annealing in *DASH* [2] to determine the positions of the molecular ions followed by multiple partial Rietveld refinements in *TOPAS* [3] to locate the Ca ions and missing water molecules. This combination was made easier by the recently developed link between the programs *DASH* and *TOPAS*, which automatically generates an input file for TOPAS including all restraints. Finally the structures were Rietveld refined with the use of restraints (bond lengths, bond angles and planarity of aromatic ring systems) with *TOPAS*.

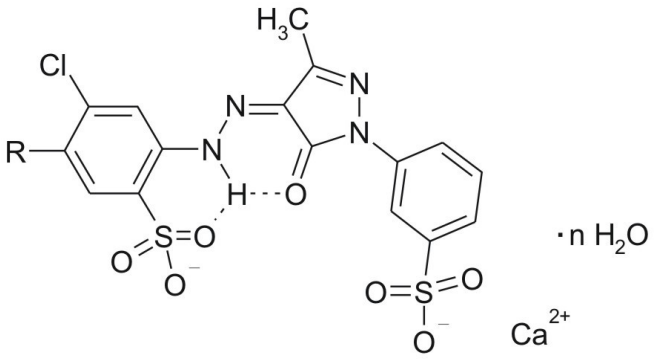

1: R= CH_3 n = 1 - 3

2: R= Cl

[1] A. Boultif & D. Louër, *J. Appl. Crystallogr*. **24** (1991), 987.

[2] W.I.F. David, K. Shankland, J. van de Streek, E. Pidcock, W. D.S. Motherwell & J.C. Cole, *J. Appl. Cryst*. **39** (2006), 910.

[3] A.A. Coelho, TOPAS-Academic 4.0 Version 4 (2007).

17:50 Oral

Dynamic re-definition of variable space during direct-space structure solution from powder X-ray diffraction data

Zhongfu Zhou, Kenneth Harris

Cardiff University, School of Chemistry, Park Place, Cardiff CF103AT, United Kingdom

e-mail: zhouz5@cardiff.ac.uk

Structure determination of organic molecular solids from powder X-ray diffraction data is nowadays carried out widely, in particular using the "direct-space" strategy for structure solution [1]. In our current implementation of this approach, the structure solution process involves exploring a powder-profile R-factor hypersurface to find the global minimum with respect to the set (Γ) of structural variables that define the trial structures. In principle, any technique for global optimization may be used, and our own current work in this field is focused on the use of a Genetic Algorithm (GA) [2] search algorithm, implemented in the program EAGER [3]. Conventionally, the structural variables in the set Γ comprise, for each molecule in the asymmetric unit, the position and orientation of the molecule with respect to the unit cell axes, and a set of variable torsion angles. Here we introduce an alternative approach, in which the standard set of structural variables is transformed to an alternative set of variables of the same or lower dimensionality, with this transformation carried out in a dynamic manner within the evolution of the GA calculation. Here we assess the feasibility of this approach in comparison with the standard approach. Structures containing highly flexible molecules defined by a significant number of torsional degrees of freedom represent a challenging case for direct-space structure solution [4], and our exploration of the potential advantages of altering the variable-space dynamically during GA structure solution calculations is focused in particular on examples of this type of structural problem.

[1] K.D.M. Harris, M. Tremayne, P. Lightfoot, P.G. Bruce, J. Am. Chem. Soc. 1994, 116, 3543.
[2] K.D.M. Harris, S. Habershon, E.Y. Cheung, R.L. Johnston, Z. Kristallogr. 2004, 219, 838.
[3] Z. Zhou, S. Habershon, G.W. Turner, B.M. Kariuki, E.Y. Cheung, A.J. Hanson, E. Tedesco, R.L. Johnston, K.D.M. Harris, EAGER, Cardiff University and University of Birmingham.
[4] A.J. Hanson, E.Y. Cheung, K.D.M. Harris, J. Phys. Chem. B 2007, 111, 6349.

18:10 Oral

Structure and polymorphism of trans mono-unsaturated triacylglycerols

Jan B. Van Mechelen, Rene Peschar, Henk Schenk

University of Amsterdam, HIMS, crystallography (UVA), Valckenierstraat 65, Amsterdam 1018XE, Netherlands

e-mail: mecheljb@xs4all.nl

Appropriately chosen blends of fats determine the physical properties of many food products like bakery products and table spreads. Soft natural oils often have to be hardened to give a blend the desired properties. Hydrogenation is a widespread applied hardening treatment with an undesired side effect: the (partial) isomerization of *cis* double bonds in *trans* double bonds, for example transformation of oleic acid (*cis*-9-octadecanoic acid; O) in elaidic acid (*trans*-9-octadecanoic acid; E). *Trans* fatty acids, commonly regarded as a health risk [1], supposedly replace their saturated analogues in the solid state but in fact little is known about their actual packing.

A better understanding of the influence of fatty-acid composition, conformational and packing differences on the polymorphic stability and phase-transition behavior of *trans* mono-unsaturated triacylglycerols (TAGs), and related saturated ones, can be obtained by combining X-ray powder diffraction (XRPD) techniques. Synchrotron and advanced laboratory time- and temperature-resolved XRPD can reveal the stability and phase-transition behavior of the important the β and β' polymorphs and these results can be related to the underlying crystal structure packing. In absence of single crystals, XRPD turned out to be a realistic but challenging alternative: with direct-space search techniques it was even possible to solve a β' TAG structure with two independent molecules in the asymmetric unit from laboratory diffraction data.

Results that will be discussed include novel meta-stable β' polymorphs and the structure of one them, methyl end-plane packing analysis in relation to observed melting points for various subgroups of TAGs, the difference in β' to β phase-transition behaviour of symmetric vs. asymmetric TAGs, and the influence of replacing a saturated stearic chain (octadecanoic acid; S) by an *trans* mono-unsaturated elaidic chain [2,3].

References:
[1] EFSA Journal (2004) 81, 1-49
[2] Mechelen, J.B. van, Peschar, R. & Schenk, H. (2008). Acta.Cryst. B**64**, 240-248.
[3] Mechelen, J.B. van, Peschar, R. & Schenk, H. (2008). Acta.Cryst. B**64**, 249-259.

Microsymposium 4

Programme

Saturday, 20 September

Line profile analysis
Saturday afternoon, 20 September, 16:30
Lecture Hall II
Chair: Nathalie Audebrand, Matteo Leoni

16:30 Oral

Debye equation versus Whole Powder Pattern Modelling: Real versus reciprocal space modelling of nanomaterials

Kenneth R. Beyerlein[1,2], Antonio Cervellino[3], Matteo Leoni[1], Paolo Scardi[1]

1. *Department of Material Engineering and Industrial Tecnology, University of Trento (DIMTI), v. Mesiano 77, Trento 38100, Italy* **2.** *Georgia Institute of Technology (GIT), 777 Atlantic Dr., Atlanta, GA 30332-0250, United States* **3.** *Swiss Light Source, Paul Scherrer Institute, Villigen PSI 5232, Switzerland*

e-mail: beyerle@ing.unitn.it

Real space methods like the Debye equation are increasingly being employed as an alternative to traditional line profile analysis (LPA) techniques for the study of size and strain effects in nanomaterials. Size and time scaling are the current main limits to an extensive use of Debye-based modelling, as all atomic coordinates need to be processed at each minimisation step to generate the diffraction pattern for a powder of small clusters. This limitation does not affect the alternative, reciprocal-space Whole Powder Pattern Method that, on the contrary, lacks of physical validation when applied to the study of small atomic clusters. A proper comparison between the two methods, however, has not been investigated so far. A comparison is therefore proposed here to highlight limits and potential of each method.

16:50 Oral

Microstructure of metals prepared by severe plastic deformation studied by different methods

Radomír Kužel[1], Milos Janecek[1], Jakub Cizek[1], Milan Dopita[2]

1. *Charles University, Faculty of Mathematics and Physics, Ke Karlovu 3, Prague 12116, Czech Republic* **2.** *Technical University Freiberg, Gustav Zeuner Str., Freiberg 09599, Germany*

e-mail: kuzel@karlov.mff.cuni.cz

Severe plastic deformation has become quite popular technique for production of compact ultrafine-grained materials. For better understanding of the microstructure of highly-deformed materials combination of different methods is desirable.

In present work, different samples of copper and copper composites deformed by the equal-channel angular pressing (ECAP) were studied by XRD line profile analysis, transmission electron microscopy (TEM), electron backscatter diffraction (EBSD) and positron annihilation spectroscopy (PAS).

Differences in microstructure of the samples in dependence on the number of passes (n_p = 1, 2, 4, 8) were found especially by TEM and EBSD. The latter technique is particularly useful thanks to the combination of good spatial and angular resolution. It was found that ECAP processing results in grain size reduction by a factor of about 100. Original course-grained microstructure evolves from prolate bands of cells/subgrains enclosed by lamellar nonequlibrium grain boundaries (1, 2) towards an equiaxed homogenous microstructure with equilibrium grain boundaries (8). Transition from the high fraction of the low angle grain boundaries created in the specimen during the first two ECAP passes to high angle grain boundaries as well as the pronounced increase of special coincidence site lattice (CSL) boundaries of $\Sigma 3^n$ type after 4 and 8 ECAP passes have been observed.

PAS technique revealed the presence of high density of defects (absence of the signal from free positrons in the spectra) and slight increase of dislocation density with the number of ECAP passes n_p. PAS also revealed the presence of microvoids of the diameter increasing with np from about 0.34 nm to 0.44 nm.

XRD measurements were carried out with the aid of X'Pert Pro powder diffractometer, filtered CuKα-radiation filtered, variable divergence and anti scatter slits enhancing high-angle peaks important for line profile analysis and the PIXCel position sensitive detector that enables to obtain high-quality low-noise data at reasonable collection time. Line profile analysis was done by simplified integral breadth method and total pattern fitting by the FOX program that was modified for the analysis of crystallite size and strain including dislocation-induced line broadening. Modified Williamson-Hall plots (integral breadth β vs. sin θ) do not show significant dependence on np except slightly varying typical line broadening anisotropy of the $\beta_{hhh} << \beta_{h00}$ type. However, changes of line profile shape can be clearly seen. With increasing np the tails become longer and shape is more Lorentzian. This may be a consequence of higher correlation in dislocation arrangements (which is in agreement with TEM and EBSD analysis) and results in the increase of dislocation density with n_p (in agreement with PAS).

17:10 Oral

Thermally induced microstrain broadening in polycrystalline materials: Powder-diffraction studies on hexagonal zinc metal and hexagonal ε-iron nitride

Andreas Leineweber[1], Thomas Gressmann[1], Eric J. Mittemeijer[1], Angus C. Lawson[2], James A. Valdez[2], Joice A. Roberts[2], Wolfgang S. Kreher[3]

1. *Max Planck Institute for Metals Research, Heisenbergstrasse 3, Stuttgart 70569, Germany* **2.** *Los Alamos National Laboratory (LANL), Los Alamos, NM 87545, United States* **3.** *Institute for Materials Science, Dresden University of Technology, Dresden 01069, Germany*

e-mail: a.leineweber@mf.mpg.de

Spatial variations of the thermal-expansion tensors in multiphase

materials or in non-cubic, single-phase polycrystalline materials induce upon temperature change locally varying microstresses [1]. Thus local plastic deformation or even grain-boundary cracking can occur. Understanding and experimental analysis of such thermally-induced microstresses, during production and during service, can be decisive for accurately estimating the strength properties of materials. These microstresses can be studied by analysing the associated microstrains by powder diffraction, because (within the Stokes-Wilson approximation [2]) the line broadening of a reflection *hkl* is determined by the projection of the microstrain distribution on the diffraction vector.

In the present contribution monophase hexagonal polycrystals showing anisotropic thermal expansion are considered. If the polycrystal is stress-free at T_0, temperature change to T_1 will lead to thermal misfit between differently oriented grains causing the above-mentioned thermal microstresses and microstrains. The corresponding multivariate Gaussian microstrain distribution can be calculated (neglecting plastic deformation and surface effects; assuming randomly oriented grains) on the basis of statistical and internal-energy considerations [1,3]:

(i) The average strain leads to average lattice parameters somewhat different from the equilibrium lattice parameters at T_1. The average strain can be used to define a strain scale with $<\Delta\varepsilon_{ij}> = 0$.

(ii) The joint second central moments $<\Delta\varepsilon_{ij}\Delta\varepsilon_{mn}>$ of the microstrain distribution around the average $<\Delta\varepsilon_{ij}> = 0$ are proportional (constant K) to the corresponding components of the elastic compliance tensor in the crystal's frame of reference, $<\Delta\varepsilon_{ij}\Delta\varepsilon_{mn}> = Ks_{ijmn}$. On the basis of these second moments the expected *hkl*-dependent microstrain broadening can be calculated [4].

The following experimental model cases were considered:

(a) Neutron-diffraction experiments on polycrystalline hexagonal zinc at ambient temperature (T_0, microstrain-free state) and after cooling to T_1 = 10 K.

(b) Synchrotron X-ray diffraction applied to polycrystalline hexagonal ε-iron nitride after cooling from 673 K (production temperature, T_0) to ambient temperature, T_1.

Both materials exhibit *hkl*-dependent microstrain broadening at T_1. For zinc this broadening is especially pronounced for 00*l* reflections, which is compatible with zinc's high elastic compliance along [001] directions. In both cases, comparison of the experimental data with theory [1,3] indicates that local plastic deformation had occurred. This conclusion is also supported by the observed characteristic reflection asymmetries, where the skewnesses of the *hk*0 and 00*l* reflections have inverse signs.

[1] W. Kreher, W. Pompe, Internal Stresses in Heterogeneous Solids, Akademie-Verlag Berlin (1989).

[2] A. J. C. Wilson, Nuovo Cimento 1 (1955) 277.

[3] W. S. Kreher, Comp. Mater. Sci. 7 (1996) 147.

[4] A. Leineweber, J. Appl. Cryst. 39 (2006) 509.

17:30 Oral

A general approach for determining the contrast factor of dislocations

Jorge Martinez-Garcia[1], Matteo Leoni[2], Paolo Scardi[2]

1. *Ecole Polytechnique Federale de Lausanne (EPFL), Lausanne 1015, Switzerland* **2.** *Department of Material Engineering and Industrial Tecnology, University of Trento (DIMTI), v. Mesiano 77, Trento 38100, Italy*

e-mail: jorge.martinezgarcia@epfl.ch

Dislocations are known for their peculiar effect on the diffraction line profile. Each given dislocation type, defined by the slip system and dislocation character, produces a specific anisotropic line broadening basically determined by the so-called Contrast Factor (CF). The determination of CFs is made difficult by a complex elastic strain and geometrical problem, which is strongly dependent on the symmetry of the crystal lattice. As a consequence, CF calculations were so far limited to some high symmetry - cubic and hexagonal - lattices. In the present work a general algorithm is presented for the calculation of CFs for any dislocation configuration and lattice symmetry. It will be shown that numerical values can be obtained in the general case, and that explicit analytical expressions can be found in some relevant cases.

17:50 Oral

Physical models for size broadening in the Whole Powder Pattern Fitting

Davor Balzar, Nicolae C. Popa

University of Denver, 2112 E Wesley Ave, Denver 80208, United States

e-mail: balzar@du.edu

Several physical models for description of size broadening that are convenient for implementation into the Rietveld programs are described. First, isotropic models are discussed and illustrated on powder patterns of cerium oxide. Second, a new anisotropic size-broadening model, based on spherical-harmonics representation allowing determination of both volume- and area-averaged apparent crystallites, is presented. The model effectiveness is demonstrated on a zinc oxide powder pattern exhibiting strongly anisotropic size broadening and pronounced super-Lorentzian peak shapes. It is shown how the apparent crystallites can be interpreted in terms of physical models by using ellipsoidal and cylindrical crystallites with lognormal size distributions.

18:10 Oral

Twinning together with dislocations and crystallite size in hexagonal materials determined by X-ray line profile analysis

Tamás Ungár, Levente Balogh

Eötvös University, Pázmány Péter sétány 1/A, Budapest H-1117, Hungary

e-mail: ungar@ludens.elte.hu

The effect of twinning and faulting on X-ray line broadening is worked out theoretically to a large extent for the close packed planes in *fcc* crystals [1-6]. Profiles of faulted or twinned crystals consist of sub-profiles which satisfy specific conditions for the *hkl* indices. Especially in *fcc* crystals, these conditions are that: (i) planar faults affect line profiles if, and only if: $h+k+l \neq 3m$, and that (ii) for a particular {*hkl*} reflection both, the FWHM and the shifts of sub-profiles are strictly proportional to $|h+k+l|$ [1], where m is an arbitrary integer [3]. The profile function of a specific sub-profile corresponding to twins or stacking faults can be shown to be the sum of a symmetrical and an antisymmetrical Lorentzian function [5,6]. In *fcc* crystal faulting or twinning occures on the close packed {111} planes which repeat periodically in the directions normal to the planes. In hexagonal materials, especially in titanium, zirconium, magnezium ant their alloys the dislocation structure and twinning are much more complicated than in *fcc* metals: (a) there are three different possible Burgers-vector types instead of one [7,8], (b) at least 11 different slip systems can operate in principle [7,8], (c) there are a variety of twinning systems, e.g., {10.1}<10.-2> and {11.2}<11.-3> compressive twins and {10.2}<10.-1> and {11.1}<-1-1.6> tensile twins [9], and (d) some slip systems may not be activated because of the large variation of the critical resolved shear stress from one slip system to another [9]. In hexagonals the crystal cannot be built up by a similar simple repetition in the normal directions to these planes. In a previous paper a numerical method was developed to give the breadths and shifts of sub-profiles as a function of fault or twin densities [10]. This procedure is extended for hexagonal crystals. The outline of the theoretical basis and a few specific applications will be presented here.

1. L. Landau, Phys. J. Soviet-Union, 12 (1937) 579.
2. S. Hendricks, E. Teller, J. Chem. Phys. 10 (1942) 147.
3. B.E. Warren, Prog. Metal Phys. 8 (1959) 147.
4. P. Scardi, and M. Leoni, J. Appl. Cryst. 32, 671 (1999).
5. L. Velterop, R. Delhez, Th. H. de Keijser, E. J. Mittemeijer, D. Reefman, J. Appl. Cryst. 33 (2000) 296-306.
6. E. Estevez-Rams, B. Aragon-Fernandez, H. Fuess, A. Penton-Madrigal, Phys. Rev. B, 68 (2003) 064111.
7. I. P. Jones, W. B. Hutchinson, Acta Metall. 29 (1981) 951-968.
8. R. Kužel Jr., P. Klimanek, J. Appl. Cryst. 22 (1989) 299-307.
9. Y. B. Chun, S. H. Yu, S. L. Semiatin, S. K. Hwang, Mat. Sci. Eng. A 398 (2005) 209-219.
10. L. Balogh, G. Ribárik, T. Ungár, J. Appl. Phys. 100 (2006) 023512.

Microsymposium 5

Programme

Sunday, 21 September

Total Scattering Analysis
Sunday morning, 21 September, 10:00
Lecture Hall I
Chair: Thomas Proffen

10:00 Oral

Total scattering analysis – how to get the most from your data

David A. Keen

Rutherford Appleton Laboratory (RAL), Chilton, Didcot, Oxon OX11 0QX, United Kingdom

e-mail: d.a.keen@rl.ac.uk

Total scattering - that is an absolutely normalised powder diffraction pattern including the diffuse scattering component - may be used to extract the average crystal structure (via Rietveld refinement) and local atom pair correlations (via a sine Fourier transform of the data). Atomistic models that are derived from this local and average information may be used to aid the understanding of crystal structures and this approach is especially helpful if the structures are complicated by a degree of local disorder.

I will illustrate how total scattering data may be collected, analysed and modelled using a number of examples and highlighting the additional insight made possible from this analysis over and above an interpretation based on the average structure alone. In this talk there will also be examples from our recent work, which uses RMCProfile modelling [1], including a structural explanation of pressure-induced amorphisation and negative thermal expansion in ZrW_2O_8 [2-4] and how weak argentophilic interactions govern the colossal (positive and negative) thermal expansion in $Ag_3[Co(CN)_6]$ [5].

[1] M G Tucker, D A Keen, M T Dove, A L Goodwin and Q Hui *J. Phys.: Condensed Matter***19** 335218 (2007)
[2] D A Keen, A L Goodwin, M G Tucker, M T Dove, J S O Evans, W A Crichton and M Brunelli, *Phys. Rev. Lett.***98** 225501 (2007)
[3] M G Tucker, A L Goodwin, M T Dove, D A Keen, S A Wells and J S O Evans, *Phys. Rev. Lett.***95** 255501 (2005)
[4] M G Tucker, D A Keen, J S O Evans and M T Dove, *J. Phys.: Condensed Matter***19** 335215 (2007)
[5] A L Goodwin, M Calleja, M J Conterio, M T Dove, J S O Evans, D A Keen, L Peters and M G Tucker, *Science***319** 794-797 (2008)

10:30 Oral

Pair Distribution Function studies of nanostructured materials at the high Q resolution powder diffraction beam line at the ESRF - Investigation of CeO_2-based compounds

Michela Brunelli[1], Marco Scavini[2], Cesare Oliva[2], Serena Cappelli[2]

1. *Europen Synchrotron Radiation Facility (ESRF), 6, Jules Horowitz, Grenoble 38000, France* **2.** *Università di Milano, Dipartimento di Chimica Fisica ed Elettrochimica, via Golgi, 19, Milano 20133, Italy*

e-mail: brunelli@esrf.fr

Pair Distribution Function (PDF) analysis method is a powerful tool for the investigation of crystalline or partly crystalline materials, yielding crucial information on the atomic-scale structures of nanosized materials. An increasing number of topics are today tacked by PDF analysis by neutron and X-ray powder diffraction. Nanostructured materials, nanoporous materials, frame-host interaction in zeolites, nano-scale structures (local structures *versus* average structures) in complex materials for modern applications have been investigated using synchrotron X-ray PDF analysis at the high reciprocal-space (Q) resolution powder diffraction beam line ID31 at the ESRF (France). In this talk I will show some recent results in these areas of research from data collected using hard X-rays at ID31. I will focus on the relation between nanosize structure and superparamagnetism in $Ce_{1-x}Gd_xO_{2-x/2}$ compounds. CeO_2-based materials ($Ce_{1-x}M_xO_{2-x/2}$; M = Gd, Y, Sm) have been studied in the last years as catalysts, structural and electronic promoters for heterogeneous catalytic reactions and oxide ion conducting electrolytes for electrochemical cells, for which application they show high ion conductivity and would be able to operate at relatively low temperatures (500 - 700°C). Since thermodynamics transport and magnetic properties of nanostructured compounds can be different from those of bulk materials, the local structure of $Ce_{1-x}Gd_xO_{2-x/2}$ nanostrucured samples has been investigated by means of PDF analysis (Fig. 1). The local distortions introduced by Gd doping and nanosize in of $Ce_{1-x}Gd_xO_{2-x/2}$ samples will be discussed.

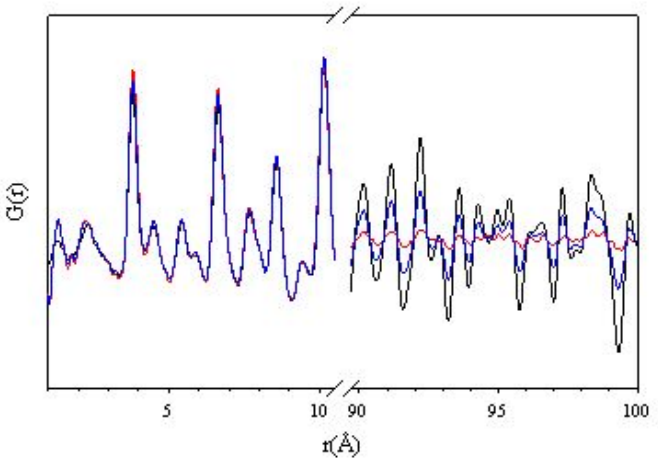

Figure 1:
G(r) function of $Ce_{0.8}Gd_{0.2}O_{1.9}$ samples: amplitude of the nanostruc-

tured samples (red) decreases rapidly at high *r* values due to the limited particle size.

11:00 Oral

Refinement of disordered structures from powder diffraction data

Reinhard B. Neder

Universität Erlangen, Kristallographie und Strukturphysik, Staudtst. 3, Erlangen 91058, Germany

e-mail: reinhard.neder@krist.uni-erlangen.de

The powder pattern of disordered structures consists of spherically integrated reciprocal space averaged over many powder particles which each may have an individual defect structure. The respective PDF is the average over all individual PDF distributions. Accordingly, the powder patter/ the PDF is best calculated by the simulation of many individual crystals, whose individual powder diffraction pattern are calculated by use of the Debye formalism, respectively, whose individual PDFs are averaged. In this presentation, a refinement algorithm that uses an evolutionary approach is presented. It allows to refine arbitrary disorder models and – for nanoparticles - arbitrary particles shapes. Besides disorder parameters, parameters that define a disorder distribution such as the size of nanoparticles can equally be refined.

As an example, the structure refinement of nanoparticles is discussed. Data were collected at the high energy beamline BW5, HASYLAB, Germany at 15K to Q_{max} = 25 Å^{-1}, and transformed to the corresponding PDF. The CdSe/ZnS core/shell particles were simulated with an elliptical CdSe core and semi-spherical ZnS shell particles, which were placed in a locally epitaxial position onto the CdSe core. Both structures were simulated as Zincblende/Wurtzite disordered structures. The refinement allows to determine structure and defect structure of the core and shell, the size and shape of the core, and the size distribution of the shell particles.

[1] R.B. Neder, V.I. Korsunskiy, Ch. Chory, G. Müller, A. Hofmann, S. Dembski, Ch. Graf and E. Rühl, phys.stat. sol. (c) **4**, 3221-3233

[2] F. Niederdraenk, K. Seufert, P. Luczak, S.K. Kulkarni, Ch. Chory, R.B. Neder and Ch. Kumpf, phys.stat. sol. (c) **4**, 3234-3243

[3] R.B. Neder and Th. Proffen, Diffuse Scattering and Defect Structure Simulation, Oxford University Press, in press

11:30 Oral

Local atomic dynamics by the Dynamic PDF method

Wojtek Dmowski[1], Takeshi Egami[1,2]

1. *University of Tennessee (UTK), Knoxville, TN, United States*
2. *Oak Ridge National Laboratory (ORNL), One bethel Valley Road, Oak Ridge, TN 37932, United States*

e-mail: wdmowski@utk.edu

Advanced neutron facilities allow use of the pair distribution function to study new aspects of local atomic structure and even dynamics. In this presentation we will describe application of the dynamic pair distribution function (D-PDF) to the study of localized atomic dynamics in a disordered relaxor ferroelectric Pb(Mg1/3Nb2/3)O3 (PMN). Lattice dynamics is usually studied by examining phonon dispersion. However, there are special cases when the phonons are localized, and phonon dispersions are ill defined. Recently, we have introduced a new approach using a Dynamic PDF (D-PDF) that overcomes this limitation. The dynamic structure factor S(Q,w) of a powder sample is measured using a time-of-flight inelastic neutron spectrometer, and then Fourier transformation over Q is performed to obtain G(r,w) or D-PDF. In our study of PMN the D-PDF was determined at various temperatures by
pulsed neutron inelastic scattering using the Pharos spectrometer of the Los Alamos Lujan Center. The D-PDF succeeded in characterizing the onset of local dynamic polarization at the Burns temperature, and its freezing at lower temperatures. We had shown that local dynamic polarization resulted in the formation of polar nano-regions and relaxor behavior. The local polarization was observed via D-PDF as a dynamic off-centering of Pb ions. Also, we measured D-PDF for a polycrystalline Ni to demonstrate the principle of the D-PDF. We observed that D-PDF captured high symmetry, non-dispersive phonons near the Van Hove singularity. Figure 1 shows the D-PDF for a polycrystalline Ni at 300K (W. Dmowski et. al,PRL 100, 137602, 2008)

This work was supported by the NSF grant DMR06-02876 and by the U.S. DOE under DE-AC05-00OR-22725.

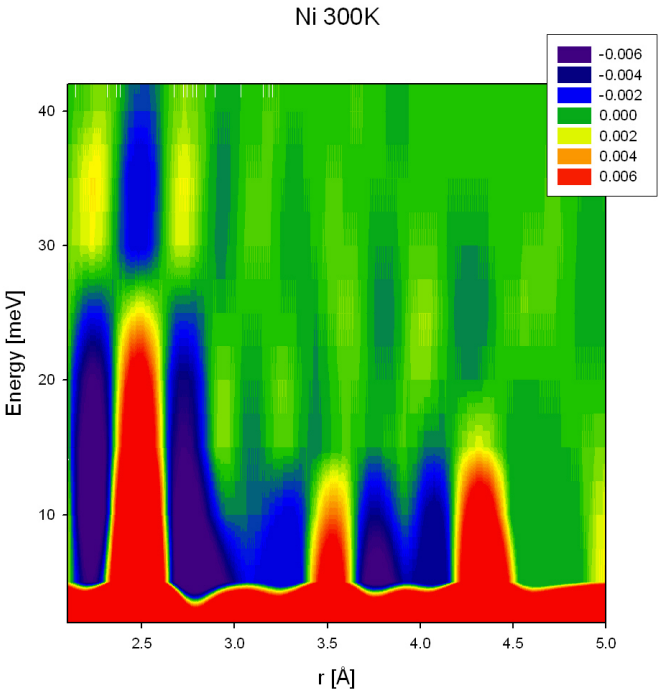

11:45 Oral

Pair distribution studies of ion-exchanged α-zirconium phosphate

Jennifer E. Readman, Victoria A. Burnell, Joseph A. Hriljac

School of Chemistry, University of Birmingham, Edgbaston, Birmingham B152TT, United Kingdom

e-mail: j.e.readman.1@bham.ac.uk

There has been a considerable amount of interest in the ion-exchange properties of layered zirconium phosphates [1-2]. This in-

terest has been renewed due to potential application in the remediation of nuclear waste and in particular for the uptake of Sr, Co and Cs nucleotides. The majority of the ion-exchange work in the literature was carried out several decades ago and little structural characterisation was undertaken [1-2]. In order for these materials to have a potential use in the nuclear waste industry it is imperative that the exchanged ions are tightly bound to the framework and therefore knowledge of their locations from structure solution plays an important role.

Here we present powder diffraction studies of hydrothermally synthesised crystalline α-zirconium phosphate ($Zr(HPO_4)_2 \cdot H_2O$) and its subsequent ion-exchange products with various monovalent and divalent cations, including Sr^{2+}, Na^{+}, Cs^{+} and Co^{2+}. The structure of α-zirconium phosphate consists of phosphate layers with water molecules located between [3]. When cation exchange occurs, the entering cation exchanges for a proton from the HPO_4 group. In some cases ion-exchange leads to a decrease in symmetry [4] and in other cases there is also a decrease in crystallinity. Traditional Rietveld methods have so far proved unsuccessful in the structure solution of these materials. Therefore attention has been turned to total scattering methods and the use of real space Pair distribution function analysis (PDF) [5-6]. The use of differential PDFs to aid cation location and structure solution will be discussed. Particular attention will be paid to the fully strontium exchanged material $ZrSr(PO_4)_2 \cdot xH_2O$, the PDF of which is shown below. The effects of ion-exchange temperature, pH etc. on the resulting PDFs will be discussed.

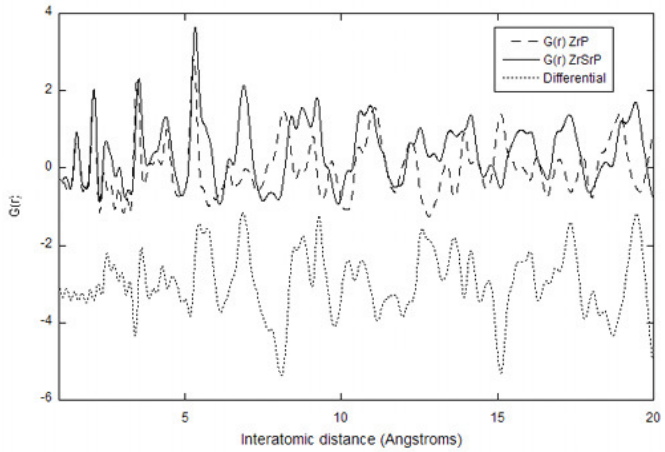

Figure: Pair distribution functions of α-zirconium phosphate, Sr^{2+} exchanged α-zirconium phosphate and the resulting differential.

References:

[1] A. Clearfield and U. Costantino*, Comprehensive Supramolecular Chemistry,***7**, 107, (1996).

[2] G. Alberti, *Acc. Chem. Res.,***11**, 163, (1978).

[3] A. Clearfield and G. D. Smith, *Inorg. Chem.,***8**, 431, (1969).

[4] D. M. Poojary and A. Clearfield, *Inorg. Chem.,***33**, 3685 (1994).

[5] S. J. L. Billinge, M. G. Kanatzidis, *Chem. Commun.,* 749, (2004).

[6] Th. Proffen and S. J. L. Billinge, *J. Appl. Crystallogr,.***32**, 572 (1999).

Microsymposium 6

Programme

Sunday, 21 September

Stress and texture analysis
Sunday morning, 21 September, 10:00
Lecture Hall II
Chair: Udo Welzel, Karen Pantleon

10:05 Oral

Problems related to near surface stress analysis by means of diffraction methods – comparison of angle- and energy-dispersive techniques

Ingwer A. Denks

Hahn-Meitner-Institute (HMI), Glienicker Str. 100, Berlin D-14109, Germany

e-mail: denks@hmi.de

Using X-ray diffraction techniques residual stress analysis (RSA) on polycrystalline material can be classified in two different methods in respect of data acquisition. The widely-used angle-dispersive (AD) method is based on scanning the Bragg angle to obtain diffraction lines in discrete positions on the 2q-scale. On the other hand, applying the energy-dispersive (ED) approach, complete energy diffraction spectra containing a multitude of diffraction lines are recorded under fixed geometrical conditions.

Both techniques are complementary, however they have their specific field of application. AD-RSA experiments being usually performed in the lab with X-rays between about 5 keV and 17 keV, are sensitive within a small surface layer of some 10 µm and therefore, well-suited for the detection of very steep residual stress gradients generated, for example, in thin films. ED-RSA using high energy photons up to 100 keV and more allow for higher penetration depths of some hundred microns, which is the transition zone between the biaxial surface and the triaxial volume stress state in the bulk of the material.

An important consequence, which follows from the different data acquisition modes concerns the information being available from AD- and ED diffraction, respectively. ED experiments with the objective of the depth resolved analysis of residual stress gradients benefit from the different energies of the individual diffraction lines $E(hkl)$ in the recorded spectrum, since each line derives from another average information depth. This additional parameter can be used to apply and advance various methods such as the 'Multi-wavelength method', the 'Universal-plot method' or the 'Scattering vector method' developed for the AD mode to the ED case of diffraction.
Stress depth profiling on the basis of the $\sin^2\psi$ measuring technique first of all yields the Laplace transform s(t) of the actual (real space) residual stress distributions s(z). The latter have to be evaluated by means of the inverse Laplace transform, which is a difficult procedure leading often to unsatisfactory results. In this respect ED diffraction opens up new prospects for direct residual stress depth scanning in the real space. The idea behind it is to carry out a quasi $\sin^2\psi$-measurement within a fixed elongated gauge volume which is aligned parallel to the sample surface. Application of this technique to multilayer systems reveals the residual stresses within buried sublayers in a depth resolution of approximately 10 µm.

10:30 Oral

Interdiffusion and stress development in thin film Ni-Cu diffusion couples

Jianfeng Sheng, Udo S. Welzel, Eric J. Mittemeijer

Max Planck Institute for Metals Research (MPI-MF), Heisenbergstrasse 3, Stuttgart 70569, Germany

e-mail: sheng@mf.mpg.de

Thin film Ni-Cu diffusion couples (individual layer thicknesses: 50nm) have been prepared by DC-magnetron sputtering on silicon substrates coated with amorphous inter-layers (Si_3N_4). The microstructural development and the stress evolution during diffusion annealing have been investigated employing *ex-situ* and *in-situ* X-ray diffraction, transmission electron microscopy and Auger-electron spectroscopy (in combination with sputter-depth profiling).
Annealing at relatively low temperatures (175°C to 350°C) for durations up to about 100 hours results in considerable diffusional intermixing. The stress changes in the bilayer system during heating and isothermal annealing have been investigated employing *ex-situ* and, in particular, *in-situ* X-ray diffraction stress measurements and have been compared to corresponding results obtained for single layers of the components in the Ni-Cu bilayers system, produced under conditions identical to those employed for the sublayers of the diffusion couple. The specific residual stresses that develop due to diffusion between the (sub)layers in the bilayer could then be identified by comparing the stress evolutions upon annealing of the single layers with those recorded for the sublayers of the bilayer. The obtained stress data are discussed in terms of possible mechanisms of stress generation.

10:50 Oral

MTEX - method, numerics, and software toolbox for texture analysis

Helmut Schaeben[1], Ralf Hielscher[2]

1. *Technische Universitaet Bergakademie Freiberg, Mathematische Geologie und Geoinformatik, Bernhard-von-Cotta Str. 2, Freiberg D-09599, Germany* **2.** *Helmholtz Zentrum Muenchen, Ingolstaedter Landstrasse 1, Neuherberg 85764, Germany*

e-mail: schaeben@geo.tu-freiberg.de

A novel method for the estimation of an orientation density function (odf) from diffraction pole figures is presented which is especially well suited for sharp textures and high spatial resolution pole figures measured with respect to arbitrarily scattered specimen directions, e.g. with an area detector. The method may be seen as a compromise of the two different approaches to approximate an odf and its pole figures suggested by the Darboux differential equation governing pole figures. Correspondingly, an odf is approximated with kernels which are well localized in spatial and frequency domain, more spe-

cifically with functions which are radially symmetric in spatial domain and with Fourier coefficients which vanish smoothly and sufficiently fast. This approach allows for multi-scale representation of the orientation and the pole density functions, respectively.

The estimated odf is computed as the solution of a minimization problem which is based on a model of the diffraction counts as a Poisson process. The algorithm applies dicretisation with radially symmetric basis functions approximated by finite harmonic series expansions and fast Fourier techniques to guarantee smooth approximation and high performance. An implementation of the algorithm is available as open source Matlab toolbox MTEX. MTEX provides all the properties of the estimated odf as C-coefficients, volume portions, texture index, entropy, etc., which are of interest.

The kernel approach is equally well appropriate to estimate an odf and its characteristic properties from individual orientation measurements by non-parametric density estimation. Choosing the Dirichlet kernel for this estimation, unbiased estimates of the C-coefficients up to any reasonably given finite order may be computed.

MTEX is not only a versatile toolbox for texture analysis and modeling but also provides a unique way to analyse texture based on integral or individual orientation measurements.

11:15 Oral

ECAP of Fe. Experiments and simulations of the in-elbow textures

Raúl E. Bolmaro[1], Javier W. Signorelli, Reny A. Renzetti[2], María José R. Sandim[2], Hugo R. Sandim[2], Maurizio Ferrante[3]

1. *Instituto de Física Rosario (IFIR), Bv. 27 de febrero 210 bis, Rosario 2000, Argentina* **2.** *Departamento de Engenharia de Materiais Escola de Engenharia de Lorena (EEL), Lorena 12600-970, Brazil* **3.** *Departamento de Engenharia de Materiais Universidade Federal de Sao Carlos (UFSCAR), Sao Carlos 13565-905, Brazil*

e-mail: bolmaro@ifir.edu.ar

The study of deformation properties of low carbon steels is of particular interest because of their many technological applications. Obtaining fine grain Fe based materials can be approached by one of the several available Severe Plastic Deformation techniques. The current paper shows experimental data and simulations of the deformation process of Fe samples by Equal Channel Angular Processing. The samples were extruded in a 120 ^{o} channel die either by one or a few passes. The heterogeneity and local development of the deformation on the elbow of the channel has been studied by X-ray measuring and simulation of the texture evolution. The Self Consistent models used for simulation allowed the calculation of the spin of the main texture components which agreed pretty well with the experiments.

11:35 Oral

Analysis of fiber diffraction transmission images using the Rietveld method

Luca Lutterotti[1], Luca Fambri[1], Mauro Bortolotti[2]

1. *Department of Material Engineering and Industrial Tecnology, University of Trento (DIMTI), v. Mesiano 77, Trento 38100, Italy* **2.** *University of California, Earth and Planetary Science Department, Berkeley, CA 94720-4767, United States*

e-mail: luca.lutterotti@ing.unitn.it

The analysis of polymer fibers by diffraction is often carried out using Laue camera and transmission images. The strong texture of the sample can be easily identified qualitatively by this method along with some informations about fiber spread and structure. Quantitative information is more difficult to get, as the material is not a single crystal nor can be approximated by a random or near random powder. With the appropriate tools and methodologies it is possible to analyze quantitatively fiber diffraction images and take advantage of the strong texture to obtain more information on the fiber structure. With this aim standard texture functions and microstructural models have been incorporated in a Rietveld like program to perform a Rietveld fit on this data. Fiber diffraction is collected on a standard Laue camera using an image plate detector in transmission. The camera is equipped with a fiber accessory to align the fibers normal to the x-ray beam. The collected images are transformed into spectra caked out from the center every 5 degrees or less (depending on the texture sharpness) and then analyzed by the Rietveld procedure to refine the fiber texture, the microstructure and the crystal structure. The entire analysis is performed in only one step through the software Maud. The methodology has been applied to industrial fibers of nylon-6, polypropylene obtained either by Bulk Continuous Filament (BCF) and Woven Nonwoven fabrics (WNW), proving to be successful in characterizing the polymers. The texture sharpness obtained by this method correlates very well with the mechanical properties and in addition some insights of the crystal structure have been obtained as well.

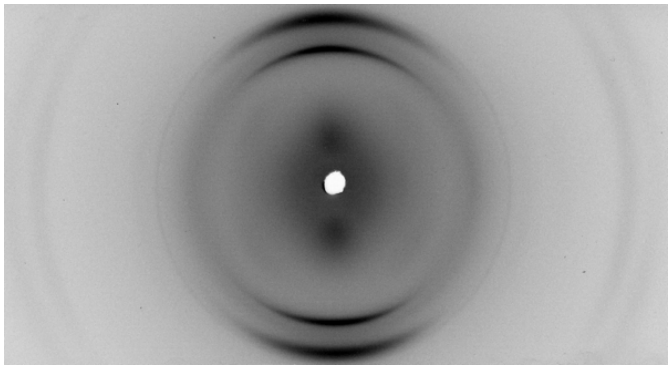

Microsymposium 7

Programme

Sunday, 21 September

Quantitative phase analysis
Sunday afternoon, 21 September, 14:00
Lecture Hall I
Chair: Ian Madsen

14:10 Oral

State-of-the-art and trends in quantitative phase analysis of geological and raw materials

Reinhard Kleeberg

Freiberg University of Mining and Technology, Mineralogical Institute, Brennhausgasse 14, Freiberg 09596, Germany

e-mail: kleeberg@mineral.tu-freiberg.de

Quantitative phase analysis (QPA) develops as a tool for scientific work and research as well as in product or process control and troubleshooting in mining and processing industry. Despite of the long history and early publications about theoretic principles and possible applications of X-ray powder diffraction (XRPD) for this purpose, the accuracy of QPA results is often discussed critically and indeed the level is not yet comparable with that usually reached in the analysis of major chemical elements. This can be shown objectively from the outcomes of inter-laboratory round robin tests. Even if the qualitative composition of mixtures is rather easy and known to the operator, significant errors and uncertainties occur in practice (Rafaja & Valvoda, 1996; Madsen et al., 2001; Scarlett et al., 2002). In the case of complex mixtures containing disordered phases like clay minerals and if the qualitative composition is unknown to the operators, the QPA results can become very inaccurate (Ottner et al., 2000; McCarty, 2002; Kleeberg, 2004). On the other hand, impressive accuracy can be obtained even for complex mixtures by careful application of well known techniques (Kleeberg, 2004; Omotoso et al., 2006). In the field of clay mineralogy, full pattern summation methods and Rietveld based techniques are dominating in the community, often combined with additional information from chemical analysis, microscopy, and mineral separation techniques. Not surprisingly, single line methods tend to perform worse than the full pattern techniques. The great impact of the users experience on the quality of the results can be seen from the very different standings of laboratories using the same software for phase quantification.

As far as the reasons for wrong QPA results can be identified from the participants reports, there seem to be some major groups of sources of errors: (i) inadequate sample preparation, (ii) wrong qualitative phase identification, and (iii) lacking understanding of the principles and weaknesses of the applied technique. In detail, well known problems like microabsorption, preferred orientation, line overlap, and uncertainties about the structural features of the phases seem to be more important than the measurement and data quality. Rietveld based techniques often suffer from convergence into wrong minima by correlation problems, mostly connected with meaningless profile shape parameters and falsified scale factors.

There are some conclusion to be drawn: In order to raise the level of QPA, first of all the basics of the methods as well as the potential sources of error must be taught to the users of the method, as detailed as possible. Combined lectures and workshops will probably the most effective way. Secondly, the developers of software for QPA should try to support the users by more user-friendly programs, stable algorithms, and physically based and tested structure models in the case of Rietveld analysis.

14:40 Oral

Rietveld quantitative phase analyses in iron alloys processed by mechanical alloying method

Hanna J. Krztoń[1], Wirginia J. Pilarczyk[2]

1. *Institute for Ferrous Metallurgy (IMZ), Karola Miarki, Gliwice 44-100, Poland* **2.** *Silesian University of Technology, Institute of Engineering Materials and Biomaterials, ul. Konarskiego 18a, Gliwice 44-100, Poland*

e-mail: hkrzton@imz.pl

Two kinds of iron alloys have been prepared: one set with 6.67wt.% C and second one with 0.4 wt% C. The alloys have been mechanically alloyed in argon atmosphere, using 8000 SPEX CertiPrep Mixer/Mill. The ratio of ball mass to powder mass (BPR) has been 2:1. X-ray powder diffraction has been used to control, up to 150 hours, the results of mechanical alloying, during the process of milling. The measurements have been performed using Philips PW 1140 diffractometer with Co radiation and diffracted beam graphite monochromator. A formation of cementite Fe_3C has been detected in the first group of alloys (Fe-6.67wt.%C) and some fraction of α-Fe has been present up to 150 hours of milling. In alloys of the second group (Fe-0.4wt.% C) only α-Fe has been observed together with amorphous component. Quantitative phase analysis has been applied to follow the changes in powders' constitution after different times of milling. The internal standard procedure has been used to detect and to calculate the fractions of amorphous component in the powders. Corundum $\alpha\text{-}Al_2O_3$ has been added as internal standard. The Rietveld method has been used to determine the fractions of components of the powders, including the amorphous phase. SIROQUANT™ software has been used in calculations.

15:00 Oral

Determination of amorphous contents with internal standards pits and traps

Martin K. Schreyer, Tim White, Stevin S. Pramana, Suo-Hon Lim

Nanyang Technological University, Singapore, Singapore

e-mail: mschreyer@ntu.edu.sg

The determination of amorphous by quantitative Rietveld analysis is in principal a very straightforward procedure: A certain amount of a fully crystalline standard is added and thoroughly mixed with the sample, X-ray powder data are collected and a quantitative Rietveld analysis is performed. The deviation of found and actual weight per-

centages of the standard can be used to compute the amorphous content of the sample. Occasionally, even that last step is already included in the Rietveld software.
However, recent investigations have shown that this method can give misleading results due to several factors which can distort the results. For one thing fully crystalline standards are much harder to obtain than assumed previously. This is best illustrated by the case of the NIST standard SRM676 which was originally assumed to be a fully crystalline material and therefore an ideal internal standard for quantitative Rietveld analysis. As of 2005 NIST admits an amorphous content of approximately 8 % which originally passed unnoticed. More seriously, microabsorption effects have been found to heavily distort the results of quantitative Rietveld analyses. This effect can under ideal circumstances be corrected with the Brindley correction. Usually, however, the premises of the Brindley correction such as spherical particle size and homogeneous particle distribution are not met and employing the Brindley correction may yield even less reliable results than overlooking the microabsorption problem altogether.
We propose to avoid these problems by developing a new set of internal standards based on ultrahard carbides. These materials are well crystalline and show a clear cleavage. Therefore amorphization on grinding is unlikely. By using carbides with a wide range of chemical composition and therefore linear absorption coefficients we aspire to minimize the absorption contrast. On this occasion we will present the first results of this approach to tackle the problems associated with the internal standard method.

15:20 Oral

The effects of particle statistics on quantitative Rietveld analysis of cement

Pamela S. Whitfield[1], Lyndon D. Mitchell[2]

1. *National Research Council Canada, Institute for Chemical Process and Environmental Technology (NRC-ICPET), 1200 Montreal Road, Ottawa K1A0R6, Canada* **2.** *National Research Council Canada, Institute for Research in Construction (NRC-IRC), 1200 Montreal Road, Ottawa K1A0R6, Canada*

e-mail: pamela.whitfield@nrc.gc.ca

Quantitative Rietveld analysis of cements is now a common tool in both industry and research. Many papers analyse cements without any additional sample preparation over and above the grinding carried out by the manufacturer. The particle sizes in cements are usually in the range of 25-40μm, which is much coarser than recommended in texts dealing with particle statistics in diffraction.

Coarse particles will have an effect on the particle statistics and consequently the reproducibility of the relative peak intensities. A systematic study has been undertaken to examine the effect of particle statistics on the results from Rietveld analysis of cements, and the influence of reducing the particle size by micronizing. In addition, the effects of changing divergence slit size and use of sample rotation have been examined.

15:40 Oral

In-situ Diffraction of Time-Resolved Processes: Application of Quantitative Phase Analysis to Large Data Sets

Daniel P. Riley[1], Erich H. Kisi[2]

1. *The Univeristy of Melbourne (UNIMELB), Grattan Street, Melbourne 3052, Australia* **2.** *The University of Newcastle, University Drive, Newcastle 2308, Australia*

e-mail: DRiley@unimelb.edu.au

With the development of high-flux neutron diffractometers (D20, ILL; GEM, ISIS; WOMBAT-HIPD, OPAL) has come the capability for investigating *in-situ* time-resolved processes. This technique may be applied to resolve either reversible (stroboscopic mode) or irreversible (e.g. chemical reactions) processes at time resolutions as low as 80ms (see Figure 1). Developments that have allowed for this research include the design of wide angular acceptance position sensitive detectors (PSDs), rapid data acquisition electronics, customisable reaction chambers, 3-dimensional visualisation programs (e.g. LAMP, ILL) and most importantly Quantitative Phase Analysis (QPA). A remaining challenge for this research is the application of QPA to large data sets; presently a time consuming and potentially inaccurate activity. To place this in perspective, it should be noted that typical *in-situ* investigations produce between 100 – 10000 sequential diffraction patterns, for which independent Rietveld refinements and QPA must be performed. Alternately, attempts at automating these analysis methods often result in inaccuracies in phase quantification at low concentrations and identification of low intensity diffraction features (e.g. superlattice reflections). It is the intended aim to present an overview of QPA as applied to large data sets; detailing limitations of this process and providing examples of relevant research.

Microsymposium 8

Programme

Sunday, 21 September

Combining powder diffraction with other methods
Sunday afternoon, 21 September, 17:30
Lecture Hall I
Chair: Lubomir Smrcok, Marek Wolcyrz

17:35 Oral

Electron diffraction, X-ray powder diffraction, lattice energy minimisation, and pair distribution function analysis to determine the crystal structures of Pigment Yellow 213, $C_{23}H_{21}O_9N_5$

Martin U. Schmidt[1], Stephan Brühne[1], Anette Rech[1], Juergen Bruening[1], Edith Alig[1], Lothar Fink[1], Christian Buchsbaum[1], Alexandra Wolf[1], Jürgen Glinnemann[1], Jacco Van de Streek[1], Fabia Gozzo[2], Michela Brunelli[3], Frank Stowasser[4], Tatiana Gorelik[5], Ute Kolb[5]

1. *Institut für Anorganische und Analytische Chemie, Johann Wolfgang Goethe-Universität, Max-von-Laue-Strasse 7, Frankfurt am Main 60438, Germany* **2.** *Swiss Light Source, Paul Scherrer Institute, Villigen PSI 5232, Switzerland* **3.** *Europen Synchrotron Radiation Facility (ESRF), 6, Jules Horowitz, Grenoble 38000, France* **4.** *Novartis Pharma AG, Basel 4002, Switzerland* **5.** *Johannes Gutenberg Universität, Institut für Physikalische Chemie, Jakob Welder Weg, 11, Mainz 55128, Germany*

e-mail: m.schmidt@chemie.uni-frankfurt.de

Pigment Yellow 213, a commercial azo pigment used for car coatings, exists in a greenish-yellow alpha-phase, and a brown beta-phase. The X-ray powder diagram of the alpha-phase could be indexed in multiple ways, and it was not possible to determine which is the correct one, even by means of LeBail fits with GSAS. Therefore the lattice parameters of the triclinic unit cell were determined by electron diffraction. Lattice energy minimisations were used to predict possible crystal structures, but attempts for subsequent Rietveld refinements were ambiguous. For all calculated structures, electron diffraction patterns were simulated and compared with the experimental electron diffraction intensities, but the correct structure could not be found, since the molecule adopts an unusual conformation which was never observed before, and which was not regarded in the lattice energy minimisations. Finally the crystal structure was solved from laboratory X-ray powder data using real-space methods with TOPAS. A subsequent Rietveld refinement (TOPAS) on synchrotron data converged with a smooth difference curve (Rp = 2.38%, Rwp = 3.12%, chi2 = 1.34). For the first time, pair distribution analyses (PDF) were applied to organic pigments. The PDF analysis of the alpha-phase, based on synchrotron powder data, confirmed the determined crystal structure. The beta-phase is a nanocrystalline powder which does not show any reliable Bragg-peak in the X-ray diffractogram. The PDF analysis of the beta-phase reveal that (1) the beta-phase exhibits a layer structure with a layer distance of about 3.3Å like the alpha-phase, (2) the local structures of the beta-phase is similar to that of the alpha-phase, and (3) the correlation length (i.e. domain size) of the beta-phase is below 5 nm. Thus the PDF method is able extract some information on the crystal structure of this organic compound from the X-ray powder diagram, although the crystallite size is so low and the powder diagram consists of some humps only. In the talk the corresponding methods (Electron diffraction, lattice energy minimisation, and pair distribution function analysis) will be briefly explained.

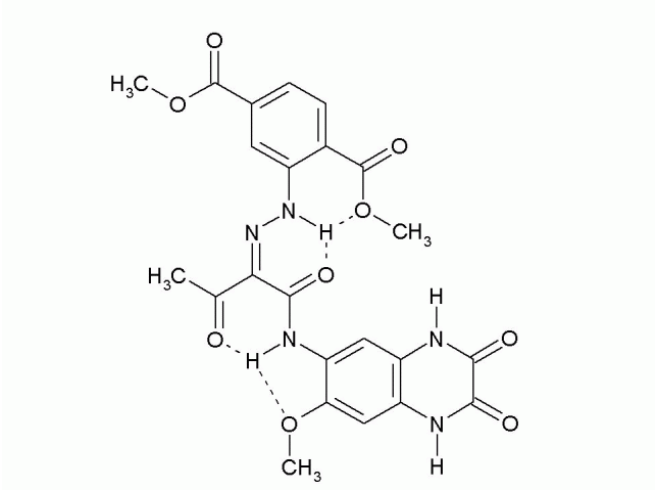

18:00 Oral

Microstructural characterization of lanthanide-doped ceria studied by XRD and TEM

Małgorzata Małecka, Leszek Kępiński

Polish Academy of Sciences, Institute of Low Temperature and Structure Research (INTiBS), Okólna 2, Wrocław 50-422, Poland

e-mail: M.Malecka@int.pan.wroc.pl

Nanocrystalline lanthanide-doped ceria is an important material widely used in catalysis and SOFC technology. Chemical activity of ceria based oxides depend strongly on a kind amount of dopant, which determine also crystal structure and stability of the particles. For low and high dopant concentrations, structures of mixed oxides are more complicated. Addition of trivalent lanthanide ions to ceria (fluorite type structure) causes the oxygen-vacancies formation, which can be arranged in an ordered way to form superstructures.

In this presentation, examples of various superstructures occuring in $Ce_{1-x}Ln_xO_{2-y}$ oxides (Ln - trivalent lanthanide ion) will be presented. X-ray powder diffraction and transmission electron microscopy (together with electron diffraction) are very effective methods often used to characterize such materials. The basic structure of the mixed oxides for given composition can be characterized by powder X-ray diffraction, but superstructure reflections due to oxygen vacancy ordering are usualy very weak and are much easier detected in electron diffraction patterns. High resolution TEM provides additional direct information on the local ordering effects on the nanometer scale.

18:20 Oral

The crystal structure of $(H_3O)Fe(SO_4)_2$

Juraj Majzlan, Cristian E. Botez, Peter Stephens, Boris Kiefer

Univ.Freiburg, Freiburg, Germany

e-mail: Juraj.Majzlan@minpet.uni-freiburg.de

$(H_3O)Fe(SO_4)_2$ is a compound that precipitates from the most acidic solutions in the system Fe_2O_3-SO_3-H_2O. We have solved the structure of this phase from synchrotron powder X-ray diffraction (XRD) data in the space group P-1. The lattice parameters are a = 4.8087(1) Å, b = 8.3180(1) Å, c = 8.3034(1) Å, α = 70.181(1)º, β = 90.276(1)º, and γ = 89.993(1)º. The unit cell volume is 312.44(1) $Å^3$. $(H_3O)Fe(SO_4)_2$ has layered structure in which the layers are built by FeO6 octahedra and SO4 tetrahedra. Three oxygen ions in the SO_4 unit are bridging and provide bonding to the Fe^{3+} ions within the layers. The fourth oxygen ion points into the interlayer space where the H_3O^+ ions are located. The structure of $(H_3O)Fe(SO_4)_2$ belongs to the yavapaiite ($KFe(SO_4)_2$) family of layered structures with octahedral-tetrahedral layers and interlayer cations and can be interpreted as a triclinic distortion of the structures of $CsFe(SO_4)_2$ or $RbFe(SO_4)_2$. The partial refinement (excluding H atoms) was augmented and supported by static ab-initio calculations. The orientation of the hydronium ions and the hydrogen bond scheme was obtained from ab-initio molecular dynamics simulations. These calculations revealed that all hydrogen atoms participate in hydrogen bonding and the hydrogens of the alternating H_3O^+ groups are oriented "up" or "down" toward the Fe-SO_4 layers. The ab-initio molecular dynamic simulations were performed at 300 K for 4.5 ps. The H_3O^+ groups re-arrange their orientation in time.

18:40 Oral

Solving solvents and solvates: structure determination using lab XRPD data and DFT optimisation

Julie Bardin[1], Francesca P. Fabbiani[3], Blair F. Johnston[1], Kenneth Shankland[2], Alastair J. Florence[1]

1. *University of Strathclyde, Strathclyde Institute for Pharmacy and Biomedical Sciences, 27 Taylor Street, Glasgow G40NR, United Kingdom* **2.** *Rutherford Appleton Laboratory (RAL), Chilton, Didcot, Oxon OX11 0QX, United Kingdom* **3.** *Universität Göttingen, GZG, Abteilung Kristallographie, Goldschmidtstr. 1, Gottingen D-37077, Germany*

e-mail: alastair.florence@strath.ac.uk

Crystal structure determination using laboratory X-ray powder diffraction data in combination with global optimisation methods is a powerful approach for accessing structural details in the absence of single crystal samples.[1] That said, the use of additional information to supplement the structure determination process can be of significant value, for example to reduce the conformational search space[2] or confirm the location of hydrogen atoms.[3] Here, we are concerned with determining the solid-state structures of a series of fluorinated ethanols with the aim of studying the molecular packing and hydrogen bonding interactions involving the solvent molecules in both pure solvent and in crystalline solvates. We report the application of geometry optimisation using CASTEP to verify the location of hydrogen atoms in the structures obtained from the simulated annealing runs. The optimised structures provide a more accurate description of the hydrogen bonding interactions in these materials. Polycrystalline samples of the solvents were obtained by cooling a liquid sample held within a glass capillary *in situ* on a Bruker-AXS D8 powder diffractometer. Despite rotating the capillaries during data collection, significant preferred orientation was encountered. Single crystal structures for two of the solvents studied were also obtained using high-P methods.

References

1. K. Shankland, W.I.F. David, L.B. McCusker, Ch. Baerlocher, ed., *Structure Determination from Powder Diffraction Data*, Oxford University Press Inc., New York, 2002.

2. I.J. Bruno, J.C. Cole, M. Kessler, Jie Luo, W.D.S. Motherwell, L.H. Purkis, B.R. Smith, R. Taylor, R. I. Cooper, S. E. Harris, A. G. Orpen, *J. Chem. Inf. Comput. Sci.*, **44**, 2133, 2004

3. C. Platteau, J. Lefebvre, F. Affouard, P. Derollez, *Acta Crystallogr.,* B**60**, 453-460, 2004.

19:05 Oral

In situ simultaneous Raman/X-ray powder diffraction study of transformations occurring at non-ambient conditions

Marco Milanesio[1], Enrico Boccaleri[1], Wouter Van Beek[1,2]

1. *Università degli Studi del Piemonte Orientale (DISTA), Via V. Bellini 25/G., Alessandria 15100, Italy* **2.** *SNBL at the ESRF, Grenoble 38000, France*

e-mail: marco.milanesio@mfn.unipmn.it

Materials containing disordered moieties and/or amorphous or liquid-like phases or showing surface- or defect-related phenomena constitute a problem for their characterization using X-ray powder diffraction (XRPD), and Raman spectroscopy can provide useful complementary information. We have designed and realized a novel experimental set-up [1] for simultaneous in situ Raman/ experiments, to take full advantage of the complementarities of the two techniques in investigating solid-state transformations at non-ambient conditions. The invaluable added value of the proposed experiment is the perfect synchronization of the two probes with the reaction coordinate and the elimination of possible bias caused by different sample holders and conditioning modes used in "in situ but separate" approaches. The set-up was developed by the Swiss-Norwegian Beamline at the European Synchrotron Radiation Facility in Grenoble and tested on three solid-state transformations: i) the kinetics of the solid-state synthesis of the charge-transfer complex fluorene:TCNQ, ii) the thermal swelling of stearate-hydrotalcite nanocomposites, iii) the photoinduced 2+2 cyclization of (E)-furylidenoxindole. The reported experiments demonstrated that, even though the simultaneous Raman/XRPD experiment is more challenging than the separated ones, high-resolution XRPD and Raman data could be collected. A gas blower allows studies from RT to 700K and 100K can be reached using a nitrogen cryostream. The experimental setup flexibility allows the addition of ancillary devices, such as the UV-lamp used to study photoreactivity.

[1] E. Boccaleri, F. Carniato, G. Croce, D. Viterbo, W. van Beek, H.

Emerich and M. Milanesio*, In situ simultaneous Raman/ high-resolution X-ray powder diffraction study of transformations occurring in materials at non-ambient conditions*, *J. Appl. Cryst.*, **2007**, *40*, 684-693.

Microsymposium 9

Programme

Monday, 22 September

Neutron scattering
Monday afternoon, 22 September, 14:00
Lecture Hall II
Chair: Hans Boysen

14:00 Oral

Towards routine refinement of hydrogenous materials by neutron powder diffraction

Paul F. Henry[1], Mark T. Weller[2], Chick C. Wilson[3]

1. *Institut Laue Langevin (ILL), 6 Rue Jules Horowitz, Grenoble, France* **2.** *University of Southampton, Department of Chemistry, Southampton SO17 1BJ, United Kingdom* **3.** *University of Glasgow, Department of Chemistry and WestCHEM research school, Glasgow G128QQ, United Kingdom*

e-mail: henry@ill.fr

Traditionally, the collection of powder neutron data from hydrogenous materials has been considered largely fruitless due to the large, wavelength variable incoherent scattering contribution from hydrogen. This, coupled with relatively low neutron fluxes, has led to disproportionately long counting times for the quality of data collected. Practically, deuteration is often assumed to be a prerequisite for a powder neutron experiment. However, in many cases, deuteration profoundly changes the properties of the material under investigation, leads to the observation of completely different structures and/or phase behaviour or is impossible or incomplete making structural work impossible due to the negative / positive scattering lengths of H / D respectively.

Materials of technological interest in the fuel cell, hydrogen storage, mineral and fast ion-conduction areas are currently hot topics in solid-state materials research. In these materials, the position of the hydrogen and its interaction with the host lattice are of utmost importance to understand the observed physical properties. As the majority of the host materials contain heavy atoms, locating the hydrogen positions and following their evolution using X-ray diffraction techniques, even using the high fluxes of a synchrotron source, is impossible.

With the advent of very-high flux, variable resolution powder neutron diffractometers such as D20 at ILL, GEM and the upgraded HRPD and POLARIS diffractometers at ISIS, WOMBAT at Opal and POWGEN at SNS as well as planned new instruments worldwide, the feasibility of studying hydrogenous materials with powder neutron diffraction needs to be revisited. The power of the currently available instruments will be illustrated using a range of example materials from the ongoing collaborative research and instrumental development programme at ILL.

14:30 Oral

Structure-function relations of novel materials studied at neutron powder diffractometer SPODI

Markus Hoelzel[1,2], Anatoliy Senyshyn[1,2], Norbert Juenke[3], Hans H. Boysen[4], Wolfgang W. Schmahl[4], Helmut Ehrenberg[5], Hartmut Fuess[1]

1. *Technische Universität Darmstadt, Institute of Materials Science, Petersenstr. 23, Darmstadt 64287, Germany* **2.** *Technischen Universität München, Forschungsneutronenquelle FRM-II (FRM2), Garching 85747, Germany* **3.** *Universitaet Goettingen, Institut fuer Physikalische Chemie, Tammanstrasse 6, Goettingen 37077, Germany* **4.** *LMU, Department of Earth and Environmental Sciences, Crystallography, Theresienstr. 41, München 81539, Germany* **5.** *Institute for Complex Materials, IFW Dresden, Helmholtzstrasse 20, Dresden 01069, Germany*

e-mail: markus.hoelzel@frm2.tum.de

In this contribution selected experimental examples are presented which demonstrate some specific advantages of neutron powder diffraction for the investigation of crystal and micro-structures and their impact on the properties of technologically important materials. All experiments have been carried out at the neutron powder diffractometer SPODI (FRMII/Garching, Germany), offering possibilities for high resolution in-situ characterisation under various environmental conditions. The instrument is equipped with 80 position-sensitive ^{3}He detectors of 300 mm active height covering an angular range of 160°. The two-dimensional raw data are treated by a sophisticated data evaluation procedure to obtain diffraction patterns with excellent profile shape. Furthermore, they allow to detect deviations from homogeneous powder particle distributions, in particular preferred orientation effects. Sample environment for in-situ methods include a tensile rig, an apparatus for gas charging over a broad temperature range, a cell for charging/discharging of Li-batteries, etc. The tensile rig (maximum force 100 kN) was used to investigate stress-induced lattice deformations, texture evolution and phase transformations in Ni-Ti shape memory alloys and superelastic alloys. Applying hysteresis loops on Ni-Ti shape memory alloys the texture development and the stress-induced formation of the rhombohedral “R-phase” was studied. The reflection intensity variations at different strain levels could be related to the corresponding twinning/detwinning processes.
Measurements on hydrogen storage materials, especially on sodium alanates ($NaAlD_4$) with different doping elements, have been performed for structure refinement and phase analysis. The studies revealed the effects of the deuterium absorption/desorption cycles on the phase composition. Recently, an apparatus for deuterium loading has been set into operation to follow phase transformations in-situ. Studies on the lithium battery material Li_xCoPO_4 ($0 < x < 1$) revealed the structural changes as a function of the Li-content. The stepwise analysis of the different compositions allowed to determine nuclear as well as magnetic contributions of the appearing phases. In particular, phase compositions, Li occupation numbers and magnetic moments were derived. Recently, first experiments on a lithium battery in operation were carried out successfully. The data are currently analysed.

14:55 Oral

Combining neutron diffraction and and XAS: gap opening through charge disproportionation in $RNiO_3$ perovskites

Marisa Medarde[1], MaríaTeresa Fernández-Díaz[2], Philippe Lacorre3, Claudia Dallera[4], Marco Grioni[5], Joël Mesot[6], María Jesús Martínez-Lope[7], Jose Antonio Alonso[7]

1. *Laboratory for Developments and Methods, Paul Scherrer Institut, Villigen PSI 5232, Switzerland* **2.** *Institut Laue Langevin (ILL), 6 Rue Jules Horowitz, Grenoble, France* **3.** *Laboratoire des Oxydes et Fluorures, Universite du Maine, Le Mans 72085, France* **4.** *INFM, Dipartamento di Fisica, Politecnico de Milano, MILANO 20133, Italy* **5.** *Institut de Physique des Nanostructures, Ecole Polytechnique Fédérale, Lausanne 1015, Switzerland* **6.** *Laboratory for Neutron Scattering, ETH Zürich and Paul Scherrer Institute, Villigen PSI 5232, Switzerland* **7.** *Instituto de Ciencia de Materiales de Madrid, CSIC (ICMM, CSIC), Cantoblanco, Madrid 28049, Spain*

e-mail: marisa.medarde@psi.ch

With the exception of metallic $LaNiO_3$, all the members of the RNiO3 series (R = rare earth and Y) undergo a sharp metal to insulator (M-I) transition at temperatures T_{MI} ranging between 130K (Pr) and 600K (Lu). The mechanism of the gap opening is not yet fully understood and has been a matter of controversy since its discovery in 1991 [1]. Recently, the existence of a symmetry decrease from orthorhombic Pbnm to monoclinic $P2_1/n$ below T_{MI} was reported for the last members of the series (Ho to Lu) and interpreted as signature of an incomplete $2Ni^{3+} ==> Ni^{3+\delta} + Ni^{3-\delta}$ charge disproportionation (CD) with $\delta = 0.3$ [2,3]. This mechanism provided a new framework for the M-I transition and, due to the diamagnetic nature of Ni^{4+}, it could also account for the unusual, non-centrosymmetric magnetic structure displayed by these compounds in the particular case of $\delta = 1$. However, due to the smallness of the associated structural changes, no diffraction studies -even on single crystals- could provide full structure refinements supporting the existence of 2 distinct Ni sites for the first members of the series (Pr to Dy).

In this study we report new, combined ultra-high resolution neutron powder diffraction and x-ray absorption measurements on the full $RNiO_3$ series. In contrast with previous studies, we observe a nearly complete charge disproportionation for the nickelates with small rare earths, as well as a progressive evolution towards a non-disproportionated state moving from Lu ($\delta = 0.8$) to Pr ($\delta = 0.2$) [4,5]. The implications of these results for the stability of the magnetic structure and the eventual existence of ferroelectricity are discussed.

.

[1] P. Lacorre, J.B. Torrance, J. Pannetier, A.I. Nazzal, P.W. Wang, T. Huang and R. Siemens, J. Solid State Chem. 91, 225 (1991).

[2] J.A. Alonso, J.L. García-Muñoz, M.T. Fernández-Díaz, M.A.G. Aranda, M.J. Martínez-Lope and M.T. Casais, PRL 82, 3871 (1999).

[3] J.A. Alonso, M.J. Martínez-Lope, M.T. Casais, J.L. García-Muñoz, M.T. Fernández-Díaz, M.A.G. Aranda, PRB 64, 94102 (2001).

[4] M. Medarde, M.T. Fernández-Díaz and P. Lacorre, submitted to PRL.

[5] M. Medarde, C. Dallera, M. Grioni, J. Mesot, M. Sikora, P. Glatzel, J.A. Alonso and M.J. Martínez-Lope, in preparation.

15:20 Oral

Application of neutron powder diffraction for the study of non-stoichiometric Ni_2MnGa based alloys

Pnina Ari-Gur[2], Giora Kimmel[1], James W. Richardson[3], Ashfia Huq[4]

1. *Institutes for Applied Research, Ben Gurion University of the Negev, Beer-Sheva 84105, Israel* **2.** *Western Michigan University (WMU), Kalamazoo 49008, United States* **3.** *Argonne National Laboratory (ANL), 9700 South Cass Avenue, Argonne, IL 60439, United States* **4.** *Oak Ridge National Laboratory (ORNL), 1 Bethel Valley Rd, Oak Ridge, TN 37831, United States*

e-mail: kimmel@bgu.ac.il

One important group of shape memory alloys is the ferromagnetic Ni_2MnGa. At room temperature, the alloy has a Heusler alloy $L2_1$ type structure. A martensitic phase transition occurs upon cooling. At the stoichiometric composition, the martensitic transformation temperature is below room temperature. Since the magnetic shape memory effect (MSM) occurs in the LT martensitic structure, non-stoichiometric alloys have been developed to enable the MSM effect at ambient conditions. One of the possibilities is the non-stoichiometric $Ni_2Mn_{1+x}Ga_{1-x}$ alloys providing modification of transformation temperature maintaining the Curie point. The deviation from stoichiometry yields non-homogenous materials after casting due to the coring effect. Another problem is that the exchange between Mn and Ga reduces the degree of order which makes neutron diffraction more sensitive to the crystallographic characterization. In this work the crystal structure of several non-stoichiometric polycrystalline alloys were investigated at several temperatures using pulsed neutron source at Argonne National Laboratory. The following parameters were studied: The deviation from stoichiometry; temperature of isothermal heat treatment for homogenization and ordering; cooling rate after homogenization. It was found that the homogenization process at high temperature following by fast cooling is essential in order to obtain single non-stoichiometric phase. There is no indication to B2 to $L1_2$ transition.

15:35 Oral

Investigation of stacking disorder in Li_2SnO_3

Nadezda V. Tarakina[1,2], Tatiana A. Denisova[1], Lidiya G. Maksimova[1], Yana V. Baklanova[1], Alexander P. Tyutyunnik[1], Ivan F. Berger[1], Vladimir G. Zubkov[1], Gustaaf Van Tendeloo[2]

1. *Russian Academy of Sciences, Ural Division, Institute of Solid State Chemistry (ISSC), Pervomaiyskay, 91, Ekaterinburg 620219, Russian Federation* **2.** *University of Antwerp, EMAT, Groenenborgerlaan 171, Antwerp B-2020, Belgium*

e-mail: tarakina@ihim.uran.ru

Depending on the sintering conditions the reactivity of Li_2SnO_3 is different. For Li_2SnO_3 annealed at 700°C the extent of the exchange of Li^+ ions for hydrogen, realized through the formation of $Li_{2-x}H_xSnO_3$, is about x=1.8, whereas for precursors annealed at 900-1100°C $x \leq 0.3$. In order to clear up the origin of this fact, a structural investigation of low-temperature Li_2SnO_3 has been carried out.

A stoichiometric mixture of SnO_2 and Li_2CO_3 (99.9 %) were annealed at temperatures up to 700ºC during 48 h. X-ray and neutron powder data yielded for Li_2SnO_3 the monoclinic unit cell, sp. gr. $C2/c$, parameters: a = 5.3033(2)Å, b = 9.1738(3)Å, c = 10.0195(2)Å, β = 100.042(2)°. In the electron diffraction patterns of Li_2SnO_3 taken along the [100]* direction lines of diffuse scattering have been observed. Random stacking of $LiSn_2O_6$ slabs shifted either over [1/2 0 0] or [1/2 1/6 0] or [0 1/6 0] can cause the appearance of diffuse intensity along c*. In order to check this assumption, simulations of X-ray and neutron powder diffraction data were performed with the DISCUS software package [1]. The best fit with the experimental patterns has been found for the model with a stacking displacement of *ab* planes over [1/2 1/6 0] with a propability of 45%. This displacement, which is equivalent to 120° rotational stacking faults was confirmed by the presence of extra spots on the ED patterns and higher intensities for (0h0), (hhl) and (-hhl) reflection series in the X-ray powder diffraction patterns. Diffraction experiments and DISCUS simulations of defect models reveal two kinds of disorder in this material: domains in *ab* planes and stacking disorder along the c-axis.

[1] Proffen Th., Neder R.B., J. Appl. Crystallogr. 30 (1997) 171-175

This work was supported by the RFBR (grant no. 06-08-00847), by Belgium Science Policy, by the Council for Grants of the President of the Russian Federation for Support of Leading Scientific Schools (grant no. NSh - 1170.2008.3).

Microsymposium 10

Programme

Sunday, 21 September

Time resolved powder diffraction
Sunday afternoon, 21 September, 17:30
Lecture Hall II
Chair: Kristina Edström, Maciej Lorenc

17:40 Oral

Time resolved measurement of the distribution of properties in dynamic systems

Gavin Vaughan

European Synchrotron Radiation Facility (ESRF), Grenoble 38043, France

e-mail: vaughan@esrf.fr

The possibility to measure in situ the temporal evolution of atomic-scale structures under dynamic conditions (i.e., temperature, pressure, strain, chemical potential…) is essential to understand many phenomena of interest to materials science and solid state chemistry. Such experiments are generally carried out using powder diffraction even when very high time resolution are required, or if the samples are amorphous or nanocrystalline. Due to advances in detector technology, powder diffraction data of sufficient quality for quantitative analysis can now be collected with millisecond time resolution [1].

If samples are sufficiently crystalline to separate the contributions of the different component crystallites (which depends on the incident beam size, where sizes down to 100s of nanometers are now achievable) and time resolution of minutes or more is satisfactory, such experiments can be carried out using polycrystalline methods [2]. Such experiments utilize multiple detectors and analytical techniques [3] to simultaneously probe length scales from Ångstoms (crystallography) to mm (sample size) by using multiple detectors. Crystal structure, microstructure, orientation, position and shape can be simultaneously measured for each crystal in polycrystalline samples, giving the actual distribution (rather than just averages) of properties in the sample, as well as the relationships between grains, and the time evolution of these properties.

In this presentation we will describe the techniques currently utilised to extract maximum information in the characteristic time scale appropriate for a given experiment.

[1] J-C Labiche, O Matho, S Pascarelli, MA Newton, G Guilera Ferre, C Curfs, GBM Vaughan, A Homs, *Rev. Sci. Instrum***78** 091301 (2007)

[2] D Juul Jensen, EM Lauridsen, L Margulies, HF Poulsen, S Schmidt, HO Soerensen, GBM Vaughan, *Materials Today***9** 18 (2006)

[3] http://fable.wiki.sourceforge.net/

18:10 Oral

Ultrafast structural dynamics in solids probed by time resolved X-ray diffraction

Faton S. Krasniqi

Swiss Light Source, Paul Scherrer Institute, Villigen PSI 5232, Switzerland Max Planck Institut for Medical Research, Heidelberg 69120, Germany

e-mail: faton.krasniqi@psi.ch

Time resolved x-ray diffraction is an attractive method of studying ultrafast structural dynamics in solids because it can directly observe the small shifts in the interatomic distance associated with the lattice dynamics. The temporal evolution of the measured x-ray diffracted intensity provides insights on the time scale of energy transfer from excited carriers to the lattice. The present talk is concerned with the laser-induced lattice dynamics (coherent acoustic phonons) in solids (InSb) and its signature in the time dependent x-ray diffracted intensity. More specifically, the following questions are addressed: (*i*) How the excitation energy (deposited by the laser pulse) is transferred to the lattice? and (*ii*) How the x-ray transient signal can be understood in frameworks of physical models that describe laser-matter interaction in conjunction with x-ray diffraction theory?

18:40 Oral

Deep restructuring of surface of Pt nanocrystals during strong adsorbate bonding - bridging the pressure gap with in situ diffraction

Zbigniew A. Kaszkur[1], Piotr R. Rzeszotarski[2]

1. *Polish Academy of Sciences, Institute of Physical Chemistry, Kasprzaka 52/56, Warszawa 01-224, Poland* **2.** *Polish Academy of Sciences, Institute of Physical Chemistry, Kasprzaka 44/52, Warszawa 01-224, Poland*

e-mail: zbig@ichf.edu.pl

Structure of a catalyst surface subjected to industrial catalytic processes may differ significantly from the surface of a single-crystal exposed to a low pressure (10^{-5}mbar) of adsorbate, as studied via surface science techniques. Lack of a suitable experimental methods enabling in situ insight into atomistic structure of the real catalyst surface in normal conditions of reaction is usually described as a pressure gap in heterogeneous catalysis. Majority of studies concern single crystals and so the conclusions drawn from them. This illustrates another gap- so called materials gap in catalysis.

Contrary to a common belief, a carefully designed in situ XRD experiment, when guided by atomistic simulations can provide data on atomistic structure of a surface layer of platinum nanoclusters. Even the adsorption process for a strongly bonded adsorbate can be monitored and interpreted, providing data that are not accessible from other technique.

Chemisorption of NO, CO and O_2 under pressure of 1 bar causes deep restructuring of surface of Pt nanocrystals supported on amorphous silica. The effect on the diffracted intensity is analogous to amorphisation of a few surface Pt layers. Diffraction peaks of Pt on exposition to NO, CO and O_2 shift at various degree to lower

angles due to surface relaxation affecting the overall lattice constant - the effect being particle size-dependent. Experiments at room temperature and at 100 deg.C shows various desorption rate in He atmosphere of preadsorbed hydrogen. A molecular model of the surface phenomena based on diffraction experiments and literature data is proposed.

19:00 Oral

Powder diffraction on a Pilatus 100K pixel detector

Bernd Hinrichsen[1], Lutz Bruegemann[1], Petr Salficky[2]

1. *Bruker-AXS (BAXS), Östliche Rheinbrückenstr. 49, Karlsruhe D-76187, Germany* **2.** *Dectris Ltd., Villigen PSI 5232, Switzerland*

e-mail: bernd.hinrichsen@bureker-axs.de

Area detectors are well established in powder diffraction, especially for *in-situ* experiments of high temporal resolution, micro-diffraction or pair distribution function data collections. Commonly gas filled detectors in laboratory equipment, or image plates at synchrotrons are used for such experiments. New solid state pixel detectors such as the Pilatus range developed at the Swiss Light Source, Villingen have now become commercially available. With readout rates of up to 200Hz and nearly perfect efficiency below 20keV this detector sets new standards in the field.

Experiments have been made on the Pilatus 100K detector on a laboratory system. As the detector was originally designed for single crystal data collection it has a considerable pixel size of 172²µm². The achievable resolution was therefore of special interest. The final quality of the pattern was surprising, and is compared to commonly used point and linear detectors.

Extracting such Rietveld quality data from a highly tilted area detector is challenging. A method for refining the detector orientation from such a small section of the diffraction space is presented.

19:20 Oral

Time resolved in situ studies of Li-ion batteries

Torbjörn Gustafsson[1], Maria J. Aragón Algarra[2]

1. *Uppsala University, Department of Materials Chemistry, Angstrom Laboratory, Uppsala, Sweden* **2.** *Departamento de Química Inorgánica, Edificio C3, Campus de Rabanales, Cordoba 14071, Spain*

e-mail: torbjorn.gustafsson@mkem.uu.se

Laptop computers and mobile phones are today powered by rechargeable Li-ion batteries. In order to reach new applications like power tools, hybrid vehicles and load levelling systems for the electrical grid, new electrode materials are developed for these batteries. A number of properties like specific energy and power, cycle-ability, safety, cost and environmental friendliness are essential to optimise. X-ray diffraction plays an important role in this work. Identification of main phases and impurities during synthesis development and rationalisation of electrochemical properties in terms of structural properties are but two examples of this.

In situ diffraction on electrochemical cells is commonly used to follow the phase evolution during lithiation and delithiation of electrode materials for Li-ion batteries.

Different designs of electrochemical *in situ* cells are used today, all with their own merits. It should be noted, however, that for studies of electrochemical systems far from equilibrium conditions, e.g. during fast charge or discharge, the *in situ* cell should mimic the "real battery" as well as possible, if the results from the *in situ* studies should be applied in the design of "real batteries". Electrode composition, layer thicknesses, diffusion paths and packing materials are essential parameters for the non-equilibrium behavior of an electrochemical cell.

Batteries in hybrid electric vehicles work within a limited charge window (e.g. 30 – 70% state of charge) and under high power conditions.

$LiFePO_4$ is a most promising candidate for the cathode material in future hybrid vehicle batteries. We have studied the non-equilibrium of this material in an *in situ* set up based on "coffee bag" cells at the beam line I911-5 at MAXlab in Lund, Sweden. The material was charged and discharged in less than ten minutes with 90% capacity retention in potential step experiments, without any deterioration of the diffraction pattern. Results from other materials studied with the same *in situ* set up will also be presented.

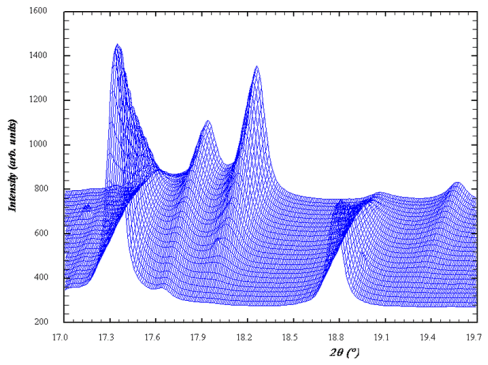

Fig1. Evoltion of the diffraction pattern from a $LiFePO_4$ electrode during fast discharge.

Microsymposium 11

Programme

Sunday, 21 September

Powder diffraction on proteins
Sunday afternoon, 21 September, 14:00
Lecture Hall II
Chair: Irene Margiolaki, Robert Von Dreele

14:05 Oral

MAD techniques applied to powder data: The method of the joint probability distribution functions

Carmelo Giacovazzo[1,3], Angela Altomare[1], Maria Cristina Burla[2], Gaetano Campi[1], Cuocci Corrado[1], Benny Danilo Belviso[1], Fabia Gozzo[4], Moliterni Anna Grazia[1], Giampiero Polidori[2], Rizzi Rosanna[1]

1. *CNR-Istituto di Cristallografia (IC), via Amendola 122/O, Bari 70126, Italy* **2.** *Università di Perugia, Dip. di Scienze dellla Terra, Perugia 06100, Italy* **3.** *Università di Bari, Dip. Geomineralogico, Bari 70125, Italy* **4.** *Swiss Light Source, Paul Scherrer Institute, Villigen PSI 5232, Switzerland*

e-mail: carmelo.giacovazzo@ic.cnr.it

The method of joint probability distribution functions has been applied to powder data to find the anomalous scatterer substructure. The method needs two wavelength data: the conclusive formulas provide estimates of the substructure structure factors, from which the anomalous scatterer positions should be found by Patterson or Direct Methods. The theory has been applied to two compounds. The crystal structure of the first, trans-dichlorido-diacetate-ammine-(1-adamantylamine) Pt(IV), C14 H26 N2 O4 Cl2 Pt was unknown: we used Pt as anomalous scatterer. The crystal structure of the second, Iron(II) phthalocyanine bis (pyridine), C32 H16 N8 Fe (C5 H5 N)2, was known: we used Fe as anomalous scatterer. Both the two substructures were correctly located.
The method of joint probability distribution of structure factors has been re-formulated to phase the full structure reflections, given the substructure. The phases so obtained resulted carefully estimated, thus leading to the solution of the (unsolved) first test structure and to confirm the solved one.

14:40 Oral

Macromolecular powder diffraction: Structure solution via molecular replacement

Jennifer A. Doebbler, Robert Von Dreele

Argonne National Laboratory (ANL), 9700 South Cass Avenue, Argonne, IL 60439, United States

e-mail: doebbler@aps.anl.gov

Macromolecular powder diffraction, though still in its nascence, is ideally suited for cases where no suitable single crystals are available. In the past seven years, the viability of the approach for several protein structures has been demonstrated. Among these initial powder studies, molecular replacement solutions of insulin and turkey lysozyme, themselves, into alternate space groups were accomplished by Von Dreele, *et al.*, and Margiolaki, *et al.*, respectively. The first molecular replacement of an unknown protein structure, the SH3 domain of ponsin, was executed by Margiolaki, *et al.*, which helped move the technique into uncharted territory.
To demonstrate that cross-species molecular replacement of larger structures is feasible, we present the solution of hen egg white lysozyme using the 60% identical human lysozyme (PDB code: 1LZ1) as the search model. We have used extracted intensities from five data sets taken at different salt concentrations in a multi-pattern Pawley refinement, in an effort to reduce the impact of overlaps. We also present a full-scale multi-species analysis, which demonstrates the reliability of the technique. Extension to higher molecular weight structures, to test the limit of this technique is ongoing.
Use of the APS was supported by the DOE/OS/BES under contract number W-31-109-ENG-38

15:05 Oral

Successful Cryocooling of Protein Microcrystalline Samples for Powder Diffraction

Yves Watier[1], Jonathan P. Wright, Irene Margiolaki[1], Andy Fitch[1], Mathias Norrman[2], Gerd Schluckebier[2]

1. *European Synchrotron Radiation Facility (ESRF), Grenoble 38043, France* **2.** *Novo Nordisk AS, Copenhagen 00000, Denmark*

e-mail: watier@esrf.fr

Modern developments of the powder diffraction technique have allowed the investigation of systems with large unit cells as proteins [1]. Protein powder specimens consist of a large number of randomly oriented diffracting micro-crystals. These micro-crystals are usually formed rapidly by batch crystallization. Frequently, the resolution and quality of the data is limited mainly by rapid deterioration of the protein crystal structure during exposure to the intense synchrotron X-ray beam. In a typical single crystal diffraction experiment radiation damage can be minimized by collecting diffraction data at cryocooled conditions (typically 100K) which requires the addition of a cryoprotecting agent to the protein sample in order to avoid freezing of the mother liquor. In this study, we succeeded in obtaining various cryocooled samples of human insulin at 100K avoiding ice formation. Powder diffraction data were collected at both room temperature and cryocooled conditions (ID31, ESRF, Grenoble, France). As expected both the cryoprotectant and the sample container have a remarkable impact on the data quality. Significant variation of the lattice parameters and peak widths with the type and concentration of cryoprotecting agent has already been observed and will be presented for the case of insulin. Preliminary data interpretation correlating these changes with the structural and microstructural characteristics of the systems under study will be shown.

[1] Margiolaki, I. & Wight, J. P. Acta Cryst. (2008). A64, 169-180

Microsymposium 12

Programme

Monday, 22 September

Instrumentation: synchrotron, neutron and laboratory
Monday morning, 22 September, 10:00
Lecture Hall II
Chair: Andy Fitch, Fabia Gozzo

10:05 Oral

New powder diffraction beamline (BL-I11) at Diamond

Chiu C. Tang, Stephen P. Thompson, Julia E. Parker

Diamond Light Source, Science Dept., Harwell Science and Innovation Campus, Chilton Didcot OX110DE, United Kingdom

e-mail: c.c.tang@diamond.ac.uk

We present the new synchrotron beamline (BL-I11) at Diamond Light Source (DLS) which is a dedicated powder diffraction instrument. The beamline receives an intense and highly collimated X-ray beam generated by an in-vacuum undulator. With the simple optics (a double-crystal monochromator, harmonic rejection mirrors and slits), a high purity beam of low energy-bandpass X-rays in the range 5-30 keV is delivered at the sample. The heavy duty diffraction instrument is designed to have the flexibility to house a variety of sample environments and to have two detection systems to collect high quality diffraction data, i.e. multi-analysing crystals for high angular resolution experiments and a fast position sensitive detector for time-resolved studies. When fully operational, BL-I11 will be a powerful state-of-the-art dedicated user facility for high resolution (d-space and time) diffraction studies of polycrystalline materials under ambient and non-ambient conditions. As the facility has very recently become operational offering the high resolution (angular) mode, the beam performance characteristics measured during the commissioning phase are presented. In addition, the first results obtained from real sample(s) are given to show the capability of this new instrument.

10:35 Oral

Diffracted-beam analyzer with multiple single crystals for high resolution parallel-beam X-ray diffraction

Hideo Toraya

Rigaku Co., Tokyo 196-8666, Japan

e-mail: toraya@rigaku.co.jp

A single-crystal analyzer is one of the best choices as an X-ray optical device for obtaining high angular resolution and low background intensities in powder and thin-film diffraction experiments. Highest performances regarding the angular resolution and intensities can be obtained when a single-crystal analyzer is coupled with a parallel-beam geometry. In synchrotron radiation (SR) experiments, a high brilliance parallel beam can be obtained from undulator or even bending magnet light sources. A single-crystal analyzer has been commonly used for diffractometer scans at many beam-lines at SR facilities worldwide. Intensity gains in high-angular-resolution and high-speed experiments at several SR facilities around the world have been further multiplied by using multiple-detector systems, each of which consists of several perfect crystal analyzers. With a laboratory X-ray source, diffracted intensities from a single-crystal analyzer are lower than those from a SR source. A popular way to improve high diffraction intensities is to use a rotating anode generator and/or a graded multi-layer mirror. Another way may be the use of a multiple-detector system similar to those presently used in several SR facilities. However, the latter choice makes the diffractometer system more complex and also very expensive.

In the present study, a new high-performance diffracted-beam analyzer consisting of several perfect crystals in a simple and compact device is proposed to increase the diffracted intensities by one order of magnitude compared to those of a single-crystal analyzer. It is commonly believed that an analyzer with high angular resolution cannot be used together with one- or higher-dimension detectors. In this presentation, a new technique using a diffracted-beam analyzer with multiple single crystals together with a one-dimensional silicon strip detector will be presented.

10:55 Oral

Advantages and disadvantages of fast XRPD measurement by using image-plate and rotating anode source

Giora Kimmel, Dmitry Mogilyanski

Institutes for Applied Research, Ben Gurion University of the Negev, Beer-Sheva 84105, Israel

e-mail: kimmel@bgu.ac.il

An image-plate detector performs simultaneous charge accumulation providing fast data collection. A high resolution Guinier image-plate camera was installed on a rotating anode source. This configuration enables fast measurement with high resolution. There are some differences between the Guinier image-plate camera (GIP) and the conventional Bragg-Brentano diffractometer (BBD). The GIP works in transmission mode with a constant focusing circle. The monochromator is attached to the source providing $K\alpha_1$ radiation. There is no background cut. The range of the scattering angles 2θ is from 1 to 100°. The BBD works in back reflection mode with multiple focusing circles. The monochromator attached to the detector cuts $K\beta$ and most of the background but without diminishing of $K\alpha_2$. The range of the scattering angles 2θ is between 0.5 and 158°. In the standard measurement procedure there are also differences in the sample loading and measurement. In GIP a thin layer of powder is loaded and the illuminated area and depth are equal for the entire 2θ range. In BBD the sample is loaded in a cavity and the illuminated area and depth are changing throughout the 2θ range. As a final point, the counting principles in GIP and BBD are totally different. Data were collected from several samples in both GIP and BBD. Most of the samples were high quality powders of well known solids like LaB_6, ZnO, α Al_2O_3, CeO_2, NIST standards, WC. More complicated structures were studied such as monoclinic HfO_2 and ZrO_2. The crystal structure characteristics including cell parameters and

atomic positions were compared. In addition, quantitative analysis was performed for mixtures of corundum and zirconia, in order to compare the results of relative phase amounts in both systems. The main tool for the data processing was the Rietveld method.

11:15 Oral

Microfocus solutions for X-ray diffractometry with area detectors

Bernd Hasse[1], Till A. Samtleben[1], Carsten Michaelsen[1], Uwe Preckwinkel[2], Holger Cordes[2], Ning Yang[2]

1. *Incoatec GmbH, Max-Planck-Str. 2, Geesthacht 21502, Germany* **2.** *Bruker Advanced X-ray Solutions (Bruker AXS), 5465 East Cheryl Parkway, Madison, WI 53711-5373, United States*

e-mail: hasse@incoatec.de

The increasing importance of X-ray diffractometry with 2-d detectors has lead to a rising demand for highly intense X-ray sources enabling the analysis of very small and weakly scattering samples in the home laboratory within a reasonable time frame. Therefore, various microfocusing sealed tube X-ray sources with focal spot sizes below 100 µm are now available.

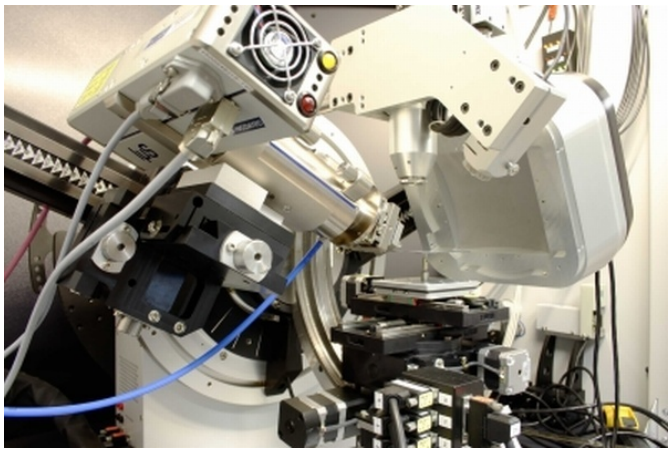

Figure 1: IµS™ for 2-d diffraction, combined with 2D VANTEC-2000 detector

For powder diffractometry IµS™ can be used either in a reflection or transmission set-up as shown in fig. 1, the IµS™ in combination with a Bruker GADDS-system with a VANTEC-2000 detector. In the transmission set-up, a focusing Quazar™ optics was used, which focused the beam into the detector. A measurement of LaB_6 showed an achievable resolution of 0.08°2θ. Measurements of a pharmaceutical powder sample (Ibuprofen) recorded with a typical parallel beam sealed tube set-up and with IµS™ with comparable 0.3 mm collimators showed that the IµS™ delivered 10 times more intensity in an 8 times shorter exposure time. Also, the spottiness of the pattern is much less for the measurement with the IµS™ because the focused beam led to a better crystallite statistics and a larger diffracting sample volume.

We have collected data of outstanding quality in applications such as protein and small molecule crystallography, phase identification, µ-diffraction, screening and small-angle scattering. The presented results demonstrate that we achieve much better data quality in XRD applications with an IµS™ coupled with a 2-d detector in comparison to the common sealed tube systems.

11:35 Oral

Optimizations in neutron powder diffraction by using divergent beam geometries in angular dispersive techniques

Alexandra Buchsteiner, Norbert Stüßer

Hahn-Meitner-Institute (HMI), Glienicker Str. 100, Berlin D-14109, Germany

e-mail: buchsteiner@hmi.de

Angular dispersive powder diffractometers define their beam divergencies by Soller type collimators. The collimators, the take-off angle at the monochromator and its mosaicity define basically the instrument performance, especially the shape of the resolution function. Changes of the instrument configuration are usually done only for different measurements of a diffraction pattern but not during a single run where the instrument configuration is generally fixed. Thus the instrument is optimized only for a certain angular range.
In order to circumvent these kinds of limitations we have developed a new type of collimator whose lamella distances can be adjusted independently at both sides of the collimator.
This allows the adjustment of the collimation as well as of the resolution function and the intensities by using focusing geometry according to the specific requirements of the experiment. Working in focusing mode can also improve significantly the resolution function in the complete angular range during a single pattern measurement by continuously adapting the collimator openings.
With these new possibilities we were able to measure powder diffraction patterns which have a high quality for structure analysis by Rietveld refinement concerning resolution, intensity and peak shapes.
We present data from the neutron powder diffractometer E6 at the Hahn-Meitner-Institut in Berlin which demonstrate the excellent advantages of the new type of collimator. Monte Carlo simulation data support the outstanding instrument setting and allow further optimization and upgrades of the instrument.

Microsymposium 13

Programme

Monday, 22 September

Challenges of nanomaterials
Monday afternoon, 22 September, 14:00
Lecture Hall I
Chair: Reinhard Neder

14:00 Oral

Total Scattering: A 'complete' structural fingerprint of nanoparticles

Thomas Proffen

Los Alamos National Laboratory (LANL), Los Alamos, NM 87545, United States

e-mail: tproffen@lanl.gov

Determination of the atomic structure is mainly based on the measurement of *Bragg intensities* and yields the *average* structure of the infinite crystalline material. However, this approach ignores any defects or local structural deviations that manifest themselves as *diffuse scattering*. It also fails in case of disordered materials, badly crystalline such as many nano-materials, or not crystalline at all, such as glasses. In some cases crystalline and amorphous phases coexist making the traditional crystallographic structure refinement difficult or incomplete. The total scattering pattern or the derived atomic pair distribution function (PDF), however, contains structural information over all length scales [1] and can be used to obtain a complete structural picture of complex materials.

One of the great advantaged of the PDF is the fact that one can limit the range on atom-atom distance over which the structural model is refined. Focusing on small distances up to a few Angstroms will illuminate the local structure where as refinements over a wide range will yield the medium and long range structure. It is interesting to consider, that instruments such as the high resolution neutron powder diffractometer NPDF located at the Lujan Neutron Scattering Center at Los Alamos National Laboratory allows the measurement of PDFs up to distances in excess of 200Å or 20nm. As a result one can obtain a 'complete' structural fingerprint of nanoparticles that are frequently smaller in size as demonstrated in a recent study of gold nanoparticles [2].

[1] Th. Proffen, S.J.L. Billinge, T. Egami and D. Louca, *Z. Krist.***218**, 132-143 (2003).

[2] K.L. Page, Th. Proffen, H. Terrones, M. Terrones, L. Lee, Y. Yang, S. Stemmer, R. Seshadri and A.K. Cheetham, *Chem. Phys. Lett.***393**, 385-388 (2004).

14:25 Oral

The Debye equation: Powder diffraction patterns directly from atom clusters. What we can really do and when it is convenient.

Antonio Cervellino[1], Antonella Guagliardi[2], Cinzia Giannini[2]

1. *Swiss Light Source, Paul Scherrer Institute, Villigen PSI 5232, Switzerland* **2.** *CNR-Istituto di Cristallografia (IC), via Amendola 122/O, Bari 70126, Italy*

e-mail: antonio.cervellino@psi.ch

The classical way of computing powder diffraction patterns is the Bragg approach, where the atomic structure of the material is intrinsically supposed to be periodic and extended to the whole space. These conditions (that can be relaxed somehow) allow to work directly in reciprocal space. The alternative is to use the Debye equation, that makes no hypothesis on the atomic structure periodicity and on its spatial extension. One sees clearly that the latter is particularly suited for nanomaterials, where one (and often both) conditions fail. The computation of a powder diffraction pattern via Debye equation involves all interatomic vector lengths; these are of order N2, where N is the number of atoms. This is clearly impossible except in few cases. However, a careful analysis shows that it is possible to proceed in two stages - first encoding the interatomic distance vectors in a sampled linear density (PDF) and then evaluating the diffraction pattern from the latter. The second stage is especially fast (order N1/3 + special FFT[1]) allowing to evaluate a full pattern in μs times. The first stage i) can be easily prototyped and it is therefore seldom required (once-over for a structure type), ii) it can be carefully tailored on the specific regularities of the system, and doing so we can lower its complexity to the order of N to N4/3. Using special methods we can also encode continuous (strain fields, dislocations) and discontinuous (stacking faults, twins) disorder types, described it by suitable statistical parameters. Such disorder forms can be treated in a variational fashion, adding little to the computational load. Therefore the Debye approach becomes suitable to describe real-world nanomaterials without restriction to crystallinity and, exploiting the optimized two-stage method, it becomes computationally effective up to the 100 nm - 108 atom limit. The computing time (first stage) extends to at most hours for the extreme cases, the second stage remains as fast. This covers completely the gap to the region of full validity of the Bragg method. Examples, simulations and applications to real systems [2-6] are shown.

1. J. Comput. Chem. 27 (2006) 995-1008
2. Phys. Rev. B 72 (2005) 035412
3. J. Appl. Crystallogr. 36 (2003) 1148-1158
4. Eur. Phys. J. B 41 (2004) 485-493
5. Nano Letters 6 (2006) 1966-1972
6. Phys. Rev. Lett. 100 (2008) 045502

14:50 Oral

Looking beyond limitations of diffraction methods of structural analysis of nanocrystalline materials

Ewa Grzanka, Svetlana Stelmakh, Stanisław Gierlotka, Bogdan F. Palosz

Polish Academy of Sciences, Institute of High Pressure Physics (UNIPRESS), Sokolowska 29/37, Warszawa 01-142, Poland

e-mail: elesk@unipress.waw.pl

There is variety of models of a nanocrystal offered in the literature, starting from the assumption that nano-crystal is basically a small single crystal. Usually, however, it is assumed that nanocrystals have a core-shell structure, where interatomic distances at the surface are different than those in the bulk. One might also consider complex models assuming a modulation of the lattice density, what is equivalent to changes of interatomic distances within the particle volume. Such a structure might look like a sequence of tensile followed by compressive strains between the surface and the grain interior. The question is, which model best describes the results of the diffraction data analysis. There are two basic methods of analysis of powder diffraction: reciprocal space analysis, which refers to characteristic Bragg scattering, and real space analysis called atomic Pair Distribution Function analysis (PDF). Both techniques give information on the atomic structure which is, however, a volumetric average of the sample. None of those techniques is capable of providing a complete, unique description of a nano-crystal, but each has a unique capabilities with respect to information about the structure. An analysis made in "reciprocal space", which refers to a unit cell and is based on examination of characteristic Bragg-type scattering, is sensitive directly to the long range-atomic order. If needed, structural refinement, e.g. with application of the Rietveld refinement software, is being done. In this case the diffuse scattering is ignored. Analysis made in "real space", which provides information on the length and abundance of interatomic distances between pairs of atoms, is based on examination of the total scattering (this includes both characteristic Bragg reflections and diffuse scattering underneath the Bragg peaks) and thus, in principle, provides information on every single atom present in the sample. The problem is that there are no simple (straightforward) methods which would allow to link specific interatomic distances to different structural components of the sample. In our case, it is impossible to find out in which part of the sample volume, the core or the surface, given interatomic distances occur. Neither real- nor reciprocal space analysis alone is well suited for nano-crystallography. The best approach encompasses a combination of both techniques, with extraction of consistent information derived from both methods. That may be a very effective searching tool for a unique model of nanocrystals. In this work we discuss various models of nanograins and compare the effects that specific structures have on Bragg scattering and on interatomic distances (determined with PDF analysis).

15:15 Oral

Possibilities of X-ray diffractometric methods by study of ultrafine-grained and nanostructured metal materials

Margarita Isaenkova, Yuriy Perlovich, Vladimir Fesenko, Olga Krymskaya

Moscow Engineering Physics Institute (MEPhI), Kashirskoe shosse, Moscow 115409, Russian Federation

e-mail: isamarg@mail.ru

By the present boom in the field of ultrafine-grained and nanostructured metal materials it is meant that there are reliable experimental methods, allowing to classify all materials from the standpoint of their grain size. However, the real situation is more complicated and requires additional methodical elaborations. When studying deformed metal materials, coherent domains and separate grains practically can not be distinguished by the X-ray line profile, since in both cases we deal with fragments of undistorted crystalline lattice, though differing in boundaries with neighbors. Methods, based on the X-ray line profile analysis, give the direct information on the size of coherent domains, but allow only indirect judgments concerning the size of grains in deformed metal materials. The profile of X-ray line (hkl), obtained by the standard geometry of diffractometric measurement, characterizes only some group of reflecting grains, corresponding to the single texture component, which in the general case can be insignificant and non-representative. Advantages of the new method of generalized pole figures (GPF) by X-ray certification of the material condition are considered. The GPF method includes reconstruction of profiles of the same X-ray line (hkl) for grains of all possible orientations and characterizes textured metal materials by distributions of substructure parameters instead of their single values.

In the case of metal materials with FCC or BCC crystalline lattice these distributions characterize relative fractions ν of axes <hkl>, along which the corresponding substructure parameter is equal to that or another value. In the case of metal materials with HCP lattice the similar histograms, constructed by X-ray reflections from basal planes (0001), show distributions of volume fractions ν of grains, characterized by different values of substructure parameters, measured along basal axes.

The most effective X-ray method to ascertain formation of ultrafine-grained or nanostructured condition under SPD bases on the quantitative texture analysis. Operation of crystallographic deformation mechanisms (slip and twinning) results in regular grain reorientation and development of textures, depending on the used deformation scheme. Since crystallographic deformation mechanisms can not operate in nano-dimensional grains, the alternative non-crystallographic mechanism of grain slippage along boundaries becomes active and results in their accidental rotations as well as in scattering of texture maxima. Measurement of this scattering and relative estimation of volume fractions, deformed by means of crystallographic and non-crystallographic mechanisms, characterizes the structure condition of material under SPD. The consideration is illustrated by numerous results, obtained by X-ray studies of SPD metal materials.

15:30 Oral

X-ray analysis of nanoscale Pt_3Co/C electrocatalysts for the low-temperature fuell cell

Igor N. Leontyev, Alexey S. Mikheykin, Andrey V. Guterman, Elena V. Pahomova

Southern Federal University (SFU), Zorge 5, Rostov-on-Don 344090, Russian Federation

e-mail: i.leontiev@rambler.ru

The composite materials containing platinum nanoparticles deposited onto carbon support are most promising electrocatalysts for the low-temperature fuel cells. However, pure Pt catalysts exhibit degradation during the operation of fuel cells as well as propensity to agglomeration of catalysts particles making their application rather difficult. These problems can be solved by using Pt alloys with Co, Ni, etc. The purpose of the present work is investigation of structural and microstructural parameters of Pt_3Co/C catalysts.

The investigated Pt_3Co/C electrocatalysts were prepared onto a high surface area carbon powder (Timrex HSAG-300) by chemical reduction of the precursors using $NaBH_4$ [1]. The water/ethyleneglycol ratio in the solvent was 1:5, 1:1 and 5:1. For estimation of corrosion and aggregate stability, as prepared samples were treated in 1M H_2SO_4 at 80^{o}C for 1 h. X-ray diffraction measurements were carried out at SNBL ESRF.

The analysis of X-ray powder patterns of all samples has shown following: 1) the average particle size *D* of synthesized Pt_3Co/C samples vary from 3 up to 4,9 nm; 2) increasing of concentration of an organic component in the solvent causes decreasing of the average particle size; 2) particle size increases by 0,8-1 nm and grain size distribution (GSD) become wider after treatment by solution H_2SO_4; 4) the narrowest GSD is observed at 1:5 ratio of the solvent; 5) the lattice parameter as a function of particle size shows nonlinear dependence both for untreated and treated by H_2SO_4 solution samples.

Increasing of anisotropic line broadening with increasing of grain size was observed for all samples studied. Nonequivalent size of particles along different crystallographic directions is the reasons of the observed behavior. The analysis of roentgenograms by means of FullProf has allowed to determine the typical shape of Pt_3Co catalyst nanoparticle. Figure illustrates SEM image (left) and shape determined from X-ray diffraction pattern (right)

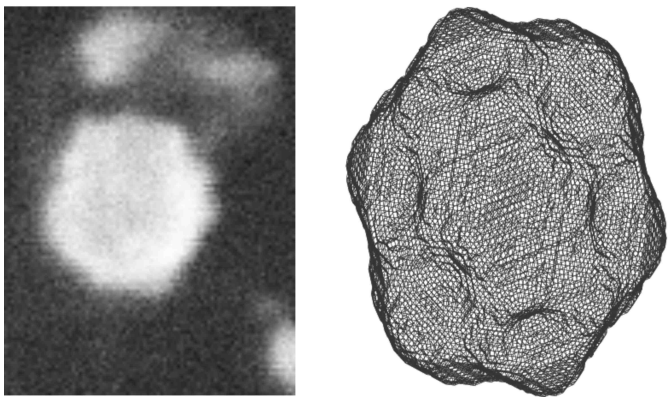

1. F.H.B. Lima et al. / Electrochimica Acta 52 (2006) 385–393

15:45 Oral

New method for detailed X-ray diffraction analysis of p6mm ordered mesoporous silicas

Stanisław Pikus

Faculty of Chemistry, Maria Curie Sklodowska University (UMCS), pl. Marii Curie Sklodowskiej 3, Lublin 20-031, Poland

e-mail: stanpik1@wp.pl

The discovery of ordered mesoporous silicas (OMSs) opened a new and rapidly growing field of modern science and technology, expanding the range of periodic porous materials into the mesopore region. The structure of the majority of OMS shows a long range ordering of amorphous elements, which can be studied by powder X-ray diffraction (XRD) and small angle X-ray scattering (SAXS) methods. On the other hand, the XRD/SAXS studies of these materials are not easy because the standard crystallographic procedures cannot be used for their characterization due to the lack of ordering at the atomic level. Various OMSs have been synthesized ranging from 2D hexagonal *p6mm* (MCM-41, SBA-15), 3D hexagonal *P6$_3$/mmc* (SBA-12), and cubic *Ia3d* (MCM-48), *Im3m* (SBA-16), *Fm3m* (FDU-1) structures to lamellar phases (MCM-50). The XRD/SAXS patterns for these OMSs contain small number of peaks (often about 3-5). They are located in the range of low angles (2q below 5^o) because of the presence of relatively large ordered pores. A major breakthrough in OMSs synthesis area was the synthesis of polymer templated OMSs (by using , for example, triblock copolymer – $PEO_{20}PPO_{70}PEO_{20}$) , namely SBA-15, which became very popular material because of larger mesopores, thicker pore walls and higher hydrothermal stability in comparison to his surfactant templated analogue, MCM-41. The XRD/SAXS patterns for the aforementioned ordered mesostructures often exhibit four or more reflections, the most intensive one, 100 peak, and three less intensive peaks, 110, 200, 210. So far, analysis of these patterns was usually limited for the evaluation of the unit cell parameter and the identification of the observed peaks. The value of unit cell parameter in combination with adsorption data provide information about the pore size and pore wall thickness.

In this work an attempt to analyze the XRD/SAXS patterns by including not only the position of observed peaks but also their intensity are presented.

On the basis of the XRD/SAXS structure modeling of the 110/200 intensity ratio in relation to the pore width/unit cell ratio the new method for estimating the pore width and pore wall thickness are presented [1]. The comparative analysis of results obtained by proposed new method and modified KJS method [2] was made.

Obtained results for many MCM-41 and SBA-15 samples (even with organic group in skeleton) indicated that the pore widths estimated on the basis of the theoretical 110/200 intensity curve for cylindrically-shaped mesopores agree well with these obtained by improved KJS methods. This result indicates that the theoretical dependence of the 110/220 intensity ratio on the pore width/unit cell ratio obtained by assuming cylindrical shape of channels in SBA-15 or hexagonal prism in MCM-41 may be used for a quick estimation of the pore widths of these materials.

[1] Pikus S., Solovyov L.A, Kozak M., Jaroniec M., Appl. Surf. Sci,

(2007), 253,5682

[2]Jaroniec M., Solovyov L.A., Langmuir, (2006), 22, 6757.

Microsymposium 14

Programme

Monday, 22 September

Non ambient conditions: phase transitions/ transformations
Monday morning, 22 September, 10:00
Lecture Hall I
Chair: Robert Dinnebier

10:00 Oral

The high pressure crystal structure of the NLO compound BiB_3O_6 from 2D powder diffraction data

Robert E. Dinnebier[1], Bernd Hinrichsen[2], Alistair Lennie[3], Martin Jansen[1]

1. *Max-Planck-Institut FKF, Heisenbergstr. 1, Stuttgart D70569, Germany* **2.** *Bruker-AXS (BAXS), Östliche Rheinbrückenstr. 49, Karlsruhe D-76187, Germany* **3.** *Daresbury Laboratory (DL), Daresbury, Warrington WA4 4AD, United Kingdom*

e-mail: r.dinnebier@fkf.mpg.de

Our recently proposed method for automatic detection, calibration and evaluation of Debye-Scherrer ellipses using pattern recognition techniques and advanced signal filtering[1] was applied to 2D powder diffraction data of the non-ferroelectric, acentric NLO compound α-BiB_3O_6 in dependence on pressure. The measurements were performed at station 9.5HPT at Daresbury. At ambient conditions, BiB_3O_6 crystallizes in space group *C*2. In the pressure range between P = 6.09 and P = 6.86 GPa, it exhibits a first order phase transition into a structure with space group B1 (phase II at P = 7.3 GPa: a=7.0228 Å, b=6.6671 Å, c=4.2019 Å, α=114.54°, β=95.00°, and γ=90.28°) (Fig. 1). A non-linear compression behavior over the entire pressure range is observed, which can be described by two Vinet relations in the ranges from P = 0. to 6.09 GPa, and from P = 6.86 to 11.6 GPa. The extrapolated bulk moduli of the high-pressure phases were determined to K0 = 38(1) GPa for phase I, and K0 = 114(10) GPa for phase II. The crystal structures of both phases are refined against X-ray powder diffraction data measured at several pressures between 0.0 and 11.6 GPa. The structural phase transition of α- BiB3O6 is mainly characterized by a reorientation of the BO_3 triangles and BO_4 tetrahedra, in order to optimize crystal packing. With increasing pressure, the lone pair which is localized at Bi^{3+} increasingly adopts pure s-character.

[1] B. Hinrichsen, R. E. Dinnebier , H. Liu, M. Jansen, Getting the maximum information out of 2D powder diffraction data: The high pressure crystal structures of tin sulfate (SnSO4), 2008, Z. Kristallo-

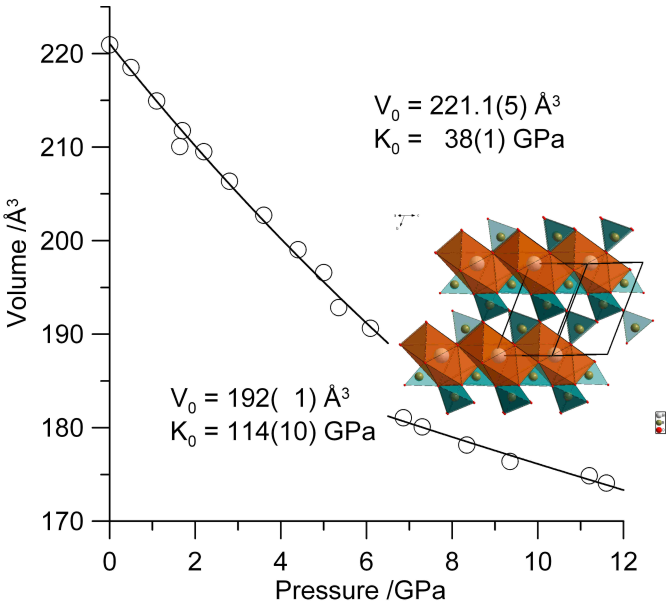

Fig. 1: Volume as a function of pressure for BiB_3O_6. The new high pressure crystal structure of BiB_3O_6 at p= 8 GPa is shown in the inset.

10:20 Oral

High-pressure behaviour of fluorides with fluorite related structures

Andrzej Grzechnik

Dpto. Física Materia Condensada, Universidad del País Vasco (UPV/EHU), Facultad de Ciencia y Tecnología, Apdo. 644, Bilbao 48080, Spain

e-mail: andrzej.grzechnik@ehu.es

In the fluorite CaF_2 structure (Fm-3m, Z = 4), the Ca atoms are surrounded by 8 fluorines at the vertices of a cube while the F atoms are surrounded by 4 Ca atoms to form a tetrahedron. It is the archetypical structure of many difluorides, dioxides, intermetallics, etc. [1-4]. The structural relation is the closest when the cation:anion ratio is equal to 1:2 with a random arrangement of cations or anions. Ordering induces low-symmetry polymorphs. Another type of superstructures is formed due to deficiency in cations or anions.

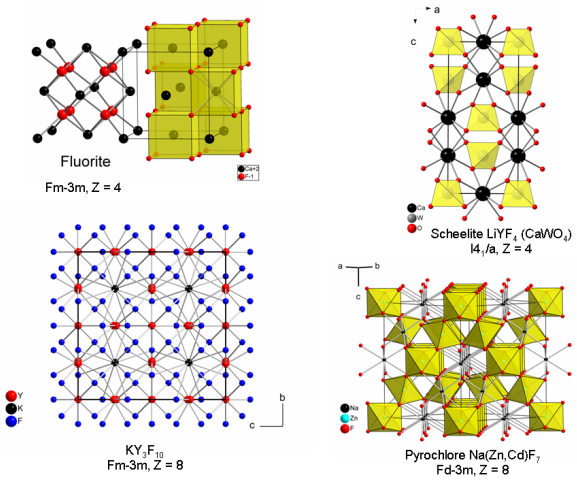

In this contribution, studies on structures, stabilities, and phase transitions of fluorides with fluorite superstructures using x-ray powder diffraction will be presented. The experimental methods include in situ measurements in diamond anvil cells and a Paris-Edinburgh press as well as synthesis in a multi-anvil.

Most of the flurite-related materials are hosts for solid state lasers. Since the optical properties mainly depend on ordering of the cations and their crystalline surrounding, a detailed study of crystal structures as a function of pressure and temperature can provide useful information on their solid state chemistry and additional data for crystal field considerations.
The discussed materials will also include systems that are important for nuclear applications. The use of such systems requires the precise characterization of not only their phase diagrams and the conditions at which they are (un)stable but also their equations of state.

1. D.J.M. Bevan, Acta Cryst. A 36, 889 (1980).
2. A.F. Wells, Structural Inorganic Chemistry, Clarendon Press, Oxford (5th Edition, 1984).
3. B.G. Hyde & S. Andersson, Inorganic Crystal Structures, John Wiley & Sons, New York (1989).
4. V.P. Korsun et al., Russ. J. Inorg. Chem. 52, 613 (2007).

10:40 Oral

Flexibility of a 3D Nickel Oxide skeleton combined with reversible repositioning of Carboxylates and hopping of metals

Nathalie Guillou[1], Carine Livage[1], Nathalie Audebrand[2], Gérard Férey

1. *Lavoisier Institute, CNRS, University of Versailles (ILV), 45 av. des Etats-Unis, Versailles 78035, France* **2.** *University of Rennes, Sciences Chimiques de Rennes, Rennes 35042, France*

e-mail: nathalie.guillou@uvsq.fr

Metal porous hybrids constitute an important new focus of research in material chemistry, offering potential applications in adsorption, catalysis, nonlinear optical devices and magnetic materials. Sorption capacities are often correlated to framework flexibility. Until now, this behaviour has mainly concerned coordination polymers and three-dimensional (3D) metal-oxide frameworks have been considered as rigid.[1] This study deals with the breathing of MIL-77 (labelled MIL-n for Materials of Institut Lavoisier), a nickel(II) glutarate with a 3D inorganic subnetwork. The as-synthesized MIL-77-*as* or $[Ni_{20}(C_5H_6O_4)_{20}(H_2O)_8].40H_2O$, is cubic [S.G.: $P4_332$, a = 16.5812(7) Å, V = 4558.8(6) Å^3] and built up from helices of edge sharing Ni octahedra with water ligands.[2] They generate corrugated 20-membered rings and very large crossing tunnels along [111] which guest water molecules. Their evacuation renders the solid porous but, curiously, this porosity drastically *decreases* after the removal of the water ligands fixed on Ni atoms. To shed light on this porosity loss, we studied dehydration/rehydration processes of MIL-77 and solved the structures from powder diffraction data after removal of guest water molecules [MIL-77-*evac* or $[Ni_{20}(C_5H_6O_4)_{20}(H_2O)_8]$, S.G.: $P4_332$ with a =16.402(2) Å, V = 4412.9(8) Å^3] and ligated ones [MIL-77-*anh* or $[Ni_{24}(C_5H_6O_4)_{24}]$, S.G.: $P4_332$ with a = 15.643(1) Å, V = 3827.8(4) Å^3]. The observed flexibility of the skeleton is very unusual for a 3D oxide framework. More amazing is the reversible hopping of nickel atoms into the voids of the skeleton and the repositioning of some carboxylate groups during the transition, explaining the decrease of porosity (see Fig. 1).

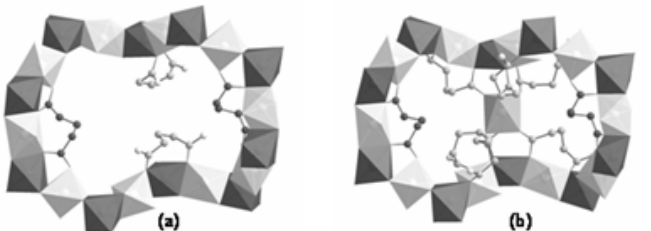

Fig.1: Polyhedral view of the corrugated twenty-membered ring with two independent glutarate ions for MIL-77-*evac* (a) and MIL-77-*anh* (b).

References:

[1] S. Kitagawa, R. Kitaura and S.-I. Noro, *Angew. Chemie Int. Ed.***2004**, *43*, 2334.

[2] N. Guillou, C. Livage, M. Drillon and G. Férey *Angew. Chem. Int. Ed*, **2003**, *42*, 5314.

11:00 Oral

Investigating phase transitions under non ambient conditions using the Incoatec Microfocus Source IμS™

Bernd Hasse[1], Till A. Samtleben[1], Carsten Michaelsen[1], Bernd Hinrichsen[2], Robert E. Dinnebier[3]

1. *Incoatec GmbH, Max-Planck-Str. 2, Geesthacht 21502, Germany* **2.** *Bruker-AXS (BAXS), Östliche Rheinbrückenstr. 49, Karlsruhe D-76187, Germany* **3.** *Max-Planck-Institut FKF, Heisenbergstr. 1, Stuttgart D70569, Germany*

e-mail: hasse@incoatec.de

The new Incoatec Microfocus Source IμS™ with molybdenum anode, a 30 W air cooled sealad tube microfocus X-ray source, with a new type of 2-dim beam shaping Montel optics, the so called Quazar™ optics, was mounted at a mar desktop beamline equipped with mar345 imaging plate detector (figure 1). This setup was used to investigate phase transitions of different samples under high pressure and high temperature. For this purpose a diamond anvil cell or a heater was mounted on the goniometer respectively.

To process the data precise information about the sample to detector distance and the detector orientation is necessary. To receive this information, measurements of the standard LaB_6 were done under the same conditions as the measurements of the samples. The data were processed using the program package Powder3D (Dinnebier et al.) for integration and visualisation.

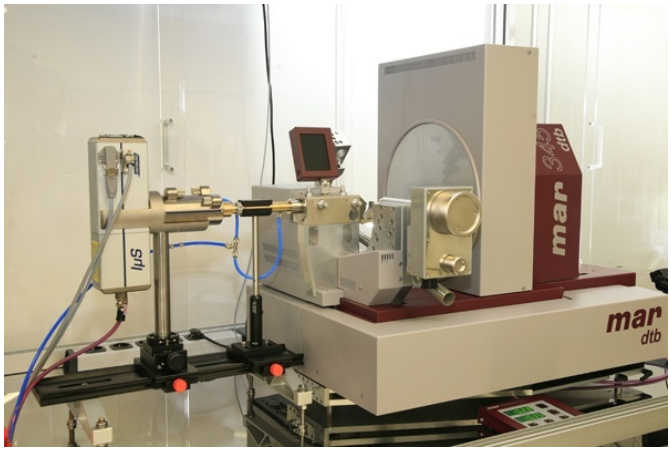

Figure 1: IμS™ for 2-dim diffraction, combined with a mar desktop beamline and mar345 imaging plate detector

11:20 Oral

High-pressure phase transitions in AI_3 (A = Rb, Cs, Tl, NH_4) Triiodides

Joseph A. Hriljac[1], Richard H. Jones[2], Alistair Lennie[3], William G. Marshall[4]

1. *School of Chemistry, University of Birmingham, Edgbaston, Birmingham B152TT, United Kingdom* **2.** *School of Physical and Geographical Sciences, Keele University, Keele ST55BG, United Kingdom* **3.** *Daresbury Laboratory (DL), Daresbury, Warrington WA4 4AD, United Kingdom* **4.** *ISIS Facility, Rutherford Appleton Laboratory (ISIS), Oxon, Chilton Didcot OX110QX, United Kingdom*

e-mail: j.a.hriljac@bham.ac.uk

The high pressure behaviour of molecular diatomic iodine is perhaps one of the most fascinating, with a gradual shortening of the intramolecular I-I contacts until they become near in value to the intermolecular I-I bonding distances. At ~18 GPa metallization occurs[1,2] even though the system remains a molecular solid.[3] With continuing pressure the distances continue to approach a similar value, finally at ~30 GPa the iodine bonds break and an extended monoatomic solid forms.[4] To date, there have been no reports of the high pressure chemistry of related simple polyhalide salts, such as the well known AI_3 (A = Rb, Cs, Tl, NH_4) systems, to explore the possibilities of similar metallisation and/or phase transitions. We have recently collected synchrotron X-ray and neutron powder diffraction data on these materials and observe phase transitions from orthorhombic to trigonal systems at very low pressures, in the range of 0.7-3 GPa. We have solved the structure of the high pressure phase, it is compared to the ambient pressure phase in Figure 1. Although the phase transition does not involve loss of triiodide units, there are drastic changes in the packing of the cations and polyhalides precluding a simple correspondence between the two polymorphs. It also appears that the phases are approaching a simple cubic AX_3 system with the A15 (Cr_3Si) structure type. In this talk, details of the novel high pressure phases and correlations between the nature of the A cation and phase transition pressure and measured bulk moduli will be presented.

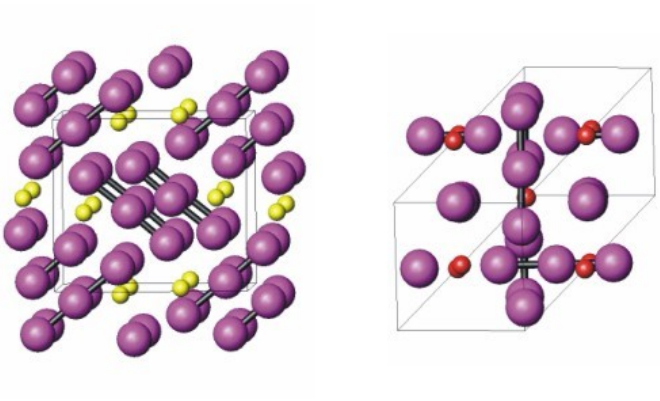

Fig. 1.Views of the ambient (left) and high (right) pressure phases

1. Balchan, A. S. & Drickamer, H., *J. Chem. Phys.***34**, 1948 (1961).
2. Riggleman, B. M. & Drickamer, H. G., *J. Chem. Phys.***38**, 2721 (1963).
3. Shimomura, O. et al., *Phys. Rev. B***18**, 715 (1978).
4. Takemura, K., Minomura, S., Shimomura, O. & Fujii, Y., *Phys. Rev. Lett.***45**, 1881 (1980).

11:40 Oral

Industrial applications of in-situ diffraction

Ian C. Madsen, Nicola V. Scarlett, Matthew R. Rowles

CSIRO Minerals, Melbourne 3168, Australia

e-mail: ian.madsen@csiro.au

Time resolved, *in-situ* diffraction can be of use in the set-up and optimisation of industrial processes by providing direct information about reaction mechanisms and kinetics. This paper will discuss several examples of this type of work which required different experimental set-ups, but which all exploited the mineralogical information (including phase quantification) provided directly by diffraction. It will present the results of both laboratory and synchrotron experiments and discusses the practice and perils of *in-situ* experimentation in general.

The first two examples are hydrometallurgical and use a novel experimental set-up employing a capillary reaction vessel, short wavelength radiation and a position sensitive detector to enable rapid, simultaneous collection of a wide range of diffraction data. The industrial processes examined are (i) the high pressure acid leaching (HPAL) of nickel laterite ores and (ii) the Bayer process for the production of alumina from bauxite. These systems have been examined using both laboratory and synchrotron X-radiation. The third example is a preliminary study into scale formation on the surface of inert anodes within electrochemical cells and utilised the penetrating power of white radiation (synchrotron) energy dispersive diffraction (EDD).

HPAL of nickel laterites

The majority of nickel is refined from sulphide ores but the oxide ores or laterites represent the largest reserves of this metal. HPAL involves leaching of laterites in sulphuric acid under hydrothermal conditions, typically 250°C and 45 atmospheres pressure. Components of the ore are known to undergo rapid changes upon cooling following HPAL thus making examination via traditional post-mortem techniques difficult.

The Bayer process

The Bayer process is used for the production of alumina from bauxite, and involves dissolving the bauxite ore in a caustic solution at temperatures between 150 – 250ºC. The process is complicated by the presence of reactive silica phases, as these also react with the aluminium and sodium to form insoluble scales. Previous studies have concentrated on *ex-situ* studies of the long term evolution of the scales. This work concentrates on the initial formation of the scale phases by examining the systems during reaction rather than after cooling, washing, etc.

Light metal production via inert anodes

Inert anodes are a proposed replacement for traditional carbon anodes in the production of light metals. The advantages of these metal oxide anodes over carbon are twofold: (i) they are not consumed during operation thus replacement is not necessary on the same timescale as carbon and (ii) they emit no greenhouse gases during operation unlike their carbon counterparts. Scale formation on the anode surface during operation can be detrimental to its operation but may actually be favourable if the scale is sufficiently thick to protect the anode but sufficiently thin to allow conduction. It is therefore vital in the development of this potentially important technology that the scale formation be characterised and understood. To date, preliminary examinations have taken place on cycled and cooled cells using white radiation and EDD. Results regarding the measurement of scales in this way will be discussed as will novel methodology for phase quantification of EDD data.

Microsymposium 15

Programme

Monday, 22 September

Powder diffraction in applied research
Monday afternoon, 22 September, 16:30
Lecture Hall I
Chair: Alessandro Gualtieri

16:40 Oral

Archaeometry: Advances with neutron and synchrotron beams

Gilberto Artioli

Dipartimento di Geoscienze, Università di Padova (UNIPD), Via Giotto 1, Padova 35137, Italy

e-mail: gilberto.artioli@unipd.it

Neutron and synchrotron X-rays probes are primary sources for the characterization of materials related to cultural heritage. Their employment in the investigation of materials related to archaeometry and conservation science encompasses imaging, chemical analysis, and crystallographic analysis, including phase identification, texture analysis, and structure and microstructure analysis. In principle, many of these information may be obtained simultaneously in a single combined experiment, thus minimizing neutron or X-rays exposure time and the risks and the costs related to object's handling.

Several trends can be acknowledged at present in the use of large facilities for cultural heritage investigations. On the one hand neutron beams, traditionally linked to neutron activation analysis and autoradiography, are increasingly used for the non-invasive characterization of large and thick objects, mainly for 3D tomographic imaging, phase identification, and crystallographic texture analysis, especially in metals. Synchrotron radiation beams on the other hand are best used for the investigation of matter at the microscale, mostly using microimaging or micromapping techniques. Although penetrating high energy X-rays have been used to probe centimeter-thick objects, the vast majority of the applications related to archaeology or art objects involve the use of XRD and XAS techniques for the identification of material heterogeneities at the micrometer level. Typical examples are the identification of pigmenting materials in paintings, analysis of glazing layers in ceramics, and interpretation of alteration layers in metal and stones.

Several examples of recent applications will be described and discussed.

17:10 Oral

In-situ hydration of activated belite cements studied by synchrotron X-ray powder diffraction

Angeles G. De la Torre[1], Miguel A G. Aranda[1], Antonio J M. Cuberos[1], Maria-Carmen Martin-Sedeño[1], Marco Merlini[2]

1. *Universidad de Malaga (UMA), Campus Teatinos, Malaga E29071, Spain* **2.** *European Synchrotron Radiation Facility (ESRF), Grenoble 38043, France*

e-mail: mgd@uma.es

The reduction of cement industry environmental impact is a challenge for researchers. On average, for every tone of cement produced, 0.97 tons of CO_2 are released into the atmosphere. So, cement industry contributes around 6% of all CO_2 anthropogenic emissions and consequently approximately 4% of the global warming of the planet. Belite cements may reduce 10% de CO_2 emissions but belite reactivity with water is slow and thus these cements develop low mechanical strengths at early stages. The attempts to enhance reactivity of these materials are being carried out by two complementary ways: i) stabilizing high temperature belite polymorphs (α-forms) and ii) producing calcium sulfoaluminate (CSA) belite cements. CSA clinkers contain calcium sulfoaluminate, $Ca_4Al_6O_{12}SO_4$, which reacts rapidly with water forming ettringite, AFt or $Ca_6Al_2(SO_4)_3(OH)_{12.26}H_2O$, and improves the development of early age mechanical strengths. CSA clinker manufacture may reduce CO_2 emissions up to ~35% by replacing some calcite by calcium sulphate(s) in the raw mixtures.
Here, we will report an in-situ synchrotron x-ray powder diffraction study of the hydration of two families of cements: i) belite cements activated using low amounts of alkaline oxides, and ii) CSA cements [nominal composition: 50 wt% of belite, 30 wt% of $Ca_4Al_6O_{12}SO_4$ and 20 wt% of ferrite]. The powder patterns were collected in transmission in BM08 beamline of ESRF using the translating image-plate detector. This methodology minimise powder averaging errors which are critical to obtain accurate phase analyses. All patterns have been analysed by the Rietveld method in order to extract the quantitative phase contents of the reacting mixtures. The water/cement ratio was 0.5. The gypsum role has been investigated by adding different amounts of this phase to cements. The starting crystalline phase assemblage and the evolution of the hydrate phases will be reported and related to the calorimetric studies.

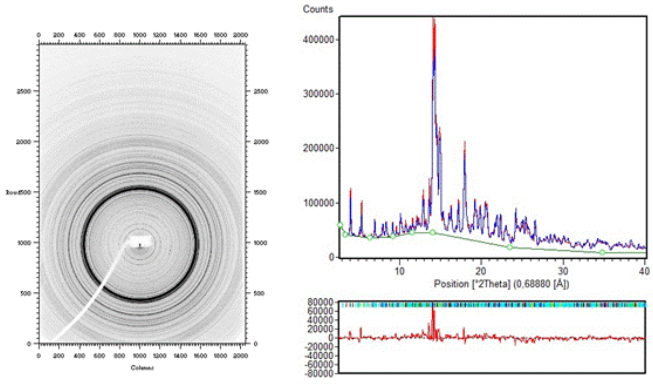

Figure 1. 2D image plate pattern for a belite cement after 9 hours of

hydration (left) and 1D integrated data fitted by the Rietveld method (right).

17:30 Oral

Structural disorder in Li_2FeSiO_4 and Li_2MnSiO_4, potential Li-battery cathode materials

Anton Meden[1], Robert Dominko[2], Marjan Bele[2], Miran Gaberšček[1,2], Janko Jamnik[2]

1. *Faculty of Chemistry and Chemical Technology, Askerceva 5, Ljubljana 1000, Slovenia* **2.** *National Institute of Chemistry (NIC), Hajdrihova 19, Ljubljana SI1000, Slovenia*

e-mail: tone.meden@fkkt.uni-lj.si

The title materials belong to a new class of Li storage materials with high Li ion exchange capacities. They are ismorphous, having an orthorhombic structure with the space group Pmn21 and the unit cell parameters approximately a = 6.27, b = 5.33 and c = 5.01 Å. This can be recognized as an ordered superstructure of a wurtzite prototype, where all cations occupy tetrahedral sites in a heaxgonal closest packing of oxygen anions.

No matter of which syntehsis procedure is used (variations of the Pechini sol-gel method and hydrothermal method were tried) the products are of low crystallinity, having broad peaks in the diffraction patterns [1]. This can be signifinicantly improved by high-temperature-high-pressure (HP-HT) treatment (performed on the Fe analogue), which gives a material with very sharp diffraction peaks. However, the intensities of the diffraction peaks of the as-made and and the HP-HT treated samples differ significantly and the subject of this contribution is to discuss this phenomenon.

Rietveld refinement, using various models on both patterns, showed that the difference is due to a disorder of cations in the as-made sample. While the HP-HT treated material is crystallographically well ordered, the scattering power, located in various interstitial sites of the oxygen packing, lead to the conclusion that two types of disorder are present in the as-made samples: a) exchange of Li and Mn over their primary sites and b) partial migration of Li, Mn and Si to alternate tetrahedral sites in the distorted HCP of oxygen atoms, just over the basal plane of the tetrahedron to the vicinal tetrahedral position, which is empty in the ordered model. The octahedral interstices are empty in all cases – no scattering power was located there.

These structural features play an important role in the electrochemical performance of the title materials. As the octahedral interstices in the HCP are face-sharing, they form channels through which the lithium ions can migrate to and from their tetrahedral sites during the electrochemical discharge-charge process. The presence of the cation disorder also facilitates the extraction-insertion of lithium ions over the empty sites and stabilizes the lithium-deficient state of the material, occurring when the battery is charged.

[1] R. Dominko, M. Bele, M. Gaberšček, M. Remškar, A. Meden, J. Jamnik, *Electrochem. commun.*, 8 (2006) 217-222.

17:50 Oral

Synchrotron X-ray diffraction studies of products of the steel pipe corrosion measured in the native aqueous suspension

Pawel Piszora[1], Jacek Nawrocki[1], Jolanta Darul[1], Waldemar Nowicki[1], Alexander Evans[2]

1. *Adam Mickiewicz University, Faculty of Chemistry, Grunwaldzka 6, Poznań 60-780, Poland* **2.** *European Synchrotron Radiation Facility (ESRF), Grenoble 38043, France*

e-mail: pawel@amu.edu.pl

Corrosion scales play an important role in modifying water quality in drinking water distribution systems. The corrosion scales from steel pipes were analyzed for their structure and composition. The tubercle deposits were collected from pipelines in the distribution systems of a large agglomeration. Scales were studied both before and after drying, and goethite, magnetite and lepidocrocite were identified as the primary constituents of the dried samples. High concentrations of layer double hydroxide (LDH) phases were detected in the samples loaded in diffractometer as a aqueous suspension in native water. Therefore the sample preparation play a key role in X-ray measurements of so labile system.

X-ray powder diffraction data were collected with the high-resolution X-ray powder diffractometer on beamline ID31 at ESRF, selecting X-rays from the white undulator source with wavelengths of 0.41274(6) Å. Small quantities of rust-in-water suspension were ground with a pestle in an agate mortar, and as a paste, introduced into 0.5 mm diameter glass capillaries, mounted on the axis of the diffractometer and spun during measurements. Data were collected for half an hour and normalized against monitor counts and detector efficiencies, and rebinned into steps of $2\theta = 0.001°$. Samples were introduced in a glass capillary for avoiding degradation of the LDH, which is sensitive to the air, but also for minimising the effect of preferential orientation.

Our synchrotron X-ray radiation studies and refinements with Rieveld method enabled to point out important differences between the corrosion products found in several different water distribution systems. The most intrinsic phases of all rust samples were LDH phases. Three of them were identified as iron(II,III) hydroxysalts commonly named green rust, which belong to the family of divalent-trivalent ions minerals, characterised by a crystal structure that consist of the stacking of brucite-like layers carrying a positive charge and layers constituted of anions and water molecules. The structure and composition of green rust depend upon the specific anions they incorporate. Products of biologically induced redox processes are proved as a result of metabolic activity of bacteria and subsequent chemical reactions involving metabolic byproducts. The organisms secrete metabolic products that react with ions or compounds on the pipe surface resulting in the subsequent deposition of mineral particles. Presented results are a part of wider studies needed to establish the role of the transitional corrosion products in the mechanism of a biotic release of iron from corroded pipes.

Acknowledgments

We acknowledge the European Synchrotron Radiation Facility for provision of synchrotron radiation facilities and we would like to

thank Dr Michela Brunelli for assistance in using beamline ID31.

18:10 Oral

X-ray powder diffraction techniques applied to criminal and environmental forensics

Mark D. Raven

CSIRO Land and Water, Waite Rd, Adelaide 5064, Australia

e-mail: Mark.Raven@csiro.au

The application of sophisticated analytical methods to forensic investigations is gaining increased importance due to advances in instrumentation and sampling techniques. Whilst X-ray diffraction (XRD) is a reasonably mature technique it is still of great importance because of its non-destructive nature; often allowing further investigations of the original intact specimens. The major strength of XRD is its ability to identify and interpret crystalline components "directly". XRD can be used to analyse all manner of crystalline materials from crime scenes such as; explosive residues, soil materials, paint chips, adhesive tapes, building materials, minerals, alloys, ceramics, gemstones and drugs. Various sample preparation techniques are employed depending on the quality and quantity of evidence available. Materials can either be analysed undisturbed on the carrier object or removed and analysed separately. Mounting the specimen in the instrument is also dependent on the size and shape of the items being investigated.

Several case studies will be presented outlining aspects of XRD analysis applied to both criminal and environmental forensics. Emphasis will be placed on case investigations where new approaches have been applied to analyse extremely small samples from shoes and clothing, and preparation procedures to obtain representative samples. These case studies will include; pinpointing the location of buried bodies, identifying the source of industrial dust, analysis of bone fragments, and matching soil material from clothing to crime scenes.

Poster Session

Posters

Sunday, 21 September

Reciprocal space methods

MS1 posters
Sunday afternoon, 21 September, 15:30

15:30	Poster	01-01

Rietveld refinement of a wrong crystal structure

Christian Buchsbaum, Martin U. Schmidt

Institut für Anorganische und Analytische Chemie, Johann Wolfgang Goethe-Universität, Max-von-Laue-Strasse 7, Frankfurt am Main 60438, Germany

e-mail: buchsbaum@chemie.uni-frankfurt.de

Generally Rietveld refinements are used to confirm or disprove crystal structures solved from powder diffraction data. If the Rietveld refinement converges with low *R* values and with a smooth difference curve, and the structure looks chemically sensible, one generally believes that the resulting structure is close to the correct crystal structure.

Here a counter example is presented: The Rietveld refinement of the X-ray powder pattern of γ-quinacridone (γ-**1**) with the crystal structure of β-quinacridone (β-**1**) gives a quite smooth difference curve, even though the crystal
structures as well as the powder patterns (Fig. 1) are completely different. The crystal structure from single data shows that in γ-1 molecular chains in a criss-cross pattern are formed; each molecule forms hydrogen bonds to 2 neighbouring molecules. In β-1 the molecules are arranged in chains; each molecule exhibits hydrogen bonds to 4 neighbouring molecules.

The crystal structure from Rietveld refinement looks reasonable in terms of molecular conformation, molecular packing and intermolecular hydrogen bonds. But neither the lattice parameters, nor the molecular packing, nor the conformation of the molecules have any similarity with the actual structure. This example shows, that a successful Rietveld refinement is not always a final proof for the correctness of a crystal structure; in special cases the resulting crystal structure may still be wrong.

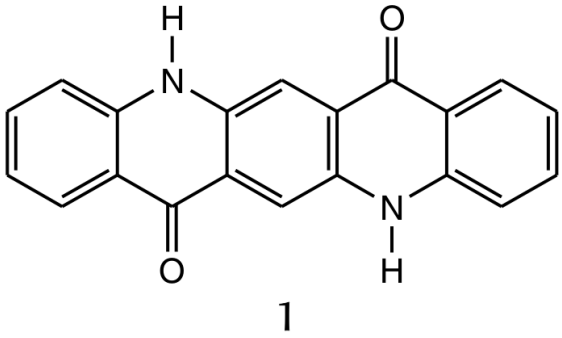

1

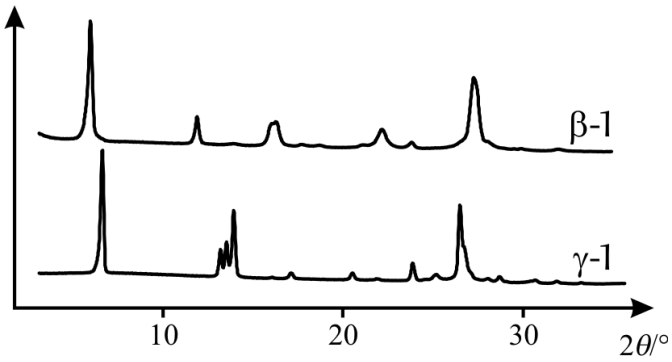

Fig. 1: Powder patterns of β-1 (top) and γ-1 (bottom).

15:30	Poster	01-02

Structural characterization of unsaturated layered metal(II) phosphonates

Aurelio Cabeza[1], Rosario Mercedes P. Colodrero[1], Laura León-Reina[1], Miguel A G. Aranda[1], Konstantinos D. Demadis[2], Gheorghe Ilia[3]

1. *Universidad de Malaga (UMA), Campus Teatinos, Malaga E29071, Spain* **2.** *Chemistry Dpt, Univ. of Crete, PO Box 1527, Heraklion 71409, Greece* **3.** *Institute of Chemistry Timisoara of Romanian Academy, Bdul Mihai Viteazul 24, Timisoara 300223, Romania*

e-mail: aurelio@uma.es

Since 1976, numerous studies have been carried out on layered metal phosphonates due to their potentially useful properties such as ion exchange, catalysis, and heterogeneous catalyst supports [1]. Zn and Cu vinylphosphonates belong to this type of layered materials, where the vinyl groups point toward the interlayer region. However, $Pb(O_3PCH{=}CH_2)$ shows a new 3D porous structure with the vinyl groups projecting into the channels [2]. In all of them, the presence of the vinyl function may be used for coordination of catalytically active species or for investigation of further organic reactions within a confined region. In this respect, the orientation/alignment of the vinyl groups within the structure may have an important effect on the reactivity [3].

In the present work, we report the synthesis and structural characterization of several divalent transition metal phosphonates containing unsaturated groups: $M(O_3PCH{=}CH_2)\cdot H_2O$ (M=Co, Ni and Cd) and

$M(O_3P\text{-}C(C_6H_5)=CH_2)\cdot H_2O$ (M=Co and Cd). These materials have been prepared by hydrothermal procedure and structurally characterized by laboratory X-ray powder diffraction. Dehydration processes in these materials were also studied. Both families of compounds show layered frameworks. $M(O_3PCH=CH_2)\cdot H_2O$ (M=Co, Ni and Cd) compounds crystallize in orthorhombic unit cells and they are isostructural to the reported Zn derivative [1]. $M(O_3P\text{-}C(C_6H_5)=CH_2)\cdot H_2O$ (M=Co and Cd) crystallize in monoclinic unit cells and their crystal structures have been solved following an *ab initio* methodology and refined by the Rietveld method. The attached figure shows the layered structure of cadmium vinylphenylphosphonate. The reactivity of these materials, under UV radiation, will be also reported.

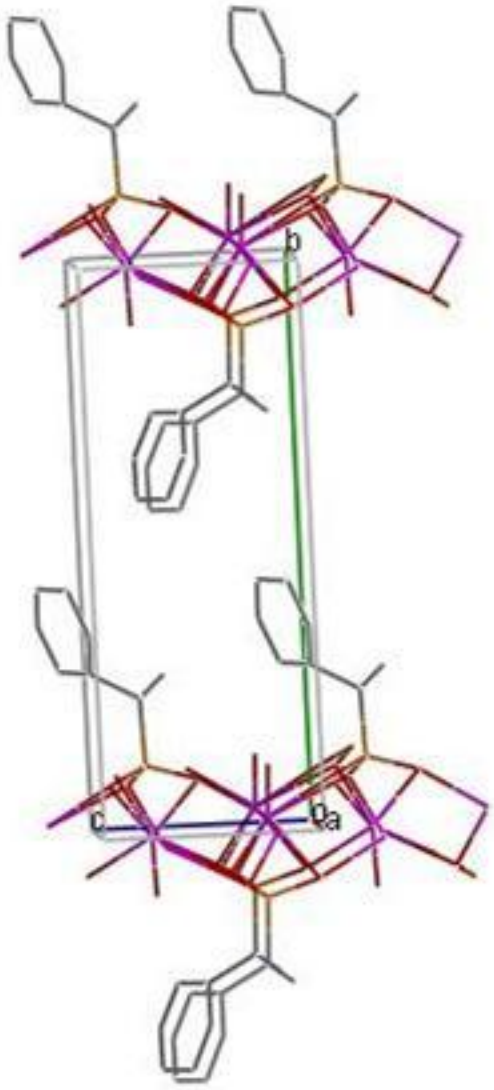

Layered framework of $Cd(O_3P\text{-}C(C_6H_5)=CH_2)\cdot H_2O$

References

[1] D.A. Knight, V. Kim, R.J. Butcher, B.A. Harper and T.L. Schull, J. Chem. Soc., Dalton Trans., 2002, 824-826.

[2] G.B. Hix,A. Turnerm K, Vahter, B.M. Kariuki, Microporous Mesoporous Mater. 2007, 99, 62-69.

[3] B. Menaa, B.M. Kariuki and I.J. Shannon, New J. Chem., 2002, 26, 906-909.

15:30 Poster 01-03

Structure studies of Fe-B-X amorphous and nanocrystalline alloys by Rietveld refinement

Małgorzata Karolus

University of Silesia, Institute of Material Science, Bankowa 12, Katowice 40-007, Poland

e-mail: karolus@us.edu.pl

From the classical point of view the structure of the amorphous materials might be done by the Radial Distribution Function and Pair Distribution Function analyses. In fact the presence of the short-range order in the amorphouse state points to the possibilities of applying the "semi" crystalline model of structure with the crystalline size up to ~10-20 nm. Than it is possible to use the Rietveld method to refining the "hypothetical unit cell" of the amorphous meterial. In this paper there are tested different models of unit cells characteristic for Fe-B-X alloys. The refinement results are compared to the RDF results (coordination radii and numbers). Thanks to applying the Rietveld method to describing the diffusion scattering there is possible to calculate parameters characterizing the searching material as crystallite size, lattice strain, changes of order in material, etc.

15:30 Poster 01-04

New approach to indexing method of powder diffraction patterns using topographs

Ryoko Oishi[1], Masao Yonemura[2], Toru Ishigaki[2], Akinori Hoshikawa[2], Kazuhiro Mori[3], Takahiro Morishima[1], Shuki Torii[1], Takashi Kamiyam[1]

1. *High Energy Accelerator Research Organization (KEK), 1-1, Oho, Tsukuba-city, Ibaraki 3050801, Japan* **2.** *Ibaraki University, Frontier Research Center for Applied Nuclear Sciences, 4-12-1 Nakanarisawa, Hitachi 316-8511, Japan* **3.** *Kyoto University, Kyoto 606-8501, Japan*

e-mail: ryoko.oishi@kek.jp

Indexing of powder diffraction patterns is considered as the most difficult part among the procedures of ab-initio powder structure determination. Recently, we devised a new indexing algorithm that can search rapidly and thoroughly for the possible solutions.

Topograph is a connected tree in the graph theory, which is a collection of relation formula given by Q(h1+h2) + Q(h1-h2) = 2 * (Q(h1) + Q(h2)). Although this formula is already known as Ito's equation and used in Ito's algorithm, it seems to have not yet displayed its real merit. We report on how it is efficient to construct an algorithm that is not affected by the extinction rule.

We proved this algorithm works completely at least for lattices of dimension 2. Although we are trying to extend this to the case of dimension 3, some uncertain part still remains.

Out method does not use any assumptions on Bravais lattice. It is efficient even if there is a false peak in the powder diffraction pattern

or the material is not a single phase.

The detail of the method and some results are introduced.

Thin films, coatings and surfaces

MS2 posters
Sunday afternoon, 21 September, 15:30

15:30	Poster	02-01

Application of position sensitive detectors for in-situ XRD investigations of electrochemical processes

Paul Angerer, Rudolf Mann, Aleksandra Gavrilovic, Werner Artner, Gerhard E. Nauer

ECHEM Kompetenzzentrum für angewandte Elektrochemie (ECHEM), Viktor-Kaplan-Strasse 2, Wiener Neustadt A-2700, Austria

e-mail: paul.angerer@echem.at

In a conventional XRD goniometer device the diffraction intensity is determined consecutively over the diffraction angle range. The development of efficient and highly sensitive image-plate detectors enables the fast and instantaneous recording of the diffraction pattern up to 140° 2θ. In addition a linear position sensitive detector (linear-PSD) with a restricted range of diffraction angle of several degrees enabling high angular resolution was used. These two types of detection instruments were applied for the in-situ study of comparatively rapid electrochemical processes on electrode surfaces at different angle of incidence. The advantages and disadvantages of these detection systems and the related measurement procedures will be discussed in detail. The use of an appropriate in-situ electrochemical cell is essential. The electric potential and current were recorded during the measurement series. The detection of the phase formation especially in the uppermost electrode surface region up to a depth of a few micrometers was achieved by variation of the penetration depth by different angles of incidence. The phase composition in the irradiated region was determined quantitatively during the electrochemical reaction by means of the Rietveld refinement method. However, the observed values are strongly influenced by the layered structure of the sample and by the different absorption coefficients of the phases. Furthermore, the absorption of the diffraction pattern of the electrode material gives information on the absorption properties of the reaction layers. Up to now our studies are focussed on different composed lead electrodes in sulphate containing electrolytes with various additives and the electrodeposition of metals on different substrates.

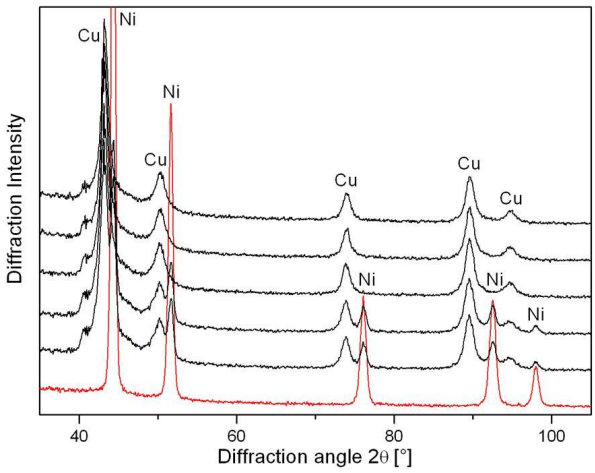

Figure 1: In-situ XRD traces of galvanostatically deposited copper on a nickel substrate with increasing deposition time.

Acknowledgements: This work was supported within the K plus programme by the Austrian Research Promotion Agency and the government of Lower Austria.

15:30	Poster	02-02

Sol-gel derived titania and silica based ceramic thin films for implant coatings - design, preparation and characterization

Justyna Krzak-Roś[1], Agnieszka Baszczuk[1], Anna Łukowiak[1], Mirosław Miller[2]

1. *Wroclaw University of Technology, Institute of Materials Science and Applied Mechanics (PWr - IMMT), Smoluchowskiego 25, Wrocław 50-370, Poland* **2.** *Wrocław University of Technology, Department of Chemistry, Wybrzeże Wyspiańskiego 27, Wrocław 50-370, Poland*

e-mail: agnieszka.baszczuk@pwr.wroc.pl

Sol-gel titania and silica thin films have received a great deal of attention in the area of bioactive surface modification of metallic implants. These materials are believed to give rise to an entirely new generation of bone-bonding materials due to their relative ease of production, ability to form a physically and chemically uniform coating over complex geometric shapes, and their potential to deliver exceptional mechanical properties due to their nanocrystalline structure.

In this work crack-free and uniform nanocrystalline titanium and silica pure oxides and Ca-doped oxides thin films were obtained. These materials prepared via sol-gel method and coated by dip-coating method onto the different substrate surface were annealed in air at 100^0C, 200^0C, 300^0C, 400^0C and 500^0C. The structural properties of the films have been evaluated using X-ray diffraction and Raman spectroscopy. Changes in morphology of ceramic films were observed using scanning electron microscopy.

15:30 Poster 02-03

Investigation of the tensile deformation of nanocrystalline palladium thin films using in-situ synchrotron x-ray diffraction

Stephen Doyle[1], Tatjana Filatova[2], Tatjana Ulyanenkova[2], Rudolf Baumbusch[3], Anna Castrup[4], Patrick Gruber[3], Tilo Baumbach[1,2], Oliver Kraft[3]

1. *Forschungszentrum Karlsruhe GmbH, Institut für Synchrotronstrahlung, ANKA (ANKA), Hermann-von-Helmholtz-Platz 1, Karlsruhe 76344, Germany* **2.** *Laboratorium für Applikationen der Synchrotronstrahlung (LAS), Kaiserstr. 12, Karlsruhe 76131, Germany* **3.** *Institut für Zuverlässigkeit von Bauteilen und Systemen, Kaiserstr. 12, Karlsruhe 76131, Germany* **4.** *Forschungszentrum Karlsruhe, Institute of Nanotechnology, P.O.B. 3640, Karlsruhe D-76021, Germany*

e-mail: doyle@iss.fzk.de

There is currently intense interest in understanding the mechanisms of plastic deformation of nano-grained metals and metallic alloys. While it is generally assumed that deformation at low extension rates and small grain sizes is governed by diffusion processes, the mechanistic processes occurring at larger strain rates are less well understood. It is expected that significant differences exist in the deformation mechanisms of nanocrystalline materials in comparison with their polycrystalline counterparts.

We report on the characterization of nanocrystalline palladium thin films prepared by sputter deposition on Kapton substrates during tensile deformation, utilising in-situ x-ray diffraction at the synchrotron radiation source ANKA in Germany. The films were subjected to defined strain regimes extending to irreversible plastic deformation. Sputtering parameters were varied to allow investigation of possible production-related effects on the thin film properties. Analysis of selected diffraction line positions and profiles leads to an evaluation of the contributions of grain-size, micro-strain and dislocation density present in the material. We interpret the x-ray diffraction data in terms of the contributions from microstrain and particle size and relate the results to deformation mechanisms as a result of the applied strain.

15:30 Poster 02-04

Microwave sintering of Ni plated SiC and Fe powders

Ayhan Erol, Ahmet Yönetken, Sabri Cevik

Afyon Kocatepe Universitesi, Afyonkarahisar 03200, Turkey

e-mail: aerol@aku.edu.tr

Ni-Fe matrix composites reinforced with SiC were produced by microwave sintering at various temperatures. A uniform nickel layer on SiC and Fe powders was deposited prior to sintering using electroless plating technique, allowing close surface contact. The formation of carbides between SiC and Fe powders is controlled through Ni layer existing on the starting powders. A composite consisting of a ceramic phase, SiC, within a matrix of Ni3Fe and NiFe, was prepared within the temperature range 500°C-900°C under Ar shroud. Characterization of composites were carried out by XRD, SEM(Scanning Electron Microscope), compressive testing and hardness measurements were employed. Results suggest that the best properties as σmax and hardness (HV) were obtained at 900°C and the microwave sintering of electroless Ni plated SiC and Fe powders is a promising technique to produce ceramic reinforced Nickel Fe composites.

15:30 Poster 02-05

Mıcrowave sıntering of electroless Ni plated B_4C powders

Ayhan Erol, Ahmet Yönetken

Afyon Kocatepe Universitesi, Afyonkarahisar 03200, Turkey

e-mail: aerol@aku.edu.tr

Nickel matrix composites reinforced with B_4C have been fabricated by microwave sintering at various temperatures. A uniform nickel layer on B_4C powders was deposited prior to sintering using electroless plating technique, allowing close surface contact than can be achieved using conventional methods such as mechanical alloying. The reactivity between B_4C powders to form compounds is controlled through Ni layer existing on the starting powders. A composite consisting of quaternary additions, a ceramic phase, B_4C, within a matrix of Ni B_4C etc., has been prepared at the temperature range 500°C-900°C under Ar shroud. XRD, SEM(Scanning Electron Microscope), compressive testing and hardness measurements were employed to characterize the properties of the specimens. Experimental results carried out for 600°C suggest that the best properties as σ_{max} and hardness (HV) were obtained at 600°C and the microwave sintering of electroless Ni plated B_4C powders can be used to produce ceramic reinforced Nickel composites.

15:30 Poster 02-06

Phase transitions in protective coatings based on ceramic oxides

Ludwik Górski[1], Andrzej Pawłowski[2]

1. *Institute of Atomic Energy, Otwock-Świerk 05-400, Poland* **2.** *Polish Academy of Sciences, Institute of Metallurgy and Materials Sciences (IMIM PAN), Reymonta 25, Kraków 30-059, Poland*

e-mail: l.gorski@cyf.gov.pl

The studied coatings containing composites based on Al_2O_3 and ZrO_2 are deposited by plasma spraying technology. These coatings belong to the group of thermal barrier acting as thermal insulators in many technical branches among others in aeronautical and automotive industry. Therefore purpose of these works has both research and practical side.

Phase transitions caused by the conditions of plasma spraying process and subsequent coatings thermal treatment are studied by X-ray diffraction. Microstructure and local changes in phase and chemical composition are observed by scanning and transmission electron microscopy combining with electron diffraction.

Different phase transitions directed to appearance of ternary oxides, solid solutions and crystal forms changing for separate oxides have been determined. In this work some results for composites belonging

to Al_2O_3 – TiO_2 and ZrO_2 – Y_2O_3 are described. In the first beside transformations in separate oxides (α – γ in Al_2O_3, anatase – rutile in TiO_2) aluminum titanate Al_2TiO_5 of high thermal resistance has been occurred. In the latter among others martensitic transformation from tetragonal to monoclinic crystal form has been observed. Transmission electron microscopy shows local areas of alternate layers: amorphous, nanocrystalline and polycrystalline of both equiaxial and columnar crystallites shape. Different changes in microscopic image caused by coatings thermal treatment are also visible.
Further studies on this topic are still in progress.

15:30 Poster 02-07

Nanophase-separated poly(pentylmethacrylate-b-methylmethacrylate) diblock copolymers: Structure investigations using X-ray scattering methods

Dieter Jehnichen[1], Doris Pospiech[1], Saija Ptacek[1], Kathrin Eckstein[1], Peter Friedel[1], Andreas Janke[1], Christine M. Papadakis[2]

1. *Leibniz Institute of Polymer Research Dresden, Dresden 01069, Germany* **2.** *Technische Universität München, Physics Department, Garching 85747, Germany*

e-mail: djeh@ipfdd.de

Nanostructured materials basing on diblock copolymers have got a soaring interest due to their opportunity to exploit the microphase/ nanophase separation behavior for developing materials with nanostructures in bulk and films or at surfaces. Nanotechnology with block copolymers (BCP) has therefore become one of the most innovative fields of polymer science. The work was directed to the development of nanostructured surfaces based on the phase separation of poly(pentylmethacrylate-b-methylmethacrylate) diblock copolymers (PPMA/PMMA). Following steps
- BCP synthesis and chemical characterization,
- phase separation in solid state (bulk) including mean field calculations,
- morphology and phase separation in thin films by combination of advanced physical methods
had to be intensively investigated. PPMA/PMMA with preferably lamellar and cylindrical structure were synthesized and subsequently tagged with functional groups for later incorporation of inorganic nanoobjects. The synthesis was performed by sequential living anionic polymerization of PMA and MMA. Polydispersities PDI of BCP with different molar masses and compositions were low as expected.
The phase separation behavior was estimated using the phase diagram obtained by mean field calculation based on an approach (Leibler, Benoit). Low PDI of BCP could be included into the calculation of the spinodals. The experimentally observed phase behavior was compared to the predicted one and a good correlation was found. Most of BCP were phase separated and did not show an order-disorder transition in T-SAXS, thus reflecting the high tendency of phase separation despite the chemical similarity of the blocks. Most of the samples formed a well-pronounced lamellar structure. Only a few ones in a quite narrow compositional region showed cylindrical structures. SAXS periodicities d corresponded to the total molar mass of BCP. Introduction of functionalities did not significantly change both, the type of morphology as well as the d-value. The wide range of lamellar structures in PPMA/PMMA compared to other types of BCP and the absence of bicontinuous structures may be explained by the chemical similarity of both blocks.
Thin films of PPMA/PMMA with cylindrical and lamellar bulk morphology on silicon wafer with film thickness between 25 and 120 nm and very low roughness were obtained by dip coating into weakly concentrated polymer solutions. The laterally demixed morphologies were examined by AFM and GISAXS. Film morphologies depended on the chemical composition of BCP (as in the bulk) as well as the molar mass. Very thin films with a thickness in the range or below dbulk indeed showed standing cylinders or standing lamellae often arranged in a wavy structure, but lateral to the surface. Thicker films with thickness higher than dbulk gave "lying" cylinders or lamellae arranged parallel to the surface. The periodicities of nanostructures in thin films were comparable to the periodicities obtained in bulk samples.

15:30 Poster 02-08

Characteristic of heat-resistant PVD coatings based on X-ray diffraction investigations

Barbara Kucharska

Częstochowa University of Technology, Armii Krajowej St., Częstochowa 42-200, Poland

e-mail: bratek@mim.pcz.czest.pl

The paper presents the results of investigations of coatings composed of chromium-nickel AISI 310S steel deposited by the magnetron sputtering method. Coatings were made for heat-resistance improvement of the steel: by the crystallites size reduction and by Al/Ir additions. During the deposition of coatings by the magnetron method, bcc structure may form in the coatings, despite the fact that the 310S steel is austenitic. During the present and other studies it has been found, that bcc phase is metastable and transform to fcc phase when the coating temperature increase.

Diffractometric measurements were made using CoKα radiation. the in this work: In the temperature range t_{room} ÷250°C the measurements were done *in-situ* using temperature attachment. At higher temperatures the measurements were done *ex-situ*, after 15 minutes of annealing of a sample at a given temperature. The temperatures were increased in steps of 50°C. It was found, that permanent effect of transformation occurred at 550°C but at lower temperatures the transformation is reversible, i.e. effect dissapear after cooling to room temperature.

The density of the coating was calculated taking into account the presence of the bcc metastable phase in the coating, which has a structure different from that of the substrate (fcc), . By using an asymmetric Bragg-Brentano diffraction geometry, the critical angles α was determined, at which radiation penetrates through the whole coating thickness. In the density calculations, the absorption coefficient, calculated from chemical composition of the coatings, and the coefficient G_x, determined experimentally, were used.

15:30 Poster 02-09

Coplanar grazing exit X-ray diffraction on thin polycrystalline films

Zdenek Matej, Lea Nichtova, Radomír Kužel

Charles University, Faculty of Mathematics and Physics, Ke Karlovu 3, Prague 12116, Czech Republic

e-mail: matej@karlov.mff.cuni.cz

X-ray powder diffraction analysis of thin polycrystalline films in the coplanar grazing exit (GE) parallel beam geometry was tested. Dependence of the diffraction peak intensity on the beam incidence/exit angle, which cannot be interpreted by a simple formula for absorption in the film [1], was observed for very thin films (<~100 nm for TiO_2). This effect is connected with the well known Yoneda peak in the transparency of the film surface interface. The refraction correction of peak positions and penetration depth [2], and also dynamical effects of multiple scattering of primary/diffracted beam in the film [3] should be considered. In comparison with the common coplanar grazing incidence geometry, by GE technique lower intensity gain for thin film can be achieved. However, if the PSD detector is used, 2D maps of scattered intensity with high resolution (because of narrow diffracted beam) can be obtained in a reasonable time. Moreover, they are not affected significantly by instrumental and sample effects. The technique is very useful for determination of the film thickness, depth profiling of phase composition, the refraction index determination and generally for study of real structure of thin films and multilayers with common laboratory diffractometers.

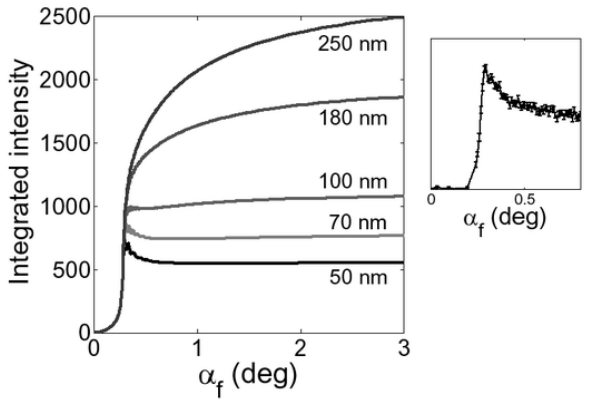

Figure: Simulated dependence of the integrated intensity of anatase (101) diffraction line on the exit angle Alpha_f, for powder TiO2 films of different film thickness. Measured intensity for the thinnest film (50 nm) is depicted in the right plot.

References:

[1] J. Lhotka, R. Kuzel, G. Cappuccio, V. Valvoda, Surf. Coat. Tech. (2001) 148 96-101

[2] G. Lim, W. Parrish, C. Ortiz, M. Bellotto, M. Hart, J. Mater. Res. (1987) 2 (4) 471-477

[3] P. F. Fewster, N. L. Andrew, V. Holy, K. Barmak, Phys. Rev. B (2005) 72 174105

15:30 Poster 02-10

Study of defects and strain in SiGe/Ge Multi Quantum Well systems using HRXRD

Antonia Neels[1], Giovanni Isella[2], Hans Von Känel[2], Alex Dommann[1]

1. *Centre Suisse d'Electronique et de Microtechnique (CSEM), Jaquet-Droz 1, Neuchâtel 2002, Switzerland* **2.** *Dipartimento di Fisica del Politecnico di Milano, Via Anzani 42, Como 22100, Italy*

e-mail: antonia.neels@csem.ch

Symmetrically strained SiGe/Ge multilayers were grown epitaxially on Si(001) by low-energy plasma-enhanced chemical vapour deposition LEPECVD. Using exceptionally high growth rates around 5 nm/s and low substrate temperatures of the order of 500^{o} C, structures containing up to 1000 SiGe/Ge double layers with a thickness of 50 nm each could be realized [1]. HRXRD methods are used to evaluate lattice strain and relaxation, lattice tilt, layer thickness, composition and dislocation densities. Single scan simulations on symmetric (004) and asymmetric (115) reflections are performed in order to obtain precise information about the Multi Quantum Wells (MQW) system. The crystalline perfection can be determined with highest precision using the reflections from the Si substrate as internal reference.

The figure 1 shows an example of a Reciprocal Space Map (RSM) in the vicinity of the Si(004) reflection, where the two main maxima correspond to diffraction from the SiGe and Ge layers, respectively, and where the superlattice reflections are clearly resolved. In addition, diffused scattering occurring around the SiGe layer diffraction peak shows the presence of defects in the MWQ. A reasonable fit of the corresponding rocking curve is only possible for such a structure if the defects are taken into account.

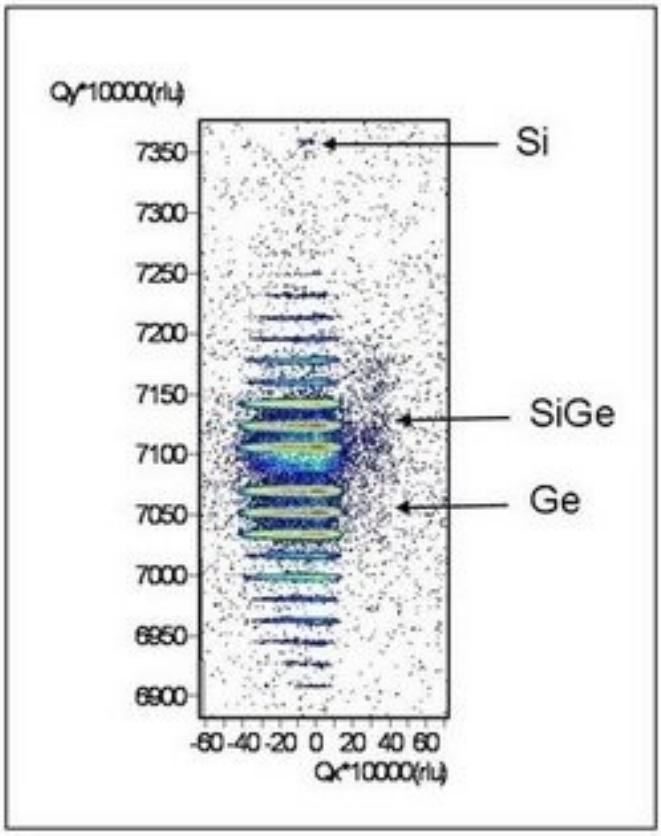

Fig. 1 RSM of (004) in a MQW

1. H. von Känel, M. Bollani, M. Bonfanti, D. Chrastina, D. Colombo, A. Dommann, M. Guzzi, G. Isella, A. Miranda, E. Müller, A. Neels, J. Osmond, B. Rössner, R. Sordan, F. Traversi, Epitaxial Si-Ge Heterostructures and Nanostructures for Optical and Electrical Applications, *Proceedings of the 2nd Conference on Nanostructures* (NS2008), 2008, Iran.

Direct space methods

MS3 posters
Sunday afternoon, 21 September, 15:30

15:30	Poster	03-01

GRINDEX - a new computer program for indexing poor powder patterns by grid search method.

Dmitry V. Albov

Chemistry Department, Moscow State University, Leninskie Gory, 1-3, Moscow 119992, Russian Federation

e-mail: albov@struct.chem.msu.ru

Indexing of powder patterns is a key step in structural characterization of an unknown powder sample. Three most popular programs – TREOR, ITO and DICVOL – often fail while dealing with poor patterns containing badly-shaped peaks and/or peaks from unidentified impurities. To help the researcher to overcome these obstacles, the new program GRINDEX (GRid search INDEXing) has been developed. In the search of correct unit cell dimensions using a list of non-ideal peak positions, GRINDEX systematically explores all possible cell parameters within specified limits. For each unit cell being tested, the calculated peak positions are compared with the experimental ones and the solution is selected by the least value of discrepancy R-factor. This is a quite heavy task but it becomes possible at present computer progress level.

GRINDEX has a friendly Windows-based interface and some useful options. It allows specifying expected volume of the asymmetric unit to reduce calculation time and to eliminate definitely erroneous solutions; in this case GRINDEX automatically uses the most frequent Z values for each crystal system. When the crystal structure is expected to be isostructural to a known structure, the user may specify different limits for all six cell parameters to test only close cells. GRINDEX accepts experimental peak positions values typed directly in its window and reads them from files. Several tests of GRINDEX with real data sets showed its efficiency, it easily indexes data sets which could not be indexed by other programs and it is resistant to the presence of some number of impurity peaks (up to 10%). The calculation time takes from seconds (cubic cell) and minutes (orthorhombic cell) to several hours (triclinic cell).

15:30	Poster	03-02

Crystal structure characterization of the single phase compounds in a $La_2Ti_2O_7 – CaTiO_3$ system

Katarina Demsar[1], Anton Meden[1], Sreco D. Skapin[2], Danilo Suvorov[2]

1. *Faculty of Chemistry and Chemical Technology, Askerceva 5, Ljubljana 1000, Slovenia* **2.** *Jozef Stefan Institute, Jamova 39, Ljubljana, Slovenia*

e-mail: katarina.demsar@fkkt.uni-lj.si

In the frame of research activities to identify novel materials for microwave applications, a systematic research of the phase relations in a ternary phase diagram system of CaO-La_2O_3-TiO_2 led, among others, to the preparation of single-phase ceramics based on $CaLa_4Ti_5O_{17}$, $CaLa_8Ti_9O_{31}$ and $Ca_2La_4Ti_6O_{20}$. Preliminary studies and structure predictions of these compounds, including the determination of their unit cells, were carried out much earlier [Nanot et al., J.Solid State Chem. 1974, 11, 272-284], but their detailed structures have not yet been published or reported in the ICSD database, resulting in a motivation to perform the structural analysis.

The three materials listed above were synthesized using a solid-state reaction method by mixing different molar ratios of $CaCO_3$, La_2O_3 and TiO_2. Their X-ray powder diffraction patterns have been collected on a PANalytical X'Pert PRO MPD diffractometer using CuKα radiation. The diffraction patterns were compared with the entries in the PDF2 database.

The structure of $CaLa_4Ti_5O_{17}$ was successfully identified using Rietveld refinement of the isostructural models found in the database by the criterion of pattern matching. The most suitable model is orthorhombic having the Pmnn space group. For the $CaLa_8Ti_9O_{31}$ and $Ca_2La_4Ti_6O_{20}$ no suitable initial model was found. The structures were solved ab initio using the Fox programme [Favre-Nicolin and Cerny, J. Appl. Cryst. 2002, A58]. Reasonable structural models were obtained; however Rietveld refinements were less successful due to poor convergence of the positions of oxygen atoms. Among the possible reasons for this are possibly incorrect space groups and fitting errors, originating from a large set of fitted parameters which is due to a large asymmetric unit. Nevertheless, all the structures ob-

tained so far are in a fair qualitative agreement with the initial predictions proposed by Nanot.
Details on the structure determinations of the listed compounds will be given and all the relevant aspect will be critically discussed.

15:30 Poster 03-03

RETRIEVE for XRD phase and structure analysis of powder patterns

Peter S. Dubinin, Igor S. Yakimov, Yaroslav I. Yakimov, Alexander N. Zaloga, Oksana E. Piksina

Siberian Federal University (SFU), Krasnoyarskii rabochii 95, Krasnoyarsk 660095, Russian Federation

e-mail: Dubinin-2005@yandex.ru

An integrated retrieval system (RETRIEVE) under MS Windows for both phase and structure XRD analysis of powder patterns is developed. An early RETRIEVE release was developed as a search/match system for phase analysis of complex powder patterns only. A special high selective query language for phase identification was designed for it. The RETRIEVE had demonstrated an excellent results on Search-Match Round Robin – 2002 (RR) where only this program among 248 participants [1] identified all test phase compositions absolutely exactly [2]. The second RETRIEVE version [3] incorporated standardless quantitative phase analysis (QPA) with two automatic methods: a modified RIR and an iterative QPA for group of powder patterns. The third RETRIEVE release is discussed here. The new RETRIEVE has following features. Problem-oriented graphical user-friendly interface (GUI) provides look-and-feel visualization and operating over experimental, reference, calculated and model fitting powder patterns. Phase identification uses the query language based on calculus predicate theory instead of simple Boolean logic using into traditional search-match. User-hidden search-match query programs are created automatically during mouse manipulations on GUI elements. The model powder pattern is built as an optimal line combination of matching reference spectrums. Standardless QPA includes two above automatic methods and additionally method similar to Rietveld analysis. The modified RIR is based on modelling powder patterns. The group QPA is based on iterative refinement of phase calibration constants and samples mass absorption coefficients. Both methods can use quantitative elemental analysis data for refinement of phase compositions. All methods show standard deviations less than 1% weight without- and less than 0.5% weight with using XRF elemental data for powder patterns of RIR on QPA three-phases mixes [4]. The RETRIEVE includes a derivative difference minimization (DDM) method [5] instead of traditional Rietveld method for refinement of profile and structure parameters as well as for QPA. A new hybrid genetic algorithm is developed for search and refinement of crystal structure models in direct space.

[1] J-M. Le Meins, L.M.D. Cranswick, A. Le Bail. Powder Diffr. 2003. 18, 106-113.
[2] Search-Match Round Robin – 2002 Results. http://sdpd.univ-lemans.fr/smrr/results/ .
[3] I.S. Yakimov. ECM24. Marrakech – Morocco. 2007. MS31 P08.
[4] I.C. Madsen, N.V.Y. Scarlett, L.M.D. Cranswick, T. Lwin. J. Appl. Crystallogr. 2001. 34, 409-426.
[5] L.A. Solovyov. J. Appl. Crystallogr. 2004. 37. 743-749.

15:30 Poster 03-04

Powder diffraction quality analysis

George Duncan-Jones, Mike Glazer

Oxford University, South Parks Road, Oxford OX1 3QZ, United Kingdom

e-mail: g.duncan-jones1@physics.ox.ac.uk

The quality of a powder diffraction pattern can be thought of as an assessment of the amount of information that can reliably extracted from a given set of data; of particular interest is an ab initio approach to this assessment that does not assume any knowledge of the circumstances that produced the pattern i.e. crystal sample, and specifications concerning the detector, source and X-ray geometry. Qualitative judgements are easily made by eye, and subjective analyses of a pattern's worth are common in disputes between biomedical firms. In this, and other, contexts a quantitative measure of quality would be a valuable resource. Software has been written to investigate the constituent parts of a powder diffraction pattern, including high frequency noise using wavelet denoising; low frequency noise using the Brückner algorithm [1]; peak search using second derivatives; determination of full widths at half maxima. It is our intention eventually to be able to combine the various constituent features in a powder pattern into a figure of merit or at least create an objective criterion that can be used to indicate the quality of a powder pattern.

[1] S. Brückner, 2000, *J. Appl. Cryst.*, **33**, 977-979.

15:30 Poster 03-05

X–ray diffraction studies of transition metal molybdates

Bartłomiej A. Gaweł[2], Wiesław Surga[3], Wieslaw Lasocha[1,2]

1. *Polish Academy of Sciences, Institute of Catalysis and Surface Chemistry, Niezapominajek 8, Kraków 30-239, Poland* **2.** *Jagiellonian University, Faculty of Chemistry, Ingardena 3, Kraków 30-060, Poland* **3.** *Świętokszyska Academy, Institute of Chemistry, Chęcińska 5, Kielce 25-020, Poland*

e-mail: gawel@chemia.uj.edu.pl

Polyoxometalate (POM) chemistry has attracted intense interest because of its fascinating structures and potential applications, such as high-density optical storage media, sensors, catalysis and biomedicine. They may self-assemble into one-, two-, and three-dimensional structures. However, it is still a challenging task in POM chemistry to assemble discrete polyanion units into one- or two-dimensional extended solid frameworks in appropriate ways. In our work we determined the structure of two molybdate hydrates, $CoMo_3O_{10} \cdot nH2O$ (I) and $CuMo_2O_{12} \cdot nH_2O$ (II). These compounds were synthezied by reaction between hot solution of $CoCO_3$ or $CuCO_3$ and suspension of MoO_3. Obtained fiber crystals were grinded with mother solution and measured using focusing mirror in capillary geometry.

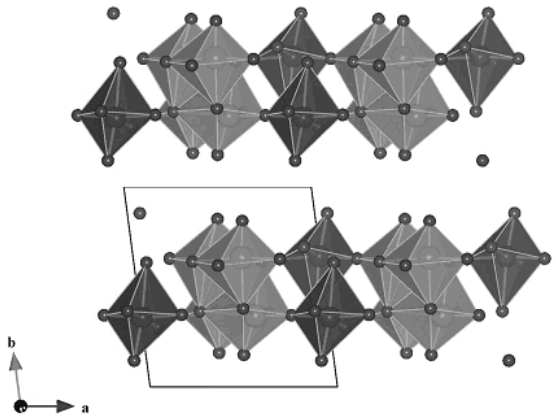

Figure 1. The unit cell of compound II.

Crystal structures of both compounds were solved using global optimization method (FOX [1]) and refined by Rietveld method (Jana2000 [2]). Compound I crystallizes in monoclinic system in the space group P $2_1/c$ with: a = 12.0698 (8) Å, b = 19.825(1) Å, c = 7.6213(8) Å, α = 90°, β = 107.584(7)°, γ = 90°, V = 1738.5(1) $Å^3$. Compound II (fig.1) crystallizes in triclinic system in the space group P -1 with: a = 8.6800 (9) Å, b = 9.2894(8) Å, c = 6.0643(8) Å, α = 90.72(1)°, β = 96.00(1)°, γ = 97.43(2)°, V = 482.06(7) $Å^3$.

Literature:

1. Favre-Nicolin V., Cerny R., J. Appl. Cryst. 35 (2002) 734
2. Petricek V., Dusek M. & Palatinus L.(2000). Jana2000. Institute of Physics, Praha, Czech Republic

Supported by the Polish MEiN grant 1T09A 07730.

15:30	Poster	03-06

Powder diffraction studies of 1,2- and 1,3-diaminopropane octamolybdates

Maciej P. Grzywa[1], Wieslaw Lasocha[1,2]

1. *Institute of Catalysis and Surface Chemistry, Polish Academy of Sciences (ICSC), Niezapominajek 8, Kraków 30239, Poland* **2.** *Jagiellonian University, Faculty of Chemistry, Ingardena 3, Kraków 30-060, Poland*

e-mail: grzywa@chemia.uj.edu.pl

Molybdates are very important compounds which are used in a wide range of applications such as lubricants, catalyst and corrosion inhibitors. In this work, synthesis and results of powder diffraction studies of 1,2- and 1,3-diaminopropane octamolybdates are presented.

The compounds have been obtained by reaction of molybdic acid with 1,2-diaminopropane and 1,3-diaminopropane in acidic solution (acetic acid, formic acid), respectively. Crystal structures have been determined by X-ray powder diffraction method.

The lattice parameters and space groups were determined using PROSZKI package [1]. The crystal structure models were obtained by global optimization methods (FOX program [2]) and by direct methods (EXPO program [3]). Final refinements by the Rietveld method were performed using Jana2000 [4] and GSAS [5-6] programs.

Investigated octamolybdates crystallize in the monoclinic space groups: P $2_1/n$ and P $2_1/c$ with: a=11.524(2), b=17.415(3), c=7.900(2) Å, β=109.87(2)°, V=1491.0(4) $Å^3$ (1,2-diaminopropane) and a=12.696(2), b=15.176(2), c=7.838(2) Å, β=96.89(2)°, V=1499.2(4) $Å^3$ (1,3-diaminopropane). Both compounds were also investigated using TG/DSC, IR and XRPD thermal decomposition studies.

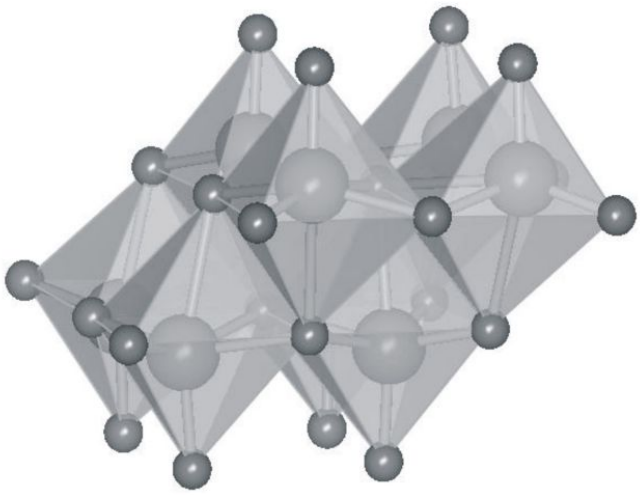

Fig.1. Structure scheme for $[Mo_8O_{26}]^{4-}$ anion.

[1] W. Łasocha, K. Lewinski, PROSZKI–a system of programs for powder diffraction data analysis, J. Appl. Crystall., 27, 1994, 437-438
[2] V. Favre–Nicolin, R. Cerny, J. Appl. Cryst., 2002, 35, 734–743
[3] A. Altomare, M. C. Burla, M. Camalli, B. Carrozzini, G. L. Cascarano, C. Giacovazzo, A. Guagliardi, G. Moliterni, G. Polidori, R. Rizzi, J. Appl. Cryst., 1999, 32, 339–340
[4] V. Petricek, M. Dusek, L. Palatinus, Jana2000. The crystallographic computing system. Institute of Physics, Praha, Czech Republic, 2000
[5] A. C Larson, R. B. Von Dreele, GSAS, Los Alamos National Laboratory Report LAUR 86-748, 2000
[6] B. H. Toby, EXPGUI, J. Appl. Cryst. 34, 2001, 210-213

The support of the Polish MEiN; grant 1T09A 07730 is gratefully acknowledged.

15:30	Poster	03-07

Crystal structure of ZSM-12 with tetraethylammonium cations from X-ray powder diffraction data

Marta Kasunič[1], Jure Legiša[1], Andrew M. Beale[2], Nataša Zabukovec Logar[3], Anton Meden[1], Amalija Golobič[1]

1. *Faculty of Chemistry and Chemical Technology, Askerceva 5, Ljubljana 1000, Slovenia* **2.** *Inorganic Chemistry and Catalysis, Utrecht University, Sorbonnelaan 16, Utrecht 3584CA, Netherlands* **3.** *National Institute of Chemistry (NIC), Hajdrihova 19, Ljubljana SI1000, Slovenia*

e-mail: marta.kasunic@fkkt.uni-lj.si

High-silica MTW (ZSM-12) was prepared by using a »two-silica« source strategy with tetraethylammonium hydroxyde (TEAOH), acting as a simple structure directing agent [A. Mitra et al., Micropor.

Mesopor. Mater. 54, 2002, 175-186]. On the basis of conventional laboratory X-ray powder diffraction data (PANalytical X'Pert PRO MPD), a structure determination of this compound by using Topas Academic program suite was performed.

Due to the resemblance between powder patterns of calcined ZSM-12 (crystallizing in *C*2/*c* space group with unit cell parameters *a*=24.8633(3), *b*=5.01238(7), *c*=24.3725(7) Å, *β*=107.721(6)°) and that of ZSM-12 with TEA cations, the former was used as a starting model [ICSD Code 40137]. However, the powder pattern of the new compound possesses some additional diffraction peaks with *k* index not divisible by three revealing superstructure with three times longer edge *b* (15.1908(4) instead of 5.01238(7) Å). This is a consequence of ordered arrangement of TEA cations in silicate framework: in each channel traversing along *b* edge two of them (a repeating unit) are settled, what is also consistent with the results of TGA measurements. According to the results of Raman spectroscopy only TEA cations of *tt.tt* conformation are present. They were presumed to behave as rigid bodies and positioned by the use of simulated annealing approach. In space group *C*2/*c*, the obtained solution had some short contacts between the cations and the framework. Therefore, a decision to lower the symmetry and solve the structure in *Cc* space group with the absence of two-fold rotation axis in the channels (which allowed only rotations of TEA cations around *b* axis) was taken. It yielded a reasonable arrangement of TEA cations and acceptable agreement between calculated and observed powder patterns with R_{wp} 9.86%.

15:30 Poster 03-08

Grid extension and structure-classification extension for FOX code

Jan Rohlicek, Michal Husak, Bohumil Kratochvil

Institute of Chemical Technology (VSCHT), Technicka 5, Prague 16628, Czech Republic

e-mail: rohlicej@vscht.cz

Parallel computing is a widely used method for speeding up a time consuming computing process. This process uses simultaneous execution of the same task (split up and specially adapted) on multiple processors or on two or more computers. These computers are communicating with each other over a network in order to synchronize their work. The idea is based on the fact that the process of solving a problem usually can be divided into smaller tasks, which may be carried out independently with some coordination.

We managed to modify the FOX [1] code for parallel computing method as mentioned above. Modified FOX [1] program (FOXGrid) can be executed as a server or as a client. Server is a control element and clients are working elements. Server manages the basic data: job list, client list and result list. During the computing, server sends jobs to clients and waits for results. After solving the job, the client sends the results back to server and request new work. The communication between server and client use TCP/IP protocol. The data are formatted in xml standard. Client can be executed on the same computer as the server or on another computer in the net. The method can be used for full utilization of multi-core and hyper threading PC by running multiple clients on the same PC.

Both FOX and FOXGrid typically produce multiple similar results during the structure solution run. The question is how to identify the identical solution and reject them from the result list? The idea is to compute fingerprints (1D or 2D plots) that are comparable among each other. We created a simple code, which is computing distances between atoms. These distances are used for creating distance histogram – fingerprint (thanks a lot to Vincent Favre-Nicolin for this idea). The code reads results generated by the FOX [1] program. It creates a similarity matrix. This approach was up to now successfully tested on simple organic structures.

Work on the 'FOXGrid' project is supported by a grant from Czech Grant agency (GAČR 203/07/0040) and by the research program MSM6046137302 and 2B08021 of the Ministry of Education, Youth and Sports of the Czech Republic.

[1] V. Favre-Nicolin and R. Cerny, J. Appl. Cryst. 35 (2002), 734-743.

15:30 Poster 03-09

Ab-initio structure determination of $Y_5(SiO_4)_3N$ from a 3-phase powder diagram

Julius Schneider, Wolfgang W. Schmahl

LMU, Department of Earth and Environmental Sciences, Crystallography, Theresienstr. 41, München 81539, Germany

e-mail: julius.schneider@lrz.uni-muenchen.de

Although $Y_5(SiO_4)_3N$ ocurs as an auxiliary phase in Si_3N_4 ceramics as a host for sinter additives such as Y_2O_3, it's structure was hitherto not described in detail. For synthesis a mixture of Si_3N_4, SiO_2 and Y_2O_3 powders with the nominal composition was heated to 1600°C under flowing nitrogen gas in a graphite furnace and reground and reheated three times.

The resulting product was investigated by $CuKa_1$-X-ray diffraction on a STOE-Stadi-P powder diffractometer in transmission geometry. Qualitative analysis yielded a mixture of 3 phases: a) Y_2SiO_5, sp.gr. I2/a, /1/, b) cuspidine-type $Y_4Si_2O_7N_2$, sp.gr.$P2_1/c$, /2/ and c) the title compound $Y_5(SiO_4)_3N$ (PDF 33-1459). The presence of two impurities with large monoclinic unit cells complicated the analysis, yet a 2-phase Rietveld refinement of the known structures of phase a) and b) allowed to separate the reflections of phase c). Indexing yielded the known hexagonal unit cell and cell dimensions of a=9.3671(5)Å and c=6.7727(3)Å. Integrated intensities of this phase were extracted by adding a LeBail refinement of phase c) to the Rietveld refinements of phases a) and b). Subsequent introduction of this information into the real space ab-initio structure determination program Endeavour produced an apatite-related structure of $Y_5(SiO_4)_3N$ with space group $P6_3/m$ (R-factor=4.6%, cost function=0.4586).

Final 3-phase Rietveld refinement of these X-ray data and of former neutron data /3/ obtained on instrument D1A at ILL will be compared and combined.

/1/ B.A.Maximov, V.V.Ilyukin, Y.A Kharitonov, N.V.Belov, Kristallografiya **15** (1970) 926

/2/ K.J.D.MaxKenzie, G.J.Gainsford, M.Y.Ryan, J.Eur.Ceram.Soc. **16** (1996) 553-560

/3/ W.W.Schmahl, M.Györfi, K.G.Nickel, A.Hewat, ECM **18** (1998) 288

15:30 Poster 03-10

Two-level genetic algorithm for a full-profile fitting of X-ray powder patterns

Yaroslav I. Yakimov, Eugeny S. Semenkin, Igor S. Yakimov

Siberian Federal University (SFU), Krasnoyarskii rabochii 95, Krasnoyarsk 660095, Russian Federation

e-mail: yar_yakimov@mail.ru

Genetic algorithms (GA) are efficient global optimization techniques in which the fittest individuals of a population survive and spawn next improved generations. They give the opportunity to find some rough crystal structure models of powders. In order to refine the structural model it is essential to use a full-profile fitting of powder patterns by Rietveld method. That fitting is based on non-linear least-square method (NLSM) requiring good initial approximations of refined parameters. Thereby its convergence for solutions found by conventional GA is unlikely in cases of complicated multi-phases samples. This work is dedicated to GA spread-out to Rietveld method including full-profile fitting and refinement of crystal structure models. A two-level hybrid genetic algorithm has been developed for this purpose. The hybrid algorithm is based on composition of the dual GA with the NLSM designed as follows. First-level GA chromosomes comprise values of profile and structure parameters used in the Rietveld method. Second-level GA chromosome is a bit string containing one bit per each parameter, where bit values define parameters to be refined with the NLSM on a current iteration. GA fitness function is based on the usual weighted profile R-factor (Rwp). The first-level GA is helpful in searching initial parameter values of acceptable Rwp and overcoming local minima. The second-level GA manages NLSM full-profile fitting with found initial parameter values. It also gives the opportunity to reduce dimensionality of the problem by using number of the user-defined parametric masks that correspond to empiric refinement techniques. The algorithm was implemented as a shell over the full-profile analysis program DDM [1] and was tested on some powder patterns of single and multi-phases samples with known stable crystal structures. 1. Solovyov L. A. // J. Appl. Cryst. 2004. 37. 743-749.

Line profile analysis

MS4 posters
Sunday afternoon, 21 September, 15:30

15:30 Poster 04-01

The evaluation of the microstructures of ceria applying variance method and line profile analysis

Seyed Rouhollah Aghdaee, Vishtasb Soleimanian

e-mail: aghdaee@iust.ac.ir

A comparison has been carried out of different methods of X-ray diffraction line broadening analysis for the determination of crystallite size and microstrains, namely line profile analysis and two approaches based on variance method. The analyses have been applied to data collected on ceria sample conducted by IUCr commission on powder. In variance method Voigt function and its approximation Pseudo-Voigt function were fitted to X-ray diffraction line profile. Based on fit results the variances of line profiles were calculated and then the crystallite size and root mean square strain were obtained from variance coefficients. A ss plot of Langford and Fourier analysis have also been carried out based on powder pattern fitting and crystal size and microstrain were determined. The values of area-weighted and volume-weighted domain size determined from variance method are in agreement with those obtained from line profile analysis within a single (largest) standard uncertainly. But the results of r.m.s. strain calculated from variance are larger than those of determined from LPA or reported by other authors.

15:30 Poster 04-02

Twinning in coarse grain and nanocrystalline Zr, Ti and Mg determined together with dislocations and crystallite size by X-ray line profile analysis

Levente Balogh, Tamás Ungár

Eötvös University, Pázmány Péter sétány 1/A, Budapest H-1117, Hungary

e-mail: levente@metal.elte.hu

Dislocation structure and twinning are much more complicated in Zr, Ti and Mg, and its alloys than in *fcc* materials because: (i) there are three different possible Burgers-vector types instead of one [1,2], (ii) at least 11 different slip systems can operate in principle [1,2], (iii) there are a variety of twinning systems, e.g., {10.1}<10.-2> and {11.2}<11.-3> compressive twins and {10.2}<10.-1> and {11.1}<-1-1.6> tensile twins [3,4], and (iv) some slip systems may not be activated because of the large variation of the critical resolved shear stress from one slip system to another [5]. It will be shown that the standard method to evaluate the effect twinning and faulting in *fcc* crystals on X-ray line broadening [6,7] cannot be applied for twinning on the above slip systems in hexagonal crystals. The reason for this is that, unlike in *fcc* materials where twinning and faulting occures on the close packed planes with the repetition of three normal to these planes, in *hcp* crystals, especially for the planes listed above, the crystal cannot be built up by a similar simple repetition in the normal direction. Therefore, the method developed earlier for *fcc* crystals [8] has been extended for *hcp* materials. The scattered intensity from twinned hexagonal crystals has been calculated in reciprocal space by using the DIFFaX [9] free software. A periodic behaviour of scattering has been observed which is used to simplify the numerical procedure in determining twinning together with dislocation densities and crystallite size in *hcp*-s. It is shown that in hot worked commercial purity Ti {10.2} tensile twins are by far more frequent than other twins. In tensile deformed Mg we found {10.1} compressive twinning whose frequency decreases with the temperature of deformation. In compression deformed Zr {10.2} tensile twinning is observed where twinning frequency decreases with deformation.

1. I. P. Jones, W. B. Hutchinson, Acta Metall. 29 (1981) 951-968.
2. R. Kužel Jr., P. Klimanek, J. Appl. Cryst. 22 (1989) 299-307.
3. Y. B. Chun, S. H. Yu, S. L. Semiatin, S. K. Hwang, Mat. Sci. Eng. A398 (2005) 209- 219.

4. N.E. Paton, W.A. Backofen, Metallurgical Trans. 1 (1970) 2839-2847.
5. H. Francillette, B. Bacroix, M. Gasperini, J. L. Béchade, Acta Mater. 46 (1998) 4131- 4142.
6. L. Velterop, R. Delhez, Th. H. de Keijser, E. J. Mittemeijera, D. Reefman, J. Appl. Cryst. (2000). 33, 296-306
7. E. Estevez-Rams, B. Aragon-Fernandez, H. Fuess, A. Penton-Madrigal, Phys. Rev. B, 68 (2003) 064111
8. L. Balogh, G. Ribárik, T. Ungár, J. Appl. Phys. 100 (2006) 023512.
9. M. M. J. Treacy, J. M. Newsam, M. W. Deem, Proc. Roy. Soc. London A433 (1991) 499-520.

15:30 Poster 04-03

Evolution of size and shape of mullite crystallites in triaxial porcelains

Angel Sanz[1], Joaquin Bastida[1], Angel Caballero[2], Marek A. Kojdecki[3], Francisco J. Serrano[1]

1. *Valencia University, Department of Geology, Dr. Moliner, 50, Valencia 46100, Spain* **2.** *Consejo Superior de Investigaciones Cientfificas (ICV), Cº Valdelatas, SN, Madrid 2809, Spain* **3.** *Wojskova Akademia Techniczna, Warsaw 00908, Poland*

e-mail: bastida@uv.es

Triaxial porcelains are complex ceramic materials consisting of glass and crystalline phases (mainly mullite) produced from a mixture of clay, feldspar and quartz, fired at about 1300ºC (1, 2). Potash feldspars (microcline and orthoclase) are common fluxes and usually appears associated with plagioclases.

This paper concerns the crystallite size and shape evolution of mullite by firing triaxial compositions at different temperature and with different fluxing agent (K-feldspar or Li bearing petalite).

Two compositions were studied: 14% quartz, 53% kaolin, 33% K-feldspar (MGS) and 14% quartz, 53% kaolin, 33% Li-feldspar (MGC). Firing conditions were: heating ratio 2ºC/min , 180 min at T max and different (T ºC max, rising time in minutes) respectively: 1270, 815 (L1), 1300, 830 (L2), 1320, 840 (L3) and 1340, 860 (L4).

X Ray diffraction patterns of powdered samples were obtained in a Bruker D5005 diffractometer in the range 10–110 º (2 theta) at scan step (0.02 º ,20 sec). Complementary SEM observations of fired samples, were made in an Hitachi S-4100 microscope.

Crystallite size and shape were obtained by the Kojdecki method (3,4,5) using LaB_6 (NIST SRM660a) as standard. The Table includes the obtained shape and size data for modelation of prism crystallite shape The parameter C/A, is almost constant in MGS samples but not in MGC samples where the higher size the higher C/A value, so there is a preferred crystallite growth from 1300 to 1340ºC .

The difference between the evolution of crystallite growth in MGC respect MGS compositions is in agreement with the morphologies observed by SEM (greater development of mullite.

Sample	A (Å)	B(Å)	C (Å)	C/A	$V^{1/3}$
MGCL1	442	450	762	1,724	533
MGCL2	387	395	1010	2,610	536
MGCL3	488	496	1180	2,418	659
MGCL4	690	704	2196	3,183	1022
MGSL1	441	450	913	2,070	566
MGSL2	428	436	836	1,953	538
MGSL3	503	512	772	1,535	584
MGSL4	414	422	753	1,819	508

In K-feldspar formulation (MGS) there is no size growth for mullite crystallites with increasing temperature, while in petalite formulations the higher temperature the bigger crystallite sizes. Moreover different features have been found for crystallite growth in this case at highest temperature respect to that found in simple sintering or reactive sintering, with clear decrease for C/A shown at 1300ºC (5) whereas slight increases are found for mullites obtained from 3:2 gels in the range 1300-1500ºC (6).

References

1 Norton, F.H. (1988) Fine Ceramics: Technology and Applications. McGraw-Hill Inc. New York.
2. Kingery, W.D. (1976) Introduction to Ceramics. Wiley. New York.
3. Kojdecki, M. A. (2001) Mater. Sci. Forum, 378–381, 12–17
4. Kojdecki, M. A (2004) Mater. Sci. Forum, 443-444, 107-110
5. Kojdecki, M. A., Bastida, J., Serrano, F. J. & Clausell, J. V. (2001) Mater. Sci. Forum, 378–381, 747–752
6. Kojdecki, M. A., Ruiz de Sola E, Serrano F.J; Delgado Pinar V, Raventós M, Esteve V.J (2007) J. Appl. Cryst. 40, 260–276

Acknowledgements. Generalitat Valenciana project: No GV02-527.

15:30 Poster 04-04

Microstructural evolution and formation of titania-doped mullites from heated single-phase gels

Marek A. Kojdecki[1], Javier Alarcón[2], Esther Ruiz de Sola[2], Francisco J. Serrano[3], José M. Amigó[3]

1. *Military University of Technology, Institute of Mathematics and Cryptology (WAT), gen S. Kaliskiego 2, Warszawa 00-908, Poland* **2.** *Universidad de Valencia, Departamento de Química Inorgánica (UV), C/ Doctor Moliner 50, Burjasot 46100, Spain* **3.** *Universidad de Valencia, Departamento de Geología (UV), C/ Doctor Moliner 50, Burjasot 46100, Spain*

e-mail: m_kojdecki@poczta.onet.pl

The crystalline microstructure of titanium dioxide doped mullites prepared from monophasic gels thermally treated at temperatures 900°C, 1100°C, 1200°C, 1400°C, 1500°C and 1600°C was analysed. Two series of gels with nominal compositions $3(Al_{2-x}Ti_xO_3)\cdot 2(SiO_2)$ and $2(Al_{2-x}Ti_xO_3)\cdot(SiO_2)$ for x=0.00, 0.02, 0.05, 0.07, 0.10 and 0.15 were prepared [1,2].

X-ray diffraction analysis was performed by using an X-ray diffractometer in the Bragg-Brentano geometry, equipped with Cu K? X-ray tube and a graphite monochromator, operating at 30kV and 40mA. X-ray diffraction patterns were recorded in the range between 15° and 90° (2θ), with a step size of 0.02° (2θ) and a counting time of 10s per step. Lattice parameters were determined by using ZnO as standard and least square fit. The instrumental peaks were recorded from lanthanum hexaboride (NIST 660a SRM) and from them the standard line profiles corresponding to Bragg angles for mullite were calculated. Pure X-ray diffraction line profiles were computed by using a stable deconvolution algorithm. Several pure line profiles, corresponding to the strongest reflections, were simultaneously analysed for each sample [3] to estimate prevalent crystal-

lite shape and to determine a volume-weighted crystallite size distribution and a second-order crystalline lattice strain distribution. The crystallites were modelled in four different shapes, as tetragonal or orthorhombic prisms, cylinders and spheres; the shape was modelled as the ratio of characteristic dimensions (such as prism edge lengths). The shape anisotropy of the crystallites was found. The dependence of crystalline microstructure of the solid solutions on the titanium contents was observed. A characteristic feature of all volume-weighted crystallite size distributions was their bimodality; each distribution could be well approximated as the sum of two logarithmic-normal distributions. This bimodality is explained as a result of nucleation and initial growth of crystallites in two stechiometric forms of mullite that happened during thermal treatment. Mean crystallite sizes, calculated from the size distributions, were in agreement with results of scanning electron microscopy observations. In general, crystallite were larger with increasing either the content of dissolved titanium oxide or the final treatment temperature. A mechanism of formation of titania-doped mullite solid solutions is suggested and the limit of solubility of titania in mullite is estimated on the basis of the interpretation of the structural and microstructural evolution from gels to doped mullites.

[1] E. Ruiz de Sola, F. Estevan, J. Alarcón: Low-temperature Ti-containing 3:2 and 2:1 mullite nanocrystals from single-phase gels; J. Eur. Ceram. Soc. 27 (2007), 2655-2654.

[2] E. Ruiz de Sola, F. J. Serrano, E. Delgado-Pinar, M. M. Reventós, A. I. Pardo, M. A. Kojdecki, J. M. Amigó, J. Alarcón: Solubility and microstructural development of TiO_2-containig $3Al_2O_3.2SiO_2$ and $2Al_2O_3.SiO_2$ mullites obtained from single-phase gels; J. Eur. Ceram. Soc. 27 (2007), 2647-2654.

[3] M. A. Kojdecki, E. Ruiz de Sola, F. J. Serrano, E. Delgado-Pinar, M. M. Reventós, V. J. Esteve, J. M. Amigó, J. Alarcón: Microstructural evolution of mullites produced from single-phase gels; J. Appl. Cryst. 40 (2007), 260-276.

15:30 Poster 04-05

Refinement of layer-faulting in Nb_2Co_7 intermetallic compound using DIFFaX+

Andreas Leineweber[1], Matteo Leoni[2]

1. *Max Planck Institute for Metals Research, Heisenbergstrasse 3, Stuttgart 70569, Germany* **2.** *Department of Material Engineering and Industrial Tecnology, University of Trento (DIMTI), v. Mesiano 77, Trento 38100, Italy*

e-mail: a.leineweber@mf.mpg.de

The crystal structure of the intermetallic Nb_2Co_7 phase was identified [1] to be similar to monoclinic Zr_2Ni_7 [2,3]. Parallel layers with a complex internal atomic structure, arranged in a close packed fashion, can be recognised.

The X-ray synchrotron diffraction pattern (ID31 beamline, ESRF, Grenoble -France, λ = 0.400094 Å) of a Nb_2Co_7 powder containing a minor fraction of C15-$NbCo_2$ Laves phase (employed to identify the crystal structure of Nb_2Co_7 [1]), exhibits complex line broadening features (cf. Figure):

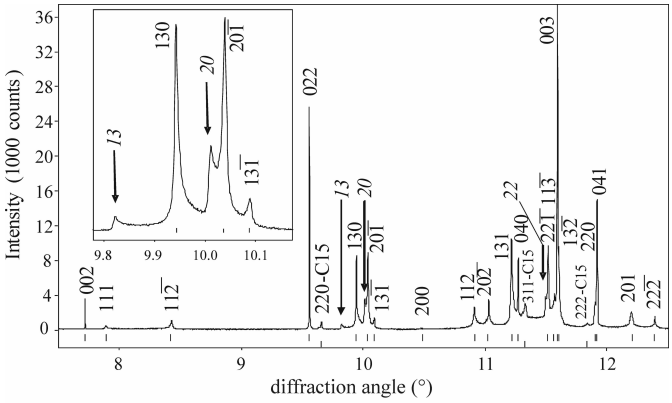

(a) 0*kl* and 5*kl* reflections are narrow. All other reflections are broad.

(b) some unindexed intensity maxima remain.

Those features can be described by an irregular stacking of the above mentioned layers, forming faults in the ideal monoclinic stacking. These faults correspond to local occurrence of the stacking sequence of orthorhombic Yb_2Ag_7 [4], which contains the same type of layers as Nb_2Co_7. Such type of faulting should indeed leave the 0*kl* and 5*kl* reflections unbroadened. Moreover, the unindexed intensity maxima can be understood as low-angle cut-offs of diffuse *hk* intensity bands (see Figure, italic numbers) parallel to **c***. A combined refinement of the crystal and fault structure was performed using the DIFFaX+ software [5], correctly reproducing the mentioned features in the powder diffraction pattern.

[1] A. Leineweber, D. Grüner, F. Stein et al. to be published.

[2] F. R. Eshelman, J. F. Smith, Acta Cryst. B 28 (1972) 1594.

[3] E. Parthé, R. Lemaire, Acta Cryst. B 31 (1975) 1879.

[4] G. Cordier, R. Henseleit, Z. Kristallogr. 194 (1991) 146.

[5] M. Leoni, A. F. Gualtieri, N. Roveri, J. Appl. Cryst. 37 (2003) 166.

15:30 Poster 04-06

Modeling crystallites and r.m.s. microstrain distributions with anisotropic broadening in the Rietveld method

Luca Lutterotti

Department of Material Engineering and Industrial Tecnology, University of Trento (DIMTI), v. Mesiano 77, Trento 38100, Italy

e-mail: luca.lutterotti@ing.unitn.it

Rietveld refinement programs even if they may include some fundamental parameter approach to model instrument broadening, they always rely on a functional description of line broadening due to microstructural characteristics. For anisotropic broadening instead they include either the description of Popa [1] or Stephens [2] to account for it. A methodology is presented here as used in the Maud Rietveld program to model line broadening using directly crystallite size and r.m.s microstrain distributions without resorting to any line profile function. The peak profile is computed directly from the convolution of the two distributions and finally convoluted also with the instrumental part. Combination of lognormal and gamma distributions are used for the crystallites and an appropriate function is used for the microstrain distribution as described by Lutterotti et al. [3]. The

methodology follow closely the description in [3] but has been adapted to the Rietveld method incorporating also a general description of the anisotropic crystallite shape and microstrain in analogy to what presented by Popa and Balzar in [1]. The methodology prove to be robust for Rietveld refinement and the computation speed is sufficient for normal refinements. The method has been successfully applied to different samples and in some cases the fitting quality improves significantly respect to an equivalent approach (even using anisotropic broadening) constrained by functional peak description as used traditionally by Rietveld programs. When applied to the broadened ceria sample of the Size-Strain-Round-Robin for the ESRF BM16 beamline data the Rwp of the fitting drop from 4.6% to 3.9% using distributions instead of peak functions to model the broadened profile (see figure). The size-strain results using the distribution modeling are in agreement with the assessed results, not showing problems related to gaussian crystallite broadening as in the case of peak function fitting.
[1] Popa N. and Balzar D. (2005). Acta Cryst., A61, C79. [2] Stephens P. W. (1999). J. Appl. Cryst., 32, 281-289. [3] Lutterotti L. and Scardi P. (1992). Advances in X-Ray Analysis, 35A, 577-584.

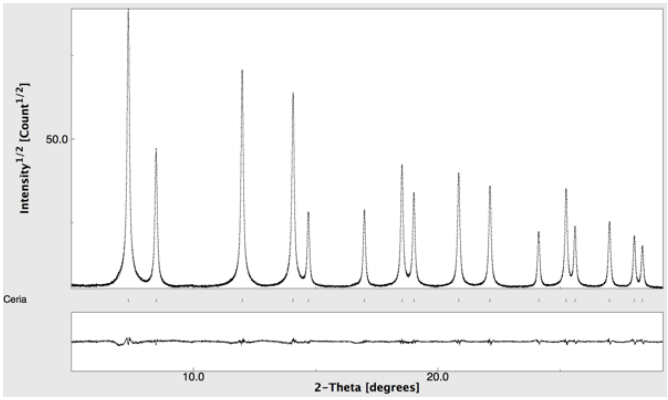

15:30 Poster 04-07

Crystallite size of kaolinites as indicator of different geochemical types of bauxite in Maestrazgo area (NE Spain)

Guillermo Cozzi[1], Joaquin Bastida[2], Ángel Álvarez Larena[3], Marek A. Kojdecki[4], Pablo R. Pardo[2]

1. *Servicio Geológico Minero (SEGEMAR), Julio Argentino Roca, 651, Buenos Aires 1067, Argentina* **2.** *Valencia University, Department of Geology, Dr. Moliner, 50, Valencia 46100, Spain* **3.** *Universidad Autónoma de Barcelona, Barcelona 08193, Spain* **4.** *Wojskova Akademia Techniczna, Warsaw 00908, Poland*

e-mail: pablo.pardo@uv.es

Classification in 4 types for bauxites of NE, Spain was stated by Combes (1) and then updated in several papers (29, (3), (4).
The Type 1 bauxites correspond to “ss” bauxites of Bardossy (5) and contains the kaolinites of lower FWHM values (6), and were formed from deposits of Types 2 and 3, (1) (4).
A set of kaolinite rich samples representative of different types of bauxites in the Maestrazgo was studied by powder XRD (Philips XPERT diffractometer PW302, data collection: step scanning: 0.02º - 20 sec from 11 to 13.2º 2θ for microstructural analysis of kaolinite in clay fractions. Mineral contents estimation in whole samples was determined by the reference intensity method (7)). Microstructural analysis of kaolinite was performed by the Voigt function method (8) using 001 reflection and LaB6 (NIST SRM660a) as standard. Winfit software (available at http://www.ccp14.ac.uk) was used for fitting.
The ranges of the found values for FWHM (º2θ), <Dv> (Å) and e, are respectively: 0,148-0,428, 150-815 and 0,0019-0,0135.
No clear differences were found in the mineralogical composition of the different types of bauxites, being the main feature of type 1 bauxites the greater values for volume weighted <Dv> sizes from 001 kaolinite reflections. That characteristic for this type of bauxite is related to a longer crystallite growth along ferrallitic alteration and subsequent processes, in agreement with the geological properties of the bauxite deposits.
The highest values for the e strain parameter have been found in kaolinites of bauxites of types 2 and 3 bauxites. The performed sampling does not allow the identification of lower e values for the type 1 bauxite.

References

1. Combes, P.J.: Mém. Centre d'Etudes et Rech. Geol. et Hydrogéol. Montpellier 1969.
2. Molina, J.M.; Salas, R.: Cuad. Geol. Ibérica, 7 (1993), 207-230.
3. La Iglesia, A.; Ordoñez, S.: Bol. Soc. Esp. Mineral, 13(1990), 81-90.
4. Ordóñez, S.; Fort, R.; Bustillo, M.: Est. Geol., 46 (1990), 373-384.
5. Valeton, I.: Bauxites. Developments in Soil Science., Nº 2. Elsevier, Amsterdam 1972
6. Cozzi, G.; Bastida, J.; Alvarez Larena, A.; Martinez, S.; Pardo, P: Geo-Temas, 8 (2005), 42-46.
7. Hubbard, C. R.; Snyder, R.: RIR - Measurement and Use of RIR in Quantitative X-ray Diffraction. Powder Diff. 3 (1988), 2, 74-77.
8. Langford, J.I.: A rapid method for analysing the breadths of diffraction and spectral lines using the Voigt function. J. Appl. Crystallogr. 11 (1978), 10–14.

Acknowledgements. Generalitat Valenciana project: No GV02-527.

15:30 Poster 04-08

Dynamical features of X-ray integrated diffracted intensity from small crystallites

Michael B. Shevchenko

G. V. Kurdyumov Institute for Metal Physics of the National Academy of Sciences (IMP), Vernadsky Blvd. 36, Kiev UA03680, Ukraine

e-mail: mishevch@yahoo.com

As it is well known, integrated intensity is one of the most important characteristics of X-ray diffraction analysis which is widely used for study of microstructure of materials [1]. However, simulation of this value may run into serious difficulties in the case of deformed crystallites. Therefore, a further development of theoretical foundations of X-ray diffraction with lattice distortions is an actual physical problem.

In the present paper, integrated diffracted intensity is calculated for strongly bent crystallites, which are entirely randomly oriented as well. The dynamical ‘fine structures’ effects, predicted early for X-ray rocking curve [2], are also established for the integrated intens-

ity. These extinction effects are due to the X-ray interbranch scattering, activated by strong deformations. It is necessary to note that they are size-related effects occurring for crystallites the thickness of which is of the order of the interbranch extinction length. This length is of a small value being considerably less than the X-ray extinction length for an ideal crystal. Moreover, it is shown that the interbranch anomalies of the integrated intensity depend on the value of Bragg angle, such that they increase significantly with increasing the angle.

It is worth to point out that the described effects, such as asymmetrical broadening and splitting of the main peak of the integrated intensity are caused by the long–range strain field which varies with depth. At the same time, the field changing along the surface may be responsible for shift of the main peak. These facts could be of interest for study of topology of the strain fields inside the given crystallite.

References:

[1] Mittemeijer E., Scardi P., *Diffraction Analysis of Microstructure of Materials*, (Springer, Berlin 2004)

[2] Shevchenko M., *Acta Crystallogr.* A 63 (2007) 273-277

15:30 Poster 04-09

Comparison of two standards for powder X-ray diffraction

Marek A. Kojdecki, Witold Z. Mielcarek, Krystyna Prociów, Joanna B. Warycha

Electrotechnical Institute, Division of Electrotechnology and Materials Science (IEL), M. Skłodowskiej-Curie 55/61, Wrocław, Poland

e-mail: m_kojdecki@poczta.onet.pl

Instrumental line-profiles measured as parts of X-ray diffraction patterns may be interpreted as convolutions of instrumental line-profiles and pure line-profiles, containing information on crystalline microstructure of investigated materials. Instrumental line profiles are important for precision of powder X-ray diffraction analyses. They can be measured from a standard material of same composition as a studied material that consists of sufficiently big and unstrained crystallites to ensure negligible contribution to line-profiles from crystalline microstructure in comparison to contribution from all instrumental factors. Frequently such standard can be hardly obtained and some standard reference material should be used instead. This substitution makes necessary further numerical procedure for determining instrumental line-profiles corresponding to Bragg angles for a material under study. In this work two standard materials, lanthanum hexaboride and zinc oxide, are compared and possible source of little discrepancy between X-ray diffraction patterns from them is revealed. Lanthanum hexaboride (NIST SRM 660a) was supported by NIST (with certificate No MD20899, mean crystallite size of 8.8 μm and cubic unit cell parameter of 0.41569162 nm ± 0,00000097 nm). Zinc oxide powder was produced by crystallisation from vapour. The measurements were performed by using a powder diffractometer (DRON) in the Bragg-Brentano configuration with radius of 180 mm, equipped with a cobalt X-ray tube (BWS-29), emission slits of 2 mm, receiving slit of 0.5 mm and Soller slit of 2°30'. X-ray diffraction pattern were recorded in range 20°-164° 2θ in scanning mode with step of $\Delta 2\theta=0.01°$ and counting time 3sec/step. The line profiles from lanthanum hexaboride were described by using fundamental parameter approach [1] and from them the line profiles corresponding to Bragg angles from zinc oxide were computed and compared with those from zinc oxide. The crystalline structure of SRM 660a was accounted [2]. The conclusions will be presented.

[1] R.W. Cheary, A. Coelho: A fundamental parameter approach to X-ray line-profile fitting, J. Appl. Cryst. 25 (1992), 109-121.
[2] C.T. Chantler, N.A. Rae, C.Q. Tran: Accurate determination and correction of the lattice parameter of LaB_6 (standard reference material 660) relative to that of Si (640b), J. Appl. Cryst. 40 (2007), 232-240.

Total scattering

MS5 posters
Sunday afternoon, 21 September, 15:30

15:30 Poster 05-01

Total scattering and Pair Distribution Function analysis of size-stabilised cubic/tetragonal zirconia

Giulio Borghini[1], Monica Dapiaggi[1], Filippo Maglia[2]

1. *Università di Milano, Dipartimento di Scienze della Terra, via Botticelli 23, Milano 20133, Italy* **2.** *Università di Pavia, Dipartimento di Chimica Fisica, viale Taramelli 16, Pavia 27100, Italy*

e-mail: giulio.borghini@unige.it

Zirconia (ZrO_2) primarily exists in three different polymorphs at ambient pressure: monoclinic (room temperature-1175°C), tetragonal (1175-2370°C), and cubic (2370-2680°C). The high-temperature ZrO_2 phases are suitable for various industrial applications such as solid electrolytes in solid oxide fuel cells and sensors, as a catalyst/catalyst support, and as membranes and dispersed phase in composite materials. Traditionally, high temperature ZrO_2 phases have been stabilized at room temperature by doping bi and trivalent cations, such as Y, in the ZrO_2 lattice. The high-temperature cubic or tetragonal phases can also be stabilized at room temperature without doping, provided ZrO_2 is synthesized in its nanocrystalline form with a grain size lower than a critical value (about 20-30 nm). Five different ZrO_2 samples were studied, with the following compositions: sample 1 (pure ZrO_2, no doping), sample 2 (0.5% Y), sample 3 (1% Y), sample 4 (2% Y) and sample 5 (4% Y). The aim of this study is double-fold: on one side the standard crystallographic techniques were used to check for the presence of size-stabilised polymorphs and to evaluate the crystal size and the microstrains present, while, on the other side, a PDF study of size-stabilised zirconia would provide information on local distortions of the nano-particles, on their temperature evolution, and on the eventual presence of significant surface defects, together with their nature. Moreover, such a study provides the relationship of the presence of size-stabilised polymorphs with the actual size of the particles and their local distortions, supplying thus a major step in the understanding of the profound reasons for size-stabilisation effects. Only the two samples with the higher Y content showed no monoclinic zirconia at all. All

the other samples showed small amounts of the monoclinic phase (no more than 10% wt of monoclinic ZrO_2). Moreover, the higher the Y content, the less distorted the structure: sample 4 and 5 could be fitted (in a classical Rietveld refinement) with the cubic structure (fluorite type), while the others were fitted with the tetragonal structure. Total scattering experiments produced well defined PDFs, where the monoclinic polymorph was easily distinguishable from the tetragonal one. As an add on to traditional crystallography, the PDF fits showed a misfit in the low R region (below about 10 Å), probably due to a distortion in the local structure, produced by the limited spatial coeherency of the nano-particles. The origin of the local distortion is still under study.

15:30	Poster	05-02

Nanosize and superparamagnetism in $Ce_{1-x}Gd_xO_{2-x/2}$ samples investigated by PDF and EPR

Michela Brunelli[1], Marco Scavini[2], Cesare Oliva[2], Serena Cappelli[2]

1. *Europen Synchrotron Radiation Facility (ESRF), 6, Jules Horowitz, Grenoble 38000, France* **2.** *Università di Milano, Dipartimento di Chimica Fisica ed Elettrochimica, via Golgi, 19, Milano 20133, Italy*

e-mail: brunelli@esrf.fr

CeO_2-based materials ($Ce_{1-x}M_xO_{2-x/2}$; M = Gd, Y, Sm) have been intensively studied in the last years as catalysts, structural and electronic promoters for heterogeneous catalytic reactions and oxide ion conducting electrolytes for electrochemical cells. In particular, for use in electrochemical cells, $Ce_{1-x}Gd_xO_{2-x/2}$, solid electrolytes are characterised by an ion conductivity higher than conventional Yttria-Stabilized-Zirconia-based ones and would be able to operate at lower temperatures (500 - 700°C).

Thermodynamics transport and magnetic properties of nanostructured compounds can be quite different from that of bulk materials. In our recent works, the relation between the magnetic properties and the nanosize of Ce0.8Gd0.2O1.9 samples have been investigated. It will be shown that nanostructured Ce0.8Gd0.2O1.9 samples shows superparamagnetic behaviour. The extent of the inner field Ha is a function of the particle dimension (see Fig.1).

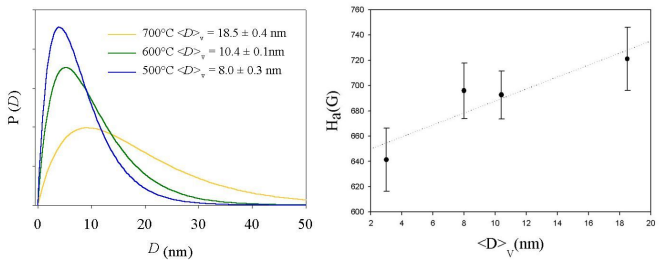

Figure 1: Left particle size distribution P(D) obtained throughout Warren-Averbach analysis for $Ce_{0.8}Gd_{0.2}O_{1.9}$ nanocrystals; right internal field Ha as a function of particle diameter (DV) for the same composition.

The local structure of $Ce_{1-x}Gd_xO_{2-x/2}$ samples has been investigated by means of PDF analysis. In Fig. 2 the *G(r)* function of a microstructured $Ce_{0.8}Gd_{0.2}O_{1.9}$ sample (black) is shown as well as the *G(r)* function relative to two nanostructured phases of the same compound. The *G(r)* amplitude of the nanostructured samples decreases rapidly at high *r* values due to the limited particle size.

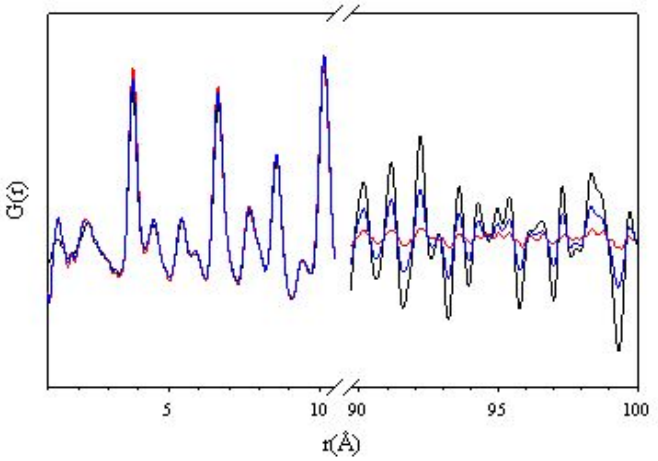

Figure 2: *G(r)* function relative to $Ce_{0.8}Gd_{0.2}O_{1.9}$ samples in the 1.5 < *r* < 10 Å and 90 < *r* < 100 Å regions. Black = microstructured; blue = sol-gel nanosample annealed at 700 °C; red = sol-gel nanosample annealed at 500 °C.

The local distortions introduced by Gd doping and nanosize structure of $Ce_{1-x}Gd_xO_{2-x/2}$ samples will be discussed.

15:30	Poster	05-03

Powder diffraction studies of mixed titanium zirconium phosphates

Victoria A. Burnell, Jennifer E. Readman, Joseph A. Hriljac

School of Chemistry, University of Birmingham, Edgbaston, Birmingham B152TT, United Kingdom

e-mail: vxb216@bham.ac.uk

Issues relating to the removal and storage of radionuclides are important as they are a key component for the use of nuclear power to generate energy and because of the threat of "dirty bombs" by terrorists. Therefore, research into materials that can sequester cations like Sr^{2+} from water must continue and consequently there has been a renewed interest in layered zirconium phosphates due to their ion-exchange abilities [1, 2]. It has been suggested that the ion-selectivity of zirconium phosphate could be altered by the presence of titanium [3]. Only two previous literature reports of mixed titanium zirconium phosphates exist, but these were poorly crystalline materials [3, 4] so little structural characterisation was undertaken. Here we present the synthesis and structure of a series of crystalline layered mixed titanium zirconium phosphates ranging from α-zirconium phosphate to α-titanium phosphate, and in situ powder XRD studies of their thermal decomposition.

Both traditional Rietveld methods and pair distribution function analysis (PDF) of powder X-ray diffraction data [5] are being used to characterise the structures. It was found that at low doping levels the materials are structurally similar to the end member that they are compositionally closest to, and no ordering of the titanium or zirconium was found. However, at higher substitution levels PDF methods suggest the presence of two closely related phases, thus implying that there are solubility limits for both series end members.

PDF studies are currently being used to refine the local and long range ordering enabling a comparison of the Ti:Zr ratio within these areas to the average structure.

The exchanged phases were thermally decomposed and monitored with variable temperature XRD.

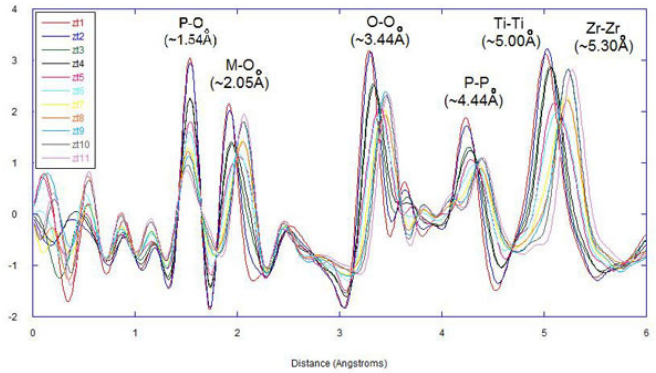

Figure 1: PDF results for the series $Zr_xTi_{1-x}(HPO_4)_2.H_2O$ where x = 0, 0.1, 0.2, 0.3, 0.4, 0.5, 0.6, 0.7, 0.8, 0.9 and 1. The peaks represent the atomic distances within the structures.

References:
1) Clearfield,A., Costantino,U., Comprehensive Supramolecular Chemistry 7, 107, (1996).
2) Alberti,G., Acc. Chem. Res., 11, 163, (1978).
3) Clearfield, A., Frianeza, T. N., J. Inorg. Nucl. Chem. 40, 1925, (1978).
4) Jingnasa, A., Rakesh, T., Uma, T., J. Chem. Sci. 118, 185, (2006).
5) Billinge, S. J. L., Kanatzidis, M. G., Chem. Commun. 749, (2004).

15:30 Poster 05-04

Structural anisotropy in metallic glasses induced by mechanical deformation

Wojtek Dmowski[1], Takeshi Egami[1,2]

1. *University of Tennessee (UTK), Knoxville, TN, United States*
2. *Oak Ridge National Laboratory (ORNL), One bethel Valley Road, Oak Ridge, TN 37932, United States*

e-mail: wdmowski@utk.edu

Advanced X-ray facilities allow use of the pair distribution function to study new aspects of local atomic structure. The anisotropy in a metallic glass is usually ignored because it is small and difficult to measure. However, the use of an area detector and high flux/high energy X-ray sources makes such studies practical. In particular it is interesting to examine structural changes induced by a mechanical deformation. There is general consensus that glass deformation must be accompanied by some local rearrangement of atoms to accommodate shear strain. However, disordered nature of a glass and small deformation volumes make it difficult to observe such atomic rearrangement experimentally. In addition the elastic strain induces structural anisotropy. Consequently, spherically averaged Fourier transformation cannot be used to obtain the pair distribution function, and for example, strain-stress analysis becomes confounded. However it is feasible, in case of high symmetry deformation, to perform expansion in terms of the spherical harmonics of both structure and pair distribution functions, whose anisotropic components are now related by the spherical Bessel transformation. We studied in-situ structure of a glass under macroscopic external stress in an elastic regime and during, and after homogenous plastic deformation (high temperature creep). The experiment was carried out at APS using high energy X-ray setup (~ 100 keV). We examined structural anisotropy and processed the data using the expansion in terms of Legendre polynomials (l=2, uniaxial anisotropy). We found that mechanical deformation involved rearrangement in clusters of atoms by local bond exchange. Such events are the atomistic mechanism of anelastic and plastic deformation and supports structural anisotropy in the deformed state. Figure 1 shows evidence of a structural anisotropy after the creep deformation.

This work was supported by the U.S. DOE under DE-AC05-00OR-22725.

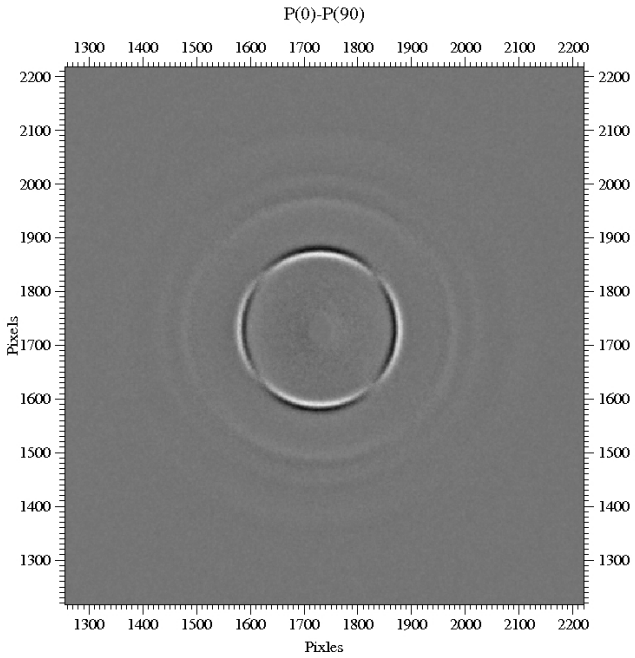

15:30 Poster 05-05

Possibilities and limitations of X-ray diffraction using high-energy X-rays on a laboratory system

Hans Te Nijenehuis, Milen Gateshki, Martijn Fransen

PANalytical, Lelyweg 1, Almelo 7600AA, Netherlands

e-mail: Milen.Gateshki@panalytical.com

Recent interest in nanomaterials has increased the need to analyze structures on a local (nano) scale. However, the atomic structures of nanoparticles and nanostructured materials are not accessible by conventional methods used to study crystalline materials because of

the short ordering range in these materials. One of the most promising techniques to study nanostructures using X-ray diffraction is the total scattering pair distribution function (PDF) analysis. This technique is successfully applied in a number of areas in materials science and technology.

The PDF analysis technique makes use of high quality, high energy X-ray scattering data, usually obtained at synchrotron facilities, available in several national and international research centers around the world.

Despite the advantages that measurements at synchrotron beam lines offer to the researcher, in practice it can be difficult and time-consuming to obtain access to the facilities required. In order to be prepared as good as possible and to make optimal use of the valuable experiment time offered, it is highly desirable to perform selective measurements on candidate samples in one's own research laboratory.

New developments in XRD technology have been directed towards the possibility of performing nanocrystallography experiments on a standard laboratory X-ray diffraction system. In this presentation we will report on the possibilities and limitations of the use of high-energy X-rays on a laboratory system.

15:30 Poster 05-06

Crystal structure solution from pair distribution function

Pavol Juhas[1], Phillip M. Duxbury[2], Simon J. Billinge[1]

1. *Columbia University, New York, NY 10027, United States* **2.** *Michigan State University (MSU), East Lansing, MI 48824-1322, United States*

e-mail: pj2192@columbia.edu

The atomic Pair Distribution Function (PDF) technique has been increasingly used to study local structure deviations in crystalline materials or nano-crystalline materials that are not accessible to traditional crystallographic methods. However, PDF analysis is not simple and typically consists of time consuming trial-and-error tests of different structure models. Recently we have demonstrated that a different approach - the Liga algorithm where trial models are built iteratively [1] - can solve the structure of fullerene molecules from PDF data alone. The Liga procedure did not require any prior structure model, however it was restricted to single-component molecules. We have extended the method to handle periodic boundary conditions and multi-component systems. We will demonstrate how it can be used to solve structures of several common crystals from both artificial and experimental PDFs. The application to materials with partially known structures will be discussed as well. [1] P. Juhas, D. M. Cherba, P. M. Duxbury, W. F. Punch, S. J. L. Billinge, Ab initio determination of solid-state nanostructure, Nature 440, 655-658 (2006).

15:30 Poster 05-07

Structure and microstructure of Mg-vermiculite

Arancha Argüelles[1,2], Matteo Leoni[3], Charles H. Pons[4], Cristina De la Calle[5], Jesús A. Blanco[1], Celia Marcos[6]

1. *University of Oviedo, Department of Physics, C/ Calvo Sotelo, Oviedo 33007, Spain* **2.** *Instituto Tecnologico de Materiales (ITMA), Parque Tecnológico del Principado de Asturias, C/ Calafates, Parcela L-3.4, Avilés 33417, Spain* **3.** *Department of Material Engineering and Industrial Tecnology, University of Trento (DIMTI), v. Mesiano 77, Trento 38100, Italy* **4.** *Institut des Sciences de la terre d'Orléans (ISTO), 1A, rue de la férollerie, Orléans 45071, France* **5.** *Instituto de Ciencia de Materiales de Madrid, CSIC (ICMM, CSIC), Cantoblanco, Madrid 28049, Spain* **6.** *University of Oviedo, Jesus Arias de Velasco, Oviedo Oviedo, Spain*

e-mail: Matteo.Leoni@unitn.it

Mg-vermiculite from Santa Olalla (Spain) has been the object of several studies in the literature, although controversial results still exists on its crystal structure. Traditional Rietveld refinement based on literature data does not lead to satisfactory modeling of the experimental powder diffraction pattern, due to the presence of features which are typical of disordered layered silicates. New results relative to the structure and microstructure have been recently obtained. Powder diffraction data has been refined by means of the DIFFaX+ software, showing the lattice to possess just 2D periodicity instead of a tridimensional one: the structure can be described as a disordered sequence of two different types of layers. Stacking probabilities were refined and the effect of water in the interlayer is evidenced.

15:30 Poster 05-08

Neutron diffraction and total scattering for the study of solid state ionics materials

Lorenzo Malavasi[1], Cristina Tealdi[1], Hyunjeong Kim[2], Thomas Proffen[2], Simon J. Billinge[3], Giorgio Flor[1]

1. *Università di Pavia, Dipartimento di Chimica Fisica, viale Taramelli 16, Pavia 27100, Italy* **2.** *Los Alamos National Laboratory (LANL), Los Alamos, NM 87545, United States* **3.** *Michigan State University (MSU), Chemistry Bldg, Lansing 48824, United States*

e-mail: lorenzo.malavasi@unipv.it

In this work we are going to present recent results on the application of neutron diffraction and neutron total scattering for the study of solid state ionics material, in particular of fast oxygen ion conductors (such as $La_2Mo_2O_9$, LAMOX, and $Ba_2In_2O_5$) and proton conductors oxides (barium cerates). It will be shown that in several cases the only application of neutron diffraction does not reveal all the features of these materials, particularly in the conducting phases, even though ND is a power tool in order to extract information on oxygen and proton ions within these compounds. On the other hand, pair distribution function analysis of total neutron scattering data (which takes into account both the Bragg peaks and the diffuse scattering) allow to correlate the local structure between the low-T (not

conducting) and high-T (conducting) phases of a solid state ionics materials.

References:

[1] L. Malavasi, C. Ritter, G. Chiodelli, *Chem. Mater*. (2008) **20** 2343-2351.

[2] L. Malavasi, H. Kim, S.J.L. Billinge, Th. Proffen, C. Tealdi, G. Flor, *J. Am. Chem. Soc.* (2007) **129** 6903-6907.

[3] C. Tealdi, L. Malavasi, C. Ritter, G. Flor, G. Costa, *J. Solid State Chem.* (2008) **181** 603-610.

15:30 Poster 05-09

Long and short range order in Laves phase deuterides

Radovan Cerny[1], Joanna Ropka[1], Valérie Paul-Boncour[2], Michel Latroche[2]

1. *University of Geneva, 24 quai Ernest-Ansermet, Geneva 1211, Switzerland* **2.** *Institut de Chimie et des Matériaux Paris Est (ICMPE), 2-8, Henri Dunant, Thiais 94320, France*

e-mail: Joanna.Ropka@cryst.unige.ch

The deuterides of cubic (C15) Laves phases have been widely studied for the influence of deuterium absorption on their magnetic properties. The systems YFe_2D_x and YMn_2D_x are particularly interesting due to the large variety of crystal structures depending on the D content [1,2]. When absorbing deuterium the metallic matrix retains the cubic cell (*Fd*3*m*) above the deuterium ordering temperature. Below this temperature the symmetry is lowered and a fully ordered coordination of metals by deuterium atoms is obtained in the deuterium rich phases. Complex structures with up to 12 metal atoms and 18 deuteriums in the asymetric unit as for monoclinic $YFe_2D_{4.2}$ [3] are formed. Little is known about the local deuterium configuration around the transition metal atoms in the disordered phase even if a considerable amount of diffuse intensity was reported in the neutron powder patterns.

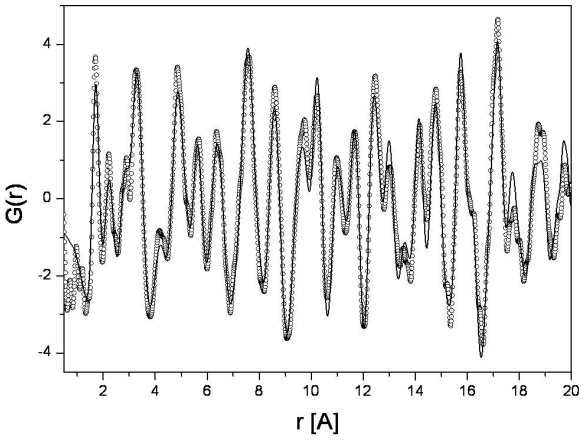

Figure 1. Observed PDF (points) of $YFe_2D_{4.2}$ in disordered state: Modelling (solid line) by same local order of deuterium atoms around iron as in the ordered phase.

Analysis of YFe_2D_x and YMn_2D_x by Rietveld and Pair Distribution Function (PDF) methods will be presented. Neutron Time-of-Flight (ToF) data were collected at IPNS, Argonne, and Lujan Center, Los Alamos on series of samples with different deuterium content. Each sample was measured below and above the temperature of deuterium ordering. The PDF in ordered and disordered states look very similar up to the radial distance of ~ 8 Å, which is comparable with the lattice parameter of a cubic Laves phase deuteride. The observed PDF was modeled in the disordered state using the same local model as in the ordered phase (Figure 1).

[1] Latroche M., Paul-Boncour V., Przewoznik J., Percheron-Guégan A. & Bourée-

Vigneron F.; *J. Alloys Compounds***231** (1995) 99-103

[2] Paul-Boncour V., Guénée L., Latroche M., Percheron-Guégan A., Ouladdiaf B. &

Bourée-Vigneron F.; *J. Solid State Chem*. **142** (1999) 120-129

[3] Ropka J., Paul-Boncour V. & Černý R.; in preparation

Stress and texture analysis

MS6 posters
Sunday afternoon, 21 September, 15:30

15:30 Poster 06-01

Effect of texture heterogenities on the shape memory properties of rolled Fe-Mn-Si SMA

Ana V. Druker[1], César E. Sobrero[1], Jorge A. Malarría[1], Ulf Garbe2, Heinz-Gunter Brokmeier[2], Raúl E. Bolmaro[1]

1. *Instituto de Física Rosario (IFIR), Bv. 27 de febrero 210 bis, Rosario 2000, Argentina* **2.** *GKSS Research Centre, Geesthacht, Germany, Geestacht, Germany*

e-mail: bolmaro@ifir.edu.ar

We have investigated an Fe-30Mn-4Si shape memory alloy to clarify the effect, on the bulk texture, of the shear layers resulting of two different thermo-mechanical treatments. RX analysis has shown the existence of texture heterogeneity through the rolled sheets thickness, due to the effect of friction between sheet and rolls. Neutron diffraction reveals that textured layers affect the whole volume. Texture found on the surface of the sheet rolled at 600ºC, is the most favourable for the $\gamma \rightarrow \varepsilon$ martensitic transformation witch is the origin of the shape memory effect. Comparing these results with those obtained on sheets rolled at room temperature, we found that shear deformation gradients produce changes on the material bulk texture. Tensile tests induce martensitic transformation initially in those grains favourably oriented. As a result, those favourable orientations disappear in remnant austenite.

15:30 Poster 06-02

Experiments and simulation evaluation in quartz veins textures in the Guamanes shear belt, Córdoba Pampean Ranges, Central Argentina

Andrea L. Fourty[1], Heinz-Gunter Brokmeier[2], Roberto D. Martino3, Raúl E. Bolmaro[1]

1. *Instituto de Física Rosario (IFIR), Bv. 27 de febrero 210 bis, Rosario 2000, Argentina* **2.** *GKSS Research Centre, Geesthacht, Germany, Geestacht, Germany* **3.** *Universidad Nacional de Córdoba (UNCOR), Av. Velez Sarsfield 299, Córdoba 5000, Argentina*

e-mail: bolmaro@ifir.edu.ar

Texture characterization of deformed rocks allows the confirmation of kinematically determined deformation processes occurring during geologic events at plate margins and in intraplate settings. The understanding of such processes is of both basic and economical importance to decipher deformation regimes, mechanisms and PT conditions. The Guamanes deformation belt (GDB) is a shear zone at Sierras de Córdoba (Argentina) which extends approximately 45 kilometers parallel to the 64°50'00" meridian. Its width varies in between 1 and 4 kilometers and can be subdivided in a northern and southern tracts. The southern part has been already quite well studied with a complete description of its milonitic rocks and the kinematic. Filonites in the northern tract and milonites with filonites and non deformed rocks in the southern tract apparently separate two well defined domains of deformation. Two different deformation events, one ductile followed by a brittle stage, have been identified. We will present ductile textures developed in quartz veins included in strongly deformed granitic pegmatites which were intruded in the shear belt during the deformation. The data will be analyzed by regular texture analysis and viscoplastic self consitent simulations. The kinematic inferred from the simulations indicates a main reverse sense of displacement with a minor sinistral component developed in a simple shear regime.

15:30 Poster 06-03

A primer on whole through processing simulation understanding of high temperature rolling - phase transformation - low temperature rolling and annealing textures in low carbon steels

Analía Roatta, Andrea L. Fourty, Raúl E. Bolmaro

Instituto de Física Rosario (IFIR), Bv. 27 de febrero 210 bis, Rosario 2000, Argentina

e-mail: bolmaro@ifir.edu.ar

Processing steels to achieve particular useful properties is a science as well as an art. Many of the properties of modern steels are a successful combination of empiric and scientific knowledge. Deep drawing low carbon steels have been used and improved through many decades of research and technological advance. However the micro mechanisms involved in the development of particular microstructures and properties are still under discussion. The current paper shows an integrated attempt to obtain consistent microscopical data from micromechanical simulations coupled with recrystallization and phase transformation codes. The simulations are performed in a way such that the information obtained from certain temperature, level or process is used in the next step to proceed further. The goal is not avoiding experiments but having a whole through scale and time integration for judging the validity of similar parameters and assumptions during the different processing steps. The simulations include high and low temperature deformation and recrystallization in the austenite region, phase transformation to room temperature, low temperature deformation and recrystallization in the ferrite phase region. The results are compared with experiments available in the literature.

15:30 Poster 06-04

Investigation of microstructural anisotropy of limestone

Ladislav Kalvoda[1], Maja Dlouhá[1], Martin Dráb[1], Jan Drahokoupil1, Alexander Grishin[1], Jiri Marek[1], Petr Sedlak[2], Stanislav Vratislav[1], Jindrich Hladil[3], Martin Chadima[3], Winfried Kockelmann[4]

1. *Czech Technical University in Prague, The Faculty of Nuclear Sciences and Physical Engineering, Trojanova 13, Prague 2, Prague 12000, Czech Republic* **2.** *Institute of Thermomechanics v.v.i., Academy of Sciences of the Czech Republic, Dolejskova 5, Prague 12000, Czech Republic* **3.** *Czech Academy of Sciences, Institute of geology (IG), Rozvojová 269, Prague 16500, Czech Republic* **4.** *Science and technology facilities council, Rutherford Appleton laboratory, Didcot OX110QX, United Kingdom*

e-mail: ladislav.kalvoda@fjfi.cvut.cz

Composition, crystalline structure and microstructural anisotropy of limestone is investigated by means of instrumental neutron activation analysis (INAA), X-ray diffraction (XRD), neutron diffraction (ND) and measurement of anisotropy of magnetic susceptibility (AMS) and anisotropy of resonant ultrasound spectroscopy (ARUS). The samples were collected near Choteč, Bohemia (Na Škrábku quarry, SE corner; 49°59'19.57" N, 14°16'44.16" E), from a single overturned/recumbent fold. Elementary composition of the investigated limestone (INAA) is dominated by Ca (34.72 mass %), Mg (4733 ppm), Fe (2253 ppm), K (1967 ppm) and Al (1185 ppm). In addition, traces of another 33 elements are present having concentration higher then 1 ppm. Total organic carbon (TOC) concentration is only ~0.15 mass %. Calcite (~ 98.5+-1 mass %) and quartz (~ 1.5+-1 mass %) were identified by phase analysis of XRD powder patterns as the prevailing mineral phases. Based on ND powder data, crystalline structure of calcite was refined within the space group R-3c giving the lattice parameters a = 0.4915(4) nm and c = 1.6800(14) nm. Crystallographic preferential orientation (CPO) of the crystalline calcite cement filling the initial sediment pores is weak (XRD and ND data). Obtained ARUS patterns exhibit sharp resonances approving the complete pore filling. The calculated sharpness (f) of the orientation distribution functions (ODF) calculated for individual samples was f < 3. The observed mean polar angle (Beta) between the c-poles and the original sedimentation direction (SD) varies with the point of sample collection within the broad range: Beta = 0^{o} - 60_{o}. Orientation of (110) poles around the <0001> direction is practically isotropic.
Small positive values of the mean magnetic susceptibility (χ) were obtained by KLY-2 bridge measurement): $\chi = 3 - 8 \times 10^{-9}$ m^3 kg^{-1}. It

is apparent that the intrinsic diamagnetic contribution of calcite is balanced by an extrinsic para-/ferro-magnetic contribution. Noisy AMS results caused only the direction of the pole to the magnetic foliation (MF) could be identified. The observed mean MF deflection from SD varies in accord with the textural Beta-value.

This research has been supported by grants MSM6840770040, AV0Z30130516 and GACR205/08/0767.

15:30 Poster 06-05

The use of extinction phenomenon for investigation of textured thin film microstructure

Tetyana G. Kryshtab, Andriy Kryvko, Jose Alberto Andraca-Adame, Gabriela Gomez Gasga

Instituto Politécnico Nacional, Depto. de Ciencia de Materiales, (ESFM), Unidad Prof. ALM, Edif. 9, Zacatenco, Zacatenco, México 07338, Mexico

e-mail: tkrysh@esfm.ipn.mx

Texture and microstructure (domain size, dislocation density, concentration and effect of dopants incorporation, etc.) of thin films strongly influence on device operating characteristics. An increase of grain size and the improvement of grain crystalline quality lead to decrease of diffraction peak broadening when the evaluation of microstructure by common methods is impossible. In this case the dynamic scattering processes can take place and phenomenon of extinction can be observed. The characteristics of the primary and secondary extinction are related to the crystal microstructural feature and can be used for its evaluation [1]. It was shown in our previous work [2] that the phase transition temperature of ZnS:Cu thin films can be decreased by using of Cl as co-doping element and some annealing conditions. The explanation of the effect on the base of thin film microstructure was proposed.

We present the results of the structural investigations of ZnS:Cu thin films as-deposited and after a special annealing. The evaluation of thin film microstructure was performed by separation of the extinction phenomenon in pole density (PD) and determination of the coefficients of the primary and secondary extinction. To the best of our belief, the primary and secondary extinction simultaneously for microstructure determination of textured thin films have not been applied.

The ZnS:Cu thin films were deposited by electron beam evaporation method onto $BaTiO_3$ substrates with thickness of 0.8 – 1.6 μm. The annealing and doping with Cu, Cl and Ga were carried out at 800 - 950° C during one hour. The structural analysis was carried out by XDR techniques using D8 Bruker X-ray diffractometer with two non-polarized Cu and Co radiations. Low and high index reflections were measured. As-deposited ZnS:Cu films were strongly textured in <111> direction and had a cubic structure. After the annealing of ZnS:Cu films and doping with Cu, Cl and Ga a phase transition at lower temperature was observed. The values of PD in pole figures for the films measured for the first and second order reflections, showed the presence of extinction. The determined parameters of the extinction allowed to evaluate the domain thickness from the values of the primary extinction and the extinction length, and the average domain misorientation angle from the value of the secondary extinction and also the dislocation density N_D at domain boundaries. In the films with the strong phase transition the dislocation density decreased noticeably that leads to more homogeneous distribution of Cu and Cl in Zn and S sublattices and, hereby, increase the amount of Cu-Cl binding that affects the phase transition temperature.

1. Kryshtab T., Palacios-Gomez J., Mazin M. and Gomez-Gasga G., Acta Materialia, 2004, 52/10, 3027.

2. T. Kryshtab, V.S. Khomchenko, J.A. Andraca-Adame, V.B. Khachatryan, M.O. Mazin, V.E. Rodionov, M.F. Mukhlio, J. Crystal Growth 275, 2005, e1163.

15:30 Poster 06-06

Comparison of hkl-dependent microstrain broadening and of hkl-dependent macrostress-induced sample-orientation dependent peak shifts in cementite, Fe_3C, compound layers grown on α-iron

Thomas Gressmann, Marc Nikolussi, Andreas Leineweber, Eric J. Mittemeijer

Max Planck Institute for Metals Research, Heisenbergstrasse 3, Stuttgart 70569, Germany

e-mail: a.leineweber@mf.mpg.de

Macrostressed polycrystalline thin surface layers will in case of intrinsic elastic anisotropy and variable grain orientation also exhibit microstrain. The microstrain distribution will lead to microstrain broadening of the diffraction peaks, which may provide valuable information about the overall state of stress/strain in the layer (see e.g. [1]). However, most macrostress-studies by diffraction techniques, e.g. using the $\sin^2\psi$ method, do not consider the line broadening of the diffraction peaks. That is partly due to the often relatively large instrumental broadening of the diffractometers dedicated to (macro)stress analysis, masking the structural line broadening.

The present contribution deals with synchrotron X-ray powder diffraction measurements (B2, HASYLAB Hamburg) on cementite layers (thickness 4.6 μm) grown on α-iron using gaseous nitrocarburising [2]. The instrumental configuration was chosen to combine the possibility for specimen tilting with high instrumental resolution. Analysis of the average reflection positions as a function of the specimen-tilting angle ψ reveals compressive stresses in the cementite. The slopes of the largely linear $\sin^2\psi$ plots depend strongly on the reflection indices *hkl*, i.e. the maximum and minimum slopes differ by a factor of about 1.7. This *hkl*-dependence can be explained by the strong elastic anisotropy of cementite [3].

The microstrain broadening of the different reflections is also strongly *hkl* dependent. In fact, those reflections showing large widths exhibit also large (in absolute terms) slopes in the $\sin^2\psi$ plots (cf. Figure). Methods for a systematic comparison of the *hkl*-dependent slopes and line widths will be presented.

[1] C. M. Sayers, Phil. Mag. A 49 (1984) 243.

[2] T. Gressmann, M. Nikolussi, A. Leineweber, E. J. Mittemeijer, Scr. Mater. 55 (2006) 723.

[3] M. Nikolussi, S. L. Shang, T. Gressmann, A. Leineweber, E. J. Mittemeijer, Y. Wang, Z.-K. Liu, submitted for publication.

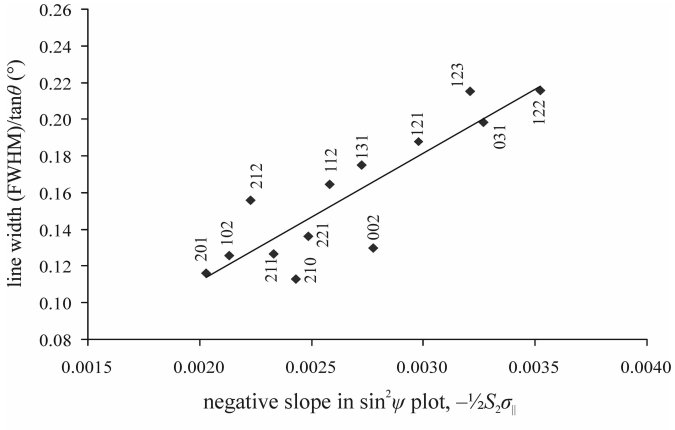

15:30 Poster 06-07

Extracting single crystal like structure factors simultaneously with the texture analysis from powder diffraction

Luca Lutterotti

Department of Material Engineering and Industrial Tecnology, University of Trento (DIMTI), v. Mesiano 77, Trento 38100, Italy

e-mail: luca.lutterotti@ing.unitn.it

As already demonstrated by Wessel et al. it is possible to take advantage of texture to extract single crystal like structure factors. Their actual procedure involves: a) the preparation of a textured sample, b) the analysis of the ODF (Orientation Distribution Function) by a dedicated measurement and analysis using the traditional pole figure measurement and c) few high resolution spectra measurements to extract structure factors using the ODF as input. In the present work we outline a procedure to make a joint extraction of structure factors and ODF simultaneously. In particular the structure factors and the ODF are simultaneously refined in subsequent iteration cycles using only one set of data that may include or not high resolution spectra. The ODF is analyzed from the same spectra used for the structure factors extraction using a Rietveld like texture analysis. Everything has been implemented in the Rietveld software Maud. For the texture part the EWIMV method incorporated in Maud is well suited for general textures, where the standard components method may give better convergences for highly monomodal texture functions as found in fiber materials. The structure factor extraction is performed through a modified Le Bail procedure that can limit the overlapping part by using a reduced peak range. All the extracted structure factors from different spectra are weighted using the ODF obtained by the simultaneous texture analysis and are used as starting point for the subsequent iteration cycle. Cell, line profile parameters and errors are also refined all together in a Rietveld like fashion refinement. Minor phases or a second phase may be incorporated as well, so not limiting the procedure to only pure compounds. The main advantages of this procedure are: 1) only one measurement/instrument is needed for the experiment, thus eliminating possible misplacements between one measurement and another and reducing the total experimental time, 2) only one analysis tool is needed and 3) the joint refinement aim to improve the accuracy of the extracted structure factors. There are also some disadvantages as the structure factor extraction needs indeed high resolution spectra with long measurement time where the texture need more spectra at different tilting of the sample to be measured. The two goals are not easily comprised in one experiment/instrument. We will show how the joint extraction can be done and how it can improve the accuracy of the extracted structure factors or otherwise being conducted on a lesser resolution set of data. Wessel T., Baerlocher Ch. and McCusker L. B. (1999). Science, 284, 477-479.

15:30 Poster 06-08

Extinction of X-ray diffraction from strong textured silver samples

Jesús Palacios Gómez, Elsa Yazmín León Marroquín

Instituto Politécnico Nacional, ESFM, Depto. de Ciencia de Materiales, Unidad Prof. ALM (ESFM), Edif. 9, Zacatenco, México, Zacatenco, México 07338, Mexico

e-mail: palacios@esfm.ipn.mx

Pole figures 111 and 222 of annealed high purity silver samples with a strong texture were measured with X-ray diffraction in order to estimate secondary extinction influence on texture determination. Since both pole figures arise from the same planes, and lower index reflections are more strongly affected by extinction, differences of pole densities between both pole figures should be attributed to this phenomenon.

Samples were first slightly rolled and then heated to 600ºC through a ramp rate of 300ºC/h and kept at this temperature for 4 hours. Then they were 91.5% cold rolled and heated to 800ºC through a rate of 600ºC/h and kept at this temperature for 4 further hours. As a result a strong one component texture was obtained.

Maximum pole densities of pole figure 222 were about 25% higher than those of pole figure 111, as expected when extinction is present. In order to rule out that this difference comes from primary extinction, the sample was slightly hammered out and then measured again, delivering similar results.

Conventional mosaic crystal extinction correction techniques were applied to obtain the true maximum pole densities. Corrected maximum pole density was about 39% higher than the one of pole figure 111 and about 9% higher than that of pole figure 222.

However secondary extinction parameter g resulted about 10^5 which implies an average crystallite orientation deviation of about 1 second of arc. This seems not consistent with the width of the texture peak which has a broadening of about 1º. Although no clear argument could be made for this result, it could be interpreted in the following way: the beam diffracted from the strong textured polycrystal can substantially be diffracted again out of the detector direction, only by a second crystallite with a very close orientation to the first diffracting crystallite.

Anyway it is clear that the conventional correction for mosaic crystals should be improved to be applicable to textured polycrystals.

15:30 Poster 06-09

Structural characterization of surface layers in Distaloy-AE and DistaloyHP

Stanisław J. Skrzypek[1], Anders Bergmark[2], Marcin Goły[1], Wiktoria Ratuszek[1], Krzysztof Chruściel[1]

1. *AGH, Faculty of Metals Engineering and Industrial Computer Science, 30 Mickiewicza Av., Kraków 30-059, Poland* **2.** *Höganäs, Höganäs 263-83, Sweden*

e-mail: skrzypek@agh.edu.pl

Purpose of this paper is to elaborate X–ray diffraction methodology for to characterize some chosen qualitative parameters of products made of AE and HP Distalloys. The beneficial feature of diffraction methods is non-destructive character and large number structural informations contained in diffraction pattern. Therefore they have potential ability in application to technological operations and fatigue or corrosion life control.

Design/methodology/approach. The qualitative and quantitative phase analysis (Tab.1) classical *sin²?* and modified *g-sin²?* methods were used (Tab.2). The profile diffraction line analysis (PDLA) was used to lattice distortion <e> and to average crystalline size evaluation. All methods were elaborated for both i.e. classical Bragg-Brentano (BB) and grazing incidence angle X-ray diffraction (GID) geometry. In the case of last one, the mentioned above properties can be scanned versus depth under surface in non–destructive way

Tab.1. Results of QXDPA with texture correction method and GID geometry. Wavelength lCoK$_a$, RA – retained austenite (non-destructive mode).

Sample - side B(r), method		GID – 10 peaks, Thickness of Measured Layer [mm]					
3.8	7.2	10.3	14-15	16-19			
a5	*RA vol.[%]*	18.2	19.6	17.9	18.4	18.1	
a8	*RA vol.[%]*	27.2	30.1	32.8	29.4	30.9	
h6	*RA vol.[%]*	19.8	22.1	23.1	26.8	24.3	
h8	*RA vol.[%]*	37.1	40.1	39.0	41.3	37.6	

Tab.2. Tab.2. Results of residual macro-stresses in measured points on samples. Wavelength lCoK$_a$, direction of measurement for residual stress: x - longitudinal, y– transverse, diffraction line {211}Fe$_a$, , σ_x, σ_y –*sin²y* method, σ_x – *g-sin²y* method.

Sample			Layer thickness [μm], *g-sin²y*					B-B (211), *sin²y*
3.8	**7.2**	**10.3**	**14-15**	**16-19**				
a5	σ_x [MPa]		134	93	84	8	20	36
	σ_y [MPa]		-	-	-	-	-	68
a8	σ_x [MPa]		142	37±4	22±4	43±8	20±5	38
	σ_y [MPa]		-	-	-	-	-	-5
h6	σ_x [MPa]		21±2	121±21	146±20	71±9	84±11	23
	σ_y [MPa]		-	-	-	-	-	17
h8	σ_x [MPa]		64±6	94±11	169±13	66±7	-9±3	84
	σ_y [MPa]		-	-	-	-	-	53

Findings in this type of sintered samples diffusion growth in solid along grains take place during sintering. The gradients of elements concentration versus grain cross-section and the irregular space distribution of retained austenite make this alloy as composite with gradient-like microstructure. This gradient-like structure is confirmed here by residual macroscopic stresses measurement, quantitative X ray diffraction phase analysis, micro-stresses and texture factor.

Research limitations/implications. The irregular distribution of retained austenite indicates to no uniformity in larger scale then the irradiated volume due to particular X-ray diffraction method (compared results for BB and GID diffraction). The ability of X-ray diffraction methods based on GID geometry to scan structural properties layer by layer is promising to this type of composite-like materials. Whole these results confirm non-uniformity of structural and phase composition. This approach can be used to characterize structural properties of thin surface layer or film invisible with traditional geometry.

Practical implications Relations between above structural features and some properties at selected points on the samples will hopefully provide more general concluding and beneficial issues in term of quality of sinters.

15:30 Poster 06-10

Neutron RTOF Diffractometers for residual stress investigation at FLNP JINR

Andrey Tamonov, Anatoli Balagurov, Gizo Bokuchava, Vyacheslav Sumin, Igor Papushkin

Joint Institute for Nuclear Research, Dubna, Russian Federation

e-mail: tamonov@nf.jinr.ru

Two special time-of-flight diffractometers are used for residual stress measurements at FLNP JINR at IBR-2 pulsed reactor in Dubna, Russia. These are High Resolution Fourier Diffractometer (HRFD) [1] and Fourier Stress Diffractometer (FSD) [2] and their principle operation is based on an application of the reverse time-of-flight (RTOF) method – a kind of correlation technique – at long pulsed neutron sources. Such a way, high resolution in interplanar spacing ($Dd/d \approx 1 \cdot 10^{-3}$) can be achieved, while maintaining high flux at the instrument. The main advantage of the RTOF-method, as well as of the usual TOF-method, is the possibility to measure simultaneously several reflections, fact which allows to determination the residual strains along various (hkl) directions in a crystal. Moreover, the HRFD resolution function has rather simple dependence on interplanar spacing *d*, which allows one to easily estimate microstrain averaged on all (hkl) directions from analysis of width of several diffraction peaks.

Nowadays, all necessary equipments for a such an experiment (the linear scanner, 5-axis goniometer "HUBER" for a measurement of the full residual strain tensor, the loading machine "TIRA-test" for in-situ experiments and definitions of materials elastic properties, a mirror furnace for an investigation of materials at high temperatures [up to 1000°C]) are operable. All of these devices can be used simultaneously that allows expanding experiment's opportunities and for example allows defining the dependence of material elastic properties on temperature etc.

This work presents the results obtained from residual stress measurements in various materials and devices spent in FLNP JINR.
References:

1. V.L.Aksenov, A.M.Balagurov, V.G.Simkin, V.A.Trounov, P.Hiismaki et al., *J.Neutron Research*, **v.5**, p.181, 1997.
2. A.M. Balagurov, G.D. Bokuchava, E.S. Kuzmin, A.V. Tamonov, V.V. Zhuk., *Zeitschrift fur Kristallographie,* 2006, Supplement Issue no. 23, pp.217-222.

15:30 Poster 06-11

Synchrotron investigations of non-uniformly shaped shot-peened samples

Andrew M. Venter[1], Corrie La Grange[3], Felix Hofmann[2], Teasung Jun[2], Jonathan Belnoue[2], Rudolph Van Heerden[1], Alexander M. Korsunsky[2], Alexander Evans[4]

1. *Necsa Limited (NECSA), Church Street West Extension, Pretoria 0001, South Africa* **2.** *Oxford University, Department of Engineering Science, Oxford OX13PJ, United Kingdom* **3.** *LIW Division of Denel, Pretoria 0001, South Africa* **4.** *European Synchrotron Radiation Facility (ESRF), Grenoble 38043, France*

e-mail: amventer@necsa.co.za

Shot peening is an important surface impact treatment widely used in industry to improve the performance of metallic parts subjected to fatigue loading, contact (fretting) fatigue, stress corrosion and other damage mechanisms by inducing beneficial compressive residual stresses in the surface region. Residual stresses induced by shot-peening are not limited to the material surface regions, but may extend to depths of up to 1mm into steel, depending on the shot-peening intensity and the material properties. The conditioning process is quantified using the ALMEN calibration method where a flat reference plate is simultaneously shot blasted in parallel to the sample being treated. This verification procedure however does not take into account differing material geometries, surface properties and residual stresses existing in practical specimens due to their manufacture. Direct quantification of the extent of the beneficial compressive residual stresses induced through the shot-peening process has become essential due to the occurrence of premature fatigue failures through cracking. We report a quantitative assessment of the efficiency of shot-peening on conical samples treated at three different shot-peening intensities, compared to a water quenced (without shot peening conditioning), as well as a control sample (as reference).

Investigations were performed at the ID31 instrument on 2mm thick slices wire EDM cut from the respective bulk conically shaped 17-4PH stainless steel samples to facilitate transmission measurements at contant pathlength through the sample thickness as function of depth below the surface. Results of the in-plane and surface normal components of residual strain indicate significant differences between line scans taken at three locations from the tip, reflecting an underlying material thickness dependence. An exploratory line scan taken at 3mm from the tip in the bulk of a conical sample indicates substantially larger compressive strains existing at the near surface region. The latter indicates that significant relaxation of the residual strains had occurred due to the sectioning of the slices.

15:30 Poster 06-12

Texture research of metals, polymers and rocks on the KSN-2 neutron diffractometer

Stanislav Vratislav, Maja Dlouhá, Ladislav Kalvoda, Martin Dráb

Czech Technical University in Prague, The Faculty of Nuclear Sciences and Physical Engineering, Trojanova 13, Prague 2, Prague 12000, Czech Republic

e-mail: stanislav.vratislav@fjfi.cvut.cz

From the industrial point of view the research activities of the Laboratory of Neutron Diffraction (Faculty of Nuclear Sciences and Physical Engineering CTU Prague) are concentrated to the quantitative texture analysis based on the ODF (orientation distribution function). We have developed the experimental and data treatment procedures for this type research. The texture experiments were carried out on the neutron diffractometer KSN-2 using the TG-1 texture goniometr. This diffraction device offers good intensity with wavelengths in the range 0.095 to 0.141 nm and the best resolution value of $\Delta d/d = 0.007$ was reached in the region $d \sim 1.0 \div 0.1$ nm (d is interplanar spacing).

Now, the KSN-2 was upgraded by means of the (311) bent monochromator unit and by the PSD system consists the bank of the three linear position tubes with 25.7 mm in the diameter and 670 mm in the active length and the resolution was improved to the $\Delta d/d = 0.002$ in the d-region from 1.4 to 0.075 nm, the neutron flux on sample is about 2.5 times higher, the sample volume is 4.5 times smaller and "in-situ" experiments are available.

The quantitative texture analysis of neutronographic pole figures or inversion pole figures recorded is treated by means of these codes: popLA, TODF-N, MAUD and Rietveld analysis method (texture analysis version: GSAS package, FULLPROF).

Quantitative texture analysis by means neutron diffraction data were used on the investigation of the many samples of the technically interesting materials. For example, we have determined the texture parameters on the oriented Si steel sheets, the zirconium alloys (tubes for nuclear reactors), polymer materials (PVC foils) and rock materials (CaCO3 test samples).

On the basis of our results we have proved that the KSN-2 diffractometer together with the above mentioned software codes is very important and powerful tool for understanding the texture development with respect to the mechanical and the thermal processes.

This research has been supported by the MSM6840770021 project.

15:30 Poster 06-13

Evaluation of macro and micro-strain in the surface modification layer peened by cavitation shotless peening

Nao Yamada[1], Arnt A. Kern[2], Lutz Bruegemann[2], Hitoshi Soyama[3]

1. *BRUKER AXS K.K, 3-9-A, Moriya-cho, Kanagawa-ku, Yokohama-shi, Kanagawa 221-0022, Japan* **2.** *Bruker-AXS (BAXS), Östliche Rheinbrückenstr. 49, Karlsruhe D-76187, Germany* **3.** *Graduate School of Engineering Tohoku University,Department of Nanomechanics, Sendai 980-8579, Japan*

e-mail: nao.yamada@bruker-axs.jp

Abstract. In order to verify the detail of macro and micro-strain in the surface modification layer peened by cavitation shotless peening (CSP), macro and micro-strain is investigated using X-ray diffraction method, as macro-strain is evaluated by residual stress and micro-stain is evaluated by profile fitting approach. Surface modification is effective solution for improving strength on material surface, and there were three kinds of method, which are shot peening (SP), laser peening (LP), and CSP. CSP is using cavitation impact, and is not required shot in the process. In order to establish optimised surface modification, accurate evaluation for macro and micro-strain are required. In previous researches, compressive residual stress is introduced as macro-strain and full width of half maximum (FWHM) of peak profile is wide before SP. However, it was found that compressive residual stress is introduced as macro-strain, even though FWHM of peak profile is sharp before peening in the case of CSP. As the results of analysing peak profile using fundamental parameter (FP), it was observed that micro-strain is released in surface modification layer by CSP.

1. Introduction

Peening method for metal surface making use of cavitation impacts is called "cavitation shotless peening (CSP)"[1-4], as shot in the process is not required. It was proven that CSP improved fatigue strength and life time for forging die[5] and gears[3] using various metals[1-4]. There have been some interest reports that CSP is possible to improve fatigue strength with compressive residual stress less than SP[2], and compressive residual stress is observed, even though FWHM of peak profile is decreased before peening. FWHM of peak profile in XRD measurement depends on X-ray geometry, crystallite size, and crystallite strain (micro-strain). Thus, in the case of CSP, there is possibility that micro-strain is released with introducing compressive residual stress as macro-strain at the same time. However, macro-strain in the surface modification layer has been evaluated by conventional method as $\sin^2\psi$ method, and micro-strain has been evaluated as FWHM value of peak profile so far. In the present paper, it was found that the transition of macro and micro-stress is evaluated with the processing time of CSP, as macro-strain is approached by 2D method[7] using triaxial stress model, and micro-stress is evaluated by fundamental parameter (FP) [8-9].

2. Experiments

CSP instrument which can generate a cavitation jet in air[6] was used in this testing. The tested material was tool steel alloy Japan Industrial Standard (JIS SKD61). The size of specimen was 45 mm in length, 15 mm in width, and 18 mm in thickness. The processing

time per unit length t was defined from the scanning speed v and number of scans n as equation (1).

$$t=n/v \qquad (1)$$

Micro-strain of the specimen was calculated from peak profile using FP. The XRD data for micro-strain were collected by θ–θ diffractometer and Bragg Brentano geometry equipped with Cu tube operated at 40 kV, 40mA and Cu $K\alpha$ radiation was used. The step size of scan was set as 0.02 degrees and the exposure time was set as 20 seconds per step. Divergence slit and anti-scattering slit were set as 0.5 degrees, receiving slit was set as 0.1 mm, and axial soller slit was set at incident side and receiving side as 2.5 degrees. Detector was chosen as solid state detector. α-Fe (110), (200), and (211) were collected for micro-strain analysis. The data for macro-strain were collected by horizontal diffractometer using two-dimensional (2D) detector equipped with Cr tube operated at 35 kV, 40mA and flat graphite monochromator was used at incident side and Cr $K\alpha$ radiation was used. X-ray beam was collimated as 0.8 mmφ. α-Fe (200) (2θ =106 degrees) was collected for residual stress measurement. Exposure time was set as 10 minutes per frame and 21 frames were collected with changing φ and ψ axis. The residual stress of normal stress σ_{11}, σ_{22}, σ_{33} and shear stress σ_{12}, σ_{13}, σ_{23}, were calculated from 21 frames by using 2D method. Young's modules and Poison's ratio were used 210 GPa and 0.28.

3. Results and Conclusions

The σ_{11} direction of residual stress on the surface as a function of processing time per unit length is shown figure 1. The compressive residual stress was increased approximately -600 MPa to -1000 MPa with increase of the processing time by CSP. The compressive residual stress is saturated and almost stable with an increase the processing time $t \geq 4$ s/mm. However, the compressive residual stress was obviously increased with an increase the processing time $t \leq 2$ s/mm. This means that the compressive residual stress is certainly increased as macro-strain by CSP. Figure 2 shows that the micro-strain, which was evaluated using FP at α-Fe 110, 200, and 211 reflections. The micro-strain was decreased with increase of the processing time by CSP at all reflections

In the present paper, it was proven that the micro-strain, which might be introduced by the heat treatment and mechanical finishing, was released less than 1/10 by CSP, even though CSP introduced the compressive residual stress. Additionally, it was concluded that the micro-strain in the face of metal polycrystalline is possible to be evaluated using FP.

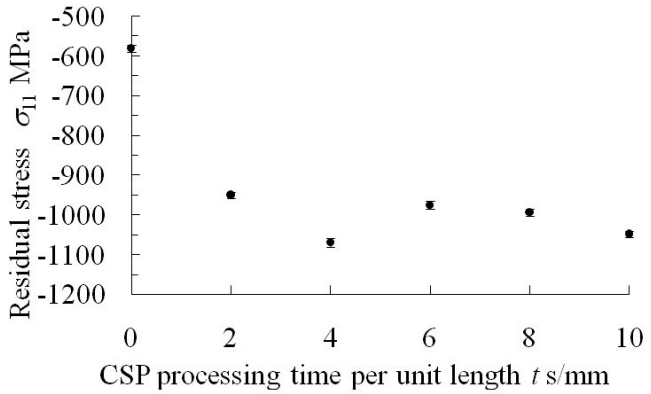

Figure1. Introduction of residual stress σ_{11} by CSP

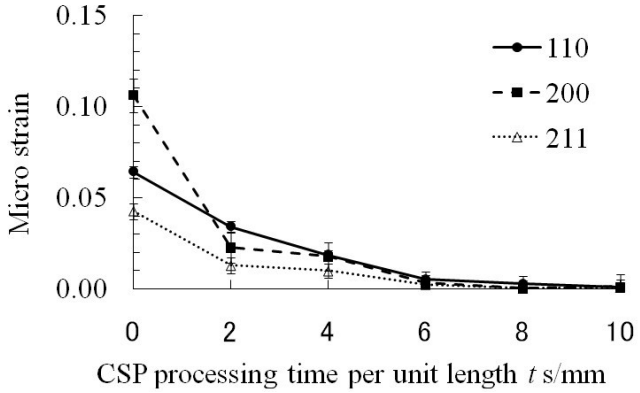

Figure 2. Releasing micro strain by CSP

References

1. H. Soyama, K. Saito and M. Saka, *Journal of Engineering Materials and Technology, Trans. ASME*, **124**-2, 2002, pp. 135-139.

2. D.Odhimbo and H. Soyama, *International Journal of Fatigue*, **25**-9~11, 2003, pp.1217-1222.

3. H. Soyama and D. O. Macodiyo, *Tribology Letters*, **18**-2, 2005, pp. 181-184.

4. H. Soyama, *Metal Finishing News*, **7**-2, March Issue, 2006, pp. 48-50.

5. H. Soyama, Y. Takano and M. Ishimoto, *Technical Review of Forging Technology*, **25**-82, 2000, pp. 53-57 (in Japanese)

6. H. Soyama, *Journal of Engineering Materials and Technology*, *Trans*. *ASME*, **126**-1, 2004, pp. 123-128.

7. B. B. He and K. L. Smith, *Proc*. *Inter*. *Conf*. *OnResidual Stress*, 1997, pp. 634-639.

8. H. P. Klug and Alexander, *X-ray Diffraction Procedures – 2nd Edition*, J. Wiley and Sons Inc., New York, 1974, pp.996.

9. A. A. Kern and A. A. Coelho, A New Fundamental Parameters Approach in Profile Analysis of Powder Data, Allied Publishers Ltd., 1998, pp.141-151.

Acknowledgements. This work was partly supported by Japan Society for the Promotion of Science under Grant-in-Aid for Scientific Research (B) 17360047.

Quantitative phase analysis

MS7 posters
Sunday afternoon, 21 September, 15:30

15:30	Poster	07-01

Quantification of complex disordered phases by a parallelized Rietveld program

Joerg Bergmann[1], Kristian Ufer[2], Reinhard Kleeberg[2]

1. *Private, Ludwig-Renn-Allee 14, Dresden 01217, Germany*
2. *Freiberg University of Mining and Technology, Mineralogical Institute, Brennhausgasse 14, Freiberg 09596, Germany*

e-mail: email@jbergmann.de

The correct modeling of diffraction patterns of disordered layered structures within the Rietveld method is a need for more accurate quantitative phase analysis (QPA) e.g. of clay-bearing rocks. Different approaches have been developed to approximate the diffraction profiles of distorted layered structures. Simple anisotropic (hkl dependent) line broadening models based on small ideal unit cells are often not sufficient to describe the real disorder features. Alternative approaches like the one-dimensional elongation of cells in the "single layer approach" (Ufer et al., 2004), combined with the recursive description of layered structures (Treacy et al., 1991) result in the generation of a large number of atomic positions respective a high number of diffraction peaks. This leads to an immense computational effort.

Especially the recursive calculation method requires large quantities of computing power. Nowadays, multi-core CPUs become more accessible and widely used in modern PCs. So it suggested itself speeding up these calculations by parallelizing the Rietveld code. Consequently, the used Rietveld program BGMN was multithread-enabled.

As a principle of development, the BGMN system remains highly portable. Wrapper functions were written for the basic multithreading operations. Therefore, the parallelized BGMN remains usable under Windows as well as under Linux. The principles of parallelization will be described in brief.

The capability of the enhanced computation procedure will be demonstrated on multiple examples. Benefits and features of this Rietveld code will be discussed. The speedup of computation on different hardware/operating systems, for simple mixtures as well as for samples containing multiple disordered phases, will be shown. In practice, a phase quantification of mixtures containing up to 14 minerals including 4 heavily disordered clay minerals was possible with satisfying results within 30 min on a dual Quad Core computer.

[1] K. Ufer, G. Roth, R. Kleeberg, H. Stanjek, R. Dohrmann, J. Bergmann,
Description of X-ray powder pattern of turbostratically disordered layer
structures with a Rietveld compatible approach.
Z. Kristallogr. 219 (2004) pp. 519-527
[2] M. M. J. Treacy, J. M. Newsam, M. W. Deem,
A general recursion method for calculating diffracted intensities from
crystals containing planar faults.
Proc. R. Soc. London A433 (1991) 499-520

15:30 Poster 07-02

Quantitavive analysis and FT-IR study of clay raw materials and thermal treated bricks

Juan A. G Carrió[1], Izabela C A. Dutra[1], Mauro C. Terence[1], Rosane Toledo[2], Denise R. Santos[2], Edmar V. Mota[2]

1. *Presbyterian University Mackenzie (UPM), Rua da Consolação 930, Sao Paulo 01302-907, Brazil* **2.** *Universidade Estadual do Norte Fluminense Darcy Ribeiro (UENF), Ave. Alberto Lamego 2000, Campos do Goytacazes 28013-600, Brazil*

e-mail: jgcarrio@mackenzie.br

In this work we present results on the structutural properties of clay deposits localized in northern Rio de Janeiro sate in Brazil, where this kind of soil is abundant and used for production of ceramics, maily brics and roof tiles. The soil samples were dried, grounded and passed through a sieve with nominal aperture of 840 μm. The resulting homogeneus powder was very representative of the natural soil, which presents 95% particles with grain sizes below 50 μm. This powder was extruded in order to obtain bricks with average dimensions of 100 X 20 X 10 mm. The bricks were dried in air at room temperature during one week and subsequently at 110 ^{o}C during 24 hours. Thereafter the bricks were submitted to a slow firing process in a furnace of high heat capacity. The temperature was slowly raised up to 600 ^{o}C and kept constant during 60 minutes in order to avoid cracks owing to a quartz phase transition that occurs at 575 ^{o}C. Then the temperature was increased to a firing temperature T_f, and kept at this value during 180 min. Subsequently the sample was cooled at a controlled rate of 1.5 ^{o}C/min. Similar procedures were applied for preparing bricks with T_f = 300, 400, 500, 600, 700, 800, 900, 950, 1000, 1050, 1100 and 1200 ^{o}C. Powder diffraction data were collectes from the treated brick with a conventional diffractometer Seifert URD65. The experimental conditions were $3^{o} \leq 2\theta \leq 75^{o}$, $\Delta 2\theta = 0{,}02^{o}$ and counting time 3 s. A granulometric study of untreated samples was performed and alowed a quantitative analyse of three different fractions by the Rietveld method using the refinement program GSAS. Samples from differents soil depths treated at 1200 ^{o}C were also quantitatively analyzed and showed small differents in their compositions of cristobalite, mullite and hematite. The effect of the thermal treatment in the clay structural properties was also analyzed by FT-IR spectroscopy. In the IR region of 780 cm^{-1} to 1010 cm^{-1} were detected different peaks of silicates in dependence of the temperature T_f.

References:

1. Toledo R., Dos Santos D.R., Faria Júnior, R.T., Carrio J.G., Auler L.T., Vargas H.. Gas release during clay firing and evolution of the ceramic poperties. Appl. Clay Sci., Amsterdam, 27, 3-4, 151-157, 2004.

2. Dos Santos D.R., Toledo R., Faria Júnior, R.T., Carrio J.G., Silva M.C., Auler L.T., Vargas H., Evolved gas analysis of clay materials. Rev. Sci. Instrum., Melville, 74, 1, 663-666, 2003.

3. A.C. Larson, R.B. Von Dreele, Los Alamos National Laboratory. Los Alamos, EUA. Copyright, 1985–2000, The Regents of the University of California, 2001.

Acknowledgments: Mackpesquisa, CAPES, FAPERJ

15:30 Poster 07-03

Multidisciplinary analysis of a slope failure at the "Obri Hrad" site in the Sumava Mts.

David Havlicek[1], Filip Hartvich[2]

1. *Charles University, Faculty of Science, Albertov 6, Prague 12843, Czech Republic* **2.** *Czech Academy of Sciences, Institute of Rock Structure and Mechanics, V Holešovičkách 41, Prague 18209, Czech Republic*

e-mail: havlicek@natur.cuni.cz

In this contribution we describe various scientific techniques, which

were used during the research of a multigeneration slope deformation on the archeological Celtic site of "Obri Hrad" near Kasperske Hory (SW Bohemia). Due to a specific local condition, practically no accumulations were left, thus we had to work with other, mostly indirect signs and traces of the older generations of the slope. We have used methods of geomorphology, of engineering geology and geophysics, and last but not least, of X-ray diffraction analysis which has helped to determine the origin of morphologically unclear accumulation remnants.The X-ray diffraction analysis was performed on the samples collected along selected profile. The method was employed in order to validate a hypothesis that the remnants of the accumulation on the right bank of the river are accumulations of a slide, originating on the left bank of the river. In total we have analyzed 11 samples, but one sample (No. 7) was omitted – it has too biased powder pattern, probably due to the weathering. In the samples were qualitatively and semiquantitatively determined a-quartz (33-1161), muscovite 2M2 (25-649), muscovite 2M1 (6-263), muscovite 1M (7-25), microcline (19-932), orthoclase (31-966), biotite 1M (42-1437) and sillimanite (38-471).If we project the results into the profile, interesting features can be observed. Generally, it can be said that samples 3-5 from the center of the slope are very much alike, and they are also very similar to sample 6, which was taken from the presumed slide accumulation. The sample No. 11 is also similar, particularly due to the presence of the sillimanite. The content of biotite 1M differentiates the samples No.8 and No.9. The projection into the profile might suggest a logical conclusion that the mineral content changes not only horizontally, but also vertically with the respect to the foliation planes.

15:30	Poster	07-04

Quantification of active substance in drug by Rietveld analysis

Marta Łaszcz

Pharmaceutical Research Instititute, Rydygiera 8, Warszawa 01-793, Poland

e-mail: m.laszcz@ifarm.waw.pl

The X-ray powder diffraction has variety applications in the pharmaceutical industry. The most popular is a polymorphs diagnostic of an active substance (API - Active Pharmaceutical Ingredient). If API has more than one crystalline form there is a risk that during following steps like: synthesis, milling, formulation and storage an undesirable form appears. For this reason powder diffraction is a main tool for qualitative and quantitative analysis.

The aim of this work was to apply the quantitative Rietveld analysis for an evaluation of API in few commercial drugs. For example, VFEND (Pfizer) tablets contain voriconazole as API. The inactive ingredients include: lactose monohydrate, pregelatinized starch, croscarmellose sodium, povidone, magnesium stearate. Voriconazole[1], lactose[2] and magnesium stearate are crystalline. The others ingredients are amorphous or semi-crystalline. Qualitative analysis detected only voriconazole and lactose. Relative phase amounts, in weight percent, are following: voriconazole 35.63%, lactose 47.39% and amorphous 16.98% (figure below). The calculated voriconazole content is close to the real quantity which is equal 30%.
Measurement time 60min. GOF 5.86, R_{exp} 1.15, R_{wp} 6.74, R_p 5.31.

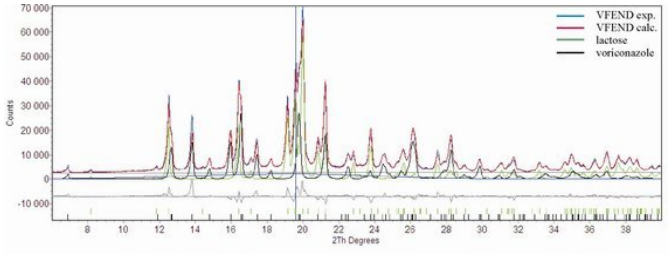

Fig. Quantitative Rietveld analysis of VFEND.

References

[1] K. Ravikumar, B. Sridhar, K. D. Prasad, A. K. S. B. Rao (2007) *Acta Crystallogr., Sect. E.: Struct. Rep. Online*, 63, o565,
[2] J. H. Noordik, P. T. Beurskens, P. Bennema, R. A. Visser, R. O. Gould (1984) *Z. Kristallogr.,* 168, 59.

Acknowledgements

The X-ray measurements were undertaken in the Structural Research Laboratory at the Chemistry Department of the University of Warsaw.

15:30	Poster	07-05

Quantifying uncertainty of the intensity of diffraction peak due to crystallite statistics

Andrzej Zieba

AGH University of Science and Technology (AGH), al. Mickiewicza 30, Kraków 30-059, Poland

e-mail: zieba@novell.ftj.agh.edu.pl

Fluctuations of the diffracted beam intensity resulting from the finite number of diffracting crystallites is called "crystallite statistics". This source of measurement uncertainty is more important that the "counting statistics" for crystallite size larger that one or few micrometers. Nevertheless, hitherto existing investigations of this effect are scarce [1] - [4].

Quantitative input data for quantifying the crystallite statistics are variation of peak intensity I_i observed when the powder sample is rotated or oscillated in step-like manner. The recorded values I_i (i = 1, ... n) are autocorrelated because each diffracting crystallite contributes to a few subsequent data points.

The proper statistical procedures for proceeding the autocorrelated data were given only recently [5], [6], [7]. Standard deviation of the single observation s and standard deviation of the mean s_{mean} are related by the formula $s_{mean} = s /(n_{eff})^{1/2}$ in which n_{eff} is the *effective number of observations* [6] smaller than the number of experimental points n. The value of n_{eff} can be estimated from the experimental autocorrelation function. The proper formula for the unbiased estimator for the variation of the mean reads $s^2_{mean} = [(\mathrm{SUM} (x_i - x_{mean})^2] / [n(n_{eff} - 1)]$ [7].

For crystallite statistics effect standard deviation s represents the uncertainty of the diffraction peak intensity for the fixed sample position and s_{mean} quantifies the effect of averaging due to oscillation or rotation of the sample. Experimental examples are given for both measurement geometries. For Al_2O_3 sample with 30 micrometer grain size its oscillating in the range +/- 1 deg causes a decrease of the relative standard deviation from 6,6% to 1,2%. Spinning of the other exemplary sample decreases the effect by the factor $(n_{eff})^{1/2} = 6$.

This uncertainty of peak intensity propagates directly into uncertainty of the phase content in multiphase sample. It also affects the accuracy of atomic positions in structural analysis. On the other hand quantyfying the crystallite statistics effect makes possible a rough estimate of the crystallite size. This method is effective for grain size range for which the line broadening method cannot be used.

[1] L. Alexander, P. K. Harold, E. Kummer. J. Appl. Phys. 19 (1948) 742.
[2] P. M. De Wolff, J. M. Taylor, W. Parrish. J. Appl. Phys. 30 (1959) 63.
[3] N. J. Elton, P. D. Salt, Powder Diffraction 11 (1996) 218.
[4] D. K. Smith, Powder Diffraction 16 (2001) 186.
[5] Dorozhovets M., Warsza Z. L. Pomiary Automatyka Robotyka, no. 1/2007, p. 18. In Polish with English Summary and Figure Captions.
[6] N. F. Zhang, Metrologia 43 (2006) S276.
[7] A. Zięba. Materials of the conference: *Basic Problems of Metrology* (PPM'08), Sucha Beskidzka, 11-14 May 2008. In Polish with English Summary and Figure Captions.

Combining powder diffraction with other methods

MS8 posters
Sunday afternoon, 21 September, 15:30

15:30	Poster	08-01

X-Ray and electron diffraction studies on layered martensite structures of Copper based shape memory alloys

Osman Adiguzel

Firat University, Department of Physics, Elazig 23169, Turkey

e-mail: oadiguzel@firat.edu.tr

The shape-memory is a particular result of a displacive solid state phase transformation, martensitic transformation, with which the lattice structure changes abruptly. Copper based binary and ternary alloys exhibit shape memory effect in metastable beta-phase field. Martensitic transition occurs in homogenised B2(CsCl) or DO_3(Fe_3Al) -type ordered structures of beta-phase on cooling from high temperatures. Martensitic transformations occur by two or more lattice invariant shears on a {110}-type plane of austenite matrix which is basal plane or stacking plane for martensite, as a first step, and the transformed region consists of parallel bands or layered structures containing alternately two different variants. These variants form internally twinned martensite regions. The product phases have the unusual complex structures, long period layered structures such as 3R, 9R or 18R, depending on the stacking sequences on the close-packed planes of lattice.

Copper alloys are very sensitive to aging effect due to metastable character, and aging in martensitic condition give rise lattice changes and reorganization of atom in lattice sites. This effect leads to martensite stabilization with which atom exchanges occur among the lattice sites in material. This behaviour is a result of diffusional process which affects the character of diffraction profile together with the peak locations and intensities. Both martensitic and post-martensitic transition requires special changes in symmetry and relations between the lattice parameters. In the present contribution, x-ray diffraction and transmission electron microscopy (TEM) studies were carried out on two copper based ternary alloys.

15:30	Poster	08-02

Determination of crystal structures of two new scandium squarates hybrids with powder X-ray diffraction and solid state NMR

Nathalie Audebrand[1], Thierry Bataille[1], Laurent Le Pollès[1], Eva Kotulanova[1,2], Denis Dorso[1]

1. *University of Rennes, Sciences Chimiques de Rennes, Rennes 35042, France* **2.** *Czech Academy of Sciences, Institute of Inorganic Chemistry, Rez near Prague 250 68, Czech Republic*

e-mail: nathalie.audebrand@univ-rennes1.fr

Porous hybrid materials (Material Open-Frameworks MOFs) give rise to numerous applications in gas or solvents storage, catalysis, drug delivery [1-4]... The design of their crystal structures is based on the concept of building units, in which metals and organic ligands are joined according to the most foreseeable connections. In that way, the planar ligand squarate, $C_4O_4^{2-}$, possesses various connexion modes allowing the formation of 2D and 3D frameworks [5,6]. We particularly focused our studies on scandium compounds, because of the duality rare earth – $3d^0$ transition metal. Two isostructural hybrid materials, $(A)_{0.5}Sc(C_4O_4)_2.xH_2O$ [A = $C_4H_{12}N_2$ (**I**) and $C_2H_{10}N_2$ (**II**)], have been prepared as powdered samples by slow precipitation at room temperature. Their crystal structures have been determined *ab initio* from X-ray powder diffraction data and solid state CPMAS NMR. Comp. **I**: a = 12.1080(6) Å, b = 8.2806(3) Å, c = 6.9139(3) Å, a = 91.419(3) °, b = 90.814(3) °, g = 95.489(3) °, V = 689.72(5) Å^3, Z = 2, S.G. P-1. The crystal structure of both hybrids, is constituted of anionic layers of scandium squarates in between which protonated amines and water molecules are intercalated. Nevertheless, examination of difference Fourier maps evidences non negligible residual electronic around the amines. The analysis by solid state NMR 13C spectroscopy (CPMAS), combined to X-ray powder diffraction data, suggests that amines can adopt two different orientations around an inversion centre.

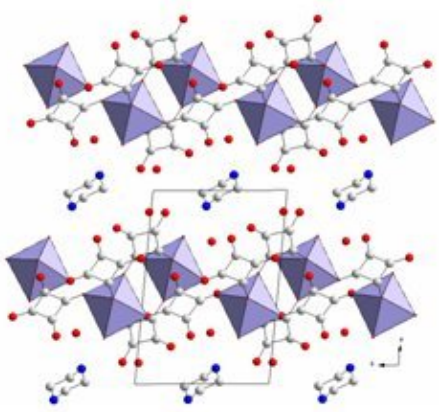

Crystal structure of $(C_4H_{12}N_2)_{0.5}[Sc(H_2O)(C_4O_4)_2]\cdot 3H_2O$

References
[1] G. Férey, Chem. Soc. Rev., 37 (2008) 191.

[2] S. Kitagawa, R. Kitaura, S.-I. Noro, Angew. Chem. Int. Ed, 43 (2004) 2334.
[3] J.L.C. Rowsell, O.M. Yaghi, Angew. Chem. Int. Ed, 44 (2005) 4670.
[4] C. Serre, C. Mellot-Draznieks, S. Surblé, N. Audebrand, Y Filinchuk, G. Férey, Science, 315 (2007) 1828; P. Horcajada, S. Surblé, C. Serre, M. Vallet-Regí, M. Sebban, F. Taulelle, G. Férey, Chem. Comm., 27 (2007) 2820; P. Horcajada, C. Serre, G. Maurin, N. A. Ramsahye, M. Vallet-Regí, M. Sebban, F. Taulelle, G. Férey, J. Am. Chem. Soc., 130 (2008) 6774.
[5] N. Mahé, T. Bataille, Inorg. Chem., 43 (2004) 8379.
[6] S. Neeraj, M. L. Noy, C. N. R. Rao, A. K. Cheetham, Solid State Sci., 4 (2002) 1231.

15:30 Poster 08-03

Structure and thermal behavior investigation of new lanthanide oxalato-squarates by using laboratory X-ray diffraction and TG/DTA combined with simultaneous MS

Patricia Bénard-Rocherullé[1], Hocine Akkari[2]

1. *University of Rennes, Sciences Chimiques de Rennes, Rennes 35042, France* **2.** *Laboratoire de Chimie Moléculaire, Contrôle de l'Environnement et de Mesures Physico-Chimiques, route de Ain El-Bey, Constantine 25000, Algeria*

e-mail: patricia.benard-rocherulle@univ-rennes1.fr

The recent exponential interest in the synthesis and characterization of new hybrid materials with 'organic-inorganic' open-framework have revealed the diversity of such materials in terms of structure, topology, composition. One of the most innovating approaches in microporous materials arises from metal-organic or metal-coordination chemistry where organic moieties act as spacer or linker between metal blocks. The use of oxalates, oxocarbon entities with aromaticity or aliphatic dicarboxylates has increased providing spectacular examples of how the organic ligand symmetry as well as the metal geometry can be exploited for conceiving novel architectures with a view to exploiting interesting properties as magnetism, porosity, ion-exchange ability. The introduction of lanthanides centers within the skeleton create unusual prototype open-frameworks and may give unique properties stemming from their *f-f* electronic transitions for optical properties (oxalic acid has been reported to form, with neodymium, a chiral mixed carboxylate exhibiting NLO properties). For the preparation of new 3D frameworks with potential properties, the use of two anions of different geometry and chemical functions offers immense scope, but has not been investigated systematically with the squarate dianion. The group presents, with the rare-earth elements, a high diversity of unusual coordination modes, including chelation. Our aim is to create novel mixed materials based on lanthanides combined with two anions but wherein an organic rigid moiety is one of the components. By using hydrothermal methods, the first hydrated lanthanum sulfato-squarate has been obtained [1]. Otherwise, as the oxalate acid has been often used to form novel porous metal dicarboxylates, our synthetic efforts have also focused on the possibility to prepare oxalato-squarates. Among our successful productions, pure isostructural *Ln* dicarboxylates [$Ln_2(C_2O_4)_2(C_4O_4)(H_2O)_2$, *Ln* = La, Ce, Pr, Nd] have been obtained hydrothermally, their crystal structure solved by X-ray diffraction. For *Ln* = La and Ce, the thermal decomposition from the hydrated precursor to the finely divided oxide [La_2O_3 (550°C)/CeO_2 (250°C)] has been investigated by X-ray thermodiffractometry. The TDXD results show a common first step of dehydration at 200°C leading to the formation of unknown well crystallized phase, $Ln_2(C_2O_4)_2(C_4O_4)$. After, the two decomposition mechanisms proceed through different steps. For a better understanding of the processes, complementary TG/DTA combined with simultaneous evolved gas analysis using mass spectrometry were carried out. The structure determination from X-ray powder diffraction of the stable anhydrous monoclinic phase $La_2(C_2O_4)_2(C_4O_4)$ is in progress. Finally, an isostructural (La/Eu) phase doped with europium(III) was recently prepared allowing for an extension of our interest to the field of luminescent hydrid phases based on rare earth metals.

[1] H. Akkari *et al.*, Solid State Sci. 8 (2006) 704.

15:30 Poster 08-04

Crystal structure determinations of fluorescent organic yellow pigments from X-ray powder data

Juergen Bruening, Christian Buchsbaum, Edith Alig, Lothar Fink, Jacco Van de Streek, Martin U. Schmidt

Institut für Anorganische und Analytische Chemie, Johann Wolfgang Goethe-Universität, Max-von-Laue-Strasse 7, Frankfurt am Main 60438, Germany

e-mail: bruening@chemie.uni-frankfurt.de

Organic pigments generally have a low solubility. Due to this property single crystals of suitable sizes are rarely obtained. Thus many structures of this class of compounds are determined from the powder patterns. The derivatives of Pigment Yellow 101 [1], compounds **1**-**4**, are almost insoluble in most organic solvents even at 200°C. All compounds show fluorescence in the solid state.

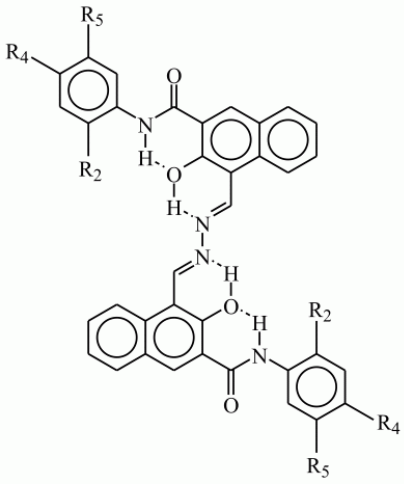

	R_2	R_4	R_5
1:	H	H	H
2:	H	OCH_3	H
3:	H	Cl	H
4:	Cl	H	Cl

The crystal structures of **1**, **2** (α-phase), **3**, and **4** could be determined from laboratory powder data. The powder patterns were measured in transmission on a STOE STADI-P diffractometer with a linear PSD (Cu-$K\alpha_1$, Ge(111)-monochromator). The powders of **1**-**4** showed good crystallinities and the data could be indexed unambiguously using DICVOL. The structure of **1** was solved by lattice energy minimisation using the program CRYSCA [2]. Energy calculations were performed in five space groups. Simulated powder patterns of the proposed structures were compared to the experimental powder dia-

grams. The best matching structure was refined with the program GSAS [3] using restraints for bond lengths, bond angles and planar groups. The structures of compounds **2-4** were solved by real-space methods using the simulated-annealing program DASH [4]. Rietveld refinements were performed using the program TOPAS [5].

[1] W. Herbst, K. Hunger, "Industrial Organic Pigments", 3rd ed., Wiley-VCH, Weinheim, **2004**, S. 570.

[2] M. U. Schmidt, H. Kalkhof, CRYSCA, Frankfurt am Main, **1999**.

[3] A. C. Larson, R. B. von Dreele, GSAS. Los Alamos National Laboratory Report, **1994**, 86-748.

[4] W. I. F. David, K. Shankland, J. van de Streek, E. Pidcock, W. D. S. Moherwell, J. C. Cole, *J. Appl. Cryst*., **2006**, *39*, 910-915.

[5] A. A. Coelho, TOPAS Academic, version 4.1, **2007**.

15:30 Poster 08-05

Crystal structure refinement of Fe^{3+}-rich aerinite from synchrotron powder diffraction and Mössbauer data

Anna Crespi Revuelta, Jordi Rius

Institut de Ciencia de Materials (ICMAB) - CSIC (ICMAB), Campus de la UAB, Barcelona 080193, Spain

e-mail: acrespi@icmab.es

The crystal structure of an Fe^{3+}-rich variety of aerinite has been refined from synchrotron powder diffraction data. The specimen comes from Tartareu (Catalunya, Spain) and is formed by pale-blue fibres. Unit cell dimensions and composition: $a = b = 16.9161$, $c = 5.2289$ Å, $V = 1296$ Å^3 with space group $P3c1$ and $D_{calc} = 2.46$ g/cm^3; $[(Ca_{4.3},Na_{.1})(Al_{5.3},Si_{.4},Mg_{.3})(OH)_{12}(H_2O)_{11.1}][(Fe^{3+},Fe^{2.5+})_{1.36}(Fe^{3+},Mg_{0.5},Al_{0.3})Si_{11.9}P_{0.1}O_{36}](CO_3)_{.75}(SO_3)_{.25}$ Z=1. Oxidation states of Fe were determined from Mössbauer spectroscopy. The model of the structure was refined with the Rietveld method to the residual value $R_{wp} = 0.036$ (X^2=1.73). The unit cell contains two similar basic building units (columns) formed by three pyroxene chains pointing inwards with different cation sites at the centres of the resulting face-sharing octahedra. These sites are occupied by different cation species compositions. One is formed by 68% Fe^{3+} and 32% mixed valence iron ($Fe^{2.5+}$), while the other has 60% Fe^{3+}, 25% Mg^{2+} and 15% Al^{3+}. According to the electron microprobe data and to the crystal chemical study approximately 12% of the more internal metal positions of the brucite-like layer that connects each two columns, show substitution of Al^{3+} with Si^{4+} (6.6%) and Mg^{2+} (5%). The unit cell contains in the middle of the channel 0.75 CO_3^{2-} and 0.25 sulphur atoms, presumable as SO_3^{2-}, stacked along one of the three ternary axis and mutually separated by 5.23 Å.

15:30 Poster 08-06

Nonaqueous approach to a metal-organic framework: A new vanadium-oxobenzoate as case study

Igor Djerdj[1], Minhua Cao[2,3], Radovan Cerny[4], Zvonko Jagličič[5,6], Fabia Gozzo[7], Markus Antonietti[2], Markus Niederberger[1]

1. *ETH Zürich (ETHZ), Wolfgang-Pauli-Strasse 10, Zürich 8093, Switzerland* **2.** *Max Planck Institute of Colloids and Interfaces (MPIKGF), Research Campus Golm, Potsdam 14424, Germany* **3.** *Department of Chemistry, Northeast Normal University, Changchun 13324, China* **4.** *University of Geneva, 24 quai Ernest-Ansermet, Geneva 1211, Switzerland* **5.** *Institute of mathematics physics and mechanics (IMFM), Jadranska 19, Ljubljana 1000, Slovenia* **6.** *Faculty of Civil and Geodetic Engineering, University of Ljubljana, Jamova 2, Ljubljana 1000, Slovenia* **7.** *Swiss Light Source, Paul Scherrer Institute, Villigen PSI 5232, Switzerland*

e-mail: igor.djerdj@mat.ethz.ch

Metal–organic frameworks (MOFs) based on transition metal elements are an important family of materials as they provide an opportunity to correlate their structure and magnetism, in addition to their adsorption and related properties arising from the porous structure. Among the broad family of transition metals, vanadium is particularly challenging due to its appearance in different oxidation states ranging from 2+ to 5+, which consequently exhibits an exceptionally rich variety of electronic ground states and magnetic properties. A new vanadium oxobenzoate $[VO(C_6H_5COO)_2]$ has been synthesized under solvothermal conditions by reacting $VO(OiPr)_3$, benzoic acid and toluene. The resulting powder was thoroughly investigated by a number of complementary methods like XPS, electron microscopy techniques, synchrotron X-ray powder diffraction, thermal analysis, bulk density, and magnetic DC susceptibility measurement. The compound crystallizes in the monoclinic system with $a = 20.661(2)$, $b = 6.791(1)$, $c = 9.959(1)$ Å, $b = 92.08°$, space group $C2$, and $Z = 4$. The crystal structure has been solved from synchrotron X-ray powder diffraction data using a direct space global optimization technique (program FOX) and refined by the constrained Rietveld method. The V atoms are in 4+ oxidation state as revealed by XPS. In the complex they have 5-fold coordination with respect to the oxygens, with the metal cation center in distorted squared pyramid coordination. Vanadium atoms are mutually linked via oxygen atoms forming helical zig-zag chains along the crystal *b*-axis as illustrated in Figure 1. The VO_5 inorganic layers lie at the distance of 10 Å, and are separated from each other by the organic part composed of benzoate moieties.

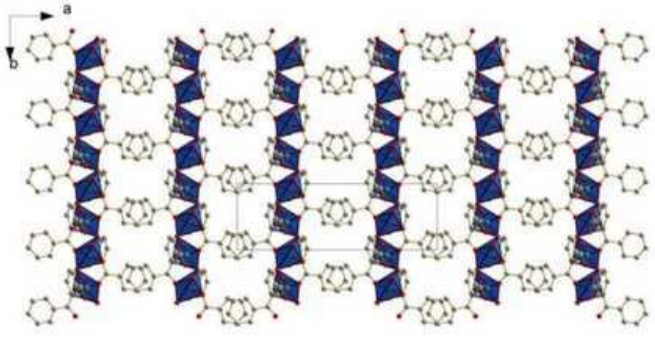

Figure 1. Molecular packing of vanadium oxobenzoate viewed along the [001] direction. The projection of unit cell is marked as a gray rectangle.

15:30 Poster 08-07

Structural and spectroscopic properties of $BaHfO_3$:Eu - the issue of the dopant location in the host lattice

Anna Dobrowolska, Eugeniusz Zych

University of Wrocław, Faculty of Chemistry, Joliot-Curie 14, Wrocław 50-383, Poland

e-mail: anilid@poczta.onet.pl

Barium hafnate, $BaHfO_3$ is a valuable host lattice for X-ray phosphors, especially due to its high absorption for ionizing radiation, which results mailny from the presence of two heavy ions, Ba^{2+} and Hf^{4+} in the lattice and density reaches 8.5g/cm^3. What is also advantageous is that $BaHfO_3$ crystallizes in cubic structure, which allows for transparent ceramics fabrication. These are potentially attractive replacements for monocrystallline materials.

Till now research on $BaHfO_3$ was concentrated on Ce-doped powders, because of its fast luminescence decay, so important in dynamic medical techniques. We choose doping with Eu as its red luminescence fits perfectly the region of the highest efficiency of CCDs, which is presently considered a detector of choice for digital planar X-ray imaging. In this technique the relatively slow decay of the Eu^{3+} luminescence is not an obstacle.

$BaHfO_3$:Eu(x%) powders were prepared with ceramic method. The products were examined with XRD technique, SEM, luminescence spectroscopy, synchrotron radiation, radioluminescence.

Analysis of the X-ray diffraction patterns of all samples (Fig.1) suggested that the dopant is distributed between both Ba^{2+} and Hf^{4+} sites. Yet, for low concentration the fractions of Eu which go the two sites are different than for higher concentration. This conclusion gor support from the results of luminescence, site selective spectroscopy, which allowed us to identify emission lines coming from Eu^{3+} located in Ba^{2+} site, as well as occupying the Hf^{4+} location, and showed that relative intensities of luminescense from the two sites vary strongly mirroring the variation of the diffraction line position (Fig.1). Surprisingly, only the Eu(Hf) ions are active in radioluminescence, while Eu(Ba) are being unable to intercept energy deposited in the host by X-rays.

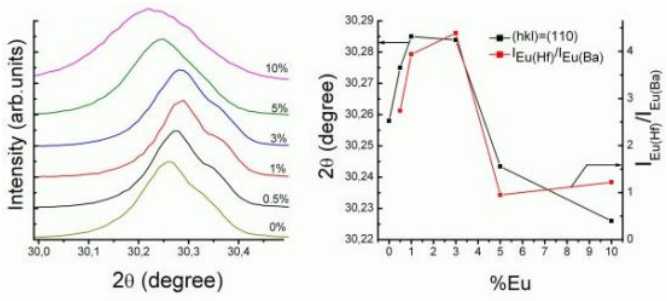

Fig. 1. Eu concentration dependance of the position of diffraction line and variation of the intensities of the emission from two sites.

15:30 Poster 08-08

Lead Free Piezoceramics. A combined neutron diffraction and TEM-study on the system BNT–BT–KNN

Hartmut Fuess, Jürgen Rödel, Wook Jo, Manuel Hinterstein, Helmut Ehrenberg, Markus Hölzel, Anatoliy Senyshyn, Jens Kling, Hans-Joachim Kleebe

Technische Universität Darmstadt, Institute of Materials Science, Petersenstr. 23, Darmstadt 64287, Germany

e-mail: hfuess@tu-darmstadt.de

Lead containing oxides with perovskite structure are widely used as sensors and actuators. Among those materials lead titanate zirconate $PbZr_{1-x}Ti_xO_3$ (PZT) and lead magnesium niobate-lead titanate, PMN-PT are the most prominent ones. The possible environmental hazard connected with lead has driven research of novel materials with comparable electrical and mechanical properties as PZT. Lead-free piezoelectric ceramics $(1-x-y)Bi_{0.5}Na_{0.5}TiO_3$-$xBaTiO_3$-$yK_{0.5}Na_{0.5}NbO_3$ ($0.05 \leq x \leq 0.07$ and $0.01 \leq y \leq 0.03$) have been synthesized by the mixed oxide route and sintering. Preliminary electromechanical characterization revealed a remarkable strain of approximately 0.4 % at an electric field of 8 kV/mm close to the boundary between two compositions with dominant ferroelectric and anti-ferroelectric properties [1, 2, 3]. Room temperature powder neutron diffraction at the SPODI diffractometer at the FRM II TU Munich showed superstructure reflections which were indexed based on the tetragonal space group P4bm [4] and the rhombohedral one R3c [5]. As no superstructure reflections were detected on a synchrotron powder run the preliminary conclusion leads to a displacement of the oxygen atoms of their positions in the cubic system. No prominent domain structure as commonly seen in PZT polycrystals was observed in TEM experiments. In contrast, electron dif-fraction revealed weak superlattice reflections in prominent zone axes. Further investigations within the composition range given above are in progress.

[1] S.-T. Zhang, A. B. Kounga, E. Aulbach, H. Ehrenberg, J. Rödel, *Appl.Phys. Lett.***91** 112906 (2007).

[2] S.-T. Zhang, A. B. Kounga, E. Aulbach, T. Granzow, Wook Jo, H.-J. Kleebe, J. Rödel, *J. Appl. Phys.***103** 034107 (2008).

[3] S.-T. Zhang, A. B. Kounga, E. Aulbach, Wook Jo, T. Granzow, H. Ehrenberg, J. Rödel, *J. Appl. Phys.***103** 034108 (2008).

[4] G.O. Jones, P.A. Thomas, *Acta Cryst. B***56**, 426 (2000).

[5] G.O. Jones, P.A. Thomas, *Acta Cryst. B***58**, 168 (2002).

15:30 Poster 08-09

XRD, TEM, neutron diffraction and EPR characterization of $LaCo_{1-y}Ni_yO_3$ perovskites obtained from citrate precursors

Sonya Ivanova[1], Anatoliy Senyshyn[2], Ekaterina Zhecheva[1], Velin Nickolov[1], Radostina Stoyanova[1], Hartmut Fuess[3]

1. *Institute of General and Inorganic Chemistry, Bulgarian Academy of Sciences (IGIC), Acad. G. Bonchev Str. bldg. 11, Sofia 1113, Bulgaria* **2.** *Lviv Polytechnic National University, 12 Bandera, Lviv 79013, Ukraine* **3.** *Technische Universität Darmstadt, Institute of Materials Science, Petersenstr. 23, Darmstadt 64287, Germany*

e-mail: sonya@svr.igic.bas.bg

It is well recognized that perspective cathode materials for intermediate-temperature solid oxide fuel cells are cobalt-based perovskite oxides. The aim of this contribution is to study in details the formation of solid solutions between $LaCoO_3$ and $LaNiO_3$ perovskites. Two methods for the preparation of $LaCo_{1-y}Ni_yO_3$ were used: (i) thermal decomposition of La-Co-Ni citrates obtained by freeze-drying of the corresponding solutions, and (ii) the method of Pechini. The distribution of Ni in $LaCo_{1-y}Ni_yO_3$ solid solutions was examined by means of neutron diffraction and EPR spectroscopy.

Rhombohedrally distorted perovskites $LaCo_{1-y}Ni_yO_3$ with 0 £ y £ 0.5 are obtained from citrate precursors at 600 °C. The oxidation state of (Co+Ni) is slightly higher than 3 for oxides prepared from freeze-dried citrates, while slightly reduced oxides are obtained by the method of Pechini. The substitution of Ni for Co leads to the increase in the unit cell parameters, which is in agreement with the different ionic sizes of Co^{3+} and Ni^{3+} ions. Oxides prepared from freeze-dried citrate precursors display plate-like aggregates with dimensions of about 5 mm, while the method of Pechini allows obtaining well separated particles. Inside the particle aggregates, hexagonal individual particles with sizes of about 70 nm were observed. In addition, HR-TEM analysis and neutron diffraction show the appearance of small spinel particles (with 10 nm sizes) deposited on the main $LaCo_{0.9}Ni_{0.1}O_3$ particles. The lattice parameter of impurity spinel phase is higher than that of pure Co_3O_4 spinel: a=8.40 – 8.45 Å as compared to a=8.08 Å, respectively.

The EPR spectra of $LaCo_{1-y}Ni_yO_3$ obtained at 600 °C consist of a signal due to magnetic Ni clusters. These magnetic clusters show a broad size distribution, the mean size being increased with the Ni content. The distribution of the Ni ions in $LaCo_{1-y}Ni_yO_3$ depends also on the preparation method. It seems that Pechini method promotes the formation of magnetic nickel clusters.

By increasing the annealing temperature up to 900 °C, the magnetic Ni clusters become invisible. In the same sequence, neutron diffraction analysis shows a random distribution of Co and Ni ions in $LaCo_{1-y}Ni_yO_3$.

Authors are grateful to EC for a grant within the FAME project (FAME FP6-500159-1) and to the Centre of Competence MISSION (SSA, EC-INCO-CT-2005-016414).

15:30 Poster 08-10

In situ study of the crystal symmetry changes in lithium titanate spinel by X-ray diffraction and Raman spectroscopy

Natasa Jovic[1], Milica Vucinic-Vasic[2], Bratislav Antic[1], Aleksandar Kremenovic[3], Volker Kahlenberg[4]

1. *VINCA Institute, POB 522, Belgrade 11001, Serbia* **2.** *Faculty of Technical Sciences, University of Novi Sad, Trg D. Obradovica 6, Novi Sad 21000, Serbia* **3.** *Faculty of Mining and Geology, Laboratory for Crystallography, University of Belgrade, Djusina 7, Belgrade 11000, Serbia* **4.** *Institute of Mineralogy and Petrography, University of Innsbruck, Innrain 52, Innsbruck A-6020, Austria*

e-mail: natasaj@vin.bg.ac.yu

$Li_{1.33}Ti_{1.67}O_4$ spinel exhibits a special interest as negative electrode material. The effect on electrochemistry by a partial substitution of lithium and/or titanium ions with transition metal ions has been studied. In the present work we have investigated the microstructure and crystal structure evolution of $LiZn_{0.5}Ti_{1.5}O_4$ obtained by high energy ball milling from an appropriate mixture of Li_2CO_3, ZnO and TiO_2 powders. For as-synthesized material the powder X-ray diffraction pattern confirms disordered spinel structure (*Fd* -3*m*). Determined cation distribution, $(Li_{0.28}Zn_{0.19}Ti_{0.53})[Li_{0.72}Zn_{0.31}Ti_{0.97}]$, is in discrepancy with the known cation site preferences and can be classified as metastable one. Microstructural size-strain analysis has been done using the FullProf computer program. The average apparent size of sample was found to be 187(12) Å, and the average apparent strain is 26(4) 10^{-4}. After annealing sample at 650 °C for 3 hours and slowly cooling down to room temperature, the superstructure reflections have been observed, indicating cation ordering at octahedral, (O_h) sublattice ($P4_332$). The order-disorder phase transition in the annealed sample was studied by *in-situ* XRD experiment. The extinction of superstructure reflections was observed between 1020 °C and 1040 °C. Disorder began with the cation migration of Li^+ and Zn^{2+} ions between the tetrahedral, 8*c* and octahedral, 4*b* sites, but the main mechanism was cation mixing inside O_h sublattice. At the temperatures higher than 1030 °C, crystal structure refinements were performed in disordered phase (*Fd*-3 *m*). The linear increase of the lattice parameter, *a*, with the temperature rise was observed, with discontinuity at the phase transition temperature. Landau theory of phase transition was used to analyze the mechanisms of the phase transitions. Analysis of the topology of the order parameter vector space could indicate biquadratic coupling between Q_1 and Q_2 parameters. In the temperature stability range of the ordered phase ($P4_332$), there is a linear relationship between Q_1 and Q_2, therefore linear-quadratic coupling is not excluded. The phase transition in $LiZn_{0.5}Ti_{1.5}O_4$ spinel has also been studied by Raman spectroscopy. Raman spectra were recorded between 500 and 1200 ºC in heating and cooling, as well as at room temperature (RT) before and after thermal treatment. Raman spectra recorded at RT shows a presence of more than five Raman mode of vibrations, as a consequence of 1:3 ordering at O_h sublattice.

15:30 Poster 08-11

Crystal structure of synthetic Hydrotungstite, $[WO_3(H_2O)](H_2O)$

James A. Kaduk, Judith B. Sentman

INEOS Technologies, 150 W. Warrenville Rd., 600-1008, Naperville IL 60563, United States

e-mail: James.Kaduk@innovene.com

Hydrotungstite, $WO_2(OH)_2(H_2O)$ or $H_2WO_4(H_2O)$ (PDF 00-016-0166 and 00-018-1420) occurs as an alteration product in the oxidized zone of a hydrothermal tungsten ore deposit at the Calacalani mine in Bolivia, and thin films of hydrotungstite have been used as humidity sensors. It is reported to crystallize in *P2/m* with a = 7.379(5), b = 6.901(5), c = 3.748(5) Å, and b = 90.36(16)°. The powder pattern of a greenish yellow precipitate from an inductively-coupled plasma (ICP) specimen preparation of a W-containing sample matched that of hydrotungstite well, but the unit cell and powder pattern were more complicated than had been reported. Application of lattice matching techniques to the reported unit cell yielded the chemically-plausible analogue "yellow molybdic acid", $MoO_3(H_2O)_2$, which has the ICSD formula type AX5. A further search for Mo-containing compounds having this formula type yielded the mineral sidwellite, $MoO_3(H_2O)_2$, which crystallizes in $P2_1/n$ with a = 10.487(1), b = 13.850(1), c = 10.617(1) Å, and b = 91.62(9)°, and has been studied using neutron powder diffraction. The sidwellite cell is an 8′ supercell of the reported hydrotungstite cell, and the sidwellite structure served as a good initial model for a Rietveld refinement of the hydrotungstite structure. The hydrogen positions were determined by a quantum chemical geometry optimization, which permitted analysis of the hydrogen bonding pattern. The structure consists of corner-sharing layers of tilted WO_6 octahedra in the *ac* plane. Pointing into the interlayer region *trans* to each tungsten atom are a coordinated water molecule and a W=O group. The interlayer region is occupied by water molecules, which are hydrogen bonded to the layers. Hydrotungstite is properly formulated $[WO_3(H_2O)](H_2O)$. The structure of the mineral tungstite, $WO_3(H_2O)$, has been reported, but the topologies of the layers in sidwellite and tungstite differ. A combination of quantum calculations and Rietveld refinement was used to determine the best model for the topology of the hydrotungstite layer. The quantum calculations help establish the relative energies of hydrotungstite and tungstite.

15:30 Poster 08-12

Phase composition study of natural minerals used as a source of white pigment production

Marcin Klepka[1], Roman Minikayev[1], Maciej Jablonski[2], Aleksander Przepiera[2], Velichka Kontozova[3], Krystyna Lawniczak-Jablonska[1]

1. *Polish Academy of Sciences, Institute of Physics, al. Lotników 32/46, Warszawa 02-668, Poland* **2.** *Technical University, Institute of Chemistry and Environmental Protection, Al. Piastów 42, Szczecin 71 065, Poland* **3.** *University of Antwerp, Department of Chemistry, Groenenborgerlaan 171, Antwerp 2020, Belgium*

e-mail: mklepka@ifpan.edu.pl

The phase composition of mineral ilmenites originated from the several places in the world (Norway, China, India, Australia) was investigated using complementary non-destructive and destructive methods. These minerals are commonly used in the white pigment production. Composition of the phases has large influence on efficiency and the quality of the final product. The non-destructive X–Ray Powder Diffraction (XRD), Single Particle Electron Probe Micro Analysis (Single Particle EPMA) and conventional X-Ray Fluorescence analysis (XRF) as well as destructive classical chemical analysis were applied for full characterisation of the mineral ilmenites. The materials have very complicated morphology, therefore conventional XRD and XRF provides confusing results which in many cases do not match. In a standard procedure composition of phases is given as a content of the most popular oxides. It does not fit to the real amount of oxygen in the material and quantity of particular chemical compounds. The diffraction pattern is complicate and several peaks overlap what make the analysis complicate and not unambiguous.

To solve this problem we applied different techniques. The XRF was used to get the knowledge about average elements content and from the balance of elements the possible phases which were assumed. To characterize the homogeneity and local composition of investigated minerals, EPMA with single particle approach and conventional φρz correction procedure were used.

The Single Particle EPMA method and integrated software have been developed at Department of Chemistry, University of Antwerp for quantification of individual aerosol particles based on an iterative reverse Monte Carlo simulations combined with successive approximation for the elemental composition. This technique allows determining the concentration of low Z elements such as carbon, nitrogen and oxygen. The analyzed particles were divided into different groups (clusters), applying Hierarchical Clustering Analysis (HCA) based on their compositional similarity and their relative abundances in the sample Next, the set of phases existing in the given cluster were proposed to keep the overall content of elements in clusters in agreement with the measurements.

These results were used as a starting point in the XRD refinement and compared with the results of chemical analysis. The chemical analysis allowed estimating the amount of majority elements (Ti, Fe) at the particular ionic state. This ionic state superimpose occurrence of the particular phase. However this analysis is laborious, very time-consuming and destructive.

Three main phases were identified in the studied minerals unambiguously by all applied methods: ilmenite ($FeTiO_3$), pseudorutile ($Fe_2Ti_3O_9$), hematite (Fe_2O_3) and several minority phases like: $MnTiO_3$, $MgSiO_3$, $MgTiO_3$, Cr_2O_3.

15:30 Poster 08-13

Structures and phase transitions of Molybdenum Phosphates

Sarah E. Lister, John Evans

Department of Chemistry, University of Durham, Science Labs, South Road, Durham DH1-3LE, United Kingdom

e-mail: Sarah.Lister@dur.ac.uk

We have an ongoing interest in metal phosphate systems whose structures can be described as containing corner-sharing polyhedra.

These systems often exhibit unusual thermal expansion, for example some materials show strong negative thermal expansion over large temperature ranges. These interesting structure-temperature relationships are often encountered alongside displacive phase transitions from the high temperature substructure to the more complicated low temperature superstructure, sometimes via a number of intermediate phases. It is from an understanding of the changing structure of the materials that the bulk material properties can be understood. As part of these studies the synthesis, structure and phase transitions of several molybdenum phosphate systems with different Mo:P ratios have been investigated.

Both in-situ and ex-situ synthetic techniques have been used to study the formation of $(Mo^{VI}O_2)_2P_2O_7$ from a hydrated precursor. These reveal the formation of two previously unknown MoPO(H) phases. Also, despite its simple formula, $(Mo^{VI}O_2)_2P_2O_7$ has been discovered to undergo a displacive phase transition just above room temperature, having a complicated structure requiring a much larger unit cell to fully describe it compared to the simple structure reported in the literature[1]. As this work has been carried out predominantly using powder XRD data, the use of complementary techniques was necessary to gain greater understanding of the transition. The observations gained from ^{31}P NMR, electron diffraction and neutron diffraction will be discussed and refinement strategies outlined which enable solution of a structure with a minimum of 60 atoms in the asymmetric unit.

1. P. Kierkegaard (1962), Arkiv Foer Kemi, 19, 1-14

15:30 Poster 08-14

Charcterization by x-ray single crystal/powder diffraction, DSC and SSNMR of new crystalline forms obtained by hetero-seeding

Lucia Maini

University of Bologna, Dipartimento di Chimica "G. Ciamician" (UNIBO), via Selmi 2, Bologna 40126, Italy

e-mail: l.maini@unibo.it

Even though *para*-methyl benzyl alcohol *p*-MeBA II and *para*-chloro benzyl alcohol *p*-ClBA are *quasi*-isostructural and share the same hydrogen bond patterns the two crystals are not isomorphous. No new polymorphs could be obtained by conventional polymorph screening based on different solvents and different crystallization conditions. A new polymorph of *p*-MeBA named *p*-MeBA I, isomorphous with the crystal of *p*-ClBA, was induced by hetero-seeding with a small quantity of powdered *p*-ClBA added to a supersaturated hexane solution of *p*-MeBA before nucleation occurred. The alternate cross-crystallization, however, failed to give a new phase of *p*-ClBA isomorphous with known crystalline *p*-MeBA II. Mixed crystals of *p*-MeBA and *p*-ClBA were also prepared with different *p*-MeBA/*p*-ClBA ratios to understand the role of different functional groups in the crystal structure. Crystal phases were characterized by a combined used of single crystal and powder X-ray diffraction, DSC and SS NMR spectroscopy.

15:30 Poster 08-15

Study of the molecular and crystalline structure of two nitrogen- sulphur pro-ligands by x-ray powder diffraction and DFTB

Edward E. Ávila[1], Asiloé J. Mora[1], Andy Fitch[2], Michela Brunelli[3], Gerzon E. Delgado[1], Ricardo R. Contreras[4], Luis C. Rincón[5]

1. *Universidad de Los Andes, Facultad de Ciencias, Laboratorio de Cristalografía, Merida 5101, Venezuela* **2.** *European Synchrotron Radiation Facility (ESRF), Grenoble 38043, France* **3.** *Europen Synchrotron Radiation Facility (ESRF), 6, Jules Horowitz, Grenoble 38000, France* **4.** *Universidad de Los Andes, Facultad de Ciencias, Laboratorio de Organometálicos, Merida 5101, Venezuela* **5.** *Universidad de Los Andes, Facultad de Ciencias, Grupo de Procesos Dinámicos en Química, Merida 5101, Venezuela*

e-mail: asiloe@ula.ve

In the last decades, inorganic chemist has faced the need to mimic the properties of metal sites in metalloproteins to synthesize new catalytic materials with advantageous properties [1]. However, one of the mayor difficulties in the synthesis of these materials has been to prepare pro-ligands with structural conformations and chemical properties close enough to the ligands around the metal in the protein to avoid problems associated with molecular recognition in the catalytic process. In this work, we have attempted to study the molecular and crystalline structure by means of X-ray powder diffraction and theoretical calculations using density functional tight-binding methods (DFTB) of two new pro-ligands of the type [NS] bidentate and $[N_2S_2]$ tetradentate: iso-butyl 2,4-bis(cyclohexane)dispiro-[1,2,3,4,4a,5,6,7]-octahydro-(1H,3H)quinazoline-8-carboxydithioate (compound I) and methyl *N*,*N*′-buthyl-bis(2-amino-1-cyclopentendi-thiocarboxidithioate (compound II) [2-4]. Powder diffraction experiments were carried out in the diffractometer of beam line ID31, ESRF, France. DFTB calculations were carried out using the computer facilities of the Theoretical Chemistry Group: Dynamical Processes, ULA, Venezuela. The structural solution was achieved using the program FOX. The Rietveld refinement of the models used the program GSAS. The molecular conformation for both compounds, which are subjected to internal hydrogen bonds and electron charge delocalization in the carboxydithioate group, and the crystal packing of the compounds are thoroughly discussed here. Finally, the molecular structures obtained by X-ray powder diffraction are compared with the ones optimized by DFTB calculations.

Acknowledgement: This study was supported by the CDCHT-ULA, FONACIT-Venezuela (Lab-97000821, Subvention-200500703) and beam line ID31, ESRF (France).

References

1. Solomon, E. I., Szilagyi, R. K., DeBeer, G. S. & Basumallick, L., 2004, *Chem. Rev*. **104**, 419-458.
2. Avila, E.E., Mora, A.J., Delgado, G.E., Contreras, R.R., Fitch, A.N. & Brunelli, M. 2008, *Acta Crystal*. **B64**, 217-222.
3. Contreras, R. R., Fontal, B., Romero. I., Briceño, A. & Atencio,

R., 2006, *Acta Cryst.***E62**, o205-o208.
4. Contreras, R. R., Fontal, B., Bahsas, A., Reyes, M., Suárez, T. & Bellandi, F. 2001, *J. Heterocycles Chem*. **38**, 1223-1225.

15:30 Poster 08-16

Synthesis, structure and magnetic properties of Fe-doped tetragonal $Li_{0.95}Mn_{2.05}O_4$

Waldemar Nowicki[1], Jolanta Darul[1], Fabiano Yokaichiya[2]

1. *Adam Mickiewicz University, Faculty of Chemistry, Grunwaldzka 6, Poznań 60-780, Poland* **2.** *Hahn-Meitner-Institute (HMI), Glienicker Str. 100, Berlin D-14109, Germany*

e-mail: waldek@amu.edu.pl

At room temperature, the lithium deficient sample of the $Li_{0.95}Mn_{2.05}O_4$ obtained by quenching shows a tetragonally distorted spinel lattice, with c/a = 0.98 [1,2]. Partial substitution with very small quantities of Fe^{3+} ions for Mn^{3+} depresses the Jahn-Teller effect, reducing the Mn^{3+} / Mn^{4+} ratio.

Series of compounds with the $Li_{0.95}Mn_{2.05-x}Fe_xO_4$ stoichiometry have been obtained by solid state reaction of Li_2CO_3 with the manganese oxide or iron-manganese oxide precursors. The samples underwent a successive thermal treatment in air, at 700°C and 800°C for 4h. After heating, the preparations were either cooled slowly to the room temperature during 24h, or quenched rapidly in the solid CO_2. The powder X-ray diffraction patterns of the substituted oxides were obtained using an X-ray diffractometer (Bruker D8 Advance), with copper K_α radiation. Neutron diffraction data were collected in the multicounter high-resolution diffractometer E9 installed at the BER II reactor in Hahn-Meitner-Institute (Berlin). The magnetometric measurements were made with DC-magnetometr/AC-susceptometer MagLab 2000 System (Oxford Instruments Ltd.). The phase identification and phase analysis were performed using the program PowderCell [3]. The structure refinement were performed using the program FullProf [4].

This study examines the effects of important processing parameters, such as composition and cooling condition. The phases obtained by quenching the products of thermal treatment, crystallize in the tetragonal system, space group $I4_1/amd$, on the other hand the samples formed as a result of slow cooling technique give nearly stoichiometric $LiMn_2O_4$, with the admixture of manganese oxides (bixbyite and hausmannite). A superexchange magnetic interaction between the Mn ions via oxygen atoms alerts, with the Fe^{3+}-content in $Li_{0.95}Mn_{2.05-x}Fe_xO_4$ increasing from x = 0.0-0.1, showing the antiferromagnetic ordering at very low temperature. The Néel point increases from 11 to 27 K.

References

[1] W. Nowicki, J.Darul, P. Piszora, C. Baehtz, E. Wolska, J. Alloys Comp.,55, **401** (2005)

[2] P. Piszora, Chem. Mater.,4802, **18** (2006)

[3] W. Kraus, G. Nolze, *PowderCell* 2.3 (1998).

[4] J. Rodriguez-Carvajal, Physica B 159, **55** (1993)

15:30 Poster 08-17

Unraveling the polimorph space of the product of a 2+2 photodimerization of (E)-furylidenoxindole by an in situ Raman/X-ray powder diffraction study

Marco Milanesio[1], Enrico Boccaleri[1], Wouter Van beek[1,2], Luca Palin[1]

1. *Università degli Studi del Piemonte Orientale (DISTA), Via V. Bellini 25/G., Alessandria 15100, Italy* **2.** *SNBL at the ESRF, Grenoble 38000, France*

e-mail: lpalin@unipmn.it

Materials containing disordered moieties and/or amorphous or liquid-like phases or showing surface- or defect-related phenomena constitute a problem for their characterization using X-ray powder diffraction (XRPD), and Raman spectroscopy can provide useful complementary information. We have designed and realized a novel experimental set-up [1] for simultaneous *in situ* Raman/ <High-resolution XRPD> experiments, to take full advantage of the complementarities of the two techniques in investigating solid-state transformations at non-ambient conditions. The invaluable added value of the proposed experiment is the perfect synchronization of the two probes with the reaction coordinate and the elimination of possible bias caused by different sample holders and conditioning modes used in "in situ but separate" approaches. The set-up was developed by the Swiss-Norwegian Beamline at the European Synchrotron Radiation Facility in Grenoble and tested on the photoinduced 2+2 cyclization of (E)-furylidenoxindole. In this experiment the surface-bulk complementarities of the Raman and XRPD probes were exploited. Raman allowed to detect the reaction speed at the surface in the first step of the reactions, when no reaction is detected by XRPD. The complex polymorph space of the product phase (one stable and two metastable crystalline phase and one amorphous phase) was fully understood and the structure of one metastable phase was also solved.

[1] E. Boccaleri, F. Carniato, G. Croce, D. Viterbo, W. van Beek, H. Emerich and M. Milanesio, *In situ simultaneous Raman/ high-resolution X-ray powder diffraction study of transformations occurring in materials at non-ambient conditions*, *J. Appl. Cryst.*, **2007**, *40*, 684-693.

15:30 Poster 08-18

Crystal structure prediction and X-ray powder diffraction of Pigment Red 168

Nadine Rademacher[1], Martin U. Schmidt[1], Graeme M. Day[2]

1. *Frankfurt University, Institute of Inorganic and Analytical Chemistry, Max-von-Laue-Str. 7, Frankfurt am Main 60438, Germany* **2.** *University of Cambridge, Department of Chemistry, Lensfield Road, Cambridge CB21EW, United Kingdom*

e-mail: nrademac@stud.uni-frankfurt.de

Pigment Red 168 (4,10-Dibromoanthanthrone, see picture) is an industrially important pigment with two known polymorphic phases. The crystal structure of the red α-phase was solved by single crystal structure analysis.[1] Since the crystallinity of the metastable orange

β-phase is always poor, powder patterns are not indexable. Therefore we tried to solve the structure by means of lattice energy minimizations.

4,10-Dibromoanthanthrone has the molecular symmetry 2/*m*. The most common space groups for molecules of 2/*m* symmetry are *P*-1, $P2_1/c$, *C*2/*c* and *Pbca* with the molecule located on the inversion centre.[2,3] The structure of the β-phase was predicted using the program CRYSCA[4]. It was assumed that the molecule is located on an inversion centre. The calculations were performed with a whole molecule in the corresponding subgroups of the above-mentioned space groups. Subsequently, the predicted structures were optimized with a force field having anisotropic atom-atom potentials, which was developed for halogenated aromatic molecules.[5] In order to find out which of the proposed structures correspond to the experimental polymorphs of α and β, powder patterns were calculated and compared with the experimental patterns.

The α-phase could be identified without problems. Due to the low crystallinity of the β-phase it was difficult to select which of the proposed structures is the correct one.

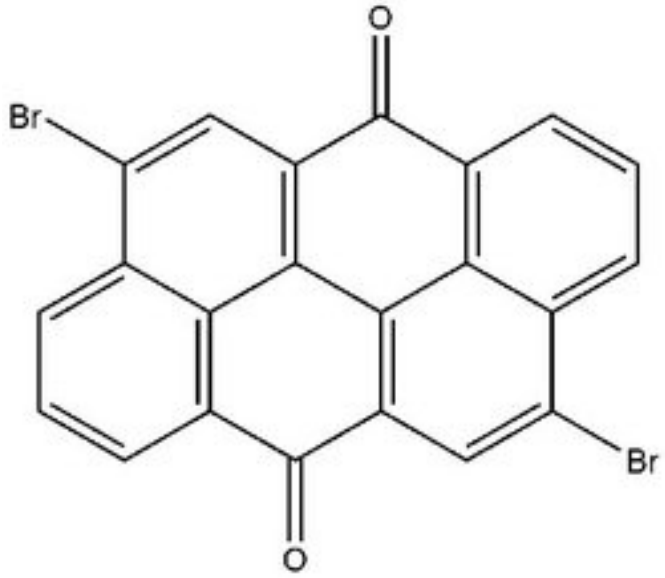

[1] E. F. Paulus, G. M. Day, M. U. Schmidt, in preparation.

[2] E. Pidcock, W. D. S. Motherwell, J. C. Cole, *Acta Cryst.***2003**, *B*59, 634-640.

[3] A. I. Kitaigorodskii: "Organic Chemical Crystallography" 1961, New York: Consultants Bureau.

[4] M. U. Schmidt, H. Kalkhof, Frankfurt am Main, 1997–2002.

[5] G. M. Day, unpublished.

15:30 Poster 08-19

Structure of K_2TaF_7 at 720°C - a combined use of synchrotron powder data and solid state DFT calculation

Ľubomír Smrčok[1], Michela Brunelli[2], Miroslav Boča[1], Marian Kucharík[1]

1. *Institute Of Inorganic Chemistry, Slovak Academy of Sciences (IIC), Dubravska cesta 9, Bratislava SK-84536, Slovakia (Slovak Rep.)* **2.** *Europen Synchrotron Radiation Facility (ESRF), 6, Jules Horowitz, Grenoble 38000, France*

e-mail: uachsmrk@savba.sk

The structure of the title compound was optimized by energy minimization in solid state using a plane waves DFT computation where the lattice parameters were obtained by LeBail method from the synchrotron X-ray powder diffraction data collected at 720°C. Owing to sample corrosiveness it had to be filled in a thin-walled Pt capillary. It was found that the structure corresponds to that of beta-K_2TaF_7 phase. It was also shown that solid state DFT methods could be an accurate alternative to Rietveld refinement, providing a remedy to the chronic pain of standard powder refinements - lack of information extractable from a powder pattern. The size of the problems tractable by the current solid state DFT methods running on a laboratory computer nowadays reaches 500-1000 atoms/unit cell, *i.e.* well exceeds widely accepted limits for unrestrained powder refinements, which frequently fail in providing accurate results even for the structures built of much smaller numbers of atoms.

Ľ.Smrčok, M.Brunelli, M.Boča and M.Kucharík *J.Appl. Cryst.* (2008) **41**(3). In press.

15:30 Poster 08-20

XRD and EPR spectroscopy for analysis of cationic distribution in layered $LiNi_{0.5}Mn_{0.5}O_2$ as cathode materials for lithium-ion batteries

Meglena Yoncheva, Radostina Stoyanova, Ekaterina Zhecheva, Gregorio Ortiz, Pedro Lavela, Jose Luis Tirado

Institute of General and Inorganic Chemistry, Bulgarian Academy of Sciences (IGIC), Acad. G. Bonchev Str. bldg. 11, Sofia 1113, Bulgaria

e-mail: meglena@svr.igic.bas.bg

Lithium-nickel-manganese oxides, $LiNi_{1/2}Mn_{1/2}O_2$, with layered crystal structure have been considered as next generation of cathode materials for lithium ion batteries. The improvement of their electrochemical performance requires a detailed study on the local cationic distribution of Li^+, Ni^{2+} and Mn^{4+} ions.

The aim of this contribution is to study the cationic distribution in $LiNi_{1/2}Mn_{1/2}O_2$ at long- and short scale range. While the Rietveld refinement of the X-ray powder diffraction patterns allows determining the extent of Li^+ and Ni^{2+} disorder between lithium and transition metal layers, the distribution of Ni^{2+} and Mn^{4+} in the transition metal layers was accessed by X-band EPR spectroscopy.

$LiNi_{1/2}Mn_{1/2}O_2$ with layered structure were synthesized by solid state reaction between lithium hydroxide and mixed Ni,Mn oxides. Two types of mixed Ni,Mn oxides were used: an ilmenite-type oxide obtained from co-precipitated Ni,Mn carbonates and a spinel-type oxide obtained from freeze-dried Ni,Mn citrates. The temperature of the solid state reaction between LiOH and Ni,Mn oxides was varied between 800 and 950 °C.

It was found that the extent of Li/Ni mixing between layers decreases with increasing the preparation temperature and is insensitive towards the precursor used. For oxides annealed at 950 °C, the EPR spectroscopy reveals the formation of large 180° Ni^{2+}-O-Ni^{2+} magnetic clusters, which include Ni^{2+} ions from both lithium and transition metal layers. This means that at lower synthesis temperatures, where the extent of the Li and Ni mixing is higher, Ni^{2+} ions from both layers are distributed in a way to avoid the formation of large 180° Ni^{2+}-O-Ni^{2+} magnetic clusters.

For $LiNi_{1/2}Mn_{1/2}O_2$, an EPR response from Mn^{4+} ions has only been detected, while Ni^{2+} ions remain EPR silent. The EPR line width increases proportionally with the Ni-to-Mn ratio in the first coordination sphere of Mn^{4+}. Analysis of the EPR line width allows determining the Ni-to-Mn ratio in the first coordination sphere of Mn^{4+} ions. It appears that the local Ni-to-Mn ratio depends mainly on the precursor used, but not on the synthesis temperature. $LiNi_{1/2}Mn_{1/2}O_2$ obtained from $NiMnO_3$-ilmenite displays a lower Ni-to-Mn ratio as compared to $LiNi_{1/2}Mn_{1/2}O_2$ obtained from Ni,Mn spinels. In addition, the different type of cationic distribution in the transition metal layers can be related with the thermal stability of $LiNi_{1/2}Mn_{1/2}O_2$. Between 800 and 950 °C, ex-spinel $LiNi_{1/2}Mn_{1/2}O_2$ is stable, while ex-ilmenite $LiNi_{1/2}Mn_{1/2}O_2$ is decomposed above 900 °C into Li_2MnO_3 and a Ni-rich layered oxide.

Authors are grateful to EC for a grant within the FAME project (FAME FP6-500159-1), to the Centre of Competence MISSION (SSA, EC-INCO-CT-2005-016414) and to the National Science Fund of Bulgaria (Contract no. Ch1701/2007).

15:30 Poster 08-21

Crystal structure solution of ECS-2, a novel crystalline hybrid organic-inorganic material

Stefano Zanardi, Giuseppe Bellussi, Angela Carati, Eleonora Di Paola, Roberto Millini, Wallace O. Parker Jr, Caterina Rizzo

Eni S.p.A., Via Maritano 26, San Donato Milanese 20097, Italy

e-mail: stefano.zanardi@eni.it

In the last years, porous organic-inorganic hybrid materials have fascinated by the potential technological application related to the combination of hydrophobic organic layers and hydrophilic inorganic ones [1]. Recently, a new class of microporous hybrid organic-inorganic alumino-silicates materials (Eni Carbon Silicate - ECS) has recently been synthesized at the Eni laboratories [2]. The crystal structure solution of ECS-2, a sodium aluminosilicate member of this new family, is here reported. The structural model was achieved by combining information obtained by high resolution X-ray Powder Diffraction (XRPD), NMR spectroscopy and high Resolution Transmission Electron Microscopy (HRTEM). ^{29}Si MAS NMR spectroscopy confirmed that the organic group was covalently bounded to the inorganic scaffolding, while ^{13}C MAS NMR clearly showed the presence of ethanol molecules, likely deriving from the hydrolysis of the organic precursor, stocked in the pores of ECS-2. HRTEM images of ECS-2 showed alternating layers suggesting that the organic layer may be stacked to the inorganic one (Fig. 1a). The XRD pattern of as-synthesized ECS-2, collected on the beam line ID-31, at ESRF in Grenoble (λ = 0.80175(2)Å), has been indexed using a monoclinic unit cell with parameters a = 7.908, b = 19.5339, c = 7.8758 Å and ß = 108.72°, and the analysis of the systematic absences indicated the $P2_1/n$ as the possible space group. The structural model of ECS-2 has been achieved by application of direct methods and can be rationalized by the stacking of alumino-silicate layers held together by phenylene groups (Fig. 1b), in agreement with the microscopy analysis. This scaffolding is characterized by the presence of large cages where the ethanol molecules find place (Fig. 1c); however, the six phenylene groups hampers the access to these cages, allowing the structure of ECS-2 to be classified as clathrate-like.

[1] B.D. Hatton, K. Landskron, W.J. Hunks, M.R. Bennet, D. Shukaris, D.D. Perovic, G.A. Ozin, Materials Today 2006, 9, 22-31

[2] A. Carati, C. Rizzo, U. Diaz Morales, G. Bellussi, S. Zanardi. W.O. Parker, Jr., R. Millini, BE 1,016,877, assigned to Eni S.p.A.

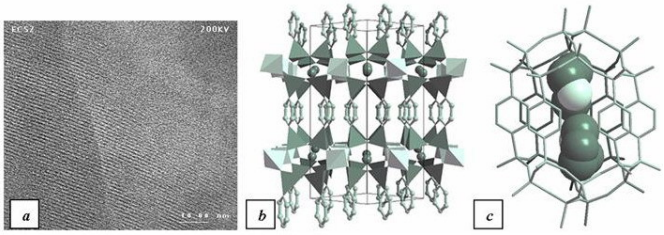

Fig. 1. a) High resolution transmission electron micrograph of ECS-2; b) Polyhedral structure of ECS-2 (dark gray small spheres are atoms of sodium); c) Six phenylene cage.

Neutron scattering

MS9 posters
Sunday afternoon, 21 September, 15:30

15:30 Poster 09-01

Structures and properties of variously doped Mayenite investigated by neutron and synchrotron powder diffraction

Hans H. Boysen[1], Ines Kaiser-Bischoff[1], Martin Lerch[2], Stefan Berendts[2], Alexander Börger[3], Dmytro M. Trots[4,5], Markus Hoelzel[5,6], Anatoliy Senyshyn[5,6]

1. *LMU, Department of Earth and Environmental Sciences, Crystallography, Theresienstr. 41, München 81539, Germany* **2.** *Institut für Chemie, TU Berlin, Straße des 17. Juni 135, Berlin 10623, Germany* **3.** *Institut für Physikalische und Theoretische Chemie, TU Braunschweig, Hans-Sommer-Straße 10, Braunschweig 38106, Germany* **4.** *Hamburger Synchrotronstrahlungslabor HASYLAB (HASYLAB), Notkestrasse 85, Hamburg D-22603, Germany* **5.** *Technische Universität Darmstadt, Institute of Materials Science, Petersenstr. 23, Darmstadt 64287, Germany* **6.** *Technischen Universität München, Forschungsneutronenquelle FRM-II (FRM2), Garching 85747, Germany*

e-mail: boysen@lmu.de

Mayenite (nominal composition $Ca_{12}Al_{14}O_{33}$), a major component of calcium aluminate cements, has recently attracted much attention for technological applications, e.g. as transparent conductive oxide, as catalyst for the combustion of volatile organic compounds or as a highly efficient oxygen ionic conductor. All this can be related to its particular crystal structure, which, in first approximation, consists of a calcium-aluminate framework, in which 32 of the 33 oxygen anions are bound. The remaining "free" oxygen is distributed at random over 1/6 of large cages in the framework and might diffuse through large openings between adjacent cages. More recent investigations [e.g. 1] have shown that the structure is heavily disordered involving e.g. displacements of Ca cations, and, at low temperatures, the presence of extra anion species like O^{2-}, O_2^{2-}, O^- and OH^-. The extra-framework oxygen can be exchanged by a variety of other an-

ions. As a new approach we have successfully substituted it by nitrogen, therewith opening up possibilities for a first pure nitrogen ionic conductor.
Four samples have been synthesized via a solid-state route with different nitrogen contents of 0 (i.e. pure O-mayenite), 0.55, 1.0 and 1.27 wt-% N. Two iron doped samples with 0.1 and 2.5 mol-% Fe (with respect to Al content) were prepared via a sol-gel route. Neutron powder diffraction experiments were carried out at instrument SPODI (FRM2/Garching) using a wavelength of 1.548 Å and an Nb vacuum furnace up to 1050 °C. Synchrotron X-ray measurements were carried out at instrument B2 (Hasylab/Hamburg) with a wavelength of 0.49324 Å up to 900 °C using a graphite furnace. Data were analysed by the Rietveld method including anharmonic Debye-Waller factors using the program package JANA2000 and by difference Fourier methods. At ambient temperature the pure and N-doped samples contained extra anion species like peroxide, superoxide, hydroxide, imide and amide, which could partly be disentangled through the complementarities of the X-ray and neutron data. They disappear above ca. 700 °C whence the samples become stoichiometric. In contrast, the Fe doped samples are stoichiometric throughout. In particular, they do not contain any hydrogen making them more apt for technical applications. Analysis of the high temperature data with respect to the diffusion properties of these materials revealed e.g. that the diffusion of oxygen proceeds via a jump-like process involving exchange of "free" oxygen with framework oxygen, coupled to relaxations of the Ca ions [1]. In contrast, nitrogen diffuses as NH^{2-} via an interstitial process. Further details, also on irreversible changes, thermal expansion, etc. will be presented in this contribution.
This work was supported by the DFG within the priority program SPP 1136 under BO 1199/2 and LE 781/10.
[1] Boysen, H., Lerch, M., Stys, A., Senyshyn, A.: Acta Crystallographica (2007) B 63, 675.

15:30 Poster 09-02

In situ neutron diffraction from Li-ion batteries

Torbjörn Gustafsson[1], Kristina Edström[1], Henrik Eriksson[1], Stefan T. Norberg[2], Peter G. Bruce[3], Stephen Hull[4]

1. *Uppsala University, Department of Materials Chemistry, Angstrom Laboratory, Uppsala, Sweden* **2.** *Chalmers University of Technology, Göteborg 412 96, Sweden* **3.** *University of St Andrews, School of Chemistry, St. Andrews KY16-9ST, United Kingdom* **4.** *Science and technology facilities council, Rutherford Appleton laboratory, Didcot OX110QX, United Kingdom*

e-mail: torbjorn.gustafsson@mkem.uu.se

In situ X-ray diffraction is today a standard tool in the study of different electrochemical processes including charge and discharge of Li-ion batteries. Many subtle structural details like lithium ion ordering and the formation of superstructures are however difficult to unravel with X-ray diffraction, due to the relatively low scattering power of lithium. Additional information from neutron diffraction would certainly be very valuable. Despite this need, there are only a few examples of *in situ* neutron diffraction experiments on Li-ion batteries in the literature. Either a special *in situ* cell is constructed or the diffraction experiment is performed on a commercial battery. Common for the purpose built *in situ* cells is the difficulty to achieve a stable long time electrochemical cycling. This is amongst other things due to the fare from optimised diffusion path for lithium in the electrolyte and the difficulty to avoid water contamination in the sensitive electrochemical processes. The huge incoherent scattering from hydrogen containing components is usually detrimental to the results when commercial batteries are used in the diffraction experiments.

As a part of the ongoing upgrade of the POLARIS diffractometer at the ISIS facility in England we try to develop an *in situ* electrochemical cell for neutron diffraction. Inspired by the success of pouch cell transmission *in situ* set ups for X-ray diffraction we aim for a sample construction very similar to an ordinary mobile phone battery. The combination of a high intensity of the primary beam and the large solid angle covered by the detector banks makes this diffractometer ideal also for time resolved *in situ* experiments. By careful choice of materials in the cell and the use of deuterated solvents in the electrolyte we will drastically reduce the incoherent background and increase the signal to noise level. Preliminary results from this work will be presented.

15:30 Poster 09-03

Quantifying the evolution of one-dimensional stacking disorder with neutron powder diffraction: formation and annealing of "cubic" ice

Thomas C. Hansen[1], Michael M. Koza[1], Andrzej Falenty[2], Werner F. Kuhs[2]

1. *Institut Laue Langevin (ILL), Avenue des martyrs, Grenoble 38042, France* **2.** *Universität Göttingen, GZG, Abteilung Kristallographie, Goldschmidtstr. 1, Gottingen D-37077, Germany*

e-mail: hansen@ill.fr

We present a data analysis strategy to extract information about one-dimensional stacking disorder and anisotropic particle sizes from high-intensity medium-resolution neutron powder diffraction performed *in situ* at D20 at ILL and to obtain a full profile refinement of the observed diffraction patterns.

Ice Ic, so-called "cubic ice", can be obtained e.g. by warming recovered high-pressure forms of ice. It is usually obtained in the form of very small crystallites leading to particle size broadening of the diffraction pattern. This pattern also contains features incompatible with a well-crystallised cubic structure, the details of which depend on the parent phase and the prevailing temperature. We have corroborated an earlier suggestion that an important number of deformation stacking faults exist in cubic ice and present a model for a quantitative description of stacking faults and anisotropic particle size broadening in ice Ic suitable for profile refinements of its complex diffraction patterns (see figure).

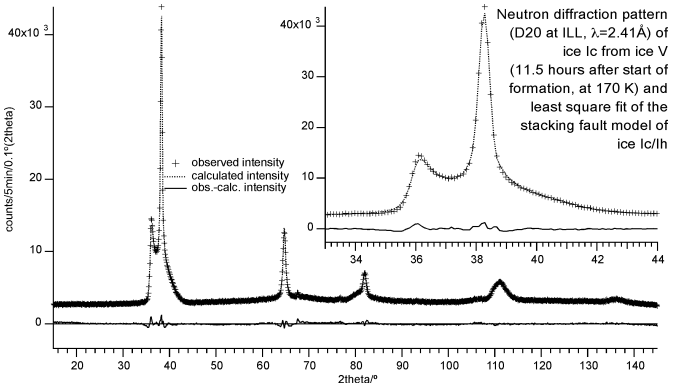

Two samples of deuterated ice Ic from ice IX and ice V have been studied *in situ* as a function of time at temperatures between 145 and 240K. Small changes of stacking fault probability occur hours after formation and continue gradually upon heating towards a higher proportion of hexagonal at the expense of cubic stacking sequences. At 190K the intensities of the Bragg reflections change considerably and the peaks become sharper. The pattern matches exactly the one of ice Ih only above 240K. We show quantitatively the time evolution of stacking disorder and crystallite size at different temperatures for ice Ic.

The kinetics of gas hydrate decomposition, below the melting point of water, is a complicated multi-phase process, due to an ice cover is produced by the initial gas hydrate decomposition at the grain surface and hindering out-diffusion of gas formed. Ice formed below 240K is stacking-faulty and shows a complicated T-dependent annealing which in turn changes the hindrance to gas diffusion leading to a "self-preservation" phenomenon above 240K where hydrates sustain in a semi-stable state for long time scales. For the data analysis of our *in situ* diffraction data we extend the presented stacking-fault model to describe the ice formed during CO_2-hydrate decomposition and its subsequent annealing behaviour.

Finally, we attempt to apply the method to a completely different system of one-dimensional stacking-disordered materials: orthorhombic copper(II)-hydroxo-oxoruthenate(VI) $CuRuO_2(OH)_4$.

15:30 Poster 09-04

Unlocking the metastable nature of Bismuth Vanadate Sillenites

Caroline A. Kirk

Loughborough University, Department of Chemistry, Epinal Way, Loughborough LE11 3TU, United Kingdom

e-mail: c.a.kirk@lboro.ac.uk

Phase formation in the bismuth-rich end of the Bi_2O_3-V_2O_5 system was investigated and a solid solution of sillenite-related phases found, $Bi_{12}(Bi_{1-x}^{3+}V_x^{5+})O_{20+(x-0.5)}$; 0.065<x<0.705. The solid solution limits were found to be far more extensive that those reported for any other sillenite-type solid solution[1].These materials are metastable and have unusual high temperature behaviour not observed in other sillenite phases. High temperature x-ray diffraction, differential thermal analysis and impedance spectroscopy have been used to characterise their high temperature properties. Structural studies of this family of bismuth vanadate sillenite materials have been carried out using powder neutron diffraction techniques to try to correlate the metastable nature of these materials to their structures. The structure of these materials is related to the sillenite structure (fig.1), but a new model was required to take into account the Bi^{3+}, with its lone pair of electrons, partially occupying the tetrahedral site along with V^{5+} (fig.2) and the non-stoichiometric nature of the oxygen lattice. It is proposed that the disordered nature of the oxygen lattice is the key to their metastable nature.

[1] Valant et al, *Chem. Mater.*, **14** (2002) 3471

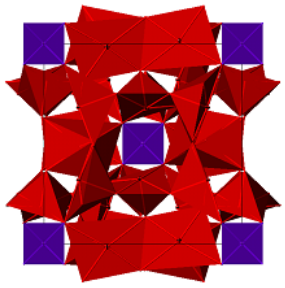

Figure 1

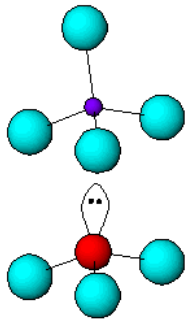

Figure 2 (V in blue, Bi in red)

15:30 Poster 09-05

Structural characterization of a coarse-grained transparent silicon carbide powder by a combination of powder diffraction techniques

Burkhard Peplinski[1], Andy Fitch[2], Alexander Evans[2], Richard M. Ibberson[3], Daniel M. Többens[4,5], Lachlan M. Cranswick[6], Ilona Dörfel[1], Franziska Emmerling[1], Ralf Matschat[1]

1. *Federal Institute for Materials Research and Testing (BAM), Richard-Willstätter-Str. 11, Berlin D-12489, Germany* **2.** *European Synchrotron Radiation Facility (ESRF), Grenoble 38043, France* **3.** *ISIS Facility, Rutherford Appleton Laboratory (ISIS), Oxon, Chilton Didcot OX110QX, United Kingdom* **4.** *Hahn-Meitner-Institute (HMI), Glienicker Str. 100, Berlin D-14109, Germany* **5.** *Institute of Mineralogy and Petrography, University of Innsbruck, Innrain 52, Innsbruck A-6020, Austria* **6.** *Chalk River Laboratories, NRC, Chalk River ON K0J1J0, Canada*

e-mail: burkhard_peplinski@web.de

Silicon carbide powders having extremely low levels of chemical impurities (a few µg per g or even less), high perfection of the crystalline lattice and a grain size of up to a hundred µm show exceptional chemical resistance (insolubility in any kind of acid), high hardness as well as unique electronic and optical properties.

Along with the lack of reliable analytical techniques for the quantitative determination of chemical trace impurities in such materials, their structural characterization is very challenging, too. One of the main problems is the considerable discrepancy between the actual grain size of the coarse-grained SiC powder samples and the ideal size for powder diffraction measurements. Any grinding bears a high risk of changing/destroying the original real structure characteristics

of the sample, e.g. the degree of stacking disorder and the polytype composition. Thus, grinding can significantly distort the outcome of the structural investigation and, therefore, should be avoided.

In an attempt to characterize the structural properties of such a material as fully as possible powder diffraction data of a large number of samples were collected applying conventional X-ray diffractometry (Bragg-Brentano geometry), constant-wavelength neutron diffractometry, time-of-flight neutron diffractometry and finally synchrotron radiation (SR) diffractometry at a dedicated beamline. All neutron and SR diffraction measurements were carried out on capillary specimens. Data evaluation was carried out with the program packages TOPAS, GSAS and FULLPROF.

The present investigation demonstrates how the specific strengths of each of these four non-destructive powder diffraction techniques complete each other very nicely. Their results go together with the outcome of a TEM investigation for which individual grains of the powder sample were thinned into 100 nm thick slices by the focused ion beam (FIB) sample preparation technique.

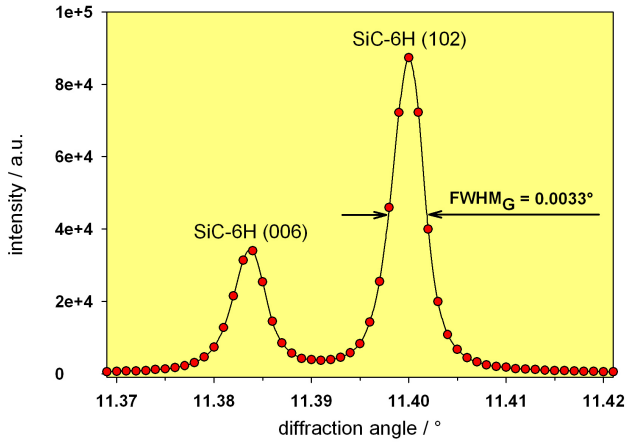

Section of the high-resolution powder diffraction pattern of a coarse-grained transparent silicon carbide powder sample collected with synchrotron radiation at the ESRF beam-line ID31 (λ = 0.050 nm)

15:30 Poster 09-06

Archaeological bronze objects studied by neutron based methods

Zsombor Sánta

Hungarian Academy of Sciences, Research Institute for Solid State Physics and Optics (SZFKI), Konkoly Thege M. út 29-33, Budapest H-1121, Hungary

e-mail: santa@szfki.hu

Neutron based non-destructive analysis methods – High Resolution Time of Flight powder diffraction (HR-TOF-D), Prompt Gamma Activation Analysis (PGAA) and Small Angle Neutron Scattering (SANS) – were applied for the investigation of archaeological bronze objects at Budapest Neutron Centre (BNC). The quantitative element analysis and phase composition analysis as well as microstructure characterization of Copper and Bronze Age axes were performed in order to reconstitute information of their ancient fabrication (hammering or casting) technology.

15:30 Poster 09-07

Rietveld refinement of TOF diffraction with multiple pulse overlap

Götz Schuck[1], Uwe Stuhr[1], Juan Rodriguez-Carvajal[2]

1. *Paul Scherrer Institut (PSI), WLGA, Villigen PSI 5232, Switzerland* **2.** *Institut Laue Langevin (ILL), Avenue des martyrs, Grenoble 38042, France*

e-mail: goetz.schuck@psi.ch

Rietveld refinement of POLDI data time-of-flight diffraction with multiple pulse overlap is enabled through the development of a POLDI data extension implemented in FullProf. [1,2]

POLDI is a multiple pulse-overlap (MP-O) diffractometer at PSI, which is designed mainly for strain-scanning experiments. The MP-O method made it possible to build a TOF diffractometer at the continuous spallation neutron source SINQ with short flight path, high resolution (1×10^{-3}) and high intensity together with a spatial resolution down to 0.6×0.6×1 mm^3. In comparison with a similar conventional TOF diffractometer at a continuous source, an enhancement of the intensity of up to two orders of magnitude is possible when the MP-O technique is applied. Typical POLDI data consists of 200000 data points (400 2theta channels x 500 time channels). As a matter of routine, calculation of the correlation diffraction pattern (CDP) or individual peak fitting (based on CDP results) is used to analyse POLDI data.[3]

The weakness of the CDP method is that the determination of the peak intensities is not precise. To overcome this and other disadvantages Rietveld refinement on the 2D (2theta - time) diffraction data can be performed using the MP-O POLDI data adaptation for FullProf (based on FullProf 3.5 Fortran code). The FullProf-POLDI data implementation has the advantage that various inherent features of FullProf (e.g.: multiphase refinement and modelling of the peak shape) can be applied for the POLDI data analysis.

The FullProf-POLDI data implementation considers the wavelength distribution of the incident beam, Bragg reflections time shifts caused due to the applied chopper speed, Bragg reflections multiplication due to the eight-chopper-slit-sequences as well as special treatment of the statistical uncertainty sigma$_i$ (average number of neutrons per data point can be lower than 1).

(1) J.K. Cockcroft, G.J. Kearley, J. Appl. Crystallogr. 17 (1984) 464

(2) J. Rodriguez-Carvajal, Physica B. 192 (1993) 55

(3) U. Stuhr, Nuclear Instruments and Methods in Physics Research A 545 (2005) 319

15:30 Poster 09-08

Indexing magnetic structures and crystallographic distortions from powder diffraction data: commensurate and incommensurate propagation vectors

Andrew S. Wills

University College London, Department of Chemistry (UCL), Gordon Street, London WC1HOAJ, United Kingdom

e-mail: a.s.wills@ucl.ac.uk

A considerable challenge is faced by researchers wishing to identify the propagation vector(s) associated with a magnetic structure or a lattice distortion from powder diffraction data, due to the severe destruction of information by powder averaging. Part of this difficulty arises from a decoupling of this procedure from the physical nature of the processes that drive the phase transition: indexing is often carried out by first extracting the peak positions and then calculating predicted peak positions for simple cells that are larger and commensurate with that of the crystal cell before the transition. Other methods use the formalism of a propagation vector, k vector, to enable the exploration of both commensurate and incommensurate trial structures, perhaps following a grid search through the possible k values. Non-linear search procedures have also been introduced that allow the k vector to be refined when in a region of reciprocal space that appears to allow the predicted peak positions to matched.

The possible values of the k vector associated with the ordering or distortion can be better understood if its physical drive is understood. In many cases of second order phase transitions, and weakly first order transitions, the observed propagation vectors correspond to the different symmetry points, lines and planes in the Brillouin zone of the crystal structure before the distortion. These correspond to different classifications of the translational symmetry of the resultant order. By using these, trial vectors can be constructed and explored that correspond in turn to the different points (no variables), lines (1 variable), planes (2 variables), and then the general position (3 variables). Sequential exploration of these can be done automatically by methods such as grid searches or trial-and-error. Reverse Monte-Carlo refinement of the moment orientations, in the case of magnetic structures, or atomic positions can then be further used to determine whether appropriate intensities can be generated at the observed positions in the powder diffraction spectrum. Together these techniques enable the characterisation of complex systems, such as those with several propagation vectors which are not symmetry related, that may otherwise have appeared to be associated with a general point in the Brillouin zone.
It should also be noted that use of an indexing procedure based on the Brillouin zone also prevents errors due to failure to take proper account of centring translations.

Time resolved powder diffraction

MS10 posters
Sunday afternoon, 21 September, 15:30

15:30	Poster	10-01

Thermal treatment on titania nanoparticles: time-resolved synchrotron x-ray diffraction studies on the effect of synthesis conditions and doping

Maria C. Dalconi[1], Francesco Matteucci[3], Giuseppe Cruciani[4], Michele Dondi[3,4], Giovanni Baldi[2], Carlo Meneghini[5]

1. *Dipartimento di Geoscienze, Università di Padova (UNIPD), Via Giotto 1, Padova 35137, Italy* **2.** *Colorobbia Italia Spa, Laboratorio di Ricerca Avanzata, Spa, Italy* **3.** *CNR-ISTEC, Institute of Science and Technology for Ceramics, Via Granarolo 64, Faenza 48018, Italy* **4.** *Università di Ferrara Dipartimento Scienze della Terra, via Saragat 1, Ferrara 44100, Italy* **5.** *Physics Department, University Roma Tre, Via della vasca navale 84, Roma 00146, Italy*

e-mail: mariachiara.dalconi@unipd.it

An important issue in development and use of nanomaterials is their ability to maintain nano-sized dimensions within extended temperature ranges or chemical conditions. Many factors control the stability and physico-chemical properties of TiO2 nanoparticles, including particle size [1], synthesis conditions [2], microstrain and morphology of crystallites [3], doping with metal oxides [4]. In our study the effect of synthesis conditions (water-based or glycol-based) and co-doping with Cr-Sb or V-Sb on the thermal behaviour of titania nanoparticles was investigated by means of temperature resolved synchrotron x-ray diffraction.
Nanocrystalline titania were produced by a novel synthesis route, consisting of a high temperature forced hydrolysis in a coordinating high-boiling solvent (and water for reference). Phase quantification of titania phases (brookite, anatase and rutile polimorphs) was obtained by quantitative Rietveld analysis using GSAS. Volume averaged apparent crystallite sizes were derived by line profile analysis with the Rietveld method (FullProf software). Phase composition and crystallite size are drastically influenced by both synthesis conditions and doping. Synthesis in water resulted in the simultaneous occurrence of anatase and brookite, transformation into rutile begins early but with a slower rate with respect to glycol-based samples (Figure 1A). Doping affected the anatese to rutile tramsformation (A→R), whose onset temperature in undoped titania (715°C) was lowered to 690°C (V-Sb) or prevented up to 950°C (Cr-Sb). Coarsening rate of anatase particle size as a function of temperature follows the A→R sequence. This confirms a particle size control on the transformation process [5].

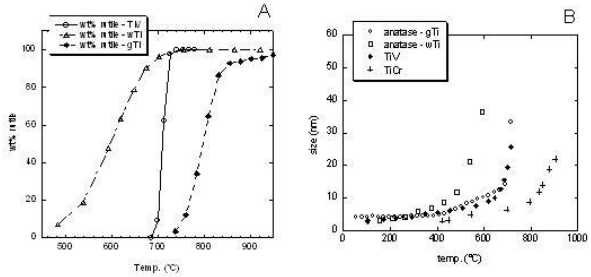

Figure 1. Legend: wTi = undoped titania in water; gTi = undoped titania in glycol; TiV = co-doped V-Sb titania in glycol; TiCr = co-doped Cr-Sb titania in glycol.

(A) temperature and rate of rutile formation: wTi (470°C) < TiV (690°C) < gTi (715°C) < TiCr (no detected rutile up to 950°C); (B) coarsening rate of anatase particle size as a function of temperature: wTi > gTi □ TiV > TiCr

References

[1] Gribb, A. A. & Banfield, J. F. (1997) Particle size effects on transformation kinetics and phase stability in nanocrystalline TiO_2. American Mineralogist, 82, 717-728.

[2] Li, Y., White, T. J. & Lim, S. H. (2004) Low-temperature synthesis and microstructural control of titania nano-particles. Journal of Solid State Chemistry, 177, 1372-1381.

[3] Penn, RL; Banfield, JF. (1999) Morphology development and crystal growth in nanocrystalline aggregates under hydrothermal conditions: Insights from titania. Geochimica Et Cosmochimica Acta, 63, 1549-1557.

[4] Reidy, DJ; Holmes, JD; Morris, MA. (2006) The critical size mechanism for the anatase to rutile transformation in TiO_2 and doped-TiO_2. Journal Of The European Ceramic Society, 26, 1527-1534.

[5] Zhang H., Banfield J. F. (2000) Understanding Polymorphic Phase Transformation Behavior during Growth of Nanocrystalline Aggregates: Insights from TiO_2. J. Phys. Chem. B, 104, 3481-3487.

15:30	Poster	10-02

Influence of superplasticizers on the hydration of Portland cement: in situ synchrotron x-ray diffraction study

Maria C. Dalconi[1], Gilberto Artioli[1], Arianna Lo Presti[2], Anna Bravo[2], Fiorenza Cella[2], Tiziano Cerulli[2]

1. *Dipartimento di Geoscienze, Università di Padova (UNIPD), Via Giotto 1, Padova 35137, Italy* **2.** *Mapei, via Cafiero, 22, Milano 20158, Italy*

e-mail: mariachiara.dalconi@unipd.it

The workability of concrete strongly depends on the rheological properties of cement pastes, which in turn are controlled by the complex system of reactions taking place during hydration process. Addition of organic additives used as superplasticizers modifies the kinetics of hydration reactions thus influencing chemical and physical properties of cement pastes. Many investigations have been carried out to disclose the effect of additives on rheological properties in cement and concrete [1-2]. Recently, detailed in-situ x-ray diffraction studies on the organic additives influence during hydration of Portland cement have been reported [3]. The present work extends the investigation to the behaviour of novel generation polymeric additives (poly-carboxylic-acid esthers based superplasticizer).

Cement pastes were prepared mixing ordinary Portland cement (CEM I 52,5) with water or solutions containing additives. To monitor the formation of gel-like (amorphous) phases during hydration process, a known amount of non-reacting internal standard (rutile) was added to the cement mixtures. Several glass capillaries were filled with the cement pastes and kept in a thermostatic bath at 40°C. The hydration process was followed for the first 8 hours, taking snapshots at different times for each sample. Time resolved x-ray diffraction measurements were performed at the Swiss Light Source Material Science beamline (X04SA) equipped with a Mythen 1-D microstrip detector.

Phase quantification by Rietveld analysis indicates different rates of ettringite formation and C3S consumption between the cement pastes with and without additives (Figure 1). The refined values of the internal standard phase fractions record a slight increase with the hydration proceeding. This reveals the presence of an evolving amorphous component in the system.

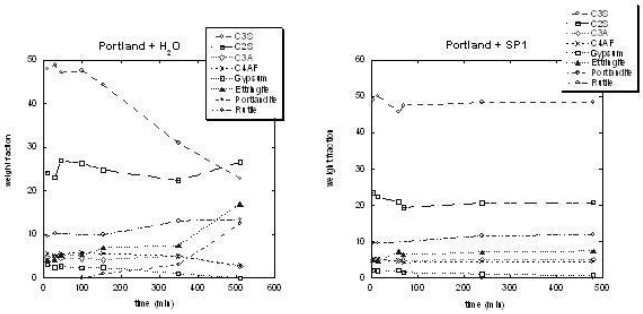

Figure 1. Phase fractions time evolution of hydrating cement pastes with and without superplasticizer additive.

References

[1] S. Hanehara, K. Yamada, Interaction between cement and chemical admixture from the point of cement hydration, absorption behaviour of admixture, and paste rheology, Cem. Concr. Res. 29 (8) (1999) 1159–1165.

[2] C. Jolicoeur, M.-A. Simard, Chemical admixture–cement interactions: phenomenology
and physico-chemical concepts, Cem. Concr. Compos 20 (2–3) (1998) 87–101.

[3] M. Merlini, G. Artioli, C. Meneghini, T. Cerulli, A. Bravo and F. Cella, The early hydration and set of Portland ements: In situ X-ray powder diffraction studies, Powder Diffraction, 22, 201-208 (2007).

15:30	Poster	10-03

The kinetics of lithium insertion in tin-based alloys studied by time-resolved synchrotron based in situ X-ray diffraction

Kristina Edström[1], Jack T. Vaughey[2], Michael M. Thackeray[2]

1. *Uppsala University, Department of Materials Chemistry, Angstrom Laboratory, Uppsala, Sweden* **2.** *Argonne National Laboratory (ANL), 9700 South Cass Avenue, Argonne, IL 60439, United States*

e-mail: kristina.edstrom@mkem.uu.se

In the search for new materials that can react and host large amounts of lithium-ions, tin has attracted a large interest. Tin can alloy with lithium with a total amount of 4 lithium per atom. Electrochemically this is occurring at low potentials vs. Li/Li^+, which makes tin interesting as an anode material for Li-ion batteries. A number of different phases are formed when lithium is alloying with tin. This electrochemical process can be followed by *in situ* powder X-ray diffraction, which today is a standard technique within the field of lithium battery research. During the lithiation process the volume of the tin particles are expanding up to 358% for the fully lithiated sample. This imposes large strains in the composite electrode matrix leading to cell failure due to crack formation of the electrode and loss of particle contact. There are different ways to circumvent this problem and we have earlier shown that forming intermetallic compound of tin with copper (that do not react with lithium) can decrease the

strain in the material [1]. We showed for Cu_6Sn_5 that lithium reacts with the formation of an intermediate phase, Li_2CuSn, while copper is being extruded from the structure and that at a potential below 0.2V vs. Li/Li^+, Li_4Sn is formed. During extraction of the lithium ions the copper is entering the structure and Cu_6Sn_5 could be re-formed.

In this study we have used a pulsed electrochemical method to study the structural kinetic response to lithium insertion in a number of Cu_6Sn_5 analogs where one of the copper atoms has been replaced with another metal: $CoCu_5Sn_5$; $ZnCu_5Sn_5$; $FeCu_5Sn_5$; and $MnCu_5Sn_5$. We show how the lithium insertion properties are influenced both electrochemically and structurally by the use of time-resolved X-ray diffraction data produced at the Swedish synchrotron MAXlab in Lund. The diffraction set-up is simple as shown in Fig. 1 and the battery is made of a polymer laminated aluminium pouch. This battery type is as similar to those used in commercial systems as possible.

Fig. 1. A battery cell connected to a potentiostat at the 711 beamline, MAXlab, Sweden.

References

[1] L. Fransson, E. Nordström, K. Edström, L. Häggström, J.T. Vaughey and M.M. Thackeray. J. Electrochem. Soc. 149 (2002) A736.

15:30	Poster	10-04

Parametric refinement of in-situ XRPD data

Rajiv Paneerselvam[1], Robert E. Dinnebier[1], John Evans[2], Martin Jansen[1]

1. *Max-Planck-Institut FKF, Heisenbergstr. 1, Stuttgart D70569, Germany* **2.** *Department of Chemistry, University of Durham, Science Labs, South Road, Durham DH1-3LE, United Kingdom*

e-mail: p.rajiv@fkf.mpg.de

Parametric refinement method [1] enables simple parallel refinements of large amount of XRPD datasets dependent on external

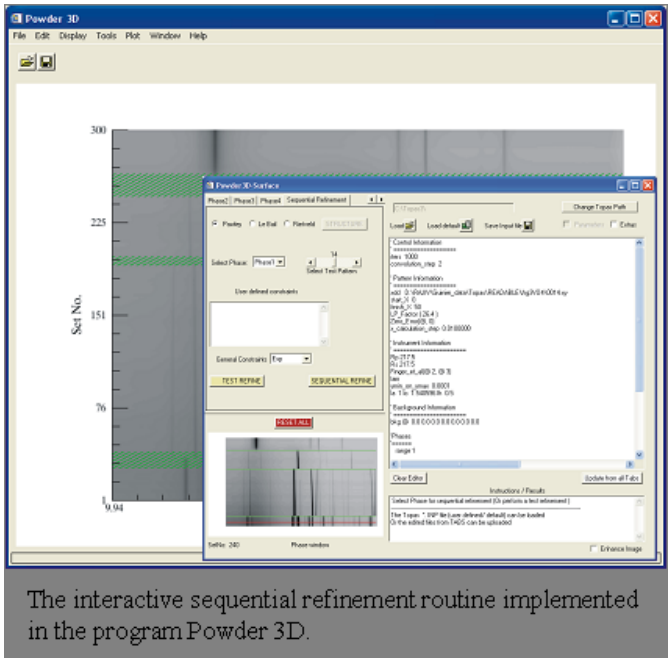

The interactive sequential refinement routine implemented in the program Powder 3D.

les. Parametric refinements are carried out by establishing non-physical models that control the convergence of refinement and physical models that describe the evolution of refinable variables with respect to the external factors (temperature, pressure, time, etc.) Parametric refinement offers ample advantages over normal sequential refinements. Parameterization of variables stabilizes the refinements and improves the precision of refined parameters [1]. It also reduces the number of free variables and creates the possibility of refining non-crystallographic quantities.

As a first step towards parametric refinement a programme that automates the process of single phase sequential Le-Bail/ Pawley refinements has been developed and presented here. The programme interacts with Topas [2] (a powerful software suite for total powder pattern analysis) for carrying out sequential and /or parallel refinements. Topas' macro language offers the flexibility to introduce user-defined constraint models in a very simple manner.

To facilitate the automation of sequential phase refinements, a general method to determine the number of phases in in-situ XRPD data has been developed. In this method, the boundaries are determined by comparing the Pearson's correlation coefficients of the neighboring patterns.

The sequential refinement routine and the phase boundaries determination routines are implemented as an interactive module in the multi pattern, data reduction software Powder 3D [3] with various options for manual interaction.

References

[1] G.W. Stinton and J.S.O. Evans, J. Appl. Cryst 40, 87–95 (2007)
[2] A.A. Coelho, TOPAS, v4.0. Bruker AXS, (2007).
[3] B. Hinrichsena, R.E. Dinnebier, and M. Jansen, Z. Krist.,Supplement Issue 23 (EPDIC-9 proceedings), 231-236 (2006)

15:30	Poster	10-05

XDB – a combined mass balance and full profile fit approach to quantitative phase analysis

István E. Sajó

Hungarian Academy of Sciences, Chemical Research Centre (CRC/HAS), Pusztaszeri ut 59-67, Budapest H-1025, Hungary

e-mail: sajo@chemres.hu

A full profile fit program was developed to evaluate X-ray powder diffraction scans with a special emphasize on quantitaive phase composition. The program runs in the 32 bit MS Windows environments and comes with an easy to use and intuitive user interface.

The software starts from PDF2 style reference data (the {d,I,*hkl*} sets of reflections) for each phase, that allows the profile fit for structureless phases too. Line shapes are modelled with the Pearson VII profile function. Appropriate corrections can be applied for preferred orientation (March-Dollase model) and mass absorption contrast (Brindley model).

Phase proportions are derived from the weight parameters of the profile fit corrected with their respective I/I_c coefficient. The calculated phase proportions depend on the particle size of the components and the absolute amounts (phase percentages) are normalized to the sum of the phases. These parameters can not be derived from the profile fit, they need to be determined independently. To improve the precision and reliability of phase quantification, the chemical composition of the sample is calculated from the phase percentages and compared to the values obtained from elemental analysis. The difference of calculated and analyzed chemistry (mass balance fit) can be refined simultaneously with the profile fit.

A fair amount of experience accumulated in analyzing various multiphase samples (ceramics, catalysts, cements, corrosion products, bauxites, ores, etc.) proves that this approach provides a fast and reliable way for phase quantification.

15:30	Poster	10-06

Modular In-Situ Reaction Chamber Design for Time-Resolved Diffraction

Mark J. Styles[1], Daniel P. Riley[1], Jason Christoforidis[2], Scott Olsen[2]

1. *The University of Melbourne, Grattan St., Melbourne 3010, Australia* **2.** *Australian Nuclear Science and Technology Organisation (ANSTO), New-Illawarra-Road.Lucas-Hieghts, Sydney 2234, Australia*

e-mail: m.styles2@pgrad.unimelb.edu.au

Progress in many technological fields including energy production, aerospace and bio-medicine is increasingly dependent upon materials with exceptional mechanical, thermal and chemical properties. Often these advanced materials are produced via complex processing techniques, making them costly both economically and environmentally. However, substantial process optimisation can be achieved through an examination of the fundamental mechanisms by which a material is formed.

Time resolved *in-situ* diffraction is a particularly powerful technique in materials research, capable of observing the time evolution of phases as they change in quantity and composition, and correlating these changes with process parameters such as temperature, pressure and time. As diffraction techniques and facilities impose unique constraints on sample geometry and processing equipment, specially designed chambers are generally required to simulate processing conditions.

To mitigate the expense of customised environment chambers, researchers at the University of Melbourne and the Australian Nuclear Science and Technology Organisation have designed and are currently constructing a modular reaction chamber, capable of separating the necessities of the diffraction technique from those of environment simulation. The *In-Situ Reaction Chamber* (Figure 1) abstracts many of the details intrinsic to the diffractometer such as beam definition, attenuation and collimation, allowing users to design inexpensive environment chambers that need only be compatible with a standard conflat flange at a set distance from the beam. The functionality of these insert chambers can then be customised to the needs of the individual user and calibration can be performed well in advance of beam time, reducing setup time to a minimum. By way of example, Figure 2 illustrates a more generic reaction chamber insert for high temperature investigations.

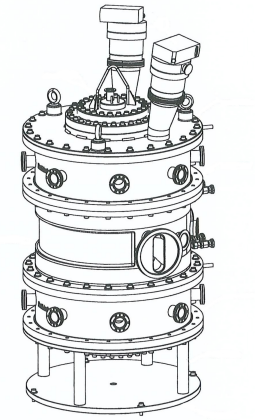

Figure 1: *In-Situ* Reaction Chamber (ISRC)

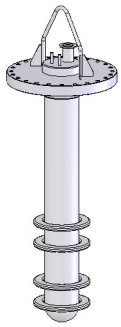

Figure2: High Temperature Insert

Powder diffraction on proteins

MS11 posters
Sunday afternoon, 21 September, 15:30

Instrumentation

MS12 posters
Sunday afternoon, 21 September, 15:30

15:30 Poster 12-01

On site x-ray diffraction: A new NDT method and technology for diagnosys of materials at the nano-scale of plants and manufactures

Giovanni Berti[1,2,3], Francesco De Marco[3], Antonio Nicoletta[3]

1. *University of Pisa, Earth Science Department and C I Material Engineering, Lab for RandD in XRD, Via S. Maria 53, Pisa 56126, Italy* **2.** *Consorzio Pisa Ricerche, Diffraction measurement and testing Centre (CPRDMTC), Corso Italia, Pisa 56100, Italy* **3.** *XRD-Tools s.r.l., Via Giuntini 25, Pisa 56023, Italy*

e-mail: g.berti@ing.unipi.it

There are some deformations of materials which progressively changes the lattice asset, the size and shape of grains which characterise the micro-nano structure of surfaces; these deformations can be used to predict dramatic damage. The ideal characteristic of the technology should be able to observe these deformations in either the plastic or viscous regime; it should have the appropriate resolution to distinguish patterns collected from materials, either affected or unaffected by such deformations.

The scale of observation is the nanometer and X-ray diffraction offers the appropriate requirements to provide the above mentioned characteristics. Appropriate mathematical theories exist, enabling the separation of contributions given by the presence of macrostrains, microsize and microistrains, even if they can be difficult to observe when using traditional X-ray diffraction technology. Moreover, since several years, experiments and measurements have been conducted by collecting data from materials under non-ambient conditions. Instruments implemented to observe X-ray diffraction from components of industrial plants or factories are, in general, so inflexible that the above-mentioned requirements are unattainable.

The implementation of an instrument fulfilling these requirements started via the cooperation between the Italian ISPESL and the University of Pisa (research contracts 67/97 and 42/98) and was based on the progress obtained since the early nineties by the cooperation between University of Pisa and Consorzio Pisa Ricerche. Little by little, measurements and testing have been performed thus giving confidence that the instrument DifRob®US7,260,178 was running correctly for the intended purposes.

The present paper reports on the advances obtained in collecting data from very brittle, thin and precious components, the surface of blocks of precious materials and from heavy and thick blocks of steel of industrial components.

15:30 Poster 12-02

New data collection subsystem for powder neutron diffractometer with position sensitive detectors

Martin Dráb, Ladislav Kalvoda, Stanislav Vratislav, Maja Dlouhá

Czech Technical University in Prague, The Faculty of Nuclear Sciences and Physical Engineering, Trojanova 13, Prague 2, Prague 12000, Czech Republic

e-mail: martin.drab@fjfi.cvut.cz

Project INDECS (Integrated Neutron Diffraction Experiment Control System) is a newly developed software system created for the purpose of data acquisition from, and controlling of, the upgraded version of the KSN-2 powder neutron diffractometer equipped with Position Sensitive Detectors. For the actual data acquisition and initial data analysis of the raw sampled signals, a special modular structure called the PSD Acquisition Path (or PSDAP) was designed. Raw sampled signals from either end of the PSD are taken as the main input to the subsystem. The signals are then split into multiple events, analyzed for the position of the obtained events on the PSD, and a histogram of the diffraction events is created as the main output of this subsystem. Moreover, the PSDAP is capable of storing the raw signals either before event splitting or after, so that later the whole process of acquisition can be replayed in software, perhaps with different settings of the processing parameters or perhaps even algorithms. It can also be switched into a mode where under special conditions a correction curve specific for the given PSD can be constructed and later, in normal operation, it can be used correct detected event positions to enhance the results on that particular PSD. This whole subsystem then acts as a single modular command unit (External Execution Module or EEM) within the entire system of project INDECS.

This research has been supported by grants MSM6840770040 and MSM6840770021.

15:30 Poster 12-03

A Monte Carlo ray-tracing model for planetary applications of x-ray powder diffraction and fluorescence

Graeme M. Hansford[1], Huawei Su[1], Richard M. Ambrosi[1], Ian Hutchinson[2]

1. *University of Leicester, University Road, Leicester LE17RH, United Kingdom* **2.** *Brunel University, London, United Kingdom*

e-mail: gmh14@star.le.ac.uk

A Monte Carlo 3D ray-tracing model for the simulation of X-ray powder diffraction and fluorescence is presented. The model is primarily intended as a tool to aid the development of a compact instrument for in-situ mineralogical and chemical analyses of planetary surfaces. A reflection geometry is assumed, along with fixed-position CCD detectors in order to avoid moving parts. In the model, X-rays are produced either by an X-ray tube or a radioactive source. The X-rays interact sequentially with a user-determined series of model elements which can include apertures, micropore collimators, söller slits and powder samples. Model samples are assumed to be ideal powders of any mineral or mixture of minerals for which the crystal structures are available. X-ray propagation ceases at the CCD detector(s), at which accurate quantum efficiency and energy redistribution effects are calculated. Given the appropriate characteristics, further source and detector types could easily be added. All model elements are treated as infinitely-thin surfaces which may be flat or curved (spherical or cylindrical).

The utility of this model lies particularly in the flexibility of the geometrical arrangement of the various elements, and the quantitative accuracy of simulations. This accuracy is illustrated in figure 1, which shows the comparison of experimental and modelled diffraction of Mn-Kα x-rays from a barite ($BaSO_4$) pressed-powder sample.

In addition, a simplified 2D model has been developed in order to determine the optimum placement of detectors with respect to 2θ resolution. The results of both models will be presented together with further comparisons with experimental data.

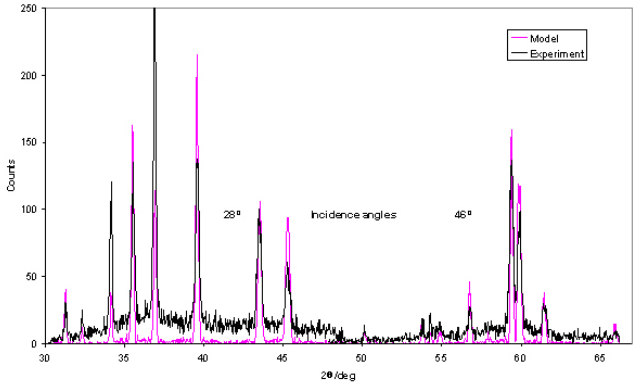

Figure 1. Comparison of experimental and modelled diffraction of Mn-Kα X-rays from a barite ($BaSO_4$) pressed-powder sample.

15:30	Poster	12-04

The Incoatec Microfocus Source IμS™ for home-lab diffractometry

Till A. Samtleben[1], Bernd Hasse[1], Jürgen Graf[1], Carsten Michaelsen[1], Uwe Preckwinkel[2], Holger Cordes[2], Ning Yang[2]

1. *Incoatec GmbH, Max-Planck-Str. 2, Geesthacht 21502, Germany* **2.** *Bruker Advanced X-ray Solutions (Bruker AXS), 5465 East Cheryl Parkway, Madison, WI 53711-5373, United States*

e-mail: hasse@incoatec.de

The Incoatec Microfocus Source IμS™ (see figure 1) is a suitable X-ray source for home-lab diffractometry applications. It incorporates an optimized combination of an extremely bright and very durable stationary air-cooled 30 W microfocus source and the newest type of 2-dim beam shaping multilayer optics, the so called Quazar™ optics.

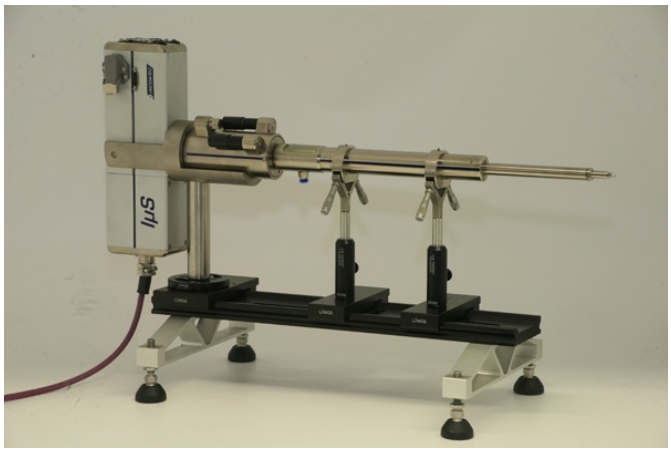

Figure 1: IμS™ with Quazar™ optics and collimator.

The IμS™ is a very versatile instrument available with copper or molybdenium anode and can be used with virtually any existing diffractometer-detector-system. Integrations are already done within Bruker and mar systems.

Due to the specially designed beam shaping Quazar™ optics, a focussing or collimating of the beam is possible. Also a hybrid-optics focussing in one direction and collimating in the other is available. The optics consist of bent substrates with shape tolerances below 100 nm, upon which multilayers are deposited with single layer thicknesses in the nanometer range and up to several hundreds of layer pairs. Additionally these multilayers were designed with lateral thickness gradients within ± 1% deviation of the ideal shape. This means that a deposition precision in the picometer range is needed. We use sputtering methods for deposition and optical profilometry in order to characterize the shape and X-ray reflectometry to characterize the multilayers. The beam parameters like monochromaticity, flux, brilliance and divergence demonstrate the quality of the multilayer optics for different lab applications, e.g. single crystal diffraction, powder diffraction, or small angle X-ray scattering. Measurements in the fields of phase identification, structure solution, stress and texture analysis and many others can be done.

We tested the IμS™ in combination with 2-dim detectors on samples in different geometries. Results of the tests are shown. They are compared with measurements of typical sealed tube and rotating anode systems.

15:30	Poster	12-05

iMATERIA - versatile neutron diffractometer at J-PARC

Toru Ishigaki[1], Akinori Hoshikawa[1], Masao Yonemura[2], Kenji Iwase[1], Dyah S. Adipranoto[1], Tuerxun Wuernisha[1], Takahiro Morishima[3], Takashi Kamiyam[3], Ryoko Oishi[3], Kazuya Aizawa[4], Masatoshi Arai[4], Makoto Hayashi[5]

1. *Ibaraki University, Frontier Research Center for Applied Nuclear Sciences, 4-12-1 Nakanarisawa, Hitachi 316-8511, Japan* **2.** *Ibaraki University, Institute of Applied Beam Science, 4-12-1 Nakanarisawa,, Hitachi 316-8511, Japan* **3.** *High Energy Accelator Research Organization, Neutron Science Laboratory (KEK), 1-1 Oho, Tsukuba 305-0801, Japan* **4.** *Japan Atomic Energy Agency, JPARC Center (JAEA), 2-4 Shirakatashirane, Tokai 319-1195, Japan* **5.** *Ibaraki prefecture goverment (IBARAKI), 978-6 Kasahara, Mito 310-8555, Japan*

e-mail: toru.ishigaki@j-parc.jp

Ibaraki prefecture, the local government of the area for the J-PARC (Japan Proton Accelaror Research complex) site in Japan, decided to build a versatile neutron diffractometer (iMATERIA, IBARAKI Materials Design Diffractometer) to promote industrial applications of neutron beam research at J-PARC. iMATERIA was planned to be a high throughput diffractometer so that materials engineers and scientists can use this diffractometer like any other chemical analytical instrument in their materials development programs. It covers in d range $0.18 < d\ (Å) < 5$ with $\Delta d/d = 0.16$ % for the high resolution bank, and covers $5 < d\ (Å) < 800$ with gradually changing resolution at three detector banks (90 degree, low angle and small angle). Typical measuring time to obtain a 'Rietveld-quality' data set is several minutes with the sample size of a laboratory X-ray diffractometer. To promote industrial applications, we will establish a support system for both academic and industrial users who are willing to use neutrons but are not familiar with neutron diffraction. The analysis software is also very important for powder diffraction experiments,

so we will also prepare a software package (Z-Code) consisting of a combination of several powder-diffraction software tools (Z-Rietveld, etc.), structural databases and visualization. The construction of iMATERIA was completed, as one of the day-one instruments for the J-PARC neutron facility. Recent data of iMATERIA will be reported.

15:30 Poster 12-06

The materials science and powder diffraction beamline at ALBA

Michael Knapp, Inma Peral, Salvador Ferrer

CELLS (ALBA), Campus UAB, Barcelona 08193, Spain

e-mail: mknapp@cells.es

We will present the design concept, and current status of the new Materials Science and Powder Diffraction beamline at ALBA. After the conceptual design report of the end-stations was presented to the user community in late 2007, it was decided that the beamline would be devoted mainly to two types of diffraction experiment: **high resolution powder diffraction** and **high pressure diffraction** using diamond anvil cells. Single crystal diffraction experiments will be possible but in a second phase of the beamline.

The beamline will operate between 8 to 50 keV. This energy range covers very well the desirable range for almost any powder diffraction experiment, and at the same time it will be possible to perform both total scattering experiments, and high pressure diffraction; for which it is desirable and sometimes necessary to have high energy sources (E > 30 keV). To accommodate the different experimental techniques there will be two experimental end stations, one devoted to powder diffraction and the second one to high pressure experiments. A third end-station is planned for a second phase, this end-station will be devoted to single crystal experiments. For this station it has been decided to install an independent and compact set-up that is commercially available and that would not compromise the rest of the layout of the beamline.

The optical elements have been recently awarded, thus the optics layout will be presented as well as the expected beam performance. The optics for the powder diffraction station includes a collimating mirror and a “double crystal” Bragg-monochromator. The energy resolution for this kind of monochromators is typically $\Delta E/E=2\cdot10^{-4}$ depending mainly on the choice of crystals. The high-pressure experiments need a beam diameter below 100µm. Therefore, a KB-mirror system will be installed behind the standard Bragg monochromator.

The end-stations layouts that have been agreed with the user community will be presented. The procurement of the different parts is now in progress; we will present the current status of the design, procurement and installation of the experimental stations.

15:30 Poster 12-07

First Results From the New Powder Diffraction Beamline (BL-I11) at Diamond

Julia E. Parker, Stephen P. Thompson, Chiu C. Tang

Diamond Light Source, Science Dept., Harwell Science and Innovation Campus, Chilton Didcot OX110DE, United Kingdom

e-mail: julia.parker@diamond.ac.uk

Beamline I11 at Diamond is the latest facility that has recently become operational for high resolution powder diffraction experiments. We present the design, key specifications and the hardware of this new beamline which receives an intense and highly collimated x-ray beam generated by an in-vacuum undulator. With the simple optics (a double-crystal monochroma-tor, harmonic rejection mirrors and slits), a high purity beam of low energy-bandpass x-rays in the range 5-30 keV is delivered at the sample. The heavy duty diffraction instrument is designed to have the flexibility to house a variety of sample environments and to have two detection systems to collect high quality diffraction data, i.e. multi-analysing crystals (MAC) for high angular resolution experiments and a fast position sensitive detector for time-resolved studies.

We have obtained results using the high resolution mode in the commissioning phase, in-cluding beam performance characteristics, powder diffraction peaks and profiles and resolu-tion function data from high quality SRM standards (Si_640c and LaB_6–660a). In addition, the first results obtained from mineralogical samples are given to demonstrate the capability of this new instrument.

15:30 Poster 12-08

A feasibility study of X-ray powder diffraction technique for synchrotron radiation under high pressure condition at the Siam Photon Laboratory

Varalak Saengsuwan[1], Thiti Bovornratanaraks[1], Wantana Klysubun[2]

1. *Department of Physics, Faculty of Science, Chulalongkorn University, 6th floor, Mahamakut Build., Payatai rd., Pathumwan, Bangkok 10330, Thailand* **2.** *National Synchrotron Research Center, P.O. Box 93, Nakhon Ratchasima, Nakhon Ratchasima 30000, Thailand*

e-mail: varalak.s@student.chula.ac.th

Nowadays the structural study of phase transitions in materials under high pressure conditions plays an important role in expanding the understanding of physical and chemical properties of materials. To support miscellaneous applications for high pressure research in Thailand, an experimental setup for X-ray powder diffraction (XRPD) under high pressure conditions using synchrotron radiation, which is based on station 9.1 at the Daresbury SRS, is developed on the bending magnet beamline BL8 at the Siam Photon Laboratory. Monochromatic X-rays with photon energy of 9000 eV are provided by a fixed-exit double crystal monochromator equipped with Ge(220) crystals. A diamond anvil cell (DAC) is used for generating high pressure conditions in powder samples. The quasi-hydrostatic pressure in the DAC is determined by the ruby fluorescent tech-

nique. In our recent study, we can record the complete diffraction pattern from the hexagonal phase of ZnO using an image plate area detector.

For the improvement of the diffraction intensity collected at this station, a double multilayer monochromator (DMM) and a focusing mirror will be used in order to provide the most suitable monochromatic X-rays, following the beamline design as shown in Figure 1. Results from ray tracing simulation for the optimization of the beamline will be presented.

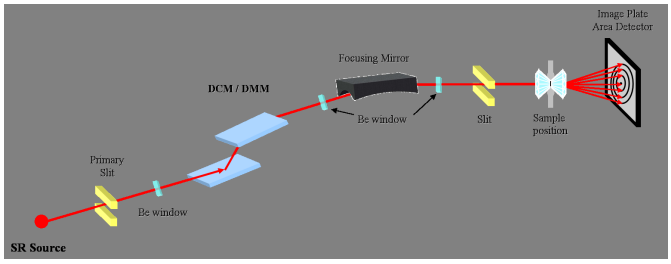

Figure 1: Schematic layout of the XRPD beamline design at the Siam Photon Laboratory

Nanomaterials

MS13 posters
Sunday afternoon, 21 September, 15:30

15:30 Poster 13-01

X-ray and electron microscopy techniques studies on nanocrystalline MgO powder materials prepared by sol-gel method

Grzegorz Dercz[1], Pająk Lucjan[1], Krystian Prusik[1], Roman Pielaszek[2], Janusz J. Malinowski[3]

1. *University of Silesia, Institute of Material Science, Bankowa 12, Katowice 40-007, Poland* **2.** *Polish Academy of Sciences, Institute of High Pressure Physics (UNIPRESS), Sokolowska 29/37, Warszawa 01-142, Poland* **3.** *Institute of Chemical Engineering Polish Academy of Sciences, Bałtycka 5, Gliwice 44-100, Poland*

e-mail: gdercz@op.pl

Materials with MgO nanocrystalites were prepared by sol-gel synthesis. Alcogels were dried either supercritically at 538 K or in supercritical CO_2. Conventional drying was also applied. Calcination of dry gels at 723 K under vacuum yielded MgO nanocrystallites. In the studied materials the amorphous phase was also stated. MgO nanocrystallites are immersed in amorphous matrix. Structure studies were performed by X-ray diffraction, scanning and transmission electron microcopies. Nitrogen adsorption/desorption measurements were also performed. Morphology of supercritically dried samples is similar; rough surface of powder particles is observed. Powder particles of conventionally dried sample are more compact. Size of MgO crystallites is generally similar for all samples and equal to about 7 nm despite of drying conditions of alcogels. Specific surface area and volume of mesopores is the greatest for sample supercritically dried at 538 K.

15:30 Poster 13-02

Characterisation of oxide nanoparticles synthesised using supercritical water

Ulrich Förter-Barth, Michael Herrmann, Maren Daschner de Tercero

Fraunhofer ICT, Joseph-von-Fraunhofer 7, Pfinztal 76327, Germany

e-mail: foe@ict.fhg.de

Near- and supercritical water is an attractive medium for the synthesis of metal oxide nanoparticles. The continuous hydrothermal synthesis is based on the mixing of a cold metal salt stream with hot compressed water. Here, it is exploited that the properties of water –in particular the permittivity– strongly change around the critical point (p = 22,1 MPa, T = 647,1 K). Mass transport related characteristics are similar to those of gases, whereas the density and the dissolving power are in the range of fluids. Thus, the formation of oxide nanoparticle dispersions without the addition of any additives is enabled.

Iron oxide nanoparticles were produced with this method by varying the mixing ratio, the flow rate and the concentration of the reactant. The size-dependent physical and chemical properties are of great importance for technical applications. Structure and properties of iron oxide nanoparticles strongly depend on the particle size, their history of formation and the surrounding medium.

The crystal structure and the mean crystallite size of the synthesised particles were investigated by powder x-ray diffraction (PXRD). A Bragg-Brentano goniometer D8 (Bruker AXS) with Cu-radiation and scintillation counter was used. The system was additionally equipped either with a secondary monochromator or two symmetrically arranged Göbel-mirrors (parallel beam geometry). The identification of the obtained material was carried out with the database Powder Diffraction Files (PDF) of the International Centre for Diffraction Data (ICDD); the evaluation of the crystallite size with the software tool TOPAS (Bruker AXS).

Particles synthesised from aqueous iron nitrate solutions could be identified as alpha-Fe2O3 (hematite) with crystallite sizes of about 35 nm. Increasing the flow rate leads to the formation of particles of less than 20 nm (confirmed by TEM-images). These samples show no or weak reflections at the positions for hematite. However, the determination of the crystallite size failed.

Magnetite (Fe3O4) was synthesised from aqueous iron acetate solutions. The crystal structure was clearly identified by PXRD with a mean crystallite size of 48 nm. TEM-images show the existence of two particle fractions, one of 50 nm – 200 nm and the other with particles below 10 nm. Stable dispersions were produced by adding nitric acid to the iron acetate solutions. Particles of about 10 nm in diameter with a narrow particle size distribution were obtained (confirmed by TEM). Again, a clear determination of the structure was not possible.

[1] M. Daschner de Tercero, J. Schubert, U. Fehrenbacher, M. Türk, U. Teipel, Kontinuierliche Herstellung von Eisenoxidnanopartikeln in überkritischem Wasser, 4. Symposium Produktgestaltung in der Partikeltechnologie, Pfinztal, 2008.

15:30 Poster 13-03

Texture analysis of an Al-evaporated thin film with powder electron diffraction data

Mauro Gemmi[1], Marco Voltolini[2], Hans-Rudolf Wenk[2]

1. *Università di Milano, Dipartimento di Scienze della Terra, via Botticelli 23, Milano 20133, Italy* **2.** *University of California, Earth and Planetary Science Department, Berkeley, CA 94720-4767, United States*

e-mail: mauro.gemmi@unimi.it

An Al thin film, produced by evaporation on an amorphous carbon film, has been investigated with selected area electron diffraction (SAED). The powder SAED patterns were collected with a CCD camera using the largest diaphragm in order to have complete diffraction discs with reliable statistics. The patterns were integrated using the software Fit2D, after refining the camera length, the beam center, and the tilt of the CCD detector. The resulting intensity vs 2Q spectrum, collected with the sample normal to the beam, was analyzed with the Rietveld method GSAS, after inserting the electron scattering factor for Al to check if a Rietveld refinement is possible. The fit is acceptable only if a strong preferential orientation of a [111] direction normal to the film is considered. In order to directly investigate the texture of the film, we tilted the sample along the two orthogonal axes of the sample holder, and collected electron diffraction patterns at 5° intervals. Texture analysis was carried out adapting a consolidated texture analysis procedure for synchrotron hard X-ray diffraction data [1] using the MAUD software. After importing the electron structure factors F_{hkl} for cubic Al, we proceeded with texture analysis using the EWIMV algorithm, refining experimental geometry parameters, peak profile function coefficients, backgrounds, scale factor and texture. Pole figures obtained for the aluminum film are plotted in the figure, and clearly show a strong (111) fiber texture. As a check, the analysis was carried out both without sample symmetry and with axial symmetry imposed and the resulting texture data are practically identical. Even without imposing symmetry the analysis was surprisingly stable. We present here for the first time, a texture analysis based on the Rietveld method applied to electron diffraction data. This new procedure seems very suitable to study textures in nanocrystalline materials and seems mature enough to be applied to more complex systems.

References:

[1] G. Ischia, H.-R. Wenk, L. Lutterotti, F. Berberich. J. Appl. Cryst., 38, 377-380, 2005.

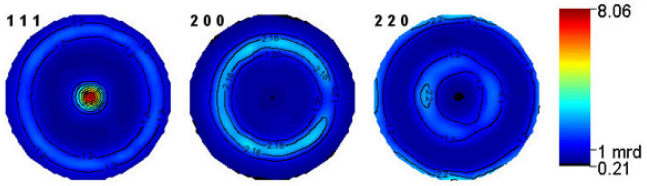

15:30 Poster 13-04

Characterization of NiS and NiCoS nanoparticles in zeolite type LTA host

Mahdi Meftah, Walid Oueslati, Abdesslem B. Haj Amara

Laboratoire de Physique des Matériaux Lamellaires et Nano Matériaux Hybrides (LPMNMH), Faculty of science of Bizerte, Bizerte 7021, Tunisia

e-mail: meftahmahdi@yahoo.fr

We report the optical and structural properties of NiS and the ternary NiCoS nanoparticles in zeolite type LTA ($|Na_{96}(H_2O)_{216}|[Si_{96}Al_{96}O_{384}]$). The samples were obtained by sulfidation of the Ni^{2+} and Co^{2+} ion-exchange zeolite in a Na_2S solution at room temperature. The optical properties of the samples were studied by UV–visible spectroscopy. Their crystalline structure and morphology were studied by XRD and scanning electron microscopy. The results show that the nanoparticles are inside the zeolite channels and cavity. Exciton absorption peaks at higher energy than the fundamental absorption edge of bulk NiS and CoS indicate quantum confinement effects in nanoparticles as a consequence of their small size. The absorption spectra show that the optical band gap varies in the range 3 – 4 eV, depending on the semiconductor material and their relative concentration.

15:30 Poster 13-05

Database on size-induced phase transitions in nanocrystals

Paweł E. Tomaszewski

Institute of Low Temperature and Structure Research, Polish Academy of Sciences, P.Nr 1410, Wrocław 50-950, Poland

e-mail: p.tomaszewski@int.pan.wroc.pl

The influence of size on physical properties of microcrystals is known from more than 50 years. Nanosized materials (nanoparticles, nanocrystals) have a different properties, e.g. transition temperature, than their coventional coarse-grained polycrystalline or bulk counterparts. During X-ray powder diffraction studies the size induced structural phase transitions to a new, previously unknown phases, are discovered for many nanocrystals. The literature data on 70 phase transitions occurring in 56 nanocrystals are presented in the form of database. Different types of phase diagrams "grain size - transition temperature" are also presented. Several such transitions in nanocrystals of double molybdates and tungstates are discovered in our laboratory.

Part of this work was supported by the Polish Ministry of Science and Higher Education under contract No 1 P03B 078 29.

Non-ambient conditions

MS14 posters
Sunday afternoon, 21 September, 15:30

15:30 Poster 14-01

Polymorphs and hydrates of lead squarate, $Pb(C_4O_4).nH_2O$ (n= 0, 1, 4): a powder diffraction study

Amira Bouhali[1], Chahrazed Trifa[1], Chaouki Boudaren[1], Nathalie Audebrand[2], Thierry Bataille[2]

1. *Laboratoire de Chimie Moléculaire, Contrôle de l'Environnement et de Mesures Physico-Chimiques, route de Ain El-Bey, Constantine 25000, Algeria* **2.** *University of Rennes, Sciences Chimiques de Rennes, Rennes 35042, France*

e-mail: thierry.bataille@univ-rennes1.fr

Lead-based oxalate compounds have been widely investigated as precursors of PZT (lead zirconium titanate) derivatives that can be obtained at moderate temperatures [1]. In order to understand the role of the carboxylic ligand in the structural arrangement of metals, we have paid our attention on the squarate group, which resembles the oxalate anion in terms of design and possible connectivity. Among the syntheses of mixed metal squarates, lead squarate and its hydrates have been obtained. The thermal decomposition of $Pb(C_4O_4).4H_2O$ [2], studied by temperature-dependent X-ray powder diffraction (TDXD) and thermogravimetry (TGA), lead to $Pb(C_4O_4).H_2O$ and three polymorphs of anhydrous lead squarate. Their formation is strongly dependent on the experimental conditions used for the dehydration.

The powder patterns of three out of the four compounds have been indexed using DICVOL06 [3]. $Pb(C_4O_4).H_2O$: a = 7.366(1) Å, b = 11.305(2) Å, c = 6.685(1) Å, β= 102.49(1)°, $P2_1/c$, Z = 4 [M_{20} = 46, F_{20} = 82(0.0071, 34)]; $Pb(C_4O_4)$ (Polymorph I): a = 24.268(4) Å, b = 15.270(3) Å, c = 7.854(1) Å, *Cmma* [M_{20} = 26, F_{20} = 64(0.0051, 60)]; $Pb(C_4O_4)$ (Polymorph II): a = 15.853(6) Å, b = 14.798(5) Å, c = 5.380(2) Å, α = 63.90(3)°, β = 103.33(4)°, γ = 115.95(3)°, P-1 [M_{20} = 27, F_{20} = 52(0.0065, 60)]. $Pb(C_4O_4)$ (Polymorph III) could be obtained as single crystals and its structure has been consequently solved from single crystal diffraction data. The crystal structure of $Pb(C_4O_4).H_2O$ was solved *ab initio* with direct-space methods using FOX [4]. The structural filiation between tetrahydrate, monohydrate and anhydrous phases are discussed.

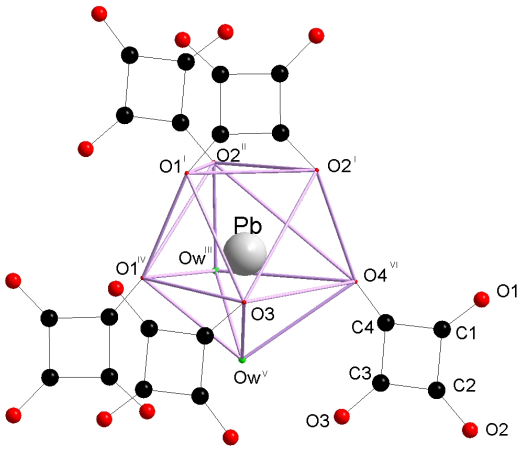

References

[1] L. A. Hall, D. J. Williams, S. Menzer, A. J. P. White, Inorg. Chem. 36 (1997) 3096.

[2] C. Boudaren, J. P. Auffredic, M. Louër, D. Louër, Chem. Mater. 12 (2000) 2324.

[3] A. Boultif, D. Louër, J. Appl. Crystallogr. 37 (2004) 724.

[3] V. Favre-Nicolin, R. Cerny, J. Appl. Crystallogr. 35 (2002) 734.

15:30 Poster 14-02

In situ XRD investigation of Co_3O_4 reduction

Olga A. Bulavchenko[1], Svetlana V. Cherapanova[1], Sergey V. Tsybulya[1,2]

1. *Boreskov Institute of Catalysis (BIC), pr. akad. Lavrentieva, 5, Novosibirsk 630090, Russian Federation* **2.** *Novosibirsk State University (NSU), Pirogov 2, Novosibirsk 630090, Russian Federation*

e-mail: isizy@catalysis.ru

The supported cobalt catalysts are widely used in Fischer-Tropsch synthesis. Catalysts are activated by reduction of Co_3O_4 in hydrogen. It is important to understand how the reduction conditions influence the structural parameters of catalyst. We investigated Co_3O_4 supported on g-Al_2O_3 and model samples to compare their behavior during reduction process. *In situ* X-ray powder diffraction was used to characterize the structure of Co catalyst supported on g-Al_2O_3 and model samples.

Initial structure of both types of samples is similar according to XRD structural analysis and contains vacancies in the cation positions. *In situ* X-ray diffraction investigations show that reduction process is different for supported and non-supported samples in hole. But there are some features which are the same for both types of the samples. The reduction process for the both types of samples begins at the same temperature (T=180°C). The structure mechanism of the reduction process beginning is also the same: we observed decreasing the quantity of cation vacancies and filling the non-spinel octahedral position by Co ions that indicates on the appearance of clusters with the structure of CoO inside the structure of Co_3O_4. Ap-

pearance of CoO clusters is common feature for both types of samples. But further reduction process is different for supported and non-supported samples. Non-supported sample is reduced to metal Co (hcp) at the temperature T=180°C without formation intermediate CoO phase i.e. non-supported sample is reduced in one step. In contrary supported cobalt oxide is reduced in two steps. Reduction of Co_3O_4 to CoO clearly identified by XRD is the first step. The second step (CoOàCo) begins at 260°C and it is not fully completed at the temperature 400°C. At this temperature two phases CoO and Co (fcc) coexist. Metallic Co (hcp) and Co (fcc) have very high concentration of staking faults. The diffraction pattern simulation showed that Co(hcp) and Co(fcc) structures contained stacking faults with concentration of about 0.2 and 0.1, correspondingly.

15:30	Poster	14-03

Effect of Zn doping on the tetragonally distorted $CuFe_2O_4$ structure

Jolanta Darul[1], Waldemar Nowicki[1], Dmytro M. Trots[2]

1. *Adam Mickiewicz University, Faculty of Chemistry, Grunwaldzka 6, Poznań 60-780, Poland* **2.** *Hamburger Synchrotronstrahlungslabor HASYLAB, Notkestrasse 85, Hamburg 22607, Germany*

e-mail: jola@amu.edu.pl

Considering the various spinel ferrites, $CuFe_2O_4$ has gained a prominent interest among materials science researchers both fundamentally and technologically for various applications. Since of Cu^{2+} is a Jahn-Teller ion, it gives the anomalous favorable properties and also exhibits phase transition from tetragonal to cubic. The partial diamagnetic substitution of Cu^{2+} for Zn^{2+} restrains the Jahn Teller effect - changes of stoichiometry reduce the crystallographic transition temperature.

Polycrystalline zinc-cooper-iron oxides were prepared by a sol-gel method. The compounds formation and crystallinity of the materials were identified by XRD patterns, which were recorded on a Bruker D8 Advance diffractometer, with CuKα radiation.

Effect of substitution with Zn^{2+} ions in $Cu_{1-x}Zn_xFe_2O_4$ system on its high-temperature structural phase transitions have been investigated on the synchrotron beamline B2 at HASYLAB (DESY, Hamburg). The structure refinement of all polymorphs using Rietveld profile analysis, based on the synchrotron X-ray data, were performed. The cation distribution of $Cu_{1-x}Zn_xFe_2O_4$ samples derived from Rietveld analysis indicates that Cu ions occupy the octahedral B-sites, so tetragonal distortion in these materials is attributed to the cooperative distortion that driven by the octahedral Cu^{2+} ($3d^9$). As Zn^{2+} substitutes Cu^{2+} in these disordered spinels, it replaces Fe^{3+} at A-site. This is due to the site preference of Zn^{2+}, which leads to transfer Fe^{3+} from A-sites to B-sites and in turns a crystallographic transformation from tetragonal to cubic structure is occurred. This transformation is attributed to the decrease of the concentration of octahedrally coordinated JT ions in the host structure and leads to the presence of high-symmetry phase.

Acknowledgements: The synchrotron measurements at DESY-HASYLAB were supported by the IA-SFS-Contract No. RII3-CT-2004-506008 of European Commission. We would like to thank Dr. D. Trots from Hasylab for his assistance during experiments.

15:30	Poster	14-04

Crystal structures and phases transitions of new double perovskite oxides $Sr_{2-x}Ca_xLnSbO_6$ (Ln= La, Sm and 0≤x≤1)

Abdessamad Faik, Edurne I. Zabalo, Irene U. Olabarria, Josu M. Igartua

Facultad de Ciencia y Tecnología (UPV/EHU), P.Box 644, Bilbao 48080, Spain

e-mail: abdessamad.faik@ehu.es

The perovskite structure type is one of the most regularly observed structure types in condensed matter sciences, as well as in advanced materials research and applications. This is due to their wide array of proprieties: superconducting, magnetoresistance,…. The double perovskite with general formula $A_2BB'O_6$ can be represented as a three-dimensional network of alternating BO_6 and $B'O_6$ octahedra, sharing the oxygens at the corners of the octahedra, with the A-cations occupying the interstitial spaces between the octahedra. The family of antimony double perovskite oxides with double perovskite has attracted a considerable attention because of the magnetic properties of some of its members, such as Sr_2FeSbO_6 [1,2].

The $Sr_{2-x}Ca_xLnSbO6$ (Ln=La,Sm) (**0≤x≤1)** materials have been elaborated by the standard solid state reaction method. Rietveld analysis of laboratory x-ray powder diffraction data at room temperature, shows that these materials are double perovskite oxides and that should be represented by $Sr_{2-x}Ln_x[Ln_{1-x}Ca_x]SbO_6$ for 0≤x≤1, and by $[Sr_{1-x}Ca_xLn]CaSbO6$ for 1≤x≤2, general formulas. In the lanthanum compounds, the A and B sites are totally occupied by La^{3+} and Ca^{2+} cations, respectively. In the samarium containing compounds, the Sm^{3+} and Ca^{2+} are partially disordered at the A and B. At room temperature, all these materials were found to have a monoclinic unit cell with a primitive space group $P2_1/n$. The high-temperature powder laboratory x-ray powder diffraction analysis has revealed that the most general temperature evolution of the crystal structures in these materials shows a double phase-transition sequence: from monoclinic (S.G. $P2_1/n$) to rhombohedral (S.G. R-3) and, then, to cubic symmetry (S.G. Fm-3m), with increasing of temperature. The transition temperatures increase as the size of the cation in the A-site decreases. Thus, the mechanism of these phase transition is related to the mistmatch between the size of the A cation and the cuboctahedral space between the BO6 and B'O6 octahedra.

[1] E.J. Cussen, J.F. Vente, P.D. Battle and T.C. Gibb (1997), J. Mater. Chem. 7 459-463. [2] N. Kashima, K. Inoue, T. Wada and Y. Yamaguchi (2002), Appl. Phys. A 74 S805-S807

15:30 Poster 14-05

Synchrotron radiation induced crystallization of amorphous Barium Titanate

Yishay Feldman[1], Vera Lyahovitskaya[1], Gregory Leitus[1], Igor Lyubomirsky[1], Ellen Wachtel[1], Vladimir A. Bushuev[2], Yuri Rosenberg[3], Gavin Vaughan[4]

1. *Weizmann Institute of Science, Rehovot 76100, Israel* **2.** *M.V. Lomonosov Moscow State University, Vorobyevy gory, Moscow 119992, Russian Federation* **3.** *Tel Aviv University (TAU), Ramat Aviv, Tel Aviv 69787, Israel* **4.** *European Synchrotron Radiation Facility (ESRF), Grenoble 38043, France*

e-mail: isai.feldman@weizmann.ac.il

A novel phenomenon of crystallization of amorphous inorganic material caused by 23 keV synchrotron X-ray beam irradiation is reported.

The structural homogeneity of self-supported buckling Barium Titanate (BTO) membrane (0.5 μm thick and 200 μm diameter), which kept amorphous after heat treatment up to 560C, has been checked with ten micron lateral resolution synchrotron radiation (SR) microbeam of ID11 Materials Science beamline of the European Synchrotron Radiation Facility. The amorphous nature of membrane was defined initially by laboratory wide angle X-ray scattering in transmission through the whole membrane area. No traces of crystalline phase were observed by optical or atomic force microscopes (AFM) as well. In the course of membrane mapping by SR, 168 two-dimensional equidistant (step size 25 μm) frames (10sec/frame) converted afterwards into standard one-dimensional X-ray diffraction (XRD) patterns were obtained in transmission. All XRD patterns confirmed unequivocally that the membrane was locally amorphous.

On the other hand, after SR irradiation a new clearly seen regular configuration of spots has emerged in membrane's optical image. The regularity of these contrast variations matches surprisingly well SR microbeam stops during mapping; this coincidence rejects any factor but SR irradiation as a reasonable cause of this pattern emergence. AFM imaging reveals that square pyramids have been appeared on the surface of amorphous BTO membrane. The AFM exposed landscape argues strongly that observed pyramids grew as a result of the membrane exposition under SR beam. Electron backscatter diffraction patterns obtained from the pyramids clearly demonstrate Kikuchi lines inherent to quite perfect single crystal.

The nature and probable mechanism of the observed phenomenon are discussed.

15:30 Poster 14-06

Iron bearing tetrahedrite and tennantite at 25ºC and 250ºC

Karen Friese[1], Andrzej Grzechnik[1], Emil Makovicky[2], Tonci Balic-Zunic[2], Sven Karup-Moller[3]

1. *Dpto. Física Materia Condensada, Universidad del País Vasco (UPV/EHU), Facultad de Ciencia y Tecnología, Apdo. 644, Bilbao 48080, Spain* **2.** *Department of Geography and Geology, University of Copenhagen, Copenhagen DK-1350, Denmark* **3.** *Institute for Environment and Resources, Danish Technical University, Lyngby DK-2800, Denmark*

e-mail: karen.friese@ehu.es

Phases in the tetrahedrite-tennantite solid solution series with the general composition $(Cu,Ag)_{10}(Fe,Zn,Hg,Cu,\ldots)_2(Sb,As)_4S_{13}$ are among the most frequent complex sulfides in ore deposits. The crystal structures of the tetrahedrite-tennantite family can be derived from the sphalerite structure type, where a part of the tetrahedra is replaced by other coordination polyhedra. $Cu(1)S_4$ tetrahedra form a tetrahedral framework with large cavities which host clusters of Cu(2) with three-fold coordination and lone electron pairs of Sb (As). These metalloids are positioned as $(Sb,As)S_3$ pyramids in the cavity walls.

The four phases investigated here do not deviate from the ideal stochiometry

$M_{12}(Sb,As)_4S_{13}$, yet some of the Cu atoms are substituted by Fe. Their compositions are $Cu_{11.4}Fe_{0.6}Sb_4S_{13}$, $Cu_{10.2}Fe_{1.8}Sb_4S_{13}$, $Cu_{11.9}Fe_{0.1}As_4S_{13}$, and $Cu_{10.8}Fe_{1.2}As_4S_{13}$. At low substitution, iron is incorporated as Fe^{3+}. With increasing substitution, Fe^{3+} is converted into Fe^{2+}, the conversion being complete at a composition of $Cu_{10}Fe_2(Sb,As)_4S_{13}$.

Rietveld refinement of x-ray diffraction data from low-Fe and high-Fe samples of both compounds, obtained at SNBL/ESRF (Grenoble) (λ=0.3748 Å) at 25^o and 250^{o}C, suggests that the coefficient of thermal expansion is highest for samples with low iron substitution. Splitting of triangular Cu(2) positions increases with temperature and the half-occupied Cu(2) positions from different coordination triangles approach each other, down to 2.70-2.75 Å in tennantite at 250^{o}C. There is insignificant residual electron density between the split Cu(2)-sites in tetrahedrite at 25^{o}C and its increase with temperature is moderate. The inter-site density is substantially higher in tennantite and increases considerably with temperature, especially in the low-Fe sample.

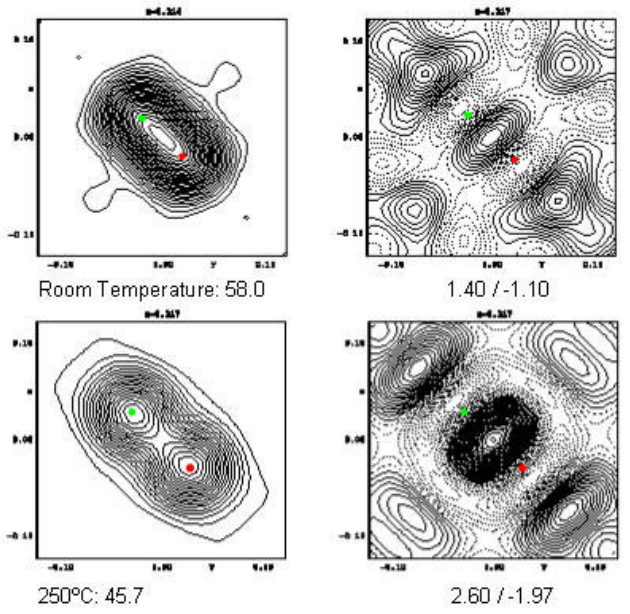

F_{obs} and difference-Fourier maps (minima/maxima in eÅ^{-3}) of $^{obs}Cu_{11.9}Fe_{0.1}As_4S_{13}$. Central point x(Cu2),0,0; distances in the three directions 2.5x2.5x2.5 Å. Contour lines 2 (Fobs) and 0.1 (difference-Fourier).

15:30 Poster 14-07

In situ high temperature synchrotron powder diffraction study of the thermal decomposition of cement-asbestos

Alessandro F. Gualtieri[1], Magdalena Lassinantti Gualtieri[1], Carlo Meneghini[2]

1. *Universita di Modena and Reggio Emilia, Modena, Italy* **2.** *Universita di Roma Tre, Roma, Italy*

e-mail: alessandro.gualtieri@unimore.it

Asbestos minerals have been extensively used since the beginning of the last century. However, use of these minerals is now banned in many countries as inhalation of asbestos fibers may cause lethal lung diseases. Consequently, the elimination of asbestos-containing materials (ACM) from the environment is of high priority. The dismissal of these hazardous materials in waste plants can not be regarded as an ultimate solution due to the risk of fiber dispersion in air during dumping operations and storage. An alternative is thermal transformation of ACM in non-hazardous minerals which can be safely recycled. A common type of ACM is cement-asbestos for which an industrial process for safe transformation has been developed in Italy. The process includes a prolonged thermal treatment (ca 1200 °C) of packages of cement-asbestos slates in a tunnel kiln. To optimize the temperature cycle of the process, it is important to gain a full understanding of the transformation sequence and kinetics. However, due to the low brightness of in-house X-ray sources, long data collection times are required to obtain adequate data. Consequently, the time resolution is strongly limited and e.g. the appearance and disappearance of metastable phases may be difficult to detect. Hence, it is necessary to use synchtrotron radiation in order to obtain a complete picture of the temperature-induced reaction pathway. For the first time, an in situ high temperature synchrotron powder diffraction study of the thermal transformation of cement-asbestos is presented. Data from a commercial cement-asbestos slate were collected at the Italian beamline BM08 (GILDA) at the European synchrotron radiation facility (ESRF), Grenoble (France), using the translating imaging-plate technique. Figure 1 shows a selected 2? range of the powder patterns collected during heating of cement-asbestos up to ca 900 °C and subsequent cooling down to ca 300 °C. Important temperature-induced changes in phase composition are clearly observed (see the Figure).

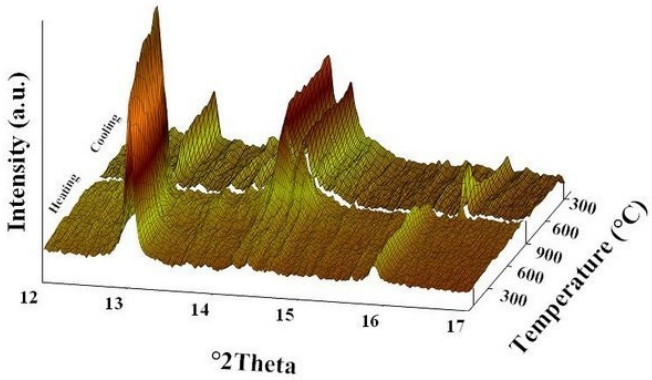

15:30 Poster 14-08

Investigation of the formation of magnesium titanate phases from xerogels using hot stage X-ray powder diffractometry

Jacob Zabicky[1], Giora Kimmel[1], Elena Goncharov[1], Francesc Guirado[2]

1. *Ben-Gurion University of the Negev, P.O.Box 653, Beer-Sheva 84105, Israel* **2.** *Universitat Rovira i Virgili (URV), Av. Països Catalans, 26, Tarragona 43007, Spain*

e-mail: kimmel@bgu.ac.il

Coprecipitated xerogel precursors of nanocrystalline magnesium titanates, with Mg:Ti stoichiometric ratio varying from 1:1 to 2:1, were subjected to thermal treatment at constant temperature in the range from 550 to 1200 °C, in air, using a hot-stage X-ray powder diffractometer. The kinetics during the first hour of the process showed dependence on the temperature and the Mg:Ti stoichiometric ratio of the precursor. At low temperatures, for compositions near 2:1, a single nonstoichiometric metastable nanocrystalline qandilite-like phase is formed; however, when the Mg content is lowered a solubility limit is reached, after which a nonstoichiometric qandilite, of fixed composition depending on the temperature, is in equilibrium with stoichiometric geikielite. The limit moves to higher Mg contents as the temperature rises. In the approximate 900-1000 °C range the metastable qandilite phases decompose into geikielite and periclase. At 1100 °C and above stoichiometric qandilite is obtained in equilibrium with geikielite. At low temperatures nanocrystalline qandilite is formed much faster than nanocrystalline geikielite, probably owing to the isotropic chemical structure of both the amorphous xerogels and qandilite. A phase diagram is proposed for the metastable nanocrystalline phases formed at low temperatures in the composition range of the present study.

15:30 Poster 14-09

High temperature X-ray investigation of liquid phase sintering of Zinc Oxide

Andreas Klimera, Mohammad Lutful Arefin, Friedrich Raether

Fraunhofer ISC (ISC), Neunerplatz 2, Würzburg 97082, Germany

e-mail: klimera@isc.fhg.de

ZnO-based ceramics doped with M_2O_3 show highly non-ohmic current voltagebehaviour that is important for surge arresting in electrical circuitry. The addition of Bi_2O_3 to ZnO lowers melting temperature and promotes liquid-phase sintering. In contrast, the presence of Sb_2O_3 influences grain size distribution and the formation of new intermediate compounds. Grain boundary phases with spinel and pyrochlore structures affect the electrical behaviour of ZnO-based varistors. In this work different compositions in the Zno-Bi_2O_3-Sb_2O_3-system were inwestigated.

High temperature in-situ X-ray diffraction by synchrotron source is used to observe successive formation of new phases during sintering. Partial evaporation of $(Bi, Sb)_2O_3$ leads to gradients in a liquid phase distribution in the surface region, so conventional HT-XRD is not reasonable because of its small penetration depht (10-20 µm).

Therefore, synchrotron X-rays were used at the Hasylab, Hamburg to analyze the phase formation in samples of 1 mm thickness. The samples were heated in a resistive furnace which was specially developed for those experiments and measured in transmission mode.

15:30 Poster 14-10

Influence of Lanthanum doping on the morphotropic phase boundary in lead zirconate titanate

Manuel Hinterstein[2], Michael Knapp[1], Kristin Schoenau[2], Hartmut Fuess[2]

1. *CELLS (ALBA), Campus UAB, Barcelona 08193, Spain*
2. *Technische Universität Darmstadt, Institute of Materials Science, Petersenstr. 23, Darmstadt 64287, Germany*

e-mail: mknapp@cells.es

Donor-doped $Pb(Zr_xTi_{1-x})O_3$ (PZT) ceramics possess various enhanced electrical and mechanical properties and are therefore frequently used in industrial applications. Despite extensive studies the microstructure of the morphotropic phase boundary (MPB) in these ferroelectric materials is still under discussion. Whereas some groups (Noheda et al [1]) fitted diffraction data by monoclinic symmetry, other groups describe the MPB as composed of a complicated system of micro- and nanodomains [2].

It would be of interest to draw a correlation between the structural stability range and enlarged dielectric properties called forth by nanodomains and the effects called forth by small percentages of dopand within the structure. A question now arising is how the stability field of nanodomain structures varies with Temperature in PLZT.

Temperature dependent synchrotron powder diffraction investigations at the beamline B2, Hasylab Hamburg across the entire compositional range of the MPB show changes in phase fractions, domain structure and phase transitions dependent on the nanodomain content. Temperatures from 20 K to 800 K were applied to PLZT compositions in the compositional range from x = 0.525 to x = 0.560 doped with 1% Lanthanum. The results will be discussed and compared with results from undoped PZT [3].

[1] Noheda et al., Phys. Rev. B 61 (2000).

[2] L. A. Schmitt et al., J. Appl. Phys. 101, 074107 (2007).

[3] K.A. Schoenau, PhD Thesis (2007).

15:30 Poster 14-11

Investigation of the products of the $BaBiO_{3-x}$ reaction with TiO_2 using the high temperature RTG attachment

Witold Z. Mielcarek, Krystyna Prociów, Joanna B. Warycha

Electrotechnical Institute, Division of Electrotechnology and Materials Science (IEL), M. Skłodowskiej-Curie 55/61, Wrocław, Poland

e-mail: mielcar@iel.wroc.pl

Varistors are the ceramic elements which are designed to protect electrical devices against overvoltage hazard. Their ability to handle the overvoltages results from the particularities of their V=R(I) characteristics i.e when exposed to high voltage transients the varistor impedance decrease many orders of magnitude, thus clamping the transient voltage to a safe level.

The ZnO varistors are processed by mixing the ZnO with a small amount of other metal oxides and although every metal oxide additive has its role to fulfill, the Bi_2O_3 is crucial for inducing the nonlinear property into ZnO ceramic. The non-ohmic behavior is brought about during varistor sintering when a number of processes and reactions is taking place in this system.

The basing process occurring during varistor sintering is the high-temperature (1050°C) $Bi_2(Zn_{4/3}Sb_{2/3})O_6$ pyrochlore phase reaction with ZnO. In the result forms alfa-$Zn_7Sb_2O_{12}$ spinel and Bi_2O_3, which is in liquid phase at this temperature. The Bi_2O_3 along with dopands dissolved in it penetrates into the intergrain regions and, by modifying them, influences varistor electrical properties. Varistor electrical properties depend also on the size of ZnO grains. The alfa-$Zn_7Sb_2O_{12}$ spinel hinders the grain growth during sintering. In this work the varistor ceramics was added with $BaBiO_{3-x}$. The $BaBiO_{3-x}$ was to act as a substitute of pyrochlore phase. As $BaBiO_{3-x}$ does not react with ZnO, as its reagent the TiO_2 was applied. The crystal phases measurements were performed with DRON 2 difractometer using Fe filtered Co radiation. The mixture of $BaBiO_{3-x}$ and TiO_2 were placed on Pt plate. As it appeared, due to the action of temperature, in the investigated ($BaBiO_{3-x}$ + TiO_2) sample the TiO_2 reflexes disappear at temperature about 700°C but quality changes of $BaBiO_{3-x}$ phase are observed at higher temperatures by appearance of ß Bi_2O_3 crystal phase, what proves that $BaBiO_{3-x}$ and TiO_2 went into reaction, although the (Ba,Ti) product of this reaction must be in subcrystalline form.

The ß Bi_2O_3 appearance give the evidence that the $BaBiO_{3-x}$ phase can be successfully applied in varistor technology.

15:30 Poster 14-12

High-pressure diffraction study of α and β Ge_3N_4

Roman Minikayev[1], Wojciech Paszkowicz[1], Jaroslaw Pietosa[1], Christian Lathe[2], Jakub Nowak[3]

1. *Polish Academy of Sciences, Institute of Physics, al. Lotników 32/46, Warszawa 02-668, Poland* **2.** *GeoForschungsZentrum Potsdam, (GFZ), Telegrafenberg A17, Potsdam D-14473, Germany* **3.** *Catholic University of Lublin, Department of Chemistry (KUL), Al. Kraśnicka 102, Lublin 20-718, Poland*

e-mail: minik@ifpan.edu.pl

The family of nitrides of group IV is mostly known due to the prediction [1] (followed by numerous experimental studies) of the shortest covalent bond in C_3N_4. The members of this family crystallise with several structures at ambient pressure and the spinel and olivine type phases at high pressures, and amorphous phase at the highest pressures. In this study the pressure behaviour of two polymorphs of a representative of this family, α- and β-Ge_3N_4 is studied.

Ge_3N_4 is a prospective material for application in photodiodes, amplifiers, optic fibres, protective coatings, it has been considered for applications as metal-insulator-semiconductor field effect transistors (MIS FET), as a possible negative electrode material for Li-ion batteries, and photocatalysts. The structure of basic polymorphs is understood since the work of Ruddlesden and Popper [2] who have confirmed that the hexagonal ($P6_3/m$) β phase is of reduced phenacite type and the (also hexagonal, $P3_1c$) α phase is structurally a closely related one.

The studied sample (ALDRICH) was a mixture of α and β polymorphs of Ge_3N_4 and contained minor amounts of germanium and germanium oxide. The high-pressure study was performed at the MAX80 diffraction press, F2.1 beamline (Hasylab, DESY). NaCl was used as a pressure standard. The experiments were performed using the energy-dispersive method at diffraction angle of 4.521º. For determination of lattice parameters of the component phases the Le Bail method was chosen. The calculations were performed using the Fullprof 2k (v. 2.70) program. The obtained bulk moduli will be discussed and compared to those reported for all Ge_3N_4 phases.

Bibliography

[1] A.Y. Liu and M.L. Cohen, *Prediction of new low compressibility solids.Science***245** (1989), p. 841.

[2] S.N. Ruddlesden, P. Popper, "On the crystal structures of the nitrides of silicon and germanium," *Acta Cryst.***11** (1958) 465-468.

15:30 Poster 14-13

Kinetics of phase transformations of copper phthalocyanine pigments

Melanie Müller[1], Robert E. Dinnebier[1], Martin Jansen[1], Stefan Wiedemann[2], Carsten Plüg[2]

1. *Max-Planck-Institut FKF, Heisenbergstr. 1, Stuttgart D70569, Germany* **2.** *Clariant GmbH, Industriepark Höchst, G 834, Frankfurt am Main 65926, Germany*

e-mail: Melanie.Mueller@fkf.mpg.de

Copper phthalocyanine (CuPC), an organometallic pigment, exists in various modifications. Of commercial interest are alpha-, beta- and epsilon-CuPC. The most stable one is beta-CuPC. All other polymorphs change into the beta-modification at 250 to 400°C.
In this case phase transfers of alpha-CuPC and epsilon-CuPC are analysed at constant temperature to get information about the kinetics. Of particular interest is the influence of additives and mixtures to the order of the reaction. Therefore, fast *in-situ* powder diffraction data were recorded at the ANKA synchrotron in Karlsruhe using MAR CCD detector. All measured data are refined by sequential Rietveld refinement and the influence of the experimental geometry is described by a resolution function derived from LaB_6 standard. The results are analyzed by using the Johnson-Mehl-Avrami equation.

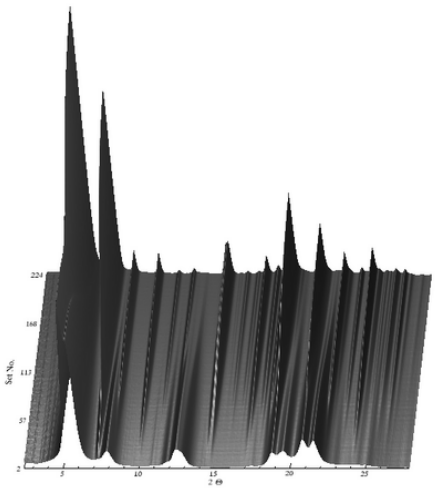

Fig. 1: Time dependent synchrotron powder diffraction data of alpha-CuPC measured at T=250°C.

References:
Erk, P. & Hengelsberg, H. (2003): In: Kadish, K.M., Smith, K.M. & Guilard, R.: The porphyrine handbook, vol.19.

15:30 Poster 14-14

High-temperature phase transitions in $La_{1-x}Sr_xFeO_{3-\delta}$ perovskite-related solid solutions

Alexander N. Nadeev, Sergey V. Tsybulya, Eugene Y. Gerasimav, Lubov A. Isupova

Boreskov Institute of Catalysis (BIC), pr. akad. Lavrentieva, 5, Novosibirsk 630090, Russian Federation

e-mail: nadeev@catalysis.ru

Nonstoichiometric ferrites of alkaline and rare earth metals with perovskite-type structure $ABO_{3-\delta}$, possess high mixed oxygen/electronic conductivity. Thus these systems are promising materials for solid oxide fuel cell electrodes, oxygen-permeable membranes for oxygen separation and catalysts for partial oxidation of hydrocarbons in catalytic membrane reactors. Using high-temperature X-ray diffraction $La_{1-x}Sr_xFeO_{3-\delta}$ ($0 \le x \le 1$) solid solutions with perovskite-related structure were investigated. Samples with $x \ge 0.6$ were cubic modification of perovskite. Heating in air up to synthesis temperature (1200 ^oC) leaved the phase composition of the sample $La_{0.25}Sr_{0.75}FeO_{3-\delta}$ unaltered, in spite of high oxygen lost. Heating in vacuum led to significant broadening of diffraction peaks concerned

with formation of two-phase region at about 900^{o}C. Adding a small quantity of Palmitic Acid to the sample resulted in decrease of phase transition temperature up to 600^{o}C and splitting of diffraction peaks. Following raise of temperature led to increase of the quantity of a new phase. The phase transition occured without changing of symmetry of unit cell. In vacuum at about 1000^{o}C the sample was monophase with cubic modification of perovskite structure. Following cooling down in vacuum up to 800^{o}C resulted in ordering of oxygen vacancies with the formation Grenier-type phase. Isosymmetrical phase transition was also observed for composition x=0.6. According to high-resolution synchrotron diffraction, significant broadening of diffraction peaks was mainly associated with the overlap of the diffraction peaks of two phases of the solid solutions with comparable lattice parameters, but not with the microstructure of the sample. Finally, under heating in air up to 1200^{o}C of the sample $SrFeO_{3-\delta}$, perovskite structure was stable. However, at about 1200^{o}C additional diffraction peak at about 32^{o} (2θ) of low-intensity (about 10% from maximal intensity) was observed. Simulated diffraction pattern of defect model of perovskite and brownmillerite layers alternation in one dimension had a good agreement with the experiment.

15:30	Poster	14-15

Lattice parameters of hard materials in the low-temperature range

Wojciech Paszkowicz[1], Pawel Piszora[2], Wieslaw Lasocha[3,4], Roman Minikayev[1], Irene Margiolaki[5], Michela Brunelli[6], Andy Fitch[5]

1. *Polish Academy of Sciences, Institute of Physics, al. Lotników 32/46, Warszawa 02-668, Poland* **2.** *Adam Mickiewicz University, Faculty of Chemistry, Grunwaldzka 6, Poznań 60-780, Poland* **3.** *Jagiellonian University, Faculty of Chemistry, Ingardena 3, Kraków 30-060, Poland* **4.** *Polish Academy of Sciences, Institute of Catalysis and Surface Chemistry, Niezapominajek 8, Kraków 30-239, Poland* **5.** *European Synchrotron Radiation Facility (ESRF), Grenoble 38043, France* **6.** *Europen Synchrotron Radiation Facility (ESRF), 6, Jules Horowitz, Grenoble 38000, France*

e-mail: paszk@ifpan.edu.pl

Hard materials such as diamond and cubic boron nitride (cBN) exhibit, due to strong covalent bonding, a very weak thermal expansion at low temperatures. Below room temperature, the total variation of the unit-cell dimension of these materials is about or less than 10^{-3} Å, being comparable to the precision of lattice-parameter determination at a typical instrument. Experimental studies have been published for diamond single crystals [1,2], whereas detailed experimental studies for polycrystalline diamond and cBN have been performed only above the room temperature. In the present study, the results of measurement of lattice parameters of commercial diamond and cBN polycrystals will be presented. The measurements were performed using Debye-Scherrer geometry at ID31 beamline (ESRF) equipped with a bank of nine detectors preceded by Si 111 **analyser crystals**. Lattice parameters were calculated using the Rietveld refinement. The obtained experimental lattice parameter and thermal expansion temperature dependencies will be discussed on the basis of available litearature data.

[1] T. Saotome, K. Ohashi, T. Sato, H. Maeta, K. Haruna, F. Ono, Thermal expansion of a boron-doped diamond single crystal at low temperatures, *J. Phys.: Condens. Matt.***10** (1998) 1267-1272

[2] T. Sato, K. Ohashi, T. Sudoh, K. Haruna, H. Maeta, Thermal expansion of a high purity synthetic diamond single crystal at low temperatures, *Phys. Rev. B***65** (2002) 092102

.[3] C. Giles, C. Adriano, A. Freire Lubambo, C. Cusatis, I. Mazzaro, M. Goncalves Hönnicke, Diamond thermal expansion measurement using transmitted X-ray back-diffraction, *J. Synchrotron Radiat.* **12** (2005) 349-353

15:30	Poster	14-16

Lattice parameters of a wurtzite-type (Zn,Mg)Se crystal as a function of temperature

Wojciech Paszkowicz[1], Pawel Piszora[2], Franciszek S. Firszt[3], Hanna Męczyńska[3], Stanisław Łęgowski[3], Carsten Baehtz[4], Michael Knapp[5]

1. *Polish Academy of Sciences, Institute of Physics, al. Lotników 32/46, Warszawa 02-668, Poland* **2.** *Adam Mickiewicz University, Faculty of Chemistry, Grunwaldzka 6, Poznań 60-780, Poland* **3.** *Nicolaus Copernicus University, Institute of Physics, Grudziądzka 5/7, Toruń 87-100, Poland* **4.** *Technische Universität Darmstadt, Institute of Materials Science, Petersenstr. 23, Darmstadt 64287, Germany* **5.** *CELLS (ALBA), Campus UAB, Barcelona 08193, Spain*

e-mail: paszk@ifpan.edu.pl

Wide gap II-VI semiconductors exhibit properties leading to various possible applications in optoelectronics. Structural and elastic properties of these materials are thus of high importance. (Zn,Mg)Se and related materials are studied since 1983 when their applications were suggested [1,2,3]. Most of considered applicatiions concern the alloys of low or moderate Mg content. Components with high-Mg-content can be used *e.g.* for control elements for IR optics [4]. Thin-film engineering involves tuning the lattice-parameter and bandgap values. The tuning is performed through selection of the given solid-solution composition, taking into account the need for lattice matching and required bandgap. Learning the structural and physical properties of the solution isa first step to design of layers and multilayers of desired characteristics. The opportunity of preparation of the solution as a single phase depends on the system and on the crystallisation process and its parameters. For the (Zn,Mg)Se system, the solid solution can be prepared in a broad range of Mg concentration, but the structure has been found to be different for bulk crystals than for epitaxial layers deposited on GaAs or InP. Alloying ZnSe with MgSe provides a way of tuning the ZnSe properties, in particular, its lattice parameters and bandgap increase with rising Mg content. Knowledge of bulk-crystal thermal expansivity is of importance for construction of optoelectronic devices, involving the (Zn,Mg)Se layers as building blocks. In this study, a wurtzite type (Zn,Mg)Se crystal grown by the high-pressure Bridgman method is studied by X-ray diffraction in the 10-290 K temperature range. The temperature variations of lattice parameter and thermal expansion coefficients are determined. An increase of thermal expansion coefficient with Mg content is observed.

[1] H.J. Lozykowski, P.O. Holtz, B. Monemar, *J. Electron.Mater*. 12 (1983) 653.

[2] T. Ohnakado, Y. Wu, Y. Kawakami, Sz. Fujita, Sg. Fujita, *Jpn. J. Appl.Phys.* 30 (1991) 1668.

[3] H. Okuyama, K. Nakano, T. Miyajima, K. Akimoto, *Jpn. J. Appl.Phys*. 30 (1991) L1620.

[3] V.M. Puzikov, Yu.A. Zagoruiko, O.A. Fedorenko, N.O. Kovalenko, *Crystallogr. Rep.* 49, 2004 215-216.

15:30 Poster 14-17

Pressure dependence of lattice parameter of Gadolinium Gallium Garnet crystals

Andrzej Durygin[2], Wojciech Paszkowicz[1], Ryszard Buczko[1], Agata Kamińska[1], Surendra K. Saxena[2], Andrzej Suchocki[1]

1. *Polish Academy of Sciences, Institute of Physics, al. Lotników 32/46, Warszawa 02-668, Poland* **2.** *CeSMEC, Florida International University, University Park, Miami FL33199, United States*

e-mail: paszk@ifpan.edu.pl

Gadolinium Gallium Garnet ($Gd_3Ga_5O_{12}$ - GGG) crystals serve as a lasing host material for various dopants. It has been shown that GGG:Yb laser crystals, showing laser action at a wavelength of about 1 μm, can be diode pumped. GGG crystals can be easily grown using various methods including a very convenient for research the micro-pulling down method.

GGG crystallises in *Ia3d* space group. Rare-earth ions in these crystals substitute Ga^{3+} at dodecahedral positions. The point symmetry of this site is D_2. Luminescence studies at high hydrostatic pressure indicate a possibility of change of the point symmetry at this site even to O_h at pressure of about 10 GPa and a return to D_2 at higher pressures. However, in the earlier experimental diffraction studies the first phase transition is observed only at much higher pressure of about 80 GPa. This intriguing behavior of site symmetry change can be observed when splitting of so called R--level ($^4F_{3/2}$) of Nd^{3+} ions is removed by applying pressure of about 10 GPa to GGG crystals. This phenomenon can occur only if Nd^{3+} ions are located at sites with O_h symmetry [1].

In this work we report high-pressure X-ray diffraction study for GGG performed at room temperature in diamond-anvil cell. In the experiment, hydrostatic conditions were well preserved at least up to 10 GPa. The measured pressure dependence of lattice parameter is compared with theoretical *ab initio* calculations and earlier theoretical estimations of bulk modulus and its pressure derivative for GGG crystals, reported in Refs [2,3]. The experimental bulk modulus was derived from the diffraction data using the EOSFIT program assuming the 3rd order Birch-Murnaghan equation of state. Our results confirm earlier theoretical estimations that the GGG crystal exhibits the smallest bulk modulus among a few other garnets containing both Gd and Ga ions. Moreover, the theory shows that at certain pressure the Ga at dodecahedral site – O distances are equal, which is a prerequisite for increase of the symmetry of this site.

Acknowledgements: The work was partially supported by a grant from the Polish Ministry of Science and Education for the years 2006–2009.

15:30 Poster 14-18

XRD study of stability of mechanoactivated oxides under non-ambient conditions

Sophia A. Petrova[1], Robert G. Zakharov[1], Anatoliy Y. Fishman[1], Vladimir B. Vykhodets[2], Elena S. Buyanova[3], Vyacheslav L. Lisin[1]

1. *Institute of Metallurgy, Urals Division, Russian Academy of Science (IMETUDRAS), 101 Amundsen, Ekaterinburg 620016, Russian Federation* **2.** *Russian Academy of Sciences, Ural Division, Institute of Metal Physics, 18 S.Kovalevskaya str., GSP-170, Ekaterinburg 620219, Russian Federation* **3.** *Ural State University (USU), Lenin avenue, 51, Ekaterinburg 620083, Russian Federation*

e-mail: danaus@mail.ru

Being non-equilibrium metastable systems, mechanoactivated materials are interesting for studying their stability. On the other hand, the main difficulties in producing compact nanomaterials from mechanochemically obtained nanopowders arise from their pressing and following annealing, which may cause an increase of grain size and lack of important features for nanomaterials. Therefore, the constancy of different mechanoactivated oxides ($LaMnO_{3\pm\delta}$, $Zr_{0.835}Y_{0.165}O_{2-\gamma}$, Mn_2O_3, Mn_3O_4, $Bi_4V_{2-x}Fe_xO_{11-x}$) produced with the help of a high-energy planetary ball mill was examined in a wide temperature range (300-1000K) in air under different partial oxygen pressures (1-10^{-18}atm). For this purpose the X-ray diffraction measurements were carried out in situ under non-ambient conditions with the help of an automated measuring complex based on a high temperature attachment with a microprocessor regulator of partial oxygen pressure. It brought out the phase composition, structural parameters and microstructural characteristics (volume averages of sizes and strains) of the samples depending on the temperature and partial oxygen pressure, as well as on the crystallite size and structural features of the oxide. Specific features of the structural phase transitions of the first order in mechanoactivated oxides with Jahn-Teller ions were also investigated. To interpret the results obtained, data on kinetics of the isotope exchange between the oxygen gas (enriched with the ^{18}O isotope) and the mechanoactivated ceramics in the temperature range of 550 – 850K gathered by using nuclear microanalysis technique, together with X-ray photoelectron spectroscopy data have been used. In particular it has been revealed, starting from some values nanosized crystallites are able to resist to heating under ambient oxygen pressure without dramatic growth. It is also true even when coming through structural phase transition. The work was supported by the Russian Foundation for Fundamental Research, grants No.06-03-32943, 06-03-32378.

15:30 Poster 14-19

Temperature dependence of microstructure of Al-Ag-Zn alloys

Stanko Popovic[1], Zeljko Skoko[1], Goran Stefanic[2]

1. *Faculty of Sciences, Dept. Physics, Bijenička 32, Zagreb HR-10000, Croatia* **2.** *Rudjer Boskovic Institute, Bijenicka cesta 54, Zagreb HR-10000, Croatia*

e-mail: spopovic@phy.hr

The precipitation sequence in ternary aluminium rich Al-Ag-Zn alloys, after rapid quenching to RT from a temperature, T_f (820 K), higher than the solid-solution temperature, T_{ss}, was found to be: GP zones (fcc) → ε′ (hcp) → ε (hcp). The as-quenched alloys contained GP zones having 3 to 4 nm in diameter as observed by XRD and TEM. During ageing of the quenched alloys at 420 K, GP zones increased in size, remaining fcc and coherent with the α-phase (fcc). In parallel, metastable precipitates, ε′, were formed; their unit-cell parameters depended on the solute content. Two mechanisms of ε′ nucleation were suggested on the basis of composite diffraction-line profiles, namely, discontinuous nucleation and a direct GP zones to ε′ transition. The unit-cell parameters of the equilibrium phase, ε, observed in the alloys slowly cooled from T_t to RT, depended on the solute content.

The alloys, that had been quenched from T_f to RT, aged at 420 K for 50 days and then prolongedly aged at RT, being two-phase system (α +ε′), were studied *in situ* at high temperature. As the temperature increased, an initial increase of diffraction-line intensities of both α and ε′ phases was observed, due to lattice strain annealing. A shift of diffraction lines due to thermal expansion took place. A small anisotropy of thermal expansion of ε′ was noticed. Above 500 K a gradual dissolution of ε′ in the α-phase started, as manifested in an enchanced decrease of diffraction-line intensities. Finally, solid solution was formed; T_{ss} depended on the alloy composition. On cooling, the alloys underwent reversal changes, exhibiting a temperature hysteresis (10 to 20 K). The dependence of the unit-cell parameters of ε′ on temperature during cooling was little different from that on heating. At RT, after a complete heating and cooling cycle, unit-cell parameters of the precipitates were close to those of the equilibrium ε-phase, while diffraction-line profiles were not composite any more.

S. Popovic and D.E. Passoja, *J. Appl. Cryst*. **4** (1971) 427-434; S. Popovic, *Cryst. Res. Technol.***19** (1984) 1351-1358; S. Popovic, Z. Skoko and G. Stefanic, *Acta Chim. Slovenica* (submitted).

15:30 Poster 14-20

Thermal behaviour of the $BaMF_4$ ferroics

Jose M. Posse[1], Andrzej Grzechnik[1], Andy Fitch[2], Karen Friese[1]

1. *Dpto. Física Materia Condensada, Universidad del País Vasco (UPV/EHU), Facultad de Ciencia y Tecnología, Apdo. 644, Bilbao 48080, Spain* **2.** *European Synchrotron Radiation Facility (ESRF), Grenoble 38043, France*

e-mail: josemaria@wm.lc.ehu.es

The isostructural piezoelectrics $BaMF_4$ crystallize in the orthorhombic space group $Cmc2_1$ at ambient conditions. The *M*-cation (*M* = Zn, Cu, Ni, Co, Fe, Mn, or Mg) is surrounded by six fluorines in an irregular octahedron. Each octahedron shares four fluorines with neighbouring octahedra forming layers perpendicular to the *b* axis. The barium atoms are accomodated in the interlayer space with coordination number nine. Individual representatives (M=Mn, Fe, Co, and Ni) of the $BaMF_4$ family show a multiferroic behaviour [1]. Based on inelastic-neutron scattering experiments [2], it was concluded that the $BaMF_4$ compounds have a structural instability at low temperatures. Up to now, this has been confirmed only for $BaMnF_4$ - a transition to an incommensurately modulated phase at temperatures below 250K being reported in [3]. $BaMnF_4$ also presents antiferroelectric anomalies in the magnetic susceptibility curve at 45K related to an intermediate magnetic phase [4].

We studied the thermal behavior of three representative members of the family (*M* = Mg, Zn and Mn) by powder diffraction measurements from 290K to 10K at the beamline ID31 (Grenoble, ESRF). No phase transition in this temperature range was observed for $BaMgF_4$ and $BaZnF_4$. However, refinements reveal a negative thermal expansion of the *a* lattice parameter and a "bump" of the *c* parameter below 70K. For $BaMnF_4$, we can confirm the transition to the incommensurate phase. However, our high resolution data cannot be explained with the model given earlier [3]. Instead, we propose a new superspace group $X2_1(½ ½ γ)$ with X=(½ ½ 0 ½). The γ-component of the q-vector increases continuously with decreasing temperature till at 45K (coinciding with the magnetic anomaly) a constant value of 0.3948$Å^{-1}$ is reached.

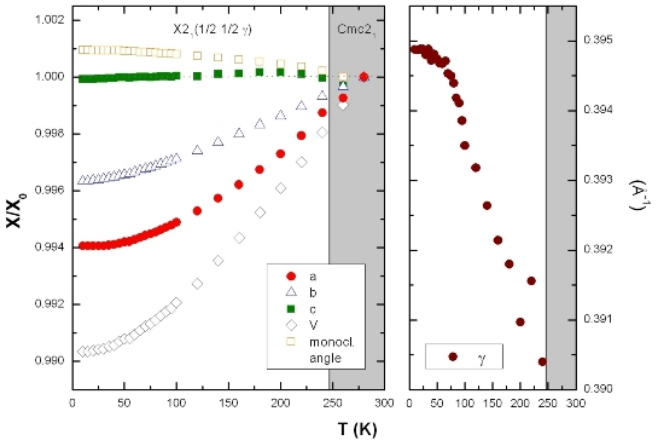

Normalized lattice parameters and γ-component of the q-vector of $BaMnF_4$.

[1]C. Ederer & N.A. Spaldin (2006) Phys. Rev. B74, 024102.

[2] R. Almairac, et al. (1997), Phys. Rev. B55, 8249.
[3] Ph. Sciau, et al. (1988), Acta Cryst. B44, 108.
[4] M. Yoshimura, et al. (2006), J. Magn. Magn. Mat. 299, 404.

15:30 Poster 14-21

In-situ high-pressure powder diffraction studies of layered metal phosphates

Jennifer E. Readman, Victoria A. Burnell, Joseph A. Hriljac

School of Chemistry, University of Birmingham, Edgbaston, Birmingham B152TT, United Kingdom

e-mail: j.e.readman.1@bham.ac.uk

The high pressure structural chemistry of zeolites has been thoroughly investigated and several unusual structural characteristics have been discovered, such as pressure induced expansion and superhydration [1-2]. However, to date few materials with layered structures have been studied [3]. Here, we present an in-situ high-pressure powder diffraction study of the layered metal phosphates α-zirconium phosphate and α-titanium phosphate [4-5]. Experiments were carried out in diamond anvil cells using a synchrotron X-ray source up to pressures of 10 GPa under hydrostatic and non-hydrostatic conditions. The GSAS suite of programs were used to

carry out Rietveld analysis at each pressure step [6]. It was found that under hydrostatic conditions there is a linear decrease in all lattice parameters with pressure, a plot of unit cell volume versus pressure is shown below and it can be clearly seen that there is little hysteresis upon pressure release. Under non-hydrostatic conditions α-zirconium phosphate is almost amorphous by 10 GPa whilst α-titanium phosphate remains crystalline. Excessive line broadening in both samples meant full Rietveld analysis could not be carried out although lattice parameters could be obtained. Full details from the refinements, changes in distances, angles and bulk moduli will be presented.

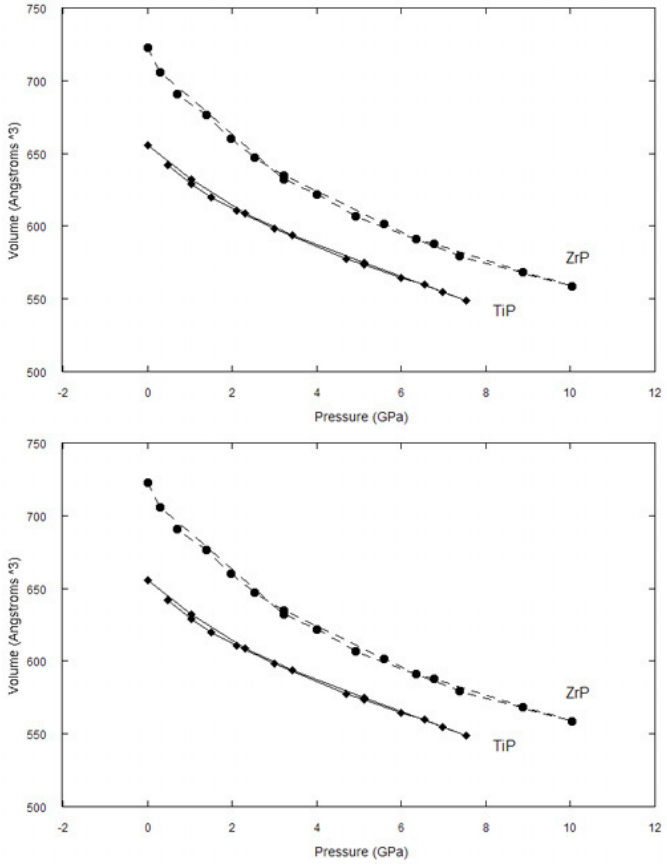

References:

[1] Y. Lee, T. Vogt, J. A. Hriljac, J. B Parise and G. Artoli, *J. Am. Chem. Soc.,***124**, 5466 (2002).

[2] J. A. Hriljac, *Cryst. Rev.,***12**, 181 (2006).

[3] S. Nakano, T. Sasaki, K. Takemura and M. Watanabe, *Chem. Mater.,***10**, 2044 (1998).

[4] A. Clearfield and U. Costantino, *Supramolecular Chemistry*, **7**, 107 (1996).

[5] S. Bruque, M. A. G. Aranda, E. R. Losila, P. Olivera-Pastor and P. Maireles-Torres, *Inorg. Chem.,***34**, 893 (1995).

[6] A. C. Larson and R. B. Von Dreele, "General Structure Analysis System (GSAS)", Los Alamos National Laboratory Report LAUR 86-748 (2000).

15:30 Poster 14-22

Structural instabilities in $LnGaO_3$ perovskites at high pressures

Anatoliy Senyshyn[1,2], Jens M. Engel[1,3], Iain Oswald[4,5], Leonid Vasylechko[2], Marek Berkowski[6]

1. *Technische Universität Darmstadt, Institute of Materials Science, Petersenstr. 23, Darmstadt 64287, Germany* **2.** *Lviv Polytechnic National University, Semiconductor Electronics Department, Bandera Street, 12, Lviv 79013, Ukraine* **3.** *Virginia Polytechnic Institute and State University, Blacksburg 24061, United States* **4.** *European Synchrotron Radiation Facility (ESRF), Grenoble 38043, France* **5.** *University of Edinburgh, Department of Chemistry, The King\'s Buildings, West Mains Rd, Edinburgh EH9 3JJ, United Kingdom* **6.** *Polish Academy of Sciences, Institute of Physics, al. Lotników 32/46, Warszawa 02-668, Poland*

e-mail: senyshyn@gmail.com

Crystal structure – property relation for perovskite type materials attract an attention of investigators over very long time. A purposeful tailoring of their physical and chemical properties requires a detailed and systematic knowledge of crystal structure behaviour under various environmental conditions and chemical composition.

Recent studies [1] resulted in obvious indications that the relative compressibilities of the A and B sites in ABX_3 perovskite structure play an important role in determining the pressure-induced structural changes of perovskites. In order to prove and extend this assumption, perovskite type rare-earth gallates $LnGaO_3$, whose crystal structure and its thermal evolution were systematically studied in the broad temperature and composition ranges [2], seem to be well-suited objects for high pressure diffraction studies, i.e. a good link between in-situ temperature- and pressure-dependent structural properties can be established. At ambient conditions all $LnGaO_3$ possess distorted $GdFeO_3$ type of structure and undergo transformation to $LaAlO_3$ structure type at elevated temperatures, where temperature of the phase transformation is proportional to tolerance factor. It is worth to mention that the high pressure phase of the first representative $LaGaO_3$ has the same symmetry as the phase found at high temperatures, i.e. $LaAlO_3$ structure type.

High pressure structural studies on perovskite type rare-earth gallates $LnGaO_3$ can resolve the set of questions collected, like:

- is the $LaAlO_3$ structure type occurring in other $LnGaO_3$ at high pressures?
- are phase transformation and elastic modules depending on perovskite tolerance factor?
- what is the agreement between experimental data and results of semiclassical simulations [3]?

In order to clarify those problems, six samples have been chosen for high pressure powder diffraction experiments, four orthogallates $LaGaO_3$, $CeGaO_3$, $PrGaO_3$, $NdGaO_3$ and two solid solutions $La_{0.50}Pr_{0.50}GaO_3$ and $La_{0.63}Nd_{0.37}GaO_3$ whose magnitude of perovskite lattice deformation is close to those of cerium gallate.

Data collection was performed in a transmission mode at beamline ID27 at ESRF (Grenoble, France) using MAR345 imaging plate detector. To fulfil the quasi-hydrostatic condition, the 4:1 methanol-ethanol mixture was used as a pressure medium for $LaGaO_3$ and $La_{0.50}Pr_{0.50}GaO_3$, whereas other samples were cryogenically embed-

ded into high purity nitrogen. More than 150 diffraction patterns were collected in a broad pressure range from 0.0001 to 40 GPa and results of such studies will be presented in the current contribution.

1. R.J. Angel, J. Zhao, N.L. Ross, Phys. Rev. Lett. 95 (2005) 025503.
2. L. Vasylechko, A. Senyshyn, U, Bismayer, in: Handbook on the Physics and Chemistry of Rare Earths, ed. K. A. Gschneidner Jr., J.-C. Bunzli, and V. Pecharsky (Elsevier, Amsterdam), Vol. 39 (2008) in print.
3. A. Senyshyn, H. Ehrenberg, L. Vasylechko, J.D. Gale, U Bismayer, J. Phys.: Condens. Matter 17 (2005) 6217.

15:30 Poster 14-23

Low-temperature structural properties of orthorhombic $TbAlO_3$, $TmAlO_3$ and $LuAlO_3$ perovskites

Dmytro M. Trots[1,2], Leonid Vasylechko[3], Anatoliy Senyshyn[2,3], Tadeusz Łukasiewicz[4]

1. *Hamburger Synchrotronstrahlungslabor HASYLAB, Notkestrasse 85, Hamburg 22607, Germany* **2.** *Technische Universität Darmstadt, Institute of Materials Science, Petersenstr. 23, Darmstadt 64287, Germany* **3.** *Lviv Polytechnic National University, 12 Bandera, Lviv 79013, Ukraine* **4.** *Institute of Electronic Materials Technology (ITME), Wólczyńska 133, Warszawa 01-919, Poland*

e-mail: dmytro.trots@desy.de

Perovskite type $TbAlO_3$ and $LuAlO_3$ rare-earth aluminates attract considerable interest as laser media [1,2]. This work is a continuation of our systematic studies on the crystal structure of perovskite type rare-earth aluminates and gallates. Here we report structural investigations on $TbAlO_3$, $TmAlO_3$ and $LuAlO_3$ at low temperatures using high-resolution synchrotron powder diffraction performed at beamline B2 (HASYLAB/DESY). All three compounds possess the $GdFeO_3$ type of structure (space group *Pbnm*) in the whole temperature range studied (20-300 K) and exhibit quite various thermal behaviours of the lattice parameters.

The thermal dependencies of the lattice parameters of $LuAlO_3$ display a rather typical (nonlinear and smooth) increase with temperature, whereas the behaviour of $TmAlO_3$ shows deviations from a "normal" law which are reflected in a "sigmoid" expansion of the lattice along the [100] direction. Unusual trends occur in the thermal behaviour of $TbAlO_3$: at T~60 K all three unique elements of the thermal expansion tensor undergo the zero value which is indicated by the observed extrema on the thermal dependencies of the respective lattice parameters. The thermal expansion coefficient in the [100] direction of the perovskite cell α_{11} achieves one more negative minimum around 130 K and then increases through the zero value (ca. 200 K). The observed smooth and nonlinear increase of the lattice dimensions in $LuAlO_3$ and the anomalous thermal behaviour occurred in $TbAlO_3$ and $TmAlO_3$ can be associated to interactions between phonons and the electron subsystem of rare-earth ions with

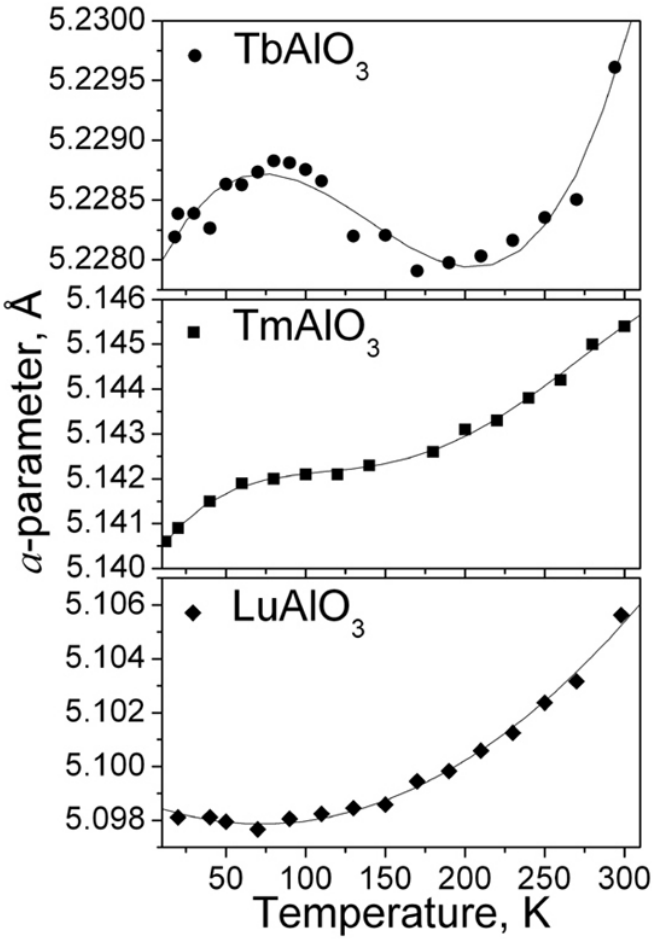

We are indebted to Andreas Berghaeuser for his help with maintenance of cryostat.

[1] Sardar et al., J APPL PHYS 100 (2006) 083108
[2] Drozdowski et al., NUCL INSTRUM METH A 562 (2006) 254
[3] Vasylechko et al., Handbook on the Physics and Chemistry of Rare-earths, ed. K. Gschneidner, J. Bunzli, and V. Pecharsky (Elsevier, Amsterdam), 39 (2008) in print

15:30 Poster 14-24

Synchrotron powder diffraction study of ionic liquids during melting and crystallisation

Kia S. Wallwork[1], Yansen Lauw[2], Theo Rodopoulos[2], Mike Horne[2], Ian C. Madsen[2], Thomas Ruether[3]

1. *Australian Synchrotron, 800 Blackburn Road, Melbourne 3168, Australia* **2.** *CSIRO Minerals, Melbourne 3168, Australia* **3.** *CSIRO Energy Technology, Bayview Ave, Melbourne 3168, Australia*

e-mail: kia.wallwork@synchrotron.org.au

Ionic liquids are salts that exist in a liquid state at, or near, room temperature. Due to their extremely low vapour pressure, high electrochemical stability, and powerful solvation properties, ionic liquids are viewed as green solvents which play an important role as electrolytes in many electrochemical applications such as lithium ion batteries, solar cells, fuel cells, electrodeposition and electroplating. Research into the structures and properties of ionic liquids has intensified in the last decade. It is apparent that fundamental studies on the

structure-property relationships of pure ionic liquids and ionic liquid solutions may provide breakthrough results in the choice of ionic liquids for specific applications.

An intensive study of ionic liquids and their possible applications in minerals and metals processing is being undertaken by CSIRO Minerals, Australia. One of the ionic liquids under investigation is 1-butyl-1-methylpyrrolidinium methanesulfonate (P_{14}MeS) which has a melting point of 65 °C. Synchrotron powder diffraction studies were undertaken in order to examine the crystalline phase transformations at solid and solid-liquid state temperatures for pure P_{14}MeS and impure P_{14}MeS containing $AlCl_3$ and water.

Powder diffraction data were collected at the Australian Synchrotron powder diffraction beamline primary end station from samples loaded in 2.0 mm capillaries. These were mounted concentrically to the rotation axis of the 3-circle diffractometer. Monochromatic X-rays of wavelength 1.0054 Å were used. The Mythen X-ray detector was used to collect data in a continuous mode throughout the temperature programme; data were collected over the angular range $0.0 \leq 2\Theta \leq 80.0^{\circ}$ with each histogram being collected for 10 s. The temperature of the sample was maintained by an Oxford Cryosystems cryostream set to a constant ramp rate of 6 ºC/min throughout the temperature cycle; the temperature programme used was a cycle between +25 to -80 to +100 to -80 to +100 to +25 °C.

During these measurements the phase transitions and hysteresis in the phase transformations was able to be observed. Such transformations give useful information about the behaviour of the ionic liquid near its melting point and also indicate the nature of aluminium speciation present in the solid phases. Further analyses are expected to reveal some information about how water affects the structure of the ionic liquid and its solutions.

15:30	Poster	14-25

In-situ GIXRD studies on $Hf_{(1-x)}Si_xO_2$ dielectrics

Lutz Wilde[1], Steffen Teichert[2], Susann Schmidt[3], Gert Jaschke[2]

1. *Fraunhofer Center Nanoelektronische Technologien, Dresden 01099, Germany* **2.** *Qimonda Dresden, Königsbrücker Straße 180, Dresden 01099, Germany* **3.** *Westsächsische Hochschule Zwickau, Dr.-Friedrichs-Ring 2A, Zwickau 08056, Germany*

e-mail: lutz.wilde@cnt.fraunhofer.de

Further shrinking of structures in DRAM cells requires the introduction of new materials with superior electrical properties. Especially, in future capacitors there is a need, to replace the traditional dielectrics by insulators having a significant higher dielectric constant κ. Among others, Si-stabilized HfO_2 is a promising candidate for 50 nm technology and beyond. The structure, in which HfO_2 crystallizes, plays an essential role, as the κ value of the cubic / tetragonal phase (CaF_2 structure) is significantly higher than that of the monoclinic phase, which is at room temperature the thermodynamically stable phase [1]. Using dopants (e.g. Si, Al or Y) the desired cubic / tetragonal phase can be stabilized at room temperature [2].

In this study, the influence of Si doping on the phase formation of Hf-Si-O_x dielectrics was investigated by means of high temperature grazing incidence XRD. Thin films of approx. 9nm thickness were deposited by ALD on a Si wafer with a 15nm TiN electrode film. A concentration split was deposited to adjust the Si/(Hf+Si) ratio within the range between 1-10%, what was checked with RBS and XPS. High temperature XRD measurements were done in a BTS-solid temperature chamber (mri) equipped with a Be dome under N_2 up to 700°C. In the temperature range between 150°C and 700°C the samples were heated with a constant ramp rate of 5 K/min. During the heating, grazing incidence XRD pattern (CuKα radiation, incidence angle ω = 0.65°) in the 2Θrange 26° - 38° were taken. Each scan lasted 5 minutes resulting in a temperature resolution of 25°C. Due to certain reasons (weak intensity, low particle size, stress in the film) it is not possible to decide if the (002) reflection is split, what would allow, to discriminate between cubic or tetragonal symmetry.

All samples were amorphous after deposition. Depending on the Si concentration, the HfO_2 crystallizes either in the cubic / tetragonal phase or in the monoclinic phase. The onset of the crystallization process is in the temperature range between 540°C for the sample with high Si content and 360°C for the samples with low Si content.

References:

[1] X. Zhao, d. Vanderbilt, Phys. Rev. **B65** (2002) 233106.

[2] K. Tomida, K. Kita, A. Toriumi, Appl. Phys. Lett. **89** (2006) 142902.

15:30	Poster	14-26

SEM investigation of Fe-Al-C alloys after thermal and high pressure influence

Oleksandra V. Zarytska[3], Yevgeniy M. Dzevin[1], Anatoliy G. Garan[2], Dmytro I. Oliferuk[1], Vladyslav A. Andryuschenko[1]

1. *G. V. Kurdyumov Institute for Metal Physics of the National Academy of Sciences (IMP), Vernadsky Blvd. 36, Kiev UA03680, Ukraine* **2.** *V. Bakul Institute for Superhard Materials NAS of Ukraine, 2, Autozavodska str., Kiev 04074, Ukraine* **3.** *Physical Engineering Centre, National Academy of Sciences of Ukraine (FTC), Vernadskiy's blvd., 36, Kiev 03680, Ukraine*

e-mail: zarickaya@rambler.ru

The samples were undergone to thermal and pressure influence in the region of pressures of 6,0 – 8,0 GPa and temperatures 1670 – 1870 K during 120 sek. Order of influence: establishment of pressure – heating – exposure – cooling – taking down of pressure.

The alloys Fe_3AlC (85,5 wt.% Fe, 12wt.%Al, 2,5 wt.%C) and $(Fe_3Al)_{40}C_{60}$ (90,3 wt.% Fe, 5,81 wt.%Al, 3,88 wt.%C) were studied in the experiment.

In the alloy Fe_3AlC using SEM method it was observed some quantity of diamond microcrystal groups (20-100 mm) in K-phase matrix.

In the $(Fe_3Al)_{40}C_{60}$ alloy after thermal and pressure influence it was observed the volumes which were filled up on 30% by diamond crystals of 50-200 mm. At that at the less thermal and pressure parameters (6 GPa and 1670K) the synthetic diamond micro crystals with developed surface forms, but at more high (8GPa and 1879 K) – diamonds like perfect octahedral micro crystals forms.

Spectral investigations in Fe- and Al-irradiation have shown the presence of 3:1 atoms of Fe and Al in diamond micro crystals.

Applied research

MS15 posters
Sunday afternoon, 21 September, 15:30

15:30 Poster 15-01

Mineral composition and monumental stones conservation studied by POL, FTIR and XRD techniques

Magdalena Aflori[1], Ana-Bogdana Simionescu[2], Mihaela A. Olaru[1], Modesto Montoto[2], Rosa Esbert[2]

1. *Petru Poni Institute of Macromolecular Chemistry of the Romanian Academy, Aleea Grigore Ghica Voda 41A, Iasi, Romania*
2. *University of Oviedo, Jesus Arias de Velasco, Oviedo Oviedo, Spain*

e-mail: maflori@icmpp.ro

A high proportion of the world's cultural heritage is built in stone, and it is slowly but inexorably disappearing. The deterioration of stone is very familiar to anyone who has looked closely at a historic stone building or monument. For the present study two types of rock, from Spain and Romania, were selected by regional significance, abundance and importance, level of usage as building materials in the construction of monumental buildings. The first selected rock is a bright white micritic dolomitic stone, typical from the Spanish region of Asturias (Oviedo), called **Laspra**, being used as one of the three main building materials of the Cathedral of Oviedo. Important parts of churches listed in UNESCO's World Heritage List: Santa Maria del Naranco and San Miguel de Lillo were built by using Laspra. The second selected stone is coming from Romania and it can be described as a bioclastic oolitic stone, named **Repedea**. One of the most important monasteries of Romania, Dobrovat, was built from Repedea.

Stone samples were first characterized by thin section polarizing microscopy POL (phase composition, texture, grain-size distribution), as well as XRD and FTIR techniques, respectively (mineral composition, crystallographic structure). Then the samples were prepared by casting the same amount of a silsesquioxanes polymer-based obtained through sol-gel approach and radical polymerization of trimethoxysilylpropyl methacrylate (TMSPMA) onto powder stones. These products polymerize within the stone pores, thereby strengthening the material. In the consolidant synthesis the sol-gel transition occurs in the presence of a surfactant. This provides an efficient means of avoiding cracking of the gel while it is drying inside the stone.

A comparative study has been made between the two types of stones consolidated with TMSPMA polymer. Due to the different composition of stones; the deposited polymer has different behaviors put in evidence by XRD and FTIR techniques. Conclusions concerning acid resistance, water repellency, stone consolidation and durability were revealed.

15:30 Poster 15-02

Grains orientation and martensitic transformation in Ni-Ti strip produced by twin roll casting technique

Tomasz Goryczka

University of Silesia, Institute of Materials Science, Bankowa 12, Katowice 40-007, Poland

e-mail: goryczka@us.edu.pl

Ni-Ti shape memory alloys are well known from their wide applications, especially in medicine. Despite the fact that they can be use as short-time implants an effort is made to improve their physical properties and biocompatibility. Particularly, an attention is paid to make a way of production short as much as possible, simultaneously keeping good quality of a final product. A twin rolls casting, which belongs to the family of rapid solidification techniques, appeared to be a useful method for Ni-Ti alloy production. In addition to economical advantages of this technique unique properties of the strip can be obtained. It combines rapid solidification together with cold-rolling. In practice, the strips are ready to use in as-cast state without additional thermo-mechanical treatment, which is needed after traditional casting for inducing shape memory effect. From the point of view of the physical properties, the main advantage of this technique is preferential grains growth. Appropriate grains orientation, originated in crystallographic description of the martensitic transformation, can increase shape memory effect.

The present work summarizes results obtained from X-ray and electron back scattered diffraction carried out for polycrystalline Ni-Ti shape memory strips produced by twin rolls casting. The strips reveal presence of the reversible martensitic transformation, which occurs between the B2, high temperature, parent phase and the B19'monoclinic martensite. The crystallization front, which simultaneously proceeds from the outer parts of the strip to its centre, causes preferentially oriented grains formation. The zones, which were in direct contact with the rotating wheels, reveal shorter grains under which the long columnar grains were extending to the centre of the strip. In the outer surfaces, two kinds of the grains can be distinguishable: equiaxial - with an average grain diameter of 5um and short columnar - 20um long. Amount of the 85% grains formed in the zone close to the surface are preferentially oriented. Texture is a mixture of the fibre <001> and <011> orientations as well as the sheet texture component {001}<100>. The columnar grains formed in the inner part of the strips are about 100 um long and reveal orientation along <001> and {001}<100> textural component.

15:30 Poster 15-03

XRD in-situ investigations on the influence of organic additives on ettringite formation in cement systems

Daniel Jansen[1], Friedlinde Goetz-Neunhoeffer[1], Juergen Neubauer[1], Wolf-Dieter Hergeth[2]

1. *Mineralogy, Geozentrum Erlangen, Universitiy Erlangen-Nuernberg,, Schlossgarten 5a, Erlangen 91054, Germany*
2. *Wacker Polymer Systems, Burghausen 84489, Germany*

e-mail: djan@geol.uni-erlangen.de

INTRODUCTION: Building materials like mortars are systems with a complex composition. Besides the anorganic binder cement, scores of organic additives give decisive properties to the products. Since ettringite is one of the hydrate phases during cement hydration, XRD investigations on the crystallography of the formed ettringite in cement systems with and without organic additives of commercial quality were carried out and the results were compared.

EXPERIMENTAL METHODS: The XRD investigations were carried out using a Siemens D5000 diffractometer assembled with a SOLX solid state detector from Bruker AXS. A special sample holder [1] with Peltier element allows isothermal conditions at 23 °C +/- 0,2 °C during measurement. Rietveld refinement was performed using the Software TOPAS V3.0 (fundamental parameters approach) and the structural models (ICSD) of all detected phases. For the refinement of ettringite a new published structure was employed [2]. Refined parameters were scale factor, sample displacement, background as Chebychev polynomial of 5th grade, crystallite size and lattice parameters of ettringite and portlandite. The lattice parameters of the cement phases were refined during quantification of the dry cement and kept fixed during refinement of the cement pastes. Furthermore the synthesis of pure ettringite using a suitable precipitation method in presence and absence of the polymer was performed and the lattice parameters were determined.

RESULTS: The investigations prove that the presence of the organic polymer shows influences on the lattice parameters of the ettringite formed during the hydration of the cement. Since there was no difference detected in the lattice parameters of the precipitated ettringites, a possible integration of the polymer in the structure of the ettringites can be excluded. The differences in the lattice parameters of the ettringites have to be caused by the offer of ions in the pore solution in the cement pastes influenced by the presence of the polymer. In hydrating cement systems on the one hand the anions CO_3^{2-} and OH^- and on the other hand the cations Fe^{3+} and Si^{4+} may play the major role for integration in the structure of the ettringite instead of SO_4^{2-} and Al^{3+} respectively and therefore influence the lattice parameters. Consequently the organic polymer may influence the availability of these different ions for the ettringite formation.

REFERENCES:

[1] Hesse, C., Degenkolb, M., Gäberlein, P., Götz-Neunheoffer, F., Neubauer, J., Schwarz, V. (2008). Untersuchungen zum Einfluss von Temperatur und w/z-Wert auf die frühe Hydratation von Weißzement, Cement International (accepted)

[2] Goetz-Neunhoeffer, F., Neubauer, J. (2006). Refined ettringite ($Ca_6Al_2(SO_4)_3(OH)_{12}*26H_2O$) structure for quantitative X-ray diffraction analysis; Powder Diffraction 21, pp. 4-11

15:30 Poster 15-04

Powder diffraction study of new compounds CoGeTe and PdSnTe

František Laufek[1,3], Jiří Navrátil[2], Anna Vymazalová[1], Jakub Plášil[3], Tomáš Plecháček[2]

1. *Czech Geological Survey, Prague 15200, Czech Republic* **2.** *University of Pardubice, Studentska, Pardubice 53210, Czech Republic* **3.** *Charles University, Faculty of Science, Albertov 6, Prague 12843, Czech Republic*

e-mail: frantisek.laufek@geology.cz

The crystal structures of two new compounds CoGeTe and PdSnTe were determined by means of conventional powder X-ray diffraction. These phases are of interest in materials science because of their possible thermoelectric applications.

The title compounds CoGeTe and PdSnTe were prepared from the elements by high-temperature solid-state reactions. The crystal structure of CoGeTe was solved by direct methods by means of EXPO2004 [1] program package and its crystal structure was found isostructural with PdSnTe. Both structures were refined by Rietveld method using FullProf program.

In the crystal structures of CoGeTe and PdSnTe (both space group *Pbca*, 3 independent atoms, $Z = 8$), each cobalt (palladium) atom is coordinated by three germanium (tin) and three tellurium atoms showing distorted octahedral coordination. One octahedral edge (Ge-Ge or Sn-Sn) in CoGeTe or in PdSnTe is shared with an adjacent octahedron, other vertices of [CoGe3Te3] and [PdSn3Te3] octahedra are connected by corners sharing. The crystal structures of title compounds can be also viewed as a ternary ordered variant of α-NiAs2 (also known as a mineral pararammelsbergite), which is transitional between the marcasite-type and the pyrite-type structures. Part of this work was submitted to the Journal of Alloys and Compounds [2,3].

1. A. Altomare, R. Caliandro, M. Camalli, C. Cuocci, C. Giacovazzo, A. Moliterni,
R. Rizzi, J. Appl. Cryst. 37 (2004), 1025.
2. F. Laufek, J. Navrátil, J. Plášil, T. Plecháček, J. Alloys Compd. (2008), in press.
3. F. Laufek, A. Vymazalová, J. Navrátil, M. Drábek, J. Plášil,T. Plecháček,
J. Alloys Compd. (2008), in press.

15:30 Poster 15-05

Reaction sequences in the thermochemical treatment of sewage sludge ashes revealed by X-ray powder diffraction - A contribution to the European project SUSAN

Burkhard Peplinski, Christian Adam, Matthias Michaelis, Gerd Kley, Franziska Emmerling, Franz-Georg Simon

Federal Institute for Materials Research and Testing (BAM), Richard-Willstätter-Str. 11, Berlin D-12489, Germany

e-mail: burkhard_peplinski@web.de

The agricultural sector requires large amounts of phosphorus (P) for

food production (in the EU consumption of fertilizer-P exceeds 1.2 million tons of P per year). However, P is a non-renewable resource, becoming scarce in the near future, and should be saved by applying *recycling technologies to P-bearing waste streams*.

One of the major carriers of P is sewage sludge. In the EU more than 10 million tons (dry mass) of sewage sludge are produced annually, which contain about 0.3 million tons phosphorous. However, sewage sludge is not only a carrier of P but it is contaminated with organic pollutants and heavy metals. Thus, the *direct* agricultural utilization of sewage sludge is a *controversial* issue.

The European project SUSAN (Sustainable and Safe Re-use of Municipal Sewage Sludge for Nutrient Recovery) bundles the research efforts of seven partners from Austria, Finland, Germany and The Netherlands, aiming at the development of a sustainable and safe strategy for *phosphorus recovery* from sewage sludge using a two-step thermal treatment including mono-incineration of sewage sludge and subsequent *thermochemical treatment* of these ashes.

One essential aspect of the thermochemical treatment is the addition of a *chlorine-donor* to the ash, leading to the conversion of the heavy metal oxide impurities into chlorides and their subsequent sublimation / evaporation. A second essential aspect is the transformation of all phosphorus-bearing components into such mineral phases that are bio-available (available for plants).

To gain insight into the chemical processes accompanying the thermochemical treatment of sewage sludge ashes X-ray powder diffraction (XRD) was applied to a large number of samples produced either in a laboratory-scale equipment or in a pilot plant. Making use of the procedure described in [1] it was shown that the thermochemical treatment is accompanied by *a sequence of chemical reactions and transformations of the phosphorus-bearing mineral phases*.

The present paper is focused on a detailed XRD-study of the reaction sequence in the thermochemical treatment of an iron-bearing sewage sludge ash using *two* alternative chlorine-donors.

[1] Peplinski B. et al., Proceedings EPDIC-9, Z. Kristallogr. Suppl. 23 (2006) p. 29

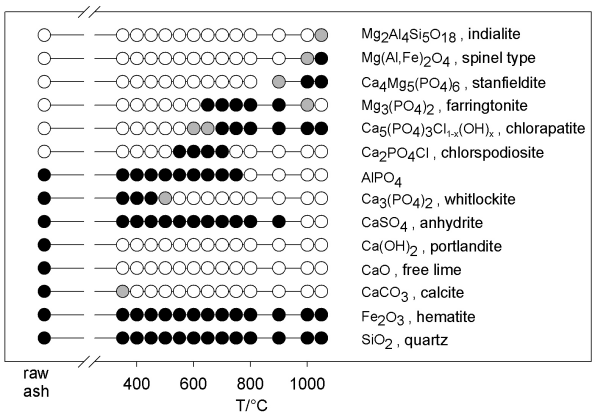

Some of the mineral phases detected by XRD in an iron-bearing sewage sludge ash before and after being thermochemically treated with magnesium chloride as a chlorine-donor at temperatures between 450 and 1050°C.
black circles = phase detected by XRD, white circles = phase not detected by XRD, grey circles = phase just (dis)appearing.

15:30 Poster 15-06

Characterization of calcium sulfates burned from gypsum at different temperatures

Sebastian Seufert, Christoph Hesse, Juergen Neubauer, Friedlinde Goetz-Neunhoeffer

Mineralogy, Geozentrum Erlangen, University Erlangen-Nuernberg,, Schlossgarten 5a, Erlangen 91054, Germany

e-mail: Sese@geol.uni-erlangen.de

INTRODUCTION: Technical OPC normally contains mixed sulfate carriers in varying amounts. Gypsum (calcium sulfate dihydrate, $CaSO_4 \cdot 2\,H_2O$) is added to the clinker before the milling process and dehydrates partially to bassanite (calcium sulfate hemihydrate, $CaSO_4 \cdot 0.5\,H_2O$) and anhydrite ($CaSO_4$). The dehydration temperature affects the resulting calcium sulfates [1]. Anhydrite exists in different polymorphes (anhydrite I-III) of which anhydrite III shows the highest reactivity with H_2O. Due to different kinetics of the calcium sulfate phases, which strongly influence hydration, it is crucial to be able to characterize the sulfate carrier composition in a cement system. Since bassanite and high reactive anhydrite III have very similar structures, a discrimination via X-ray methods is not easy. In this investigation a focus was put on the discrimination between the bassanite and anhydrite III structure as well as on transformation processes by rehydration of ambient humidity.

EXPERIMENTAL METHODS: Syntheses of different calicum sulfates were carried out by dehydration in chamber furnaces at 85 °C to 800°C ± 5 °C in air. The initial high purity gypsum ($CaSO_4 \cdot 2\,H_2O$, 99.9 %, Fluka) – was weighed in corundum crucibles of 60 ml size and dehydrated for 16 to 120 hours (deydration time is dependant on dehydration temperature). Preparation of the dehydrated gypsum samples for X-ray investigations was carried out under different humidity conditions (47 % relative humidity and 7 % relative humidity). The sample was covered by a capton film to prevent further reactions. Phase composition of the samples was examined at room temperature by quantitative X-ray powder diffraction (XRPD) with a Siemens D5000 X-ray diffractometer in combination with Rietveld refinements. Rietveld refinement was performed using the structural models (ICSD) of all occurring calcium sulfate phases. Refined parameters were: scale factor, zero displacement, background as Chebychev polynomial of 5th grade, crystallite size and lattice parameters for anhydrite III and anhydrite II. Lattice parameters of bassanite were kept fix in order to achieve stable refinement results.

RESULTS: All investigated powders consisted of at least two different calcium sulfates. Less reactive anhydrite II was found in all samples besides highly reactive anhydrite III and bassanite in different ratios. With increased dehydration temperature bassanite contents are decreasing in the samples. Anhydrite III is formed at the expense of bassanite and transformed to anhydrite II at higher temperatures. A determination of bassanite and anhydrite III in the same powder via Rietveld refinement can be accomplished with fixed lattice parameters of bassanite. Coevally, the investigations showed the hygroscopic character of dehydrated calcium sulfates. High humidity causes an instant transformation of anhydrite III to bassanite. Re-

finements of long time investigations showed a clearly detectable and continuous transformation of anhydrite III to bassanite over time. Rietveld refinement could be utilized to differentiate calcium sulfates with very similar crystalline structure and to measure transformation processes by rehydration in pure calcium sulfates.

REFERENCES:

[1] W. Abriel, K. Reisdorf, *Dehydration Reactions of Gypsum: A neutron and X-Ray Diffraction Study*, J. Solid State Chem. 85 (1990) 23-30

15:30 Poster 15-07

The X-Ray investigation of anthropogenic salinization influence on the clay mineralogy of Seriogovo soils

Yulia S. Simakova

Institute of Geology of RAS (IG), Pervomaiskaya st., Syktyvkar 167982, Russian Federation

e-mail: yssimakova@geo.komisc.ru

The objects of our investigation are the podzolic soils from the Seriogovo salt plug territory where salt mineral waters deposites are situated. Seriogovo salt plug is confined to Mezen syneclise of Russian platform. Samples were obtained from 7 soil cross sections near the Seryogovo salt deposite: R-4, R-6, R-7, PR-1 – uncontaminated (background) and R-5, R-8, R-9 – saline cross sections at the depth 0-103 cm.

The mineralogical composition of the clay fraction (<2 μm) of samples was determined by x-ray diffractometry. The clay samples were subjected to several standard treatments before XRD-analysis. Diffraction patterns were obtained of clay samples: a) air-dried, b) glycerol-saturated, c) treated by 1N HCl at 100^{o}C and d) heated for 1h at 550^{o}C. The *d*(060)-values were used to distinguish dioctahedral (0.1510 nm) and trioctahedral (0.1538 nm) minerals.

X-ray analysis indicates that almost all clay samples of background sections contain smectite, illite, chlorite, kaolinite with dominated smectite. In clay samples of saline soils chlorite, vermiculite, interstratified chlorite/vermiculite, kaolinite, illite and galite are contained. Chlorite became the predominant 1.4-nm-mineral. Smectite is the most abundant mineral in the clay fraction of uncontaminated soils. The smectite is not well ordered, evident by incomplete collapse to 1.0 nm when heated to 550^{o}C. Small amount of disordered chlorite contains in this samples. In the lower parts of saline cross sections smectite is almost absent, the most abundant minerals are pedogenic dioctahedral chlorite and interstratified minerals. The XRD patterns for the clay fraction of the uncontaminated section has an intense peak of 0.1540 nm and a smaller peak of 0.1507 nm suggesting that in this samples trioctahedral minerals are dominated, but also samples contains some dioctahedral minerals. The samples of the saline section also has both trioctahedral and dioctahedral minerals but the intensity of the peak for the dioctahedral mineral, however, is proportionally larger than in the uncontaminated clay.

The investigations display the difference between the clay minerals of saline and background soil samples of Seriogovo deposits because of their transformation under the environmental changes. The expandable layer silicates typical for the soils transformed to the unexpandable dioctahedral soil chlorite. Transformation reactions involves the introduction of non-exchangable hydroxyl-Al polymers into the interlamellar space of pre-existing smectite or vermiculite. We can propose that interlayer octahedral layers are more stable than exchangeable cations of clay minerals' crystal structure in the saline environment.The results presented suggest that chlorite was formed diagenetically by prolonged periodic percolation of salt brines through pervious layer silicates.

15:30 Poster 15-08

The Rietveld structure refinement of an exceptionally pure sample of clinoptilolite from Ecuador and its Na-, K-, and Ca-exchanged forms

Ruben A. Snellings[1], Alessandro F. Gualtieri[2]

1. *Catholic University of Leuven, Department of Earth and Environmental Sciences (KUL-EES), Celestijnenlaan 200E, Leuven 3001, Belgium* **2.** *Universita di Modena and Reggio Emilia, Modena, Italy*

e-mail: ruben.snellings@ees.kuleuven.be

Clinoptilolite is a sedimentary zeolite of extreme interest for industrial applications such as bulk separation and purification processes of waste waters and industrial effluents. It is considered a zeolite of the heulandite group with (Na+K) > Ca and Si/Al > 4. Only a few crystal structure refinements of very fine-grained (2-20 μm) natural sedimentary clinoptilolite are reported in the literature, the main reason being the presence of inseparable sample impurities such as clay minerals and feldspars intimately intergrown with clinoptilolite. The clinoptilolite studied in this work is of exceptional purity as the clinoptilolite phase fraction is around 99 wt% with trace amounts of quartz. This specimen allows for a direct structure refinement based on laboratory and synchrotron diffraction data. The sample was taken along the Rio Ayampe in the vicinity of the village of Guale and occurs as a series of white to greenish tuff layers situated in the pyroclastic Cayo Formation (Ecuador). This entirely zeolitised formation was deposited as the breakdown product of an intra-oceanic volcanic arc and constitutes a very large, recently discovered zeolite province accreted to the west Ecuadorian margin. To study the control of cation exchange on the crystal structure, the sample has been exchanged with K^{+}, Na^{+} and Ca^{2+} by immersing equal portions in a nearly saturated solution of the corresponding acetate. The separate samples were stored in sealed containers in an oven at 60 °C to promote the exchange and the solutions were renewed periodically at 1, 4 and 10 days. By means of Atomic Absorption Spectrometry the cation concentrations in the out-coming solutions were analysed to evaluate the extent of exchange. The exchange was considered as completed after 20 days. X-Ray powder diffraction data of the natural and Na-exchanged forms were collected at a lab source and at the synchrotron Italian beamline BM08 at ESRF using an imaging plate system. The in-house data were collected with a Panalytical X'Pert Pro diffractometer with a θ/θ geometry, Cu Kα radiation, and a Real Time Multiple Strip (RTMS) detector. The data of the K- and Ca-exchanged forms were collected only using a conventional source. The Rietveld refinements were conducted with both GSAS and TOPAS packages.

15:30 Poster 15-09

Langasite: Composition, color, hardness

Elena A. Tyunina, Galina M. Kuz'micheva, Elena A. Domoroschina

Moscow State Academy of Fine Chemical Technology, 86 Vernadskogo Avenue, Moscow 119571, Russian Federation

e-mail: tyunina_elena@mail.ru

Langasite (LGS, sp. gr. P321, z=1) is the most attractive materials for acoustic-volume (surface)-waves devices. Observable colouring of crystals can influence spectral-luminescent properties, is especial if it is imposed on area of generation or excitation, and also on factor transmission crystals LGS.

The aim of this work is to find a relationship between composition, color and hardness of LGS. One structural peculiarity of $La_3Ga_5SiO_{14}$ - $La_3Ga(1)Ga_3(2)(GaSi)(3)O_{14}$ is three positions for atoms of gallium: Ga(1) – octahedral, Ga(2) – tetrahedral, (GaSi)(3) - trigonal-pyramidal. Lanthanum atoms are in the centre of dodecahedron [1].

Powder samples prepared by grinding single crystals were grown by the Czochralski technique from $La_3Ga_5SiO_{14}$ (crystal I – colorless, atmosphere Ar and growth direction <01-11>; crystals: II – yellow, III – light orange, IV – orange, atmosphere Ar + O_2 and growth direction <0001>). The intensity data for Rietveld analysis were collected on a HZG-4 diffractometer (Ni – filter, CuK_α, t = 15 s, s = 0.02°, 2q 10-115°). In all calculations, we used DBWS-9411. After refining the scaling factor, zero counter position, lattice parameters, and sample displacement, the structural and profile parameters were refined by gradually introducing profile parameters at a refined background. The structural parameters were refined in several steps: first, only atomic position coordinates; then, isotropic thermal parameters at fixed positional parameters; and, finally, site occupancies at fixed positional and thermal parameters.

Crystal	H, Kg/mm^2	a, Å	c, Å	Refined composition
I - Colorless	858.33	8.1630(7)	5.0952(6)	$(La_{2.968(5)}\square_{0.032})Ga(Ga_{2.959(7)}\square_{0.041})(Ga_{1.01}Si_{0.99(1)})(O_{13.89}\square_{0.11})$
II - Yellow	1236.00	8.1668(3)	5.0966(3)	$La_3Ga(Ga_{2.978(5)}\square_{0.022})(Ga_{1.05(1)}Si_{0.95})(O_{13.94}\square_{0.06})$
III - Light orange	1460.30	8.1667(3)	5.0966(3)	$La_3Ga(Ga_{2.953(4)}\square_{0.047})(Ga_{1.02(1)}Si_{0.98})(O_{13.92}\square_{0.08})$
IV - Orange	1671.17	8.1664(3)	5.0965(3)	$La_3(Ga_{0.988(5)}\square_{0.012})(Ga_{2.96(1)}\square_{0.04})(Ga_{1.04(1)}Si_{0.96})(O_{13.90}\square_{0.10})$

i. The change in the cations site composition leads to vacancy formation.

ii. It may be stated that the experimental data prove the role of oxygen vacancies in the color of crystals. The oxygen content of yellow crystal is higher than that of colorless one.

iii. The presence of point defects lead to changes not only in lattice parameters and color but also in the hardness of these samples.

iv. The growth conditions influence the properties of LGS.

1. Mill B.V., Butashin A.V., Khodzhabagyan G.G., Belokoneva E.L., Belov N.V. “Modified rare-earth gallates with a $Ca_3Ga_2Ge_4O_{14}$ structure” // Dokl. Akad. Nauk SSSR, (in Russian) 1982, V. 264 (6), P. 1385-1389

15:30 Poster 15-10

Characterization of loosely agglomerated Lu_2O_3:Eu powders synthesized at high temperatures

Marcin Wójtowicz[1], Eugeniusz Zych[1], Leszek Kępiński[2], Joanna Trojan-Piegza[1]

1. *Wrocław University, Faculty of Chemistry, 14 F. Joliot-Curie, Wrocław 50-383, Poland* **2.** *Polish Academy of Sciences, Institute of Low Temperature and Structure Research (INTiBS), Okólna 2, Wrocław 50-422, Poland*

e-mail: mwojt@eto.wchuwr.pl

Lutetium oxide, usually activated with Eu^{3+} ions has been widely studied as a potential ionizing radiation detector. The interest in this compound comes from its unique characteristic: high density (9,4 g/cm^3), high effective atomic number (Zeff. = 67,3), which result in very high absorption coefficient for X-rays. Chemical and physical stability of lutetia are also high.

Nanocrystalline powders of Lu_2O_3 doped with 5% of Eu^{3+} with respect to Lu were synthesized by homogenous precipitation with urea at 80 °C and subsequently annealing of the raw powder at various temperatures up to 1300 °C. The homogenous precipitation from water solution was carry out in the presence of polyvinyl alcohol as

a surfactant and Li_2SO_4, which we found a good modifier preventing agglomeration upon heating at higher temperatures.
Structure and morphology of the materials were investigated using X-ray Powder Diffraction and Transmission Electron Microscopy (TEM) techniques. Spectroscopic properties were characterized using absorption, photoluminescence and radioluminescence spectroscopy.
XRD patterns, presented in Fig. 1, show transformation of the raw, basically amorphous material into $Lu_2O_2SO_4$ and finally to Lu_2O_3 upon heating. Pure oxide phase forms at 1100°C but to complete removing of OH^- groups, which have deleterious influence on luminescent properties, annealing at 1200 °C is necessary. In the presentation we shall discuss the properties of the powders in detail.

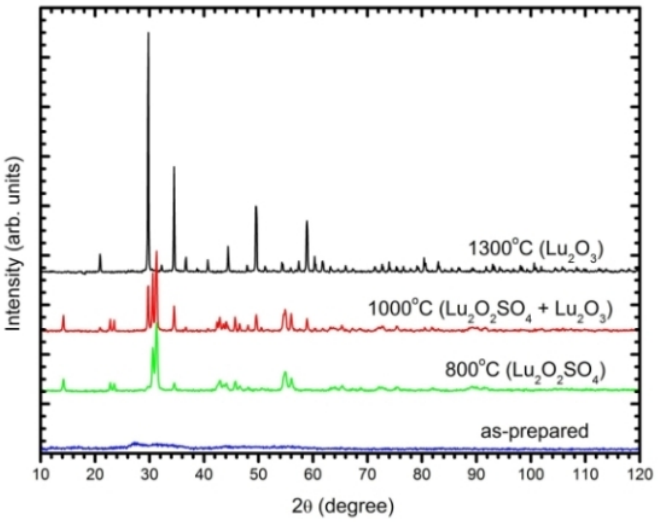

Fig. 1. XRD patterns of the materials treated at different temperatures.

15:30 Poster 15-11

Anisotropic grain growth of bismuth titanate in molten salt fluxes

Teresa Zaremba

Silesian University of Technology, Department of Inorganic Chemistry and Technology, ul. Krzywoustego 6, Gliwice 44-100, Poland

e-mail: teresa.zaremba@polsl.pl

Bismuth titanate ($Bi_4Ti_3O_{12}$) is a suitable material for applications as high temperature transducers, capacitors and sensors, due to its high Curie temperature and high piezoelectric coefficient. However, its layered structure and low crystal symmetry leads to difficulty in polarizing the conventional polycrystalline $Bi_4Ti_3O_{12}$ ceramics. It is desirable to obtain $Bi_4Ti_3O_{12}$ ceramics with textured microstructure since improved properties can be achievied in textured ceramics comparing to ceramics with randomly oriented grain structure. $Bi_4Ti_3O_{12}$ particles with plate-like morphology are preffered templates for fabricating textured $Bi_4Ti_3O_{12}$ ceramics. Molten salt synthesis (MSS) is a suitable method for synthesizing oxide powders with anisotropic particle morphologies.

$Bi_4Ti_3O_{12}$ platelets were obtained by MSS method in NaCl-KCl and Na_2SO_4-K_2SO_4 fluxes, using a mechanicaly mixed Bi_2O_3-TiO_2 mixture as the starting material. The mixtures of the precursors and salts were placed in a sealed alumina crucibles and heated at temperatures ranging from 700 to 1100ºC for a desired time period. The effects of the synthesizing temperature and time, salt species and salt content on the formation process and morphology of the $Bi_4Ti_3O_{12}$ plateletes were investigated. The morphology of the powders obtained was examined by SEM. Phases present and their crystal structures were determined by XRD.

In both fluxes, aggregate particles were formed during the initial period of reaction between Bi_2O_3 and TiO_2. The shape of the particles in the aggregate changed from lumpy to plate-like, and finally discrete plate-like particles were formed, on heating for longer periods or at higher temperatures. Plate-like $Bi_4Ti_3O_{12}$ particles with an average diameter of 5 μm and thickness <0,5 μm were obtained. The plate face was perpendicular to the crystallographic c-axis. The powders obtained during the formation process have imperfections of ionic configuration along the c-axis, which is eliminated during the growth.

15:30 Poster 15-12

Use of X-ray powder diffraction method for study on synthesis and decomposition of $K_2Ti_8O_{17}$

Teresa Zaremba, Dagmara Garczorz

Silesian University of Technology, Department of Inorganic Chemistry and Technology, ul. Krzywoustego 6, Gliwice 44-100, Poland

e-mail: teresa.zaremba@polsl.pl

Titanates, typically potassium titanates ($K_2O \cdot nTiO_2$, where n = 2, 4, 6 and 8), have been expected to be useful as a novel functional materials. The di- ($K_2Ti_2O_5$) and tetratitanates ($K_2Ti_4O_9$) possess a layered structure and have a great ion-exchange abilities. Tunnel structures have compounds with lower alkali-metal content. The hexatitanate ($K_2Ti_6O_{13}$) shows a high thermal insulating ability and chemical stability. Compare to these compounds octatitanate ($K_2Ti_8O_{17}$) has been little studied.
Potassium octatitanate possess stable tunnellike structure and exhibits characteristic properties such like as a high thermal insulating capacity and compared to $K_2Ti_6O_{13}$ a high ion conductivity. Because of these features it has been used as advanced reinforcing material for the composite and frictional material for breakes. However, it is difficult to obtain $K_2Ti_8O_{17}$ using conventional method (solid-state reaction) compared to other alkali-metal titanates. From literature data it is known that $K_2Ti_8O_{17}$ had been synthesized by hydrothermal method or host-quest reaction followed by dehydration and ion-exchange reaction. In this respect, the ion-exchange reaction method, is one of the promising synthesis method.

In the present work, we display preliminary investigation of synthesis and decomposition of $K_2Ti_8O_{17}$ using ion-exchange reaction method. This study was depend on treatment the fibrous $K_2Ti_4O_9$ with different concentrations of hydrochloric acid. Next the samples were dried and heated in determined temperatures (400÷700ºC). X-ray powder diffraction (XRD) method was used to study the formation and decomposition of $K_2Ti_8O_{17}$.
As a result, a fibrous $K_2Ti_8O_{17}$ was obtained, when heat treatment was carried out in temperature range 400÷500ºC. Investigation was

also confirmed that $K_2Ti_8O_{17}$ is decomposed above 600ºC.

Other topics

Posters
Sunday afternoon, 21 September, 15:30

15:30 Poster 16-01

Soap structured gels - The effect of soap chain length by X-ray diffraction

Ruud Adel den, Eli Roijers

Unilever (URDV), Olivier van Noortlaan 120, Vlaardingen 3130AC, Netherlands

e-mail: ruud-den.adel@unilever.com

The microstructure of soap structured gels consists of Na-soap crystals, organized in a fiber and/or ribbon structure. The dimensions of these micro structural entities depend on the soap chain length, the presence of surfactants and solvents. C16/C18 soap gives **in the absence of surfactants** soap ribbons or fibers having a width, dependent on the water/solvent ratio, in the range around 20-100 nm with crystal repeating distances of 4.5 nm. So the crystal domains are 4-20 crystal layers. **In the presence of a large amount of synthetic surfactant mixture (~ 60% w/w),** very fine soap fibers (between 10 and 20 nm) are found with crystal repeating distances of 3.3 nm. Being so thin, it is not expected to detect an X-ray diffraction line of the soap. It is hypothesised that the ribbons are curled up to fibers of a hollow tube structure. Due to the "curling-up", the soap molecules are orientated in the direction of the soap fibres resulting in a manifold repetition of the bi-layer structure and a diffraction signal is measured. In this study gels with different soap chain lengths, C8, C12, C16, Pristerene (mixture C16/C18), C22 and a reference without soap are made. In addition, temperature is an important parameter to obtain knowledge about the crystallisation behaviour of crystalline soap structures at a specific temperature.

The X-ray diffraction measurements are performed on the Bruker D8-Discover in a theta/theta configuration. A cupper anode is used and the K-alpha radiation with wavelength 0.15418 nm is selected. Long spacings are measured by performing X-ray diffraction in the transmission mode. The X-ray source and the detector are positioned in front of each other (Theta 1 and Theta 2 = 0 degrees). To prevent the detector being hit by the primary beam a leaden beam stopper is precisely positioned in the middle and just in front of the detector. The sample is placed in a Linkam temperature stage between X-ray Mylar film.

The X-ray diffraction pattern of the blank reference without soap is compared with the pattern of the Pristerene soap structured gel. A big overlap between the X-ray diffraction patterns of the blank system, showing a surfactant molecular arrangement ("ordered" L2-structure) and Pristerene is visible. Due to the absence of the theoretical expected d-value of 4.5 nm for Pristerene soap and knowing the fact that the soap fibers are very thin (10-20 nm measured with SEM), meaning less than 20 repeating layers, the question arose whether it is possible to measure soap fibres with X-ray diffraction. A way to prove this is to use longer or shorter soap chain lengths, which can possibly establish more separation between the diffraction lines of the soap and the surfactants.

It is found that very thin (10-20 nm) molecular soap arrangements in soap structured gels containing surfactants can be measured with X-ray diffraction. This is unusual, but measurable due to our hypothesis that the repeating units are in the length direction of the fiber. A large change in soap-crystal morphology and soap-crystal network structure between C12 and C16 and longer is detected with different analytical techniques in systems with large amounts of surfactants: a change in tilt-angle (XRD) and a change in the morphology of the soap-crystal network from coarse ribbons to fine fibers (SEM). The surfactants arrangement in the gel systems still exists at 80°C, while the soap is already dissolved.

15:30 Poster 16-02

The XRD studies on multicomponent ceramic of the PZT type

Bożena B. Bierska-Piech, Joanna A. Bartkowska

University of Silesia, Institute of Materials Science, 12, Bankowa Str., Katowice 40-007, Poland

e-mail: bbierska@us.edu.pl

The studing material was the multicomponent ceramic of the PZT type: $PbZrO_3$-$PbTiO_3$-$PbNb_{2/3}Mn_{1/3}O_3$-$PbW_{1/2}Mn_{1/2}O_3$. This kind of multicomponent ceramic might be used as high frequency electric converters, piroelectric detectors or useful material in acoustoelectronics as well. This ceramic was obtained by hot pressing method from simple oxides. The studied material was exposed to the external electric field. The field has ordered vectors of polarization inside the material. The polarization conditions were following: temperature of polarization T_{pol}=(410÷430) K, the external electric field E_{pol}=(2.5÷3.5) 10^6 V/m, the polarization time t_{pol}=1800 s and the environment was the silicon oil (POLSIL OM 500).

The XRD were used for the structure analysis of the non-polarized and polarized samples. The correlation with the crystal structure and ferroelectric domain structure of $PbZrO_3$-$PbTiO_3$-$PbNb_{2/3}Mn_{1/3}O_3$-$PbW_{1/2}Mn_{1/2}O_3$ were analyzed.

This study proves that the high level of the electric field causes to bigger order of 71^o and 109^o domain. According to the increase of the electric field intensity, the value of the crystal lattice deformation increases as well.

The XRD was performed using the Philips X'Pert PW 3040/60 diffractometer with the coopper radiation.
The experimental data were analyzed by the PowderCell programme v. 2.2 and the X'Pert High Score Plus software. The lattice distortions were analyzed using the Williamson–Hall method.

15:30 Poster 16-03

X-ray investigation of martensitic transformations in Fe-Ni alloys rapid quenched from melt

Volodymyr Y. Bondar, Vitaliy Y. Danilchenko, Ruslan M. Delidon

G. V. Kurdyumov Institute for Metal Physics of the National Academy of Sciences (IMP), Vernadsky Blvd. 36, Kiev UA03680, Ukraine

e-mail: vib@imp.kiev.ua

Structure-phase state and characteristics of martensitic transformations in Fe-Ni alloy (Fe - 31 wt.% Ni) ribbon quenched from melt were investigated by x-ray, optical microscopy and magnetomethric methods. X-ray investigated shown the significant texture of austenite. The peculiarities of characteristics of the direct g-a- and reverse a-g-martensite transformations connected with existence of microcrystalline and nanocrystalline component of initial austenite were founded.

15:30 Poster 16-04

Characterization of calcium phosphate synthesis products by XRD

Natalija Borodajenko, Kristine Salma, Liga Berzina-Cimdina

Riga Biomaterials Innovation and Development Centre, Riga LV-1007, Latvia

e-mail: ltmtk@inbox.lv

Calcium phosphate powders have been synthesized using wet-chemical precipitation method from $CaCO_3$ and H_3PO_4 as starting materials. Influence of technological parameters (ending pH value of calcium phosphate suspension and calcination temperature) on phase composition of final product – calcium phosphates was investigated.

The identification and phase analysis of as-synthesized and calcined calcium phosphates were investigated with X-ray diffraction and FTIR.

X-ray diffraction patterns of as-synthesized calcium phosphates showed that all powders were partially crystalline. All as-prepared calcium phosphate powders consisted of single phase - HAp as indicated by XRD.

XRD patterns of calcium phosphate samples calcined at 1000°C and above showed different phase composition (HAp, β-TCP, HAp/ β-TCP) in depending of ending pH value of calcium phosphate suspension.

The phase analysis of technologically modified calcium phosphate syntheses are shown in Fig. 1. The calcium phosphate sample (1) synthesized at pH=9 shows that the product consists of a single well crystallized phase – hydroxyapatite, sample (2) synthesized at pH=6 shows that this sample is a biphasic mixture of hydroxyapatite and β-tricalcium phosphate (β-TCP), sample (3) synthesized at pH=7 is the pure phase of β-TCP.

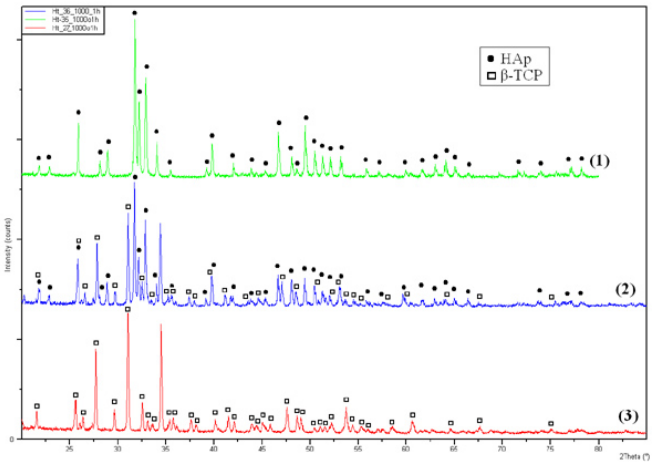

Fig. 1. X-ray diffraction patterns of calcium phosphates syntheses obtained at different pH values in the range of 6-11 and calcined at 1000°C for 1 h.

15:30 Poster 16-05

Structurally-phase state of steel under influence of laser treatment

Ruslan M. Delidon[1], Vitaliy E. Danilchenko[2]

1. *G. V. Kurdyumov Institute for Metal Physics of the National Academy of Sciences (IMP), Vernadsky Blvd. 36, Kiev UA03680, Ukraine* **2.** *G.V. Kurdyumov Institute for Metal Physics National Academy of Sciences (IMP), Vernadsky Blvd. 36, Kyiv UA03680, Ukraine*

e-mail: delrus@bigmir.net

X-ray diffraction, optical microscopy and microhardness measurements were used to study the structure formation in low carbon steel containing 0.04% C, 0.3% Mn, and 0.2% Si, 0.2% Al was subjects to laser irradiation in air with a KVANT-18 M setup using discrete 8-ms pulses. The resulting spots are either isolated (up to 2 mm in diameter) or overload, forming a track up to 40 mm long. The density of the irradiation energy was varied between 2 and 16 J/mm^2 to provide treatment conditions changing from heating into the α and γ fields (without melting) to the surface melting of the samples. Dislocation density defined on the value of a physical broadening of X-ray reflexes.

The laser treatment of low carbon steel results in a nonmonotonic distribution of dislocation density both through the laser-affected zone depth and over the diameter of an isolated laser spot in the surface layer. The maximum dislocation density was observed at a about 50 μm and in the center of the laser spot. In this case, the dislocation density observed at this depth exceeds that observed in the surface layer of the center of the laser spot. In all cases, the degree of strengthening (microhardness) is consistent with the dislocation density.

A series of structure types from dendritic and martensitic structures to fragmented grain structure with a high dislocation density inside the fragments can coexist in the laser spot and over the laser-affected zone depth. The nonmonotonic character of the microhardness distribution is mainly determined by the distribution of dislocation density. Additional contributions to the strengthening of the ma-

terial come from the structure refinement (the grain refinement, the refinement of their internal structure, and the formation of martensite).

15:30 Poster 16-06

X-ray investigations of the powders of highcarbon Fe-Al alloys phase components

Yevgeniy M. Dzevin[1], Oleksandra V. Zarytska[3], Georgiy S. Mogylniy[1], Anatoliy G. Garan[2], Dmytro I. Oliferuk[1], Vladyslav A. Andryuschenko[1]

1. *G. V. Kurdyumov Institute for Metal Physics of the National Academy of Sciences (IMP), Vernadsky Blvd. 36, Kiev UA03680, Ukraine* **2.** *V. Bakul Institute for Superhard Materials NAS of Ukraine, 2, Autozavodska str., Kiev 04074, Ukraine* **3.** *Physical Engineering Centre, National Academy of Sciences of Ukraine (FTC), Vernadskiy's blvd., 36, Kiev 03680, Ukraine*

e-mail: dzevin@i.ua

The phase components of Fe-Al-C alloys as quenched in water from melting temperature as received by melting under high pressure (7,2 GPa) have been investigated by x-ray method. It is established the presence of diamond phase in the samples which received by thermal and high pressure treatment by means of using of the monochromatic Fe $_{K\alpha 1}$-x-ray irradiation. The results of x-ray study by using monochromatic Cu $_{K\alpha 1}$-irradiation allow to conclude that the distortions of diamond crystal lattice are absent. It was defined that K-phase (carbide), independently from method of alloy receiving, did not correspond to stoichiometric structure Fe_3AlC. Its formula can be represented as Fe_{4-y}-Al $_y$-$C_{0,66}$. The diamond powder, received by dissolving of sample in acid mixture, has been investigated. The x-ray patterns obtained in Fe-irradiation have shown clear and untailed reflections of diamond phase. All the data allow unambiguously identify the diamond and confirm the possibility of receiving of the synthetic diamond powders from Fe-Al-C alloys.

15:30 Poster 16-07

XRD investigation and thermal properties of the $[Ir(NH_3)_6][Co(C_2O_4)_3]\cdot H_2O$ and $[Co(NH_3)_6][Ir(C_2O_4)_3]$ — precursors for the $Co_{0.50}Ir_{0.50}$ bimetallic phase

Evgeny Y. Filatov[1,2], Kirill V. Yusenko[1,2], Evgeny S. Vikulova[2], Pavel E. Plyusnin[1,2], Yuri V. Shubin[1,2]

1. *Nikolaev Institute of Inorganic Chemistry of SB RAS, Lavrentev 3, Novosibirsk 630090, Russian Federation* **2.** *Novosibirsk State University (NSU), Pirogov 2, Novosibirsk 630090, Russian Federation*

e-mail: decan@che.nsk.su

Solid solutions and intermetallic compounds containing platinum metals are shown to possess the greatest electrocatalytic and magnetic characteristics. The double complex salts (DCS) containing both a platinum group metal and a transition metal are attracting to researchers as precursors of bimetallic materials of various composition and structure [1, 2].

Bimetallic phase $Co_{0.50}Ir_{0.50}$ was prepared by the thermal decomposition of $[Ir(NH_3)_6][Co(C_2O_4)_3]\cdot H_2O$ and $[Co(NH_3)_6][Ir(C_2O_4)_3]$. The processes of the thermal decomposition in helium and hydrogen atmospheres were studied in details.

Decomposition of these complex salts in hydrogen atmosphere was investigated by XRD and thermal analysis. Relatively fast (0.5 hour) rise of the temperature to 550 °C and exposure of thermolysis products at this temperature during one hour results in formation of nanocrystalline bimetallic phase. The developed phase is represented by close packing crystal structure with planar defects – stacking faults. Diffraction patterns of the products can be interpreted as alloys of iridium with cobalt based on FCC structure with coherent insertion of the HCP fragments. Crystalline size of the particles is 4-5 nm.

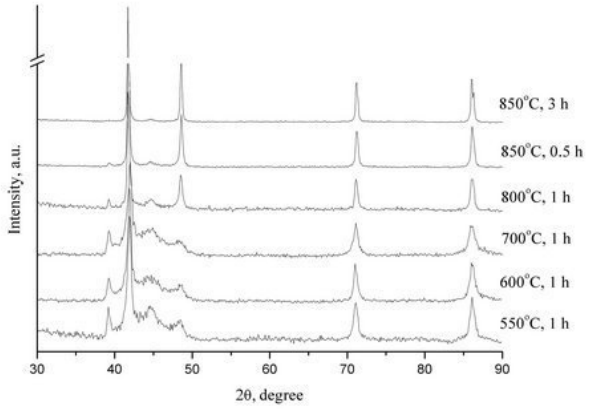

Father rise of the temperature diminishes the number of packing defects. During the annealing the positions of the reflections of the FCC lattice remains constant, while relative intensity of the peak 002 increases, and the ratio I_{002}/I_{111} approaches 0.5 (see figure). Final product is a powder of disordered solid solution $Ir_{0.50}Co_{0.50}$ (sp. gr. Fm-3m, a = 3.710(3) Å, 20-30 nm crystalline size). Size distribution and morphology of the particles were investigated by scanning electron microscopy. The composition of the all samples was confirmed by energy dispersive X-ray spectroscopy (EDS).

This work was supported by the RFBR grants 07-03-01038-a, 08-03-00603-a.

1. A.V. Zadesenets, E.Yu. Filatov, K.V. Yusenko et al., Inorg. Chim. Acta 361 (2008) 199.

2. K.V. Yusenko, E.Yu. Filatov, D.B. Vasil'chenko et al., Z. für Krist. Suppl. 26 (2007) 289.

15:30 Poster 16-08

Synthesis and Chemistry of New Layered Oxychalcogenide

David G. Free, John S. Evans

Department of Chemistry, University of Durham, Science Labs, South Road, Durham DH1-3LE, United Kingdom

e-mail: d.g.free@dur.ac.uk

We have an ongoing interest in oxychalcogenide materials. In particular those with layered structures. Layered structures are commonly found due to the different bonding requirements of oxygen and chalcogen ions in mixed metal systems. Materials with these structures are of interest due to their magnetic properties, potential use in optical devices, and as hosts in alkali ion battery technology. One of

the least studied families of oxychalcogenides is the $A_2O_3M_2Q_2$ family, where A = lanthanide ion, M = transition metal ion, Q = chalcogenide.

Synthetic studies on the $A_2O_3M_2Q_2$ family has provided a general overview of the range of the metal species for which this structure is stable. Variable temperature X-ray diffraction has shown that $Pr_2O_3Mn_2Se_2$ undergoes a structural transition at low temperatures (~150K) from a tetragonal to an orthorhombic unit cell. This transition is accompanied by ferromagnetic ordering of the moments within the structure when cooled the material in the presence of an applied magnetic field. There is also evidence for a similar structural transition in $La_2O_3Mn_2Se_2$ at lower temperatures. This poster will report synthetic, structural and magnetic characterisation of these materials.

15:30 Poster 16-09

Quantitative and qualitative analysis of clays containing poluent industrial residues

Juan A. G Carrió[1], Mauro C. Terence[1], Waldemar A. Monteiro[1], Nelson B. De lima[2], Antonio H. Munhoz Jr[1], Carolina G. Prieto[1]

1. *Presbyterian University Mackenzie (UPM), Rua da Consolação 930, Sao Paulo 01302-907, Brazil* **2.** *Instituto de Pesquisas Energéticas e Nucleares (IPEN-CNEN), Av. Prof. Lineu Prestes, 2242, USP, Sao Paulo 05508000, Brazil*

e-mail: jgcarrio@mackenzie.br

Treatment station of waste effluents at the Brazilian automotive industry obtains a considerable quantity of solid residues, which contain some heavy metal silicates. Those residues can be industrially recycled by their insertion in clays, in which they can become inert. In this work, samples of solid industrial residues were characterized by thermogravimetric analysis (TG), differential scanning calorimetry (DSC), atomic absorption spectrometry (AAS) and infrared absorption spectroscopy by Fourier transformed (FT-IR). The main elements presents in the samples were Ca, Mg, Ni and Zn. The residues were then mixed with Brazilian shale and quartz. The effect of the residues in the clay properties was analyzed by FT-IR spectroscopy and X-rays powder diffraction. In the IR region of 780 cm^{-1} to 1010 cm^{-1} were detected peaks of heavy metal silicates. X-ray powder diffraction data were collected with a Rigaku MultiFlex difractometer with a fixed monocromator. The experimental conditions were: 40kV, 20mA, $10^o < 2\theta < 100^o$, $\Delta 2\theta = 0.02^o$, λCuKα, divergence slit = 0.5^o, reception slit = 0.3 mm and step time 5 s. A quantitative analysis of the samples with and without residues was performed by the Rietveld method using the refinement program GSAS. The refinement results and Fourier differences calculations indicate that the metal atoms occupy intersticial and substitutional sites in the clay cristaline structure. This explains the results of leaching tests, in which no detectable amounts of heavy metal were found.

References:

A.C. Larson, R.B. Von Dreele, Los Alamos National Laboratory. Los Alamos, EUA. Copyright, 1985–2000, The Regents of the University of California, 2001.

Acknowledgments: Mackpesquisa, CAPES

15:30 Poster 16-10

Structural analysis of influence of dopants in the electrical conductivity of CuNi alloys

Juan A. G Carrió, Waldemar A. Monteiro, Vicene A. Rodrigues, Mauro C. Terence, Terezinha J. Masson, Leila F. Miranda

Presbyterian University Mackenzie (UPM), Rua da Consolação 930, Sao Paulo 01302-907, Brazil

e-mail: jgcarrio@mackenzie.br

It is well known that in disordered solid solutions, the resistivity of metals and alloys is strongly influenced by the atomic displacements, vacancies and intersticials. In this work, were produced samples of alloys on the base of Cu-Ni from high purity precursors, to study the interactions between the metallurgical and thermodynamic processes that determine the strength-electrical conductivity combinations of $Cu_{x\%}$ - $Ni_{y\%}$ alloys, doped with Sn, Be, Pt, Cr and Nb. A sequence of thermo mechanical treatments was developed with the intention of increasing the hardness maintaining the electrical conductivity of the alloys. Then they were characterized by optical microscopy and Vickers micro hardness measurements. Their electrical conductivity was measured with a milliohmeter Agilent (HP) 4338B. Substitutional solid solutions with the dopant Sn showed a clear increasing of hardness and decreasing of conductivity, as predicted by the literature. X-ray diffraction data of the samples were collected with a Rigaku MultiFlex difractometer with a fixed monocromator. The experimental conditions were: 40kV, 20mA, $10^o < 2\theta < 120^o$, $\Delta 2\theta = 0.02^o$, λCuKα, divergence slit = 0.5^o, reception slit = 0.3 mm and step time 5 s. Refinements of the crystalline structure of the samples were performed by the Rietveld method, using the refinement program GSAS. The refinement results and Fourier differences calculations indicate that the metal atoms occupy substitutional sites in the alloy structure. The refinements also allowed a study of the dependence of the micro-structure and the thermomechanical treatments of the samples and its relation with the strength and electrical conductivity.

References:

1. Monteiro, W. A., Cosandey, F., Bandaru, P., The effect of termo mechanical treatment on the microstructure of a Ni-Cu-Be alloy, THERMEC`97, Australia, 1997.

2. A.C. Larson, R.B. Von Dreele, Los Alamos National Laboratory. Los Alamos, EUA. Copyright, 1985–2000, The Regents of the University of California, 2001.

Acknowledgments: Mackpesquisa, CAPES

15:30 Poster 16-11

Preparation and structure analysis of gel-metal oxide composites as filling material for W-188/Re-188 generator columns

Edward Iller[1], Andrzej Deptuła[2], Jan Milczarek[3], Ludwik Górski[3], Fabio Zaza[4]

1. *Institute of Atomic Energy, Radioisotope Centre Polatom, Otwock-Świerk 05-400, Poland* **2.** *Institute of Nuclear Chemistry and Technology (IChTJ), Dorodna 16, Warszawa 03-195, Poland* **3.** *Institute of Atomic Energy, Otwock-Świerk 05-400, Poland* **4.** *ENEA, via Anguillarese 301, Roma 00123, Italy*

e-mail: l.gorski@cyf.gov.pl

Rhenium has recently shown up as a useful radioisotope in variety of clinical trials. At present the carrier –free Re-188 is obtained from W-188/Re-188 generators in which the tungsten-188 in form of sodium tungstenate W-188 solution is adsorbed on the alumina filling of generator column. A new approach to preparation of chromatographic column packing of tungsten-188/rhenium generators is application of nanocomposites obtained by mean of the sol-gel technique... A specific method for the synthesis of these materials was elaborated at INCT. The initial stage of the process is preparation of the ascorbate- NH_4^+- tungsten, next the separately prepared zirconyl or/ and silicon sols are added gradually to the reaction mixture. After a gelation step, the gels are thermal treated at temperatures indicated by thermal analysis (500, 650, 800^{o}C). This way the synthesis of nanocomposites containing of TiO_2-WO_3, ZrO_2-WO_3, ZrO_2-SiO_2-WO_3 at different ratios of oxides were carried out. The elution profile of generator column packed on gels samples activated in nuclear reactor have been studied using as eluent 0,9% NaCl solution as an eluent. The best results of elution (profile and eluent purity) appeared in the case of filling a chromatographic column by materials ;WO_3-ZrO_2 in which the oxides molar ratio was 1:2 and calcination temperature 500^{o}C and WO_3-TiO_2 with molecular ratio 1:2 and a calcination temperature of 650^{o}C. The samples containing WO_3-ZrO2-SiO_2 did reveal satisfactory elution profile. For determination of structure of ZrO2-WO3 composites the neutron scattering and X-ray diffraction analysis have been applied. The gels at different molar ratio of oxides 1:1, 2:1, 2:3 and annealed at 500^o, 650^o,800^{o}C had been examined. The atomic ordering of the composites was studied by wide range scattering angle (10^o – 110^o) neutron diffraction. The measurements were carried out with a double crystal monochromator diffractometry employing Cu single crystals with (200) reflection planes. The nanoscale structure of the composites was determined by the small angle neutron scattering in 0.1 nm^{-1} – 1 nm^{-1} region. The small angle neutron scattering was studied with λ= 0.237 nm neutrons monochromatized with double PG monochromator and filtered with 3 cm thick PG filter. In conclusion of experiments , we can state that the WO_3-ZrO_2 composites easy crystallize and the rate of process increases with the annealing temperature. In the composites annealed at 500^{o}C the inhomogenities of average diameter of 50 nm and highly warped boundary surface are found. For higher annealing temperatures the cylinder like particles are formed. Next the samples were analyzed by X-ray diffraction technique using Cu radiation and scanning range from 2Θ =3^o to 2Θ =90^o (step 0.02^o and rate 2^o/min). On the X-ray diffraction pattern WO_3-ZrO_2 (1:1, 1:2, 3:2) composites annealed at 500^{o}C practically no peaks are visible, materials are rather amorphous. After annealing at 650^{o}C, few weak peaks beyond the background level are observed . The gels annealed at 800^{o}C are fully crystalline and contain both oxides as separate phases : WO_3 as a monoclinic form and ZrO2 as the mixture of cubic and tetragonal phases. Acknowledgment: The work was supported by the research grant No 3 TO9B 042 29 of the Polish Ministry of Science and Education

15:30 Poster 16-12

Structural - phase state of maraging alloys

Vitaliy E. Danilchenko, Viktor E. Iakovlev

G.V. Kurdyumov Institute for Metal Physics National Academy of Sciences (IMP), Vernadsky Blvd. 36, Kyiv UA03680, Ukraine

e-mail: zvik83@mail.ru

Structural and composition changes in single crystals caused by heating the maraging alloys to within the (γ+α)- limits were investigated by X-ray. The heating is necessary either for producing the intermetallic phases on aging or for initiating the reverse α-γ- transition. These processes in iron-nickel alloys are accompanied by the redistribution of the alloying element between the γ- and α-phases.

The test materials were Fe-29wt.%Ni-2wt.%Ti and Fe-28wt.%Ni-2wt.%Ti-2wt.%Al alloys, which are used for the fabrication of stamps and press molds. The specimens contained (70-85)% martensite at room temperature. The reverse transition occurred on heating in salt bath at (400-500)^{0}C. The transition kinetics and the amount of martensite were controlled by magnetometry. Selected area X-ray diffraction patterns were taken on a KAMEBAX spectrometer. Nickel content of the γ-solid solution was estimated from the previously built concentration dependences of fcc-lattice parameter of binary iron-nickel alloys.

The tempering of freshly quenched alloys reduced the parameter c_α and the tetragonality c/a_α of the martensite lattice even at room temperature. At temperatures between 100 and 300^o C, the parameter c_α reduced further, and the reverse α-γ-transition occurred during tempering at 400^o C. The reduce in c_α is associated with the loss of matching of the martensite and retained austenite lattices, as well as with the formation of a Ni_3Ti-type phase and the subsequent depletion of the α-solid solution in the alloying elements due to the formation of intermetallic compounds and the nickel redistribution between the γ- and α-phases.

Annealing of the two-phase specimens at 520^{o}C for several minutes shifted the martensite reflections having high third indices toward higher Bragg angles.

The retained austenite reflections were tailed at the side of low angles, and weak first-order satellite reflections appeared at the tailing at 520^{o}C (for 10 h) or higher annealing temperature (600^{o}C) attenuated and eliminated the latter reflections, and the retained austenite reflections started blurring. Holding at 600^{o}C increased the Bragg angles and intensities of the satellite reflections. The Bragg angles of the retained austenite reflections also increased.

Thus, heating of two-phase iron-nickel alloys during the reverse α-γ- transition causes the surface lamination of the γ-solid solution. The surface of the quenched alloy is nickel because of the nickel re-

distribution between the γ- and α-phases during the α-γ-transition, selective iron oxidation, and increase in the concentration of the unoxidized component in the superficial layer.

15:30 Poster 16-13

Structure of the active phase in V-Mo-Nb-O catalysts for ethane oxidative transformations

Tatyana U. Kardash, Ludmila M. Plyasova, Dmitry I. Kochubey, Valentina M. Bondareva, Alexandr N. Shmakov, Arkady V. Ischenko

Boreskov Institute of Catalysis (BIC), pr. akad. Lavrentieva, 5, Novosibirsk 630090, Russian Federation

e-mail: tanik.kardash@gmail.com

Nonstoichiometric molybdenum oxides with tunnel structure, doped with Group IV, V and VI metals, has become the great deal of scientific attention in the last time because of their catalytic activity in the selective oxidation of alkanes C_2-C_3. For instance, triple V-Mo-Nb oxide, which in crystalline state has the Mo_5O_{14}-like structure [1], acts as an active phase in ethane selective (amm) oxidation [2-4]. During the process of catalyst genesis XRD-amorphous phase forms in the temperature range 400-550°C, crystalline phase forms at 550°C.

In the present work structures of XRD-amorphous and crystalline oxides with composition $Mo_1Nb_{0.37}V_{0.30}O_x$ are characterized by the complex of physical and chemical methods (EXAFS, HREM and XRD). Cation distribution in crystalline state is established and structure of crystalline oxide is refined by full profile analysis.

All diffraction data and EXAFS- spectra are obtained in Siberian Synchrotron Radiation Center, (Budker INP, Novosibirsk, Russia). Effect of anomalous scattering far and near the adsorption edge of niobium is used to distinguish the contribution of niobium and molybdenum to diffraction peaks. EXAFS spectra proceeding and modeling is made in VIPER software environment [5]. Rietveld refinement is performed using GSAS with EXPGUI user interface [6].

HREM investigation of the XRD-amorphous V-Mo-Nb oxide reveal 1D-ordered nanostructure with block size <10 nm and interlayer distance of 0,40 nm. . In perpendicular plane, networks are built by Me_5O_{14}-like subunits with “star shape”, which consist of MeO_7-bipiramides connected by edge with five octahedra. Cations of molybdenum and niobium are statistically distributed in the structure and located both in the centers of pentagonal bipiramides and octahedra. These Me_5O_{14}-like subunits are distributed in the distorted matrix of MeO_6 octahedra, where Me=V, Mo, Nb. Oxygen surrounding of molybdenum and niobium does not change noticeably when crystalline phase forms. The latter process is accompanied by changes in angles between polyhedra.

In the crystalline V-Mo-Nb oxide Me_5O_{14}-like subunits form tetragonal unite cell with statistical distribution of molybdenum and niobium in the structure. These subunits share corners with single octahedra, occupied either by vanadium cations or by molybdenum (niobium) ones.

Authors acknowledge the financial support of RFBR (project 07-03-00203)

References:

1. Kihlborg L., 1959, Acta Chem. Scand., 13, 95
2. Roussel M., Bouchard M. et. al., 2006, Appl. Catal. A, 308, 62
3. Bondareva V. M., Andrushkevich T.V. et. al., 2006, React. Kinet. Catal. Lett., 87, 377
4. Merzuoki M., Taouk B., Monceaux L., et al., 1992, Stud. Surf. Sci. Catal, 72, 165.
5. Klementiev K. V., 2001, J. Phys. D: Appl. Phys., 34, 209.
6. Toby B. H., 2001, J. Appl. Cryst., 34, 210-221

15:30 Poster 16-14

X-ray study of langatate

Irina Kaurova[1], Galina M. Kuz'micheva[1], Aleksandr B. Dubovsky[2]

1. *Moscow State Academy of Fine Chemical Tecnology by M. V. Lomonosov, Vernadskogo pr., 86, Moscow 119571, Russian Federation* **2.** *Russian Research Institute for the Synthesis of Minerals, Institutskaya st., 1, Aleksandrov 60165, Russian Federation*

e-mail: kaurchik@yandex.ru

$La_3Ga_{5.5}Ta_{0.5}O_{14}$ ($La_3(Ga_{0.5}Ta_{0.5})(1)Ga_3(2)Ga_2(3)O_{14}$, LGT) belongs to the langasite family (sp. gr. *P321*, z = 1). These compounds are of considerable practical interest in the context of the search for "strong" piezoelectrics. A characteristic feature of this structure is that Ga resides at three positions: octahedral, Ga(1) (partially occupied by Ta atoms); tetrahedral, Ga(2); and trigonal-pyramidal, Ga(3). The La atoms sit at the center position of dodecahedra.

The aim of the work is to determine a composition of langatate with different color for the establishment of relationship between the composition of the samples and their color.

Single crystals were grown by the Czochralski technique in an <0001> direction and have a different color: as-grown crystal - **I.1**. (yellow); crystal, annealed in air at 1400°C - **I.2**. (orange); crystal, annealed in vacuum at 1000°C - **I.3**. (colorless) (Fig.*a*); crystal, annealed in vacuum at 1200°: part **II.1**. (pale-green) and part **II.2**. (green) (Fig.*b*). The color of crystals was determined by transmission spectra using a "Specord M-40" with "Color measurement" option.

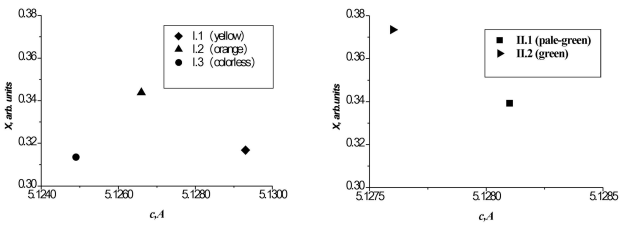

The samples were ground into fine powders and examined by XRD on HZG-4A diffractometer (room temperature, CuKα, graphite monochromator, t=15 s and a step of 0.02°, 2Θ range 10°-115°). Refinement of crystal structures was accomplished using the Rietveld suite of programs DBWS-9411.

The compositions of the samples:

I.1$La_3(Ga_{0.501}Ta_{0.499(2)})(Ga_{2.97(1)}\tilde{}_{0.03})Ga_2(O_{13.95(3)}$”$_{0.05})$;
I.2 $La_3(Ga_{0.490(2)}Ta_{0.510})(Ga_{2.95(1)}\tilde{}_{0.05})Ga_2(O_{13.94(3)}$”$_{0.06})$;
I.3$La_3(Ga_{0.487(2)}Ta_{0.513})(Ga_{2.947(4)}\tilde{}_{0.053})Ga_2(O_{13.93(4)}$”$_{0.07})$;
II.1$(La_{2.994(1)}\tilde{}_{0.006})(Ga_{0.501}Ta_{0.499(1)})Ga_3Ga_2(O_{13.99(1)}$”$_{0.01})$;
II.2$La_3(Ga_{0.486(2)}Ta_{0.514})(Ga_{2.93(1)}\tilde{}_{0.07})Ga_2(O_{13.91(4)}$”$_{0.09})$

An appearance of the crystal color for I crystals is due to the ratio of the $V_O^{\cdot\cdot}$ (oxygen vacancies):$(1/2V_O^{\cdot\cdot},e\phi)^x$ (associates-centers color): by the $V_O^{\cdot\cdot}<(1/2V_O^{\cdot\cdot},e\phi)^x$ the crystals are colored (yellow – I.1. or orange – I.2), by the $V_O^{\cdot\cdot}>(1/2V_O^{\cdot\cdot},e\phi)^x$ or without vacancies crystals are colorless. At the same time, in contrast to their results we revealed another color of II crystal. Probably, green color is associated with the precipitation of phase with Ta^{3+} ions. This phase is oriented to the host matrix LGT. The oxygen content of part II.1 is higher than that of I crystals and part II.2 and color of part II.1. near to colorless than to colored.

15:30 Poster 16-15

Synthesis and characterization of (electro)luminescent materials based on charged $[Eu^{3+}$/Organic chelate$]^-$ complexes within layered double hydroxide (Hydrotalcite) as host matrix

Sumeet Kumar, Marco Milanesio, Leonardo Marchese

Università degli Studi del Piemonte Orientale (DISTA), Via V. Bellini 25/G., Alessandria 15100, Italy

e-mail: sumeet.kumar.iitk@gmail.com

Charged anionic complexes of europium with various organic chelates have been synthesized and studied for its luminescent and further electroluminescent properties with LDH (Hydrotalcite) as host material. Synthesizing host-guest structure is a promising method to enhance charge transfer to the light emitting ion/ligands and also increase efficiency/life time of a device. The complexes and LDH are characterised by techniques (XRPD/FT-RAMAN/FT-IR/TGA/UV-Vis). Topas software is used for the analysis of the powder diffraction data. Diffraction peak shifting and peak broadening effects are realised on comparing the diffraction pattern before and after intercalation of europium complexes into the LDH.

Zn/Al LDH synthesized at a controlled pH of 5.5 - 6 and with general formula: $[Zn^{II}_{1-x}Al^{III}_x(OH)_2]^{x+}[A^{m-}_{x/m}.nH_2O]^{x-}$
where (A= nitrate, and x=0.35) has been experimentally found to be more yielding and easy to get intercalated, with NO_3^- ions being replaced by separately synthesized europium complexes, among which [europium(III)+EDTA] in a basic environment (pH=8±0.5) was difficult to intercalate into the LDH layers while experiments with the carbonate form showed no intercalation but separate phases of LDH and [europium+EDTA] complex on XRPD analysis. Tris(benzoylacetonato) mono(phenanthroline)europium(III) obtained from sigma aldrich and used without further purification is oxidised by pottasium permanganate in solution phase and the filtered sample after thorough washing with enough CO_2 free water is dissolved into decarbonized water with molar ratio of 0.5 w.r.t M(III) part of LDH, the Solution obtained is put at 100 °C for 24 hrs and filtered/washed with further drying at 60 °C for 5 hours. Similar synthesis method is applied for obtaining coumarine-3-carboxylate chelated Eu(III) complexes.

15:30 Poster 16-16

Why high resolution is absolutely needed for powder diffraction study of the crystal and magnetic structures of the complex strongly correlation systems

Alexander I. Kurbakov

St.Petersburg Nuclear Physics Institute RAS (PNPI), Orlova Roshcha, Gatchina 188300, Russian Federation

e-mail: kurbakov@pnpi.spb.ru

The absolute necessity of an application of the high resolution for understanding of the physical nature of the strongly correlation systems having tendency to the phase separation is shown by the example of the electron-doped $Sm_{0.1}Ca_{0.9-x}Sr_xMnO_3$ perovskite manganites study by powder neutron (NPD) and x-ray (XRPD) diffractions. The refinement of the room temperature XRPD data show a transition from *Pnma* for $x\leq0.4$ to *I4/mcm* space group for $0.5\leq x<0.8$. The room temperature crystallographic parameters were obtained from analysis of the high resolution NPD data confirm with the preliminary x-ray study. The *Pnma* structures are slightly distorted (the distortion parameter $[(a+c)/b\sqrt{2}]$ remains close to 1), whereas the cell parameters present a clear splitting in the *I4/mcm* space group (leading to a distortion $[a\sqrt{2}/c]$ around 0.98). Nevertheless two kinds of *Pnma* lattices are observed, $a>b/\sqrt{2}>c$ for $x<0.2$ and $c>b/\sqrt{2}>a$ for $x>0.2$. A detailed (by 5 K temperature step) study of two compounds $Sm_{0.1}Ca_{0.9-x}Sr_xMnO_3$ (x=0.3 and 0.6), belonging to each structural region, has been carried out on high intensity G4.1 diffractometer with the medium resolution. It demonstrates phase separations at low temperature, with mixtures of *C*- and *G*-type antiferromagnetisms (AF). The temperature dependence of the NPD patterns shows two magnetic transitions without structural ones for $Sm_{0.1}Ca_{0.3}Sr_{0.6}MnO_3$. At ~240K, peaks characteristic of *C*-type AF start to develop and at ~120K a peak characteristic of *G*-type AF appears. The data recorded with G4.1 for $Sm_{0.1}Ca_{0.3}Sr_{0.6}MnO_3$ were all refined by using one phase with the *I4/mcm* space group and *C*-type and then *G*-type antiferromagnetic structures were added for *T*~240 and 120K, respectively [leading to Mn magnetic moments of ≈2 and 1.1m_B, respectively (at 1.4K)]. The temperature dependence of the lattice parameters was studied from 1.4 to 300K showing a smooth evolution. The low temperature structure was then analyzed by using the higher resolution NPD-G4.2 diffractometer data. Two *I4/mcm* unit cells are needed to use to describe the low temperature state. Both unit cells are elongated along the *c* axis, the more distorted one corresponds to the main phase (70%) and *C*-type AF (with 2.3μ_B) and the more regular one (30%) is associated with *G*-type AF (2.4μ_B). The magnetic moments are along the *c* axis, corresponding to the longer Mn-O distances in the *C*-AF phase, and perpendicular to this axis in the *G*-type phase. The magnetic behavior of $Sm_{0.1}Ca_{0.6}Sr_{0.3}MnO_3$ is similar, with *C*- and *G*-type AFs establishing at ~150 and 70K, respectively. Nevertheless, accordingly to the G4.1 medium resolution data, for this compound a structural transition is associated with the magnetic one at 150K (from paramagnetic P-*Pnma* to *C*-AF-$P2_1/m$). At lower temperature, that is, around 70

K, the *G*-type AF starts to develop, without visible structural changes. The low temperature state (<70K) is thus described with one monoclinic cell associated with two AF components (with ≈2μ_B and 1μ_B for *C* and *G*, respectively). The high resolution G4.2-NPD data allow an improvement of the fit by adding a second crystalline phase of *Pnma* space group, corresponding to the *G*-type AF. At 1.5 K, the main part of the sample (~95%) corresponds to the $P2_1/m$ space group and is associated with the *C*-type AF. The magnetic moments (2.1μ_B) are lying in the basal (*x*, *z*) plane in agreement with the distortion of the cell in this plane. The two MnO_6 octahedra of this monoclinic phase exhibit the same distortion: the smaller distance is the apical Mn-O (1.890 Å in both cases) and one of the equatorial ones is longer (1.920 or 1.921 Å) than the other one (1.896 or 1.895 Å). This elongation is associated with the d_{3z2-r2} orbital polarization, characteristic of *C*-type AF. Thus decreasing the temperature, the MnO_6 octahedra become more flattened and a strong distortion appears in the basal plane. So, it is shown, that only addition of the high intensity diffraction results by the data with the high resolution, lead to a coherent physical picture. The phase separation at low temperatures occurs as from the point of view of crystal, and magnetic structures. Each magnetic phase corresponds to the crystal phase and features of a crystal phase determine type of a corresponding magnetic phase. There are the strong relationships and the correlation between structures and properties in this phase separation $Sm_{0.1}Ca_{0.9-x}Sr_xMnO_3$ series.

15:30 Poster 16-17

Crystal Structure of the $Sr_3MgSi_2O_8:Eu^{2+},Dy^{3+}$ persistent luminescence material

Jorma Hölsä[1], Marja Isotahdon[1], Taneli Laamanen[1,2], Mika Lastusaari[1], Marja Malkamäki[1,2], Maarit Myllykoski[1], Janne Niittykoski[1]

1. *University of Turku, Department of Chemistry, Turku FI-20014, Finland* **2.** *Graduate School Of Materials Research, Turku FI-20500, Finland*

e-mail: miklas@utu.fi

Silicates usually possess stable and rigid crystal structures. Thus, they make excellent host matrices for efficient luminescent materials with use in applications as lamps, cathode ray tubes, scintillators, *etc*. [1]. $Sr_2MgSi_2O_7:Eu^{2+},Dy^{3+}$ is currently the best persistent luminescence material [2]. It can store energy from *e.g.* sun or lamp light and release it as visible light persisting up to 24 hours in the dark. The applications of persistent luminescence range from the traditional luminous paints to more sophisticated fields as radiation detection, structural damage and temperature sensing as well as medical diagnostics. The other stable composition in the $Sr_nMgSi_2O_{5+n}$ series, $Sr_3MgSi_2O_8:Eu^{2+},Dy^{3+}$, also shows persistent luminescence [3].

The crystal structure of $Sr_3MgSi_2O_8$ has been suggested to be orthorhombic with unit cell parameters a = 5.4, b = 9.6 and c = 7.2 Å, Z = 2 [4,5]. However, no space group or structural details have been reported. The structure has also been referred to as merwinite ($Ca_3MgSi_2O_8$) type with the monoclinic space group $P2_1/a$ (No. 14), Z = 4 [6]. In this work, the crystal structure was investigated based on X-ray powder diffraction data.

The undoped and Eu^{2+}/Dy^{3+} codoped $Sr_3MgSi_2O_8$ samples were prepared by solid state reactions. Stoichiometric amounts of strontium carbonate, magnesium nitrate hexahydrate, silicon dioxide, europium oxide and dysprosium oxide were heated at 1250 °C for 10 hours in a reducing N_2 + 12 % H_2 atmosphere. The X-ray powder diffraction patterns were collected at room temperature by a Huber 670 Guinier camera using monochromatic copper $K_{\alpha 1}$ radiation (λ = 1.5406 Å).

The unit cell was found to be of lower symmetry than that of the glaserite type trigonal $Ba_3MgSi_2O_8$ [7]. The previously proposed orthorhombic cell could not account for all the observed reflections, either, but a doubling of the unit cell c-axis was needed. This cell corresponds to the merwinite one, but the systematic absences suggest possible space groups Cc (No. 9) or C2/c (15). Even if no clear reflection splitting was observed, the broadening and intensities of the reflections suggest a unit cell belonging to the monoclinic crystal system with a = 9.442, b = 5.452, c = 13.860 Å and β = 90.2°.

1. Shionoya S., Yen W.M. (Eds.), *Phosphor Handbook*, CRC Press, Boca Raton, FL, USA, 1999.

2. Lin T., Tang Z., Zhang Z., Wang X., Zhang J., *J. Mater. Sci. Lett.***20** (2001) 1505.

3. Lin Y., Tang Z., Zhang Z., Nan C.W., *J. Alloys Comp.***348** (2003) 76.

4. Klasens H.A., Hoekstra A.H., Cox A.P.M., *J. Electrochem. Soc.***104** (1957) 93.

5. JCPDS, 1997, *Powder Diffraction File*, entry No. 10-0075.

6. Moore P.B., Araki T., *Am. Miner.***57** (1972) 1355.

7. Aitasalo T., Hietikko A., Hölsä J., Lastusaari M., Niittykoski J., Piispanen T., *Z. Kristallogr. Suppl.***26** (2007) 461.

15:30 Poster 16-18

Determination of the crystal structure for the ferroelectric relaxor (1-x)$PbMg_{1/3}Ta_{2/3}O_3$ - x$PbTiO_3$

Agnieszka Leonarska, Antoni Kania, Joachim Kusz, Alicja Ratuszna

University of Silesia, August Chełkowski Institute of Physics, Department of Solid State Physics, Uniwersytecka 4, Katowice 40-007, Poland

e-mail: aleonars@us.edu.pl

Single crystals of (1-x)$PbMg_{1/3}Ta_{2/3}O_3$ - x$PbTiO_3$ solid solution of the concentration 0≤x≤0,4 were examined by two methods: X-ray powder (using a Siemens D-5000 diffractometer with Cu Kα radiation) and single crystal diffraction (using a four-circle KM4 diffractometer with graphite-monochromatized Mo Kα radiation).

The samples were prepared by the flux method [1]. The crystals show that with the increase of Ti content, at room temperature, symmetry changes from cubic to tetragonal.

For the $PbMg_{1/3}Ta_{2/3}O_3$, on the diffracted patterns obtained for single crystal as well as for powder apart the main lines related to cubic, perovskite structure, the additional, weak lines are observed. The calculations for the cubic model give the value of R_B about 0,10. When the model of structure with the tilts of oxygen octahedral, and with the double lattice cell was assumed the discrepancy factor is about 0,08. For these reason the model of the modulated structure has been proposed and calculated for the single crystal data.

The picture present the experimantal powder spectrum

$Ta_{2/3}O_3$ - $xPbTiO_3$ for x=0, with permit observe the additional lines. It assume that these lines are the superstructure ones.

The next studies were performed for the mixed crystals $(1-x)PbMg_{1/3}Ta_{2/3}O_3$ - $xPbTiO_3$. The diffracted pattern shows the splitting of the main diffracted lines, indicating on tetragonal distortion. The structure has been refinement using the Glazer model [2,3]. The data from the single crystal experiment confirmed the model proposed from powder.

[1] A. Kania, A. Leonarska, Z. Ujma - J.Crystal Growth **310** (2008) 594 - 598

[2] A.M. Glazer - Acta Cryst. (1972). **B28**, 3384

[3] A.M. Glazer - Acta Cryst. (1975). **A31**, 756

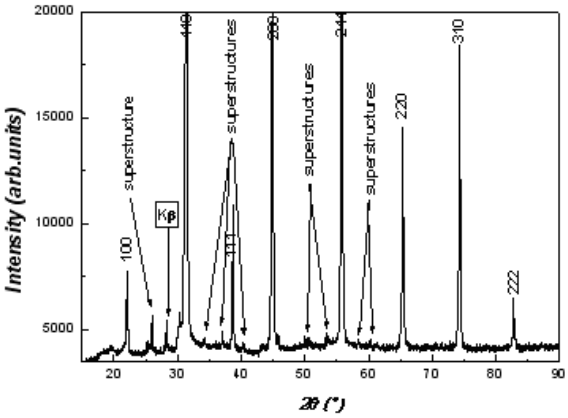

Experimental powder spectrum (1 - x)PMT - xPT for x=0

Keywords: structural phase transitions, X-ray powder diffraction and single crystal diffraction, perovskites, (1-x)PbMg$_{1/3}$Ta$_{2/3}$O$_3$ - xPbTiO$_3$. Type of contribution: **poster**

15:30	Poster	16-19

Structure and microstructure of magnetic intercalated vermiculites

Arancha Argüelles[1,2], Matteo Leoni[3], Charles H. Pons[4], Cristina De la Calle[5], Sergei A. Khainakov[6], Jesús A. Blanco[1], Celia Marcos[7]

1. *University of Oviedo, Department of Physics, C/ Calvo Sotelo, Oviedo 33007, Spain* **2.** *Instituto Tecnologico de Materiales (ITMA), Parque Tecnológico del Principado de Asturias, C/ Calafates, Parcela L-3.4, Avilés 33417, Spain* **3.** *Department of Material Engineering and Industrial Tecnology, University of Trento (DIMTI), v. Mesiano 77, Trento 38100, Italy* **4.** *Institut des Sciences de la terre d'Orléans (ISTO), 1A, rue de la férollerie, Orléans 45071, France* **5.** *Instituto de Ciencia de Materiales de Madrid, CSIC (ICMM, CSIC), Cantoblanco, Madrid 28049, Spain* **6.** *University of Oviedo, Department of organic and inorganic chemistry, C/Julián Clavería, Oviedo 33006, Spain* **7.** *University of Oviedo, Jesus Arias de Velasco, Oviedo Oviedo, Spain*

e-mail: Matteo.Leoni@unitn.it

Vermiculite Intercalation Compounds (VIC's) have been prepared from Mg-vermiculite from Santa Olalla (Huelva, Spain). Magnetic cations (Fe, Ni) have been introduced in the interlamellar space by ion-exchange, in order to study the magnetic behaviour of the resulting systems. In the present work, structure and microstructure of the VIC's resulting from these diffusion processes have been analyzed by microprobe and X-ray powder diffraction techniques. Data has been refined by means of the DIFFaX+ software, as these compounds are showed to have a semi-ordered structure, like the starting vermiculite. Variations in the structure parameters induced by the presence of the new cations (Fe, Ni) have been analyzed.

15:30	Poster	16-20

Effect of concentration of bi-ionic solutions containing (Pb^{2+}, Zn^{2+}) on the selectivity phenomenon in the case of Na montmoriollonite: "in Situ" XRD analysis

Walid Oueslati[1], Mahdi Meftah[1], Hafsia B. Rhaiem[1], Bruno Lanson[2], Abdesslem B. Haj Amara[1]

1. *Laboratoire de Physique des Matériaux Lamellaires et Nano Matériaux Hybrides (LPMNMH), Faculty of science of Bizerte, Bizerte 7021, Tunisia* **2.** *LGIT, CNRS-UJF, Grenoble BP53, France*

e-mail: meftahmahdi@yahoo.fr

This paper aims at characterizing the structural evolution and selectivity of Na-dioctahedral smectite(Wy-Na).Cation Exchange Selectivity (CES) for Wyoming montmorillonite was determined by equilibration of the clay with a mixed equinormal solution containing two competing cations (i.e Pb^{2+}, Zn^{2+}). The quantitative analysis of XRD patterns is achieved using an indirect method based on the comparison of XRD experimental patterns to calculated ones. The study is carried out in two steps: first the Cation Exchange Capacity (CEC) is saturated with one cation Pb^{2+} and Zn^{2+} (i.e. two heavy metal cations occurring in hold house trash) in order to prepared reference sample. The resulting complexes were respectively labelled Wy-Pb and Wy-Zn. Secondly the clay is placed in presence of bionic solution: Pb-Zn with different concentrations (i.e. from 10^{-2}N to 10^{-4}N) in order to understand the concentration effect on the selectivity phenomena of the clay for these cations. XRD quantitative analysis showed that for low concentrations the d_{001} spacing corresponds to the Wy-Na complex, whereas for high concentration the d_{001} spacing can be attributed to the Zn and Pb cation. This means that at low concentrations, the sample present an homogeneous state and the clay CEC is saturated with low hydration state cation (Na^+) which is characterized by one water layer (1W). For high concentrations, an interstratified behaviour appears and the clay has a tendency to fix in minor contribution the Zn^{2+} cation and in major contribution with Pb^{2+} cation characterised by a mixed hydration state between one (1W) and two water layers (2W). This result was confirmed by using in situ XRD analysis when we studied the evolution of hydration behaviour related to sample saturated Pb^{2+} and Zn^{2+}. We note large difference between those samples for suitable range of relative humidity. After there, it can be easy to identify the interlamellar space contents.

15:30 Poster 16-21

Effect of heating and reaction time on the nature of synthesized zeolites from KGa-2 kaolinite

Mahdi Meftah, Walid Oueslati, Abdesslem B. Haj Amara

Laboratoire de Physique des Matériaux Lamellaires et Nano Matériaux Hybrides (LPMNMH), Faculty of science of Bizerte, Bizerte 7021, Tunisia

e-mail: meftahmahdi@yahoo.fr

This paper explains first, the characterization of synthesize zeolites from KGa-2 kaolinite (natural and heated). The intermediate phases and final products were characterized by X-ray diffraction and high-resolution ^{29}Si and ^{27}Al MAS NMR. Secondly, we studied the thermal condition effect of starting material to judge the final zeolites phases. The process of synthesizing zeolites A and P depend in the host material heated temperature and time reaction. Indeed, when we used a natural or heated (i.e 500°C) sample we obtained characteristic lines of zeolites P. by increasing temperature degrees towards 900°C the nature of synthesized zeolites change. Indeed, for 24h time reaction we obtained characteristics lines of zeolites A. While continuing time reaction at 72h we note a structure change traduced by appearance of characteristics peaks related to zeolites P. This result was confirmed by MAS NMR spectroscopy. Indeed, the characteristic band positions of core ^{29}Si for the zeolites A are placed between -99.75 and -89.31(ppm). The zeolites P phases obtained from heated clay at 500°C present a band position between -107.36 and -87.49 (ppm). The core ^{27}Al present in the major case one characteristic resonance line at -57 ppm. Those values indicate a new crystalline phase polymerisation given by (Si m Al) with $0 \leq m \leq 4$ atoms corresponding to two different zeolites phases.

15:30 Poster 16-22

X-ray powder diffraction of the sillenite family

Tatyana I. Melnikova[1], Galina M. Kuz'micheva[1], Aleksandr B. Dubovsky[2]

1. *Moscow State Academy of Fine Chemical Tecnology by M. V. Lomonosov, Vernadskogo pr., 86, Moscow 119571, Russian Federation* **2.** *Russian Research Institute for the Synthesis of Minerals, Institutskaya st., 1, Aleksandrov 60165, Russian Federation*

e-mail: melti@list.ru

The sillenites are a crystalline material group with the general formula $Bi_{24}M^{4+}_2O_{40}$ [1] (sp.gr. *I*23, z=1), which demonstrate interesting physical properties depending on their composition. $Bi_{24}M^{4+}_2O_{40}$ are named as ideal sillenites (IS). Deviations from the M^{4+} formal charge (FC) lead to a defect structure (DS) based on vacancies ($Bi_{24}[M^{2+(3+)}_{2-y}[]_y](O_{40-d}[]_d$); []-vacancy) and/or incorporations of the O in the crystal structure ($Bi_{24}[M^{5+}_2](O_{40+d})$. There are solid solutions, which can describe as $Bi_{24}(M',M''_2)O_{40}$. They phases may be both IS and DS that depend on the FC of M' and M'' ions. The aim of this paper to determine a composition and structural peculiarities of some sillenites using results of X-ray powder diffraction.

All samples of nominal composition $Bi_{24}M^{4+}_2O_{40}$ (M^{4+}=Si, Mn) and $Bi_{24}(M',M''_2)O_{40}$ (M'=Si^{4+}, M'' = Mn, V) were synthesized by hydrothermal method. The samples ground into powder were examined by X-ray diffraction on HZG-4A diffractometer (room temperature, CuKα, graphite monochromator, a stepwise mode with an exposure time of 15 s and a step of 0.02°, 2Θ range 10°-100°). Refinement of crystal structures (the position parameters, the site occupancies and the anisotropic thermal parameters for all atoms) was accomplished using the Rietveld suite of programs DBWS-9411.

As a results of crystallochemical analysis of X-ray data and the valence force method applying the formula [2]: $k_i = v_c/[\Sigma(1/r_i)^n]$, where n=2.5 (our data for Bi), k_i (table data), and r_i Å are the experimental values of the interatomic Bi-O and M-O distances main conclusions were made:

- An increase of Bi-O average interatomic distances in BiO_5 polyhedra is associated with a reduction of M-O distances in MO_4 tetrahedra and vice versa.

- A linear dependence and negative deviation from a linear dependence of the cell parameters vs. value x for phases of the systems $(1-x)Bi_{24}(Bi^{3+}_{1.4}[]_{0.6})(O_{38.4}[]_{1.6}) - xBi_{24}Mn^{4+}_2O_{40}$ and $(1-x)Bi_{24}Si^{4+}_2O_{40} - xBi_{24}Mn^{4+}_2O_{40}$ can be caused by the FC Mn^{4+} and by the different compression of initial phases, respectively.

- The cell parameters of «$Bi_{24}V^{4+}_2O_{40}$» and «$Bi_{24}V^{5+}_2O_{41}$» phases were estimated and they were used to find the FC V in phases of systems $(1-x)Bi_{24}(Bi^{3+}_{1.4}[]_{0.6})(O_{38.4}[]_{1.60}) - x$«$Bi_{24}V^{4+(5+)}_2O_{40(41)}$» and $(1-x)Bi_{24}Si^{4+}_2O_{40} - x$«$Bi_{24}V^{4+(5+)}_2O_{40(41)}$». Obviously the anomalous behavior of the cell parameter and the M-O distance of phase with the general formula $Bi_{24}(Si^{4+},V)_2O_{40}$ is due to the presence of FC V^{4+} that promotes the green colour of this sample.

- The difference between the FC M' and M'' ions in $Bi_{24}(M',M''_2)O_{40}$ phases and the non-optimal ionic radii of M (M' and M'') ions are a possible reasons of DS formation.

1. S.F. Radaev, V.I. Simonov, *Kristallografiya*. 1992, **37**, 914
2. Y.A. Pyatenko, *Kristallografiya*. 1972, 17, 773.

15:30 Poster 16-23

The Curie point of lead-barium zirconate titanate PZT ceramic

Witold Z. Mielcarek, Dionizy Czekaj, Krystyna Prociów, Joanna B. Warycha, Lucjan Kozielski

e-mail: mielcar@iel.wroc.pl

A piezoelectric substance is one that produces an electric charge when a mechanical
stress is applied (the substance is squeezed or stretched). Conversely, a mechanical
deformation (the substance shrinks or expands) is produced when an electric field is
applied. An important group of piezoelectric materials are ceramics which are utilized
to make many useful products, such as ceramic resonators, ceramic bandpass filters,
ceramic discriminators, ceramic traps and filters.

In analogy to ferromagnetic materials, the Curie temperature is also used in

piezoelectric materials to describe the temperature above which the material loses
its spontaneous polarization and piezoelectric characteristics. In lead zirconate
titanate, the material is tetragonal below Tc and the unit cell contains a
displaced central cation and hence a net dipole moment. Above Tc, the material is
cubic and the central cation is no longer displaced from the centre of the unit cell.
Hence, there is no net dipole moment and no spontaneous polarization.

The Curie point was estimated for $PB_{0.84}Ba_{0.16}(Zr_{0.54}Ti_{0.46})O_3$ + 1mol% Nb_2O_5 ceramic.

The XRD measurements were carried out with DRON-2 deffractometer using Fe filtered Co
radiation and equipped with the high- temperature attachment.The XRD patterns were
taken in the range from 20o to 80o, as step-scans. The calculation were made with
DHN-PDS computing program.From the changes of lattice constants with temperature it
was determined that at 230oC +/-lOoC the $PB_{0.84}Ba_{0.16}(Zr_{0.54}Ti_{0.46})O_3$ + 1mol% Nb_2O_5 ceramic structure fully transformed from tetragonal to cubic one with lattice constant a=4.081 A.

15:30	Poster	16-24

Study of aluminas obtained by irradiated pseudoboehmites calcination

Antonio H. Munhoz Junior[1], Marcela Nakashima[1], Waldemar A. Monteiro[1], Amanda A. Aguiar[2], Leonardo G. Andrade e Silva[2], Leila F. Miranda[1]

1. *Presbyterian University Mackenzie (UPM), Rua da Consolação 930, Sao Paulo 01302-907, Brazil* **2.** *Instituto de Pesquisas Energéticas e Nucleares (IPEN-CNEN), Av. Prof. Lineu Prestes, 2242, USP, Sao Paulo 05508000, Brazil*

e-mail: ahmunhoz@yahoo.com

In a previous work pseudoboehmites obtained from aluminum nitrate as precursor using the sol-gel method were irradiated with electrons to study the possible effects of radiation in their properties. In this work it has been studied the effect of radiation with electron beam in a pseudoboehmite obtained by sol-gel synthesis using aluminum chloride and ammonium hydroxide as precursors. The addition of poly(vinyl alcohol) ($[C_2H_3OH]_n$) solution (8 wt% in water) in the reaction mixture was also studied. The aluminium chloride solution was mixed with the polyvinyl alcohol and the mixture was dropped into an ammonium hydroxide solution. It has been studied the effects of pseudoboehmite radiation in the aluminas structure resulted from sol-gel synthesis product calcination. The milky-white colloidal pseudoboehmite precipitate obtained by sol-gel method was filtered off, washed with distilled water, dried at 70°C, and powdered in a mortar. The sample acquired was calcined at 1100° C for 4 hours and after that the X-ray powder diffraction was performed. A well crystallized a-alumina was obtained at 1100°C from the not irradiated samples. The X-ray powder diffraction data shows that in some irradiated samples calcined at 1100° C for four hours presented θ-alumina and a-alumina. The powder dried at 70° C was also examined by thermal analysis. The Thermo Gravimetric analysis (TG) and Differential Scanning Calorimetry (DSC) were used to evaluate mass loss and the pseudoboehmite endothermic and exothermic transformations. The scanning electron microscopy was also used to analyze the samples.

15:30	Poster	16-25

Electronic structure of diamond-formating Me-Al-C alloys

Dmytro I. Oliferuk[1], Vladyslav A. Andryuschenko[1], Oleksandra V. Zarytska[2]

1. *G.V. Kurdyumov Institute for Metal Physics National Academy of Sciences (IMP), Vernadsky Blvd. 36, Kyiv UA03680, Ukraine* **2.** *Physical Engineering Centre, National Academy of Sciences of Ukraine (FTC), Vernadskiy's blvd., 36, Kiev 03680, Ukraine*

e-mail: vaavandr@i.kiev.ua

The electronic structure calculations for various phases in Me-Al-C systems (Me = Cr, Mn, Fe, Co, Ni) have been carried out using the full-potential linearized augmented plane wave (FP-LAPW) method. Possible crystal structures of non-stoichiometric carbides in these compounds are suggested. Electron density distribution, full and partial density of states spectra have been obtained. Type of magnetic ordering and varying of electronic properties depending on kinds of transition metal atoms in lattice and different carbon concentrations have been analyzed. We propose the hypotheses about effect of electronic structure of the carbon-containing phases that causing the diamond formation in these alloys.

15:30	Poster	16-26

Rietveld refinement for $Li_2Si_2O_5$ doped with vanadium

Wojciech Paszkowicz[1], Suzan Abd El All[1,2], Fathi M. Ezz-Eldin[2], Krzysztof Kaczorek[3], Ryszard Diduszko[1,3]

1. *Polish Academy of Sciences, Institute of Physics, al. Lotników 32/46, Warszawa 02-668, Poland* **2.** *Center of Research and Radiation Technology, Nasr City, Cairo 0002, Egypt* **3.** *Tele and Radio Research Institute, Ratuszowa 11, Warsaw 03-450, Poland*

e-mail: paszk@ifpan.edu.pl

Lithium-based conducting glasses are promising candidates for electrolyte materials of thin-film batteries because they exhibits isotropic ionic conductivity. However, at room temperature most of such conducting glasses exhibit relatively low ionic conductivity values, in the range 10^{-7} to 10^{-8} S/m. In order to increase the conductivity, some specific additives have been used., one of them being vanadium. In a recent work on borate glasses, vanadium dopant at a level of several percent was used for this purpose [1-3]. It has been noticed that annealing of vanadium doped borate glass results in a change of physical properties [1]. This may suggest that vanadium enters specific crystallographic sites. In this work, a related material, vanadium-doped lithium silicate glass is studied. The glass was prepared by heating a mixture of quartz (SiO_2), lithium carbonate

CO_3) and vanadium pentoxide (V_2O_5) at a level of up to 5.5 weight percent at 1400 for 3 h and then cooled. As prepared glass was annealed for four hours at 550°C. This procedure gives virtually pure $Li_2Si_2O_5$ phase of orthorhombic *Ccc*2 space group [4] with vanadium present in the lattice and traces of impuity phases. The lattice parameters are found to vary isotropically with increasing vanadium content. We notice that the observed crystallisation is faster than that reported in literature for phosphate glasses [5].

References

[1] N.A. El-Alaily, R.M. Mohamed, *Effect of irradiation on differenial thermal properties and crystallization behavior of some lithium borate glasses,* Nucl. Instrum. Meth. Phys. Res. B **179** (2001) 230-242

[2] Y.-I. Lee, J.-H. Lee, S.-H. Hong, Y. Park, *Li-ion conductivity in $Li_2O–B_2O_3–V_2O_5$ glass system*, Solid State Ionics **175** (2004) 687–690

[3] S.Y. Marzouk, N.A. Elalaily, F.M. Ezz-Eldin, W.M. Abd-Allah, *Optical absorption of gamma-irradiated lithium-borate glasses doped with different transition metal oxides*, Physica B **382** (2006) 340–351

[4] B.H.W.S. de Jong, H.T.J. Supér, A.L. Spek, N. Veldman, G. Nachtegaal, J.C. Fischer, *Mixed alkali systems: Structure and ^{29}Si MASNMR of $Li_2Si_2O_5$ and $K_2Si_2O_5$*, Acta Cryst. B **54** (1998) 568-577

[5] Y. Iqbal, W.E. Lee, D. Holland, P.F. James, *Crystal nucleation in P_2O_5-doped lithium disilicate glasses*, J. Mater. Sci. **34** (1999) 4399–4411

15:30 Poster 16-27

Probing the fluorite-pyrochlore phase boundary in bismuth oxides

Julia L. Payne, Ivana Radosavljevic Evans

Department of Chemistry, University of Durham, Science Labs, South Road, Durham DH1-3LE, United Kingdom

e-mail: J.L.Payne@durham.ac.uk

Oxides based on fluorite (MO_2) and pyrochlore ($A_2B_2O_7$) have potential uses in devices such as solid-oxide fuel cells and oxygen sensors, arising from their oxide ion conductivity. The high temperature Bi_2O_3 polymorph, δ-Bi_2O_3, adopts the cubic defect fluorite structure, where 25% of the oxygen sites are vacant and the vacancies are distributed statistically. Relative to fluorite, in a typical pyrochlore structure, $A_2B_2O_7$, only 12.5% of the oxygen sites are vacant, but the vacancies are ordered.

It has been widely reported that the formation of the pyrochlore structure over the fluorite structure depends on the cation radius ratio, r_A/r_B, with the pyrochlore forming in the range 1.46-1.78 [1]. This ratio may be adjusted by aliovalent or isovalent doping of the cation sites, which can also induce anion disorder [2]. This is especially important in the pyrochlore structure, where the oxide ion vacancies are usually ordered, hence the creation of anion disorder should result in a greater oxide ion conductivity.

Our current research efforts are focused on probing the fluorite-pyrochlore structural phase boundary in $(Bi,Zr)_4O_7$ – $Bi_2B_2O_7$ (B = Ti, Sn, Hf) systems. We have recently determined a fluorite – pyrochlore phase boundary in the $(Bi,Zr)_4O_7$ – $Bi_2Ti_2O_7$ system. Here we present some results of our recent synthetic work and in-situ variable temperature powder XRD studies.

1. M.A. Subramanian, G. Aravamundan & G.V. Subba Rao, (1983), *Prog. Solid St. Chem.***15**, 55-143

2. B.J.Wuensch, K.W. Eberman, C. Heremans, E.M. Ku, P. Onnerud, E.M.E Yeo, S.M.Haile, J.K.Stalick, J.D. Jorgensen, (2000), *Solid State Ionics*, **129**, 111-133

15:30 Poster 16-28

Error bars in powder diffraction

Roman Pielaszek

Polish Academy of Sciences, Institute of High Pressure Physics (UNIPRESS), Sokolowska 29/37, Warszawa 01-142, Poland

e-mail: roman@pielaszek.net

Imaging of atomic-scale phenomena in macroscopic world (e.g. on photographic film) made X-ray diffraction one of the most powerful experimental techniques in the history of science. This success came real in large extent due to elegant simplicity of fundamental diffraction formulas, such as Laue or Bragg equations.

Both, the diffraction phenomena and the simplicity of original theory have their sources in phase relations establishing the method. Phase-related math is extremely simple in binary (black&white) considerations that constitute the fundamental formulas. However, in any intermediate (gray) case, where $\varphi \neq n \cdot 2\pi$, the math becomes less elegant and not that simple anymore.

Obviously, the preferred solution of this problem is to tag all $\varphi \neq n \cdot 2\pi$ photons as "noise" or "parasitic intensity" and cut them off. However, in the present paper we would like to use them to determine some basic error estimates for selected quantities ibeing used n X-ray diffraction. This will help to draw error bars around readings of crystallite size, dispersion of sizes, lattice parameter or phase concentration.

15:30 Poster 16-29

Molecular and crystalline structures of (s)-4-decyloxycarbonyl-2-azetidinone and (s)-4-hexadecyloxycarbonyl-2-azetidinone

Luis E. Seijas[1], Asiloé J. Mora[1], Andy Fitch[2], Michela Brunelli[3], Francisco López Carrasquero[4]

1. *Universidad de Los Andes, Facultad de Ciencias, Laboratorio de Cristalografía, Merida 5101, Venezuela* **2.** *European Synchrotron Radiation Facility (ESRF), Grenoble 38043, France* **3.** *Europen Synchrotron Radiation Facility (ESRF), 6, Jules Horowitz, Grenoble 38000, France* **4.** *Universidad de Los Andes, Facultad de Ciencias, Laboratorio de Polímeros, Merida 5101, Venezuela*

e-mail: seijasluis@ula.ve

The compounds (S)-4-decyloxycarbonyl-2-azetidinone (I) and (S)-4-hexadecyloxycarbonyl-2-azetidinone (II) are optically active b-lactam derivatives of aspartic acid, which are used as starting materials in anionic polymerization to produce poly-b-peptides[1].

These polymers adopt conformations that resemble those of the a-helixes and display properties of liquid crystals and piezoelectricity [2-4]. In this work the structures of these (S)-4-alkoxycarbonyl-2-azetidinones were solved by means of the parallel tempering algorithm implemented in the program FOX [5]. Both compounds crystallize in monoclinic cells $P2_1$, with cell parameters a= 27.81703(3) Å, b= 5.35138(4) Å, c=5.35138(4) Å, b=92.046(1)º (compound I); and a=37.14982(7) Å, b=5.35795(6) Å, c=5.30862(1) Å, b=92.169(1)º (compound II). During the Rietveld refinement [6] with the program GSAS [7], bond distances and angles were restrained to vary within ±0.02 Å and ±1.5º, respectively. Both compounds display a similar asymmetry pattern in the distances of the azedinone ring and deviation from planarity due to the presence in the ring of different hydration states of the carbons atoms. The aliphatic chain presents normal bond distances and angles for sp^3 carbon atoms, and torsion angles close to 180º. The crystal packing is dominated by hydrogen bonds of the type N—H···O, which form extended chains running along **b** and described by the first order graph symbol C(4); additionally, van der Waals interactions between neighboring aliphatic chains help to form supramolecular zig-zag structures.

Acknowledgement: This study was supported by the CDCHT-ULA, FONACIT-Venezuela (Lab-97000821) and beam line ID31, ESRF (France).

References

1. López-Carrasquero, F., García-Álvarez, M. and Muñoz-Guerra, S. (1994). *Polymer*, **35**, 4502–4510. López-Carrasquero, F., Aleman, C. and Muñoz-Guerra, S. (1995). *Biopolymers*, **36**, 263-271.
2. Prieto, A., Pérez, R. and Subirana, J. A. (1989). *J. Appl. Phys.***66**, 803–806.
3. Muñoz-Guerra, S., López-Carrasquero, F., Aleman, C., Morillo, M., Castelleto, V. & Hamley, I. (2002). *Adv. Mater.***14**, 203–205.
4. Favre-Nicolin, V. and Černý, R. (2002) *J. Appl. Cryst.***35**, 734–743.
5. Rietveld, H. M. (1969). *J. Appl. Cryst*. **2**, 65-71.
6. Von Dreele R. B. & Larson A. C. (2007). *GSAS*: General Structure Analysis System. Los Alamos National Laboratory, Los Alamos, New Mexico, USA.

15:30 Poster 16-30

Structural transformations of metal-organic cyano-bridged chains, networks and frameworks triggered by dehydration/rehydration

Helen Stoeckli-Evans, Olha Sereda, Antonia Neels

Centre Suisse d'Electronique et de Microtechnique (CSEM), Jaquet-Droz 1, Neuchâtel 2002, Switzerland

e-mail: helen.stoeckli-evans@unine.ch

Dynamic structural transformations, based on flexible porous frameworks are a major challenge in material sciences, both from a fundamental and a practical point of view. We have constructed a number of metal-organic chains, networks and frameworks based on metallocyanides. Some of these metal-organic cyano-bridged compounds (MOCB's) show structural transformations on dehydration/rehydration. The "sponge-like" behaviour of the molecular transformations is accompanied by a colour change and it has been shown by in-situ powder X-ray diffraction and immersion calorimetry to be completely reversible. By a combination of the DSC, powder XRD and immersion calorimetry it was also possible to find the net heat of the transformation. For one such system the structural transformation, driven by solvent molecules, lead to the formation of two types of networks that show different behaviour upon drying, falling within the category of "recoverable collapsing" and "guest-induced reformation" frameworks. We will show that the synthetic strategy based on cyanide-bridged bimetallic assemblies is advantageous for the formation of flexible nanoporous materials.

15:30 Poster 16-31

X-ray powder diffraction for illite polytypes analysis

Agnese Stunda[1], Ilze Luse[2], Liga Berzina-Cimdina[1], Valdis Seglins[2]

1. *Riga Biomaterials Innovation and Development Centre, Pulka Str. 3/3, Riga LV-1007, Latvia* **2.** *University of Latvia, Raina Bulvaris 19, Riga LV1009, Latvia*

e-mail: agnese.stunda@rtu.lv

X-ray powder diffraction (XRPD) is one of main methods for clay minerals polymorphism research. For polytypes analyzing it is important to acquire unoriented clay XRPD pattern and in addition to it pattern should be intensive enough to recognize polytypes peaks.

Clay mineral crystallites have a small size and layered structure, therefore XRD pattern has a very small intensity. Polytype characterizing unbasal peaks have considerably lower intensity than basal peaks have. The aim of these studies is to achieve XRPD patterns of unoriented samples with hight resolution of unbasal reflexes. For these studies we used clay samples from Latvia with different genesis and various illite polytypes content. The samples were separated into 2 and 1 micron fractions, using different kind and different concentration of dispersants, $[Na(PO_3)]_6$ and NH_4OH. Than each sample was tested either heated at 550°C, either saturated with glycol.

Analyzing clays by X-ray diffraction it was tried in several combinations to improve the intensity keeping background smooth. Sample amount was very small, yet sample was placed in such a way, that irradiated diameter of sample reached 10 mm, thickness approximately 1 mm. We tested time prolongation from 30 till 120 s per step, split 1/4° and 1/2°, mask 5 and 10 mm and several irradiated length combinations.

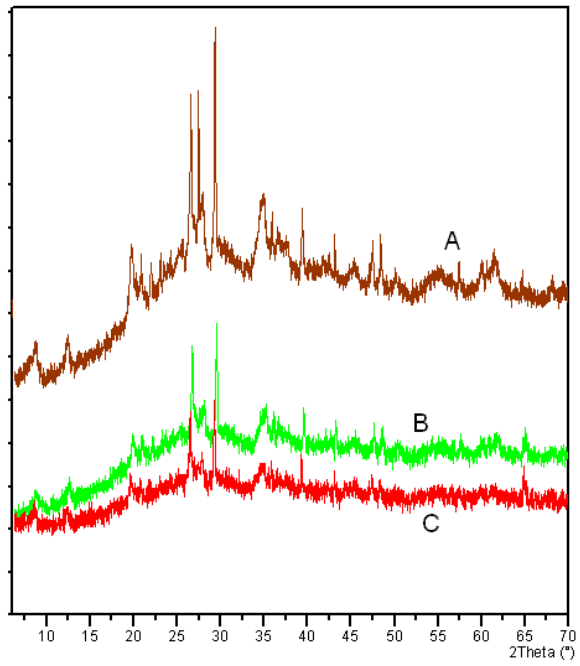

Analyzable clay samples mostly contain illite and kaolinite. Using dispersants either doesn't influences or makes X-ray pattern worse. Time prolongation and split opening improves reflection intensity, however damage background (see figure: a - 120, b - 60, c - 30 s/step), that obstruct interpretation of X-ray powder diffraction pattern.

15:30 Poster 16-32

Laboratory X-ray diffraction and fluorescence tests of the Martian analogue: The Theo's flow rock from Ontario, Canada

Huawei Su[1], Graeme M. Hansford[1], Richard M. Ambrosi[1], Antony F. Abbey[1], David Vernon[1], Ian Hutchinson[2]

1. *University of Leicester, University Road, Leicester LE17RH, United Kingdom* **2.** *Brunel University, London, United Kingdom*

e-mail: hs93@le.ac.uk

The X-ray diffraction and fluorescence tests of a Martian analogue rock carried out by the University of Leicester are presented. A simulation chamber consists of CCD, X-ray source, source collimator and sample table is designed and developed in support of the *in situ* mineralogical and chemical analysis instrument of the planetary surface exploration.

A reflection XRD geometry is selected for the benefit of wider two-theta angle coverage and easier sample preparation. In order to maximize the operation reliability of the *in situ* remote instrument, all parts are designed as the fixed components. So the 2-Dimension CCD would be a good candidate chosen for the detector, and both position and energy related X-ray events could be stored simultaneously. An array of CCDs in-line could extend the two-theta angle coverage, therefore in our chamber, we simulated this by using an XMM EPIC CCD22 manufactured by e2v Technologies mounted on a motorized rotating arm. The source we used is a conventional X-ray tube with copper anode and with anode coated by the manganese powder. Both Cu-Ka and Mn-Ka characteristic X-rays are tested in our chamber. ^{55}Fe radioactive source will be the next one to choose in the test.

The Theo's flow rock is from the Pyroxenite layer, 60 meter below the surface of Ontario Canada. It's believed that the composition of the rock is similar to the Martian Nakhlites. The sample was prepared by crushing the rock and pressing the powder into a pellet disk. The results show the X-ray spectrum and diffractogram. By analyzing these results, the possible elemental and mineral composition could be carried out. Also the sample has been tested by a commercial XRD/XRF instrument from Department of Geology in University of Leicester. The comparison of the laboratory results and commercial ones suggests that the planetary surface XRD/XRF instrument implementation is feasible. **Figure 1.** Comparison of laboratory and commercial XRD instrument diffractogram of Theo's flow rock Martian analogue sample.

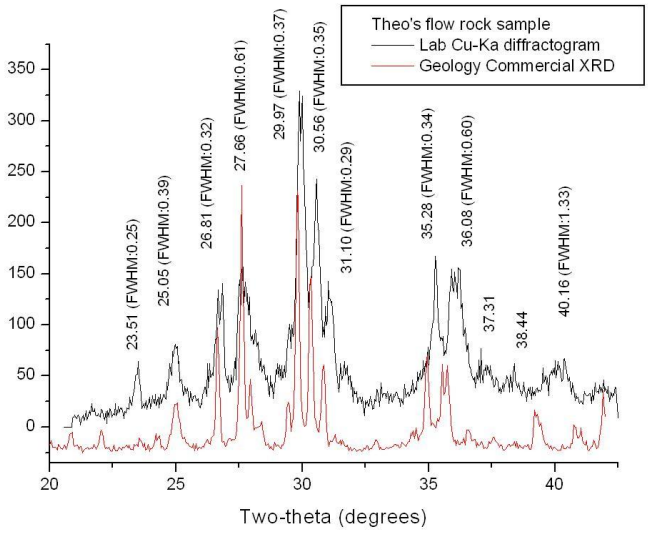

15:30 Poster 16-33

Crystal structure and optical properties of $Ln_2(Ca,Mn)Ge_4O_{12}$

Nadezda V. Tarakina[1], Vladimir G. Zubkov[1], Alexander P. Tyutyunnik[1], Ivan I. Leonidov[1], Ludmila L. Surat[1], Inna V. Baklanova[1], Lina A. Perelyaeva[1], Olga V. Koriakova[2], Joke Hadermann[3], Gustaaf Van Tendeloo[3]

1. *Russian Academy of Sciences, Ural Division, Institute of Solid State Chemistry (ISSC), Pervomaiyskay, 91, Ekaterinburg 620219, Russian Federation* **2.** *Institute of Organic Synthesis, Ural Branch of the Russian Academy of Sciences, 22 S. Kovalevskaya str., Ekaterinburg 620219, Russian Federation* **3.** *University of Antwerp, EMAT, Groenenborgerlaan 171, Antwerp B-2020, Belgium*

e-mail: tarakina@ihim.uran.ru

The new group of compounds with cyclic anions $Ln_2M^{2+}Ge_4O_{12}$ (Ln = Eu - Lu; M = Ca, Mn) which shows record Stokes shifts (3500 - 4200 cm^{-1}) upon laser pumping at λ = 976 nm has been synthesized and studied for the first time. All compounds convert the monochromatic line of the excitation laser to a shift band consisting of selected lines with a width of 5 - 8 cm^{-1}. The compounds $Ln_2M^{2+}Ge_4O_{12}$ (Ln = Eu - Lu; M = Ca, Mn) are isostructural, crystallizing in the space group *P*4/*nbm*. A peculiarity of their crystal structure is the

presence of cyclic anions $[Ge_4O_{12}]^{8-}$, consisting of four GeO_4 tetrahedra. The crystal structure of these compounds can be described as two alternating layers: one formed by Ln and (Ca,Mn) atoms and another by $[Ge_4O_{12}]^{8-}$ anions in boat-type conformation. Between these layers octahedral and square antiprismatic cavities are formed. The Ln and (Ca,Mn) atoms are positioned inside elongated oxygen octahedrons with ratio 0.5/0.5. The square antiprisms are occupied only by rare earth cations. The decreasing atomic radius of the rare earth elements leads to a change of the island structure motive to the 2D layered type. Analysis of the crystal structure and optical properties allows to conclude that the high values of the Stokes shifts are caused by inelastic interactions of excitation quanta and tetracyclic groups $[Ge_4O_{12}]$, which are harmonic oscillators. This type of vibration is almost absent in compounds with the 2D layout of tetracycles in the structure ($Yb_2CaGe_4O_{12}$, $Lu_2CaGe_4O_{12}$).

This work was supported by the RFBR (grant 07-03-00143), by Belgium Science Policy, by the Councils for Grants of the President of Russia for Support of Young Scientists (grant MK-84.2007.3) and for Support of Leading Scientific Schools (grant no. NSh - 1170.2008.3).

15:30 Poster 16-34

XRD controll of mechanical synthesis process of $(BiFeO_3)_{0.5}(BaTiO_3)_{0.5}$ multiferroic system

Wiktor Walerczyk[1], Adam Pietraszko[1], Bożena Hilczer[2], Izabella Szafraniak-Wiza[3]

1. *Institue of Low Temperature and Structure Research, Polish Academy of Sciences (INTIBS-PAN), P.Nr 1410, Wrocław 50-950, Poland* **2.** *Institute of Molecular Physics, Polish Academy of Sciences, Smoluchowskiego 17, Poznań 60-179, Poland* **3.** *Institute of Materials Science and Engineering, Poznań University of Technology, Poznań 60-965, Poland*

e-mail: w.walerczyk@int.pan.wroc.pl

The trend towards miniaturization of the devices resulted in a renaissance in the studies of materials exhibiting simultaneously ferroelectric and ferromagnetic properties. Among them $BiFeO_3$ remains still interestingas a single-phase multiferroic at room temperature (T_C=1100 K [1], T_N=420 K [2]). Bismuth ferrite is known to form solid solutions with ferroelectric perovskites [3, 4] in which one can expect an enhancement of the magneto-electric coupling due to the increase in the long-range electric order. The properties of $(BiFeO_3)_{1-x}(BaTiO_3)_x$ solution obtained by solid state reaction were studied by Kumar et al. [5] and Buscaglia et al. [6]. We used much simpler procedure to obtain of $(BiFeO_3)_{0.7}(BaTiO_3)_{0.3}$ solid solution: a direct synthesis from respective oxides at room temperature via mechanically triggered chemical reaction.

High purity Aldrich bismuth oxides in stoichiometric ratios $(Bi_2O_3 + Fe_2O_3)_{0.7}(BaO + TiO_2)_{0.3}$ were mechanically activated in SPEX 8000 Mixer Mill in the air atmosphere at room temperature during various milling time t_m. The batch contained 6 g of the oxides and the weight ratio of the stainless steel balls to the oxides was 2:1.

The mechanical synthesis of the powder after different times t_m was controlled by X-ray diffraction using a Stoe Diffraction System with Cu-$K_{\alpha 1}$ radiation. Linear position sensitive detector was used to measure the diffracted radiation in the 2θ angle from 3 to 103 degrees of arc and standard DHN-PDS reduction procedure was applied to analyze the powder diffraction pattern. The mean grain size of the powder was assessed with Scherrer method from the half-width of the (h1 k1 l1) and (h2 k2 l2) profiles with Williamson-Hall analysis. We assumed a monodispersive grain size distribution an the Lorentzian profile of the reflections.

The powder after 75 h of mechanical synthesis was found to be a single-phase $(BiFeO_3)_{0.7}(BaTiO_3)_{0.3}$ with rhombohedral symmetry and lattice parameters: a = 0.5608(5) nm, c = 1.3853(3) nm. The assessed mean grain size of the powder amounts to ~12 nm and the grains exhibit a core-shell type structure.

[1] J.R.Teague, R. Gerson, W.J. James, Solid State Commun. **8**, 1073 (1992)

[2] I. Sosnowska, M. Lowenhaupt, W.I.F. David, M.R. Ibberson, Physica B **180**, 117 (1992)

[3] R.T. Smith.G.D. Achenbach, R. Gerson, W.J. James, J. Appl. Phys. **39**, 70 (1968)

[4] T. Fuji, S. Jinzenji, Y. Y. Asahara, T. Shinjo, J. Appl. Phys. **64,** 5434(1988).

[5] M. Kumar, A. Srinivas, S.V. Suryanarayana, J. Appl. Phys. **87,** 855 (2000).

[6] MT. Buscaglia, L. Mitoseriu, V. Buscaglia, B. Pallecchi, M. Viviani, P. Nanni, A.S. Siri, J. Europ. Ceram. Soc. **26**, 3027 (2006).

15:30 Poster 16-35

Structural investigations on $(1-x)Pb(Mg_{1/3}Nb_{2/3})O_3$-$xPbTiO_3$ solid solution using the X-ray Rietveld method

Haixia Wang[1], Helmut Ehrenberg[2], Jean-christophe Jaud[1], Hartmut Fuess[1]

1. *Technische Universität Darmstadt, Institute of Materials Science, Petersenstr. 23, Darmstadt 64287, Germany* **2.** *Leibniz-Institute for Solid State and Materials Research, P.O.Box 270116, Dresden D-01171, Germany*

e-mail: saliencas@hotmail.com

Complex perovskite ferroelectrics $(1-x)Pb(Mg_{1/3}Nb_{2/3})O_3$-$xPbTiO_3$ (Abbr. PMN-PT) exhibit superior piezoelectric and electromechanical properties, which triggered an intensive interest of applications [1]. Therefore, great attention has been paid to microstructures related to special properties, of which the true symmetry is still under debate [2,3].

The transformation of spontaneous ferroelectric to relaxor (FE-R) state was evidenced as a (weak) first order phase transition in the PMN-rich side with unkown R(X) or C(X) phase [4,5] of the phase diagram associated with two branches. A detailed study at lower temperature than the transition temperature T_{FE-R} in the PMN-PT solid solutions was carried out using the X-ray Rietveld technique from the PMN end to PMN-PT (x=0.26), which is near the morphotropic phase boundary. A systematic structure analysis carried out for this series revealed the development of a polar state. Data analysis using Rietveld method combined with electron diffraction has been further performed for compositions falling in the region between the two temperatures which was dedicated to understand the structure changes within the phase diagram.

Keywords X-ray Rietveld method, electron diffraction, PMN-PT

References

[1] R.F.Service, Science 275, 1878, 1880 (1997).

[2] A.K. Singh, D. Pandey, O. Zaharko, Phys. Rev. B 74, 024101 (2006)

[3] B. Noheda, D.E. Cox, Phase Transit. 79, 5 (2006)

[4] G. Xu, D. Viehland, J. F. Li, P. M. Gehring, and G. Shirane, Phys. Rev. B 68, 212410 (2003).

[5] F. Bai, N. Wang, J. Li, D. Viehland, P.M. Gehring, G. Xu and G. Shirane, J. Appl. Phys. 96, 1620, (2004).

15:30 Poster 16-36

Effect of annealing on the structure and microstructure of Pr doped ZrO_2-Y_2O_3 nanocrystals

Ewa Werner-Malento[1], Wojciech Paszkowicz[1], Janusz D. Fidelus[2], Marek Godlewski[1,3], Sergiy A. Yatsunenko[1]

1. *Polish Academy of Sciences, Institute of Physics, al. Lotników 32/46, Warszawa 02-668, Poland* **2.** *Polish Academy of Sciences, Institute of High Pressure Physics (UNIPRESS), Sokolowska 29/37, Warszawa 01-142, Poland* **3.** *Cardinal Stefan Wyszynski University, College of Science, Warszawa, Poland*

e-mail: ewerner@ifpan.edu.pl

Yttria-stabilized zirconia (YSZ) is one of the most studied metal oxides [1–4]. It is a relatively hard and chemically inert material. YSZ is characterised by wear resistance, high-temperature stability and corrosion resistance, superionic conductivity at high temperature. The material is mostly used in jet engines, to determine oxygen content in exhaust gases, to measure pH in high-temperature water, as membranes for high temperature solid oxide fuel cell, as a component of waveguides and laser mirrors, and optical filters, as well as for electrolytes or insulators in microelectronic devices.

Several zirconia polymorphs are known (monoclinic, tetragonal, cubic and rhombohedral one). Among them, those of the highest symmetry are of most interest, due to their attractive properties. To prepare the desired cubic or tetragonal phase, thermal treatment and/or doping with yttrium or other dopants are typically used.

Nanocrystalline zirconium dioxide powder samples were characterized by X-ray diffraction using a Philips X'pert MRD diffractometer. The changes in ZrO_2 structure and microstructure due to annealing and yttrium doping were studied. Rietveld analysis, done by FullProf, based on the structure of the component phases [5] was used for quantitative phase analysis and structure refinement. In this work, the phase composition and structure of $Zr_{0.9214}Y_{0.0712}Pr_{0.0074}O_{1.9607}$ (sample A) and $Zr_{0.8962}Y_{0.0958}Pr_{0.0080}O_{1.9481}$ (sample B) prepared by treatment at two temperatures, 70 °C and 1200°C, was studied and compared with ZrO_2 structure.

The unannealed undoped sample contains the tetragonal (78%) and monoclinic (22%) phases. An addition of yttria results in disappearing of the minority monoclinic component. Moreover, the axial ratio of the tetragonal phase shows a clear decreasing tendency. The changes in the structure, phase composition and crystallite size caused by addition of yttria, Pr doping and annealing will be discussed.

References

[1] J. Ciosek, W. Paszkowicz, P. Pankowski, J. Firak, U. Stanislawek, Z. Patron, *Vacuum***72** (2004) 135–141

[2] A.C.T. van Duin, B.V. Merinov, S.S. Jang, W.A. Goddard III, *J. Phys. Chem. A***112** (2008) 3133–3140

[3] K. Muraoka, *Appl. Phys. Lett*. **80** (2002) 4516–4518

[4] C. Piconi, G. Maccauro, *Biomaterials***20** (1999) 1–25

[5] ICSD database (Karlsruhe 2008)

Figure 1. Experimental x-ray diffraction patterns of zirconia. The vertical bars show the peak positions for the tetragonal phase (upper) and monoclinic phase (lower).

15:30 Poster 16-37

Formation of nickel hydrides in reactive plasmas

Harm Wulff[1], Marion Quaas[1], Oxana Ivanova[2], Christiane A. Helm[2]

1. *Universität Greifswald, Felix-Hausdorffstr. 4, Greifswald 17487, Germany* **2.** *University of Greifswald, Felix-Hausdorff-Str. 6, Greifswald 17487, Germany*

e-mail: wulff@chemie.uni-greifswald.de

Nickel films of about 20 nm thickness and a mean domain size of 7 nm were treated in a microwave plasma (SLAN, 2.45 GHz). The nickel films were exposed to argon –hydrogen plasma using different negative substrate voltages to study the hydride formation.

The nickel hydride films were investigated by grazing incidence X-ray diffractometry (GIXD) to control the phase formation. Thickness and density were determined by X-ray reflectometry (XR); sample topology was studied by atomic force microscopy.

The effect of hydrogen plasma depends on the used negative substrate voltage. Without substrate voltage no chemical reaction occurs. Solely a partial sputtering and a recrystallization of the small Ni domains can be observed.

At negative substrate voltages (-25 V, -50 V, -75 V) a hexagonal Ni_2H phase is formed in a first quick reaction step. In a subsequent plasma chemical reaction this Ni_2H is transformed into cubic NiH. The reaction rate of the NiH formation increases with increasing negative substrate voltage.

The kinetic processes will be discussed using a modified isoconversional kinetic analysis.

15:30 Poster 16-38

Ru – Re, Ru – Os and Re – Os solid solutions – preparation under mild conditions, powder XRD investigation and phase diagrams analyzing

Kirill V. Yusenko, Il'ya V. Korolkov, Svetlana A. Martynova, Sergey A. Gromilov

Institute of Inorganic Chemistry of RAS, Novosibirsk 630090, Russian Federation

e-mail: yusenko@che.nsk.su

Control of the size, shape and phase composition of nanocrystalline materials is a key point in current nano-science research. Synthetic chemical methods have proved efficiency for the nanocrystals production with a tight size distribution and composition. Ru, Re and Os bulk and nanoscale solid solutions show high thermal, chemical and mechanical stability. Metals with hexagonal close packed (**hcp**) structures have extremely high melting points as well as Re and Os. Therefore their solid solutions are difficult to prepare. The main purpose of this work is preparation of the nanodimention solid solutions **Ru – Re**, **Ru – Os** and **Re – Os** and their characterization by powder X-ray diffraction and scanning electron microscope. Binary phase and Retgers diagrams were analyzed.

Ru – Re, Ru – Os and Re – Os bimetallic solid solutions were prepared by thermal decomposition under H_2 of bimetallic compounds: $[M^1(NH_3)_5Cl][M^2Cl_6]$ and $[M^1(NH_3)_5Cl]_2[M^2Cl_6]Cl_2$ (M^1 = Ru, Os; M^2 = Re, Os). Precursors were prepared as described previously for isoformular compounds[1].

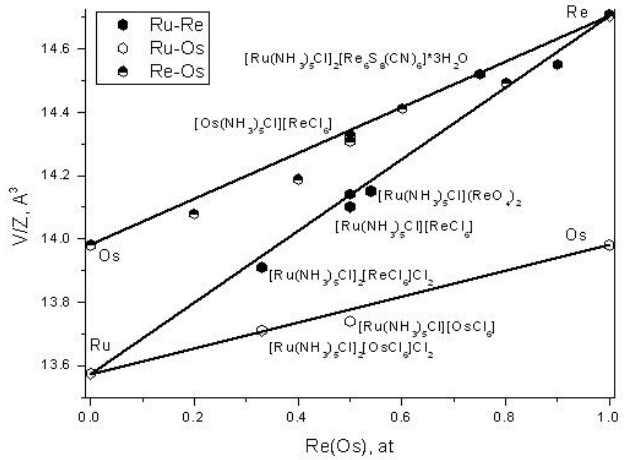

Preparation at 500 °C gives homogeneous **hcp** bimetallic solid solutions with crystallite dimensions nearly 100 Å. Additional annealing of the samples during 5 h at 800 °C does not essentially affect the unit cell parameters, but the crystallite size is doubled. The dependence of atomic volumes (**V/Z**) on the composition on the **Ru – Re**, **Ru – Os** and **Re – Os** bimetallic solid solutions is depicted here. Dependences are nearly-linear with negative deflection not more than 0.5 %. Equilibrium binary phase diagrams of given metallic systems were calculated by CALPHAD method based on an ideal solutions model. Obtained bimetallic powders are nearly equilibrium and prepared on 1/5 melting points for pure metals. It gives possibilities for the preparation of the nano-dimensional solid solutions of high melting metals for catalytic and material applications.

[1]S.A. Martynova, K.V. Yusenko, I.V. Korolkov, S.A. Gromilov (2007): *Russ. J. Coord. Chem*., 33, 530

Satellite events

Workshop WS1

Programme

Abstracts

in author alphabetical order

Oral

BRASS 2 – In der Werkzeugkiste (in the toolchest)

Johannes Birkenstock, Reinhard X. Fischer, Thomas Messner

University of Bremen, Geosciences, Klagenfurter Str. 2, Bremen 28359, Germany

e-mail: jbirken@uni-bremen.de

The "toolchest" of BRASS is directly accessible via the BRASS job explorer. Windows®-typical behaviour is routinely provided – such as drag&drop, context sensitive menus, exploring by tree structure – and in addition many tasks are directly accessed via buttons on the related pages. The following main branches represent the major tools of BRASS (branch brass database not yet active):

- raw data viewer: Display and overlay data of various file formats.
- rietveld job: Run rietveld job and use direct links to e.g. structure model display, calculation of distances and angles and fourier calculations.
- struplo job: Display crystal structure model with various options for versatile high quality drawings and perform various calculations with respect to the model (calculate distances and angles, calculate void volume after [1]).
- fourier job: Calculates and displays fourier maps and lists of maxima and minima, either from a formatted file or directly when called from the current rietveld job.
- grid search job: Displays grid search maps after calling a grid search run from the current rietveld job.

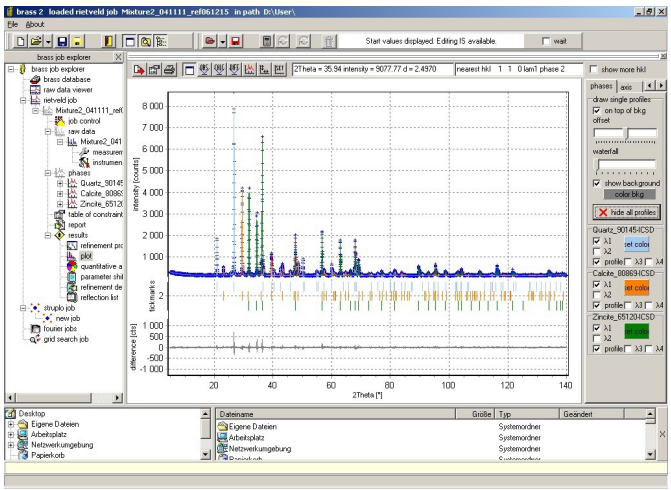

From the toolchest, among others, it will be demonstrated how to quantify a phase without having a structural model. The underlying procedure has been described earlier in [2] and [3].

[1] H. Küppers and F. Liebau (2004) On the determination of volumes and shapes of micropores in inorganic crystals. *Zeitschrift für Kristallographie.* Supplement Issue, **21**, 120.

[2] J. Birkenstock, R.X. Fischer, T. Messner (2005): *BRASS: Quantifying phases without structural model.* Abstracts of the 83rd DMG-meeting.

[3] J. Birkenstock (2005): *Absolute scaling of observed intensities for phase quantification using the Rietveld method.* Abstracts of the 83rd DMG meeting.

Workshop WS2

Programme

Thursday, 18 September

WS2
Thursday morning, 18 September, 9:00
Chair: Paolo Scardi, Scott Misture

9:00 Oral

Characterization and Measurement of Microstructures in Nanoscales and Structure-property Relations in Nanocrystalline Materials

Mo Li

Georgia Institute of Technology (GIT), 777 Atlantic Dr., Atlanta, GA 30332-0250, United States

e-mail: mo.li@mse.gatech.edu

Nanocrystalline materials have been around for well over two decades. Extensive research has been conducted with the major focus on some of the extraordinary property changes and a few structure parameters such as the grain size and grain boundaries. As a result, a systematic and complete study of how the microstructures in nanoscale affect the properties has been largely ignored. Despite the scale difference, nanocrystalline materials possess the same microstructures as those in polycrystalline materials. The microstructures have statistical properties that are characterized by the topological entities of the three dimensional grains cores, two-dimensional grain boundaries, and one-dimensional junctions, and zero-dimensional vertices. Those microstructure entities contribute collectively to the properties in nanocrystalline materials.

In this talk, I will present a systematic study of the microstructures in some model nanocrystalline materials with a particular emphasis on atomistic characterizations and measurement. A newly developed algorithm to generate realistic microstructures and the characterization tools to measure the grain cores, grain boundaries, junctions and vertices in nanoscale will be presented. The so-called digital microstructures will be examined, also with the simulated scattering from those structural entities. We show that the microstructures have intimate and complicated relations with the mechanical responses in the nanocrystalline materials. One of the conclusions we learned from this work is that we need to include as much as possible all microstructures to understand and manipulate the properties in nanocrystalline materials. Finally, the challenges and some initial efforts in connecting the digital microstructures with real experiment will be discussed.

9:45 Oral

Strain measurements at the nanoscale: microbeam Laue scattering and coherent diffraction.

Olivier Thomas

Aix-Marseille Université, Institut Matériaux Microélectronique Nanosciences de Provence, Marseille 13397, France CNRS, Faculté des Sciences et Techniques, Campus de St Jérome, Marseille 13397, France

e-mail: olivier.thomas@univ-cezanne.fr

Very high stresses arise in thin films and in nano-sized structures (lines, dots) because of the constraint of the substrate to which they are attached. The mechanical behavior of these small structures can deviate significantly from scaling laws developed for bulk materials. Moreover, the origins and magnitudes of these stresses are of great interest in technology as many fabrication and reliability problems are stress related.
X-ray diffraction is an ideal tool to measure non-destructively displacement fields at very local scales: thanks to x-ray synchrotron sources a 10 nm resolution may be achieved. Sub-micrometer x-ray beams are revolutionizing mechanics in small dimensions and it is now possible to perform micro-diffraction experiments while performing in situ mechanical testing. Another very promising approach relies on both real space and reciprocal space resolution. Coherent x-ray diffraction is highly sensitive to lattice distortions and may yield strain fields with a spatial resolution as small as 10 nm.

WS2
Thursday morning, 18 September, 11:00
Chair: Paolo Scardi, Scott Misture

11:00 Oral

Microdiffraction from individual buried dislocation cells and walls

Lyle E. Levine[1], Bennett C. Larson[2], Jon Tischler[2], Peter T. Geantil[3], Michael E. Kassler[3], Wenjun Liu[4]

1. *National Institute of Standards and Technology, Materials Science and Engineering Laboratory (NIST), Bureau Dr. 100, STOP 8553, Gaithersburg, Maryland 20899-8553, United States* **2.** *Oak Ridge National Laboratory (ORNL), One bethel Valley Road, Oak Ridge, TN 37932, United States* **3.** *University of Southern California, Los Angeles, CA 90089, United States* **4.** *Argonne National Laboratory (ANL), 9700 South Cass Avenue, Argonne, IL 60439, United States*

e-mail: Lyle.Levine@nist.gov

The existence and magnitude of long range elastic strains (and thus stresses) in dislocation cell interiors and walls in deformed metals have been the subject of extensive investigation for more than 20 years. Although numerous volume-averaged measurements have been used to infer their existence, direct measurements were not possible before the advent of high-resolution focused synchrotron X-rays. We have used depth-resolved submicrometer X-ray beams to directly measure diffraction line profiles from deeply buried indi-

vidual dislocation cell interiors and cell walls in plastically deformed copper single crystals. In the cell interiors, these spatially resolved measurements found large compressive elastic strains in the unloaded tension-deformed specimen and large tensile elastic strains in the unloaded compression-deformed specimens. The elastic strains in the cell walls were reversed with respect to those in the cell interiors. All of these results are qualitatively consistent with the Mughrabi composite model. The strains also exhibited large cell-to-cell variations that have important implications for theories of dislocation structure evolution, dislocation transport, changes in mechanical properties during reverse loading (Bauschinger effect and fatigue), and the extraction of dislocation structure parameters from X-ray line profiles.

11:45 Oral

Looking at the real structure of nanocrystals with powder diffraction: the apparent lattice parameter approach

Stanisław Gierlotka, Bogdan F. Palosz, Ewa Grzanka, Svetlana Stelmakh

Polish Academy of Sciences, Institute of High Pressure Physics (UNIPRESS), Sokolowska 29/37, Warszawa 01-142, Poland

e-mail: xray@unipress.waw.pl

It commonly agreed that the arrangement of atoms at the surface of a crystal is different from that of the bulk. Numerous simulation studies of extremely small crystallites have shown that in a few nanometers thick surface layer of a nanocrystal the interatomic distances are different from the "ordered bulk" values. As long as it's presence can be safely ignored for micrometer-sized crystallites such a layer constitutes a significant portion of a nanocrystal. The arrangement of atoms in a nanocrystal is not strictly periodic and therefore it must not described by a set of lattice parameter any more. Nevertheless diffraction patterns of the nanocrystalline samples show well developed diffraction peaks. Careful analysis of their positions shows that indeed, each diffraction peak of a nanometric material corresponds to a slightly different set of lattice parameters. This brings us to the concept of the *apparent lattice parameter (alp)*, the quantity that does not describe the crystal as a whole but is hkl-dependent. In the presentation we will show that analysis of those small deviations of peak positions form the "expected" values can bring valuable information about the true atomic structure of nanocrystals. We will show results of numerical simulations of diffraction patterns of the nanocrystals with altered surface layers and compare them to the experimental data. We will also discuss the experimental techniques that must be used, methods of data evaluation and cases where the obtained information may become useful.

.

WS2

Thursday afternoon, 18 September, 13:45

Chair: Paolo Scardi, Scott Misture

13:45 Oral

Nanomaterials and powder diffraction

Matteo Leoni

Department of Material Engineering and Industrial Tecnology, University of Trento (DIMTI), v. Mesiano 77, Trento 38100, Italy

e-mail: Matteo.Leoni@unitn.it

The different approaches available for the structural and microstructural analysis of nanostructured materials via powder diffraction can be broadly classified either as top-down or bottom-up. In the first case (e.g. Whole Powder Pattern Modelling ,WPPM) the parameters of a microstructure model are directly refined on diffraction data whereas in the second case (e.g. computer modelling followed by Debye approach), atomic positions in a model cluster should be modified until a match between model and diffraction experiment is obtained. Some features of the currently available methods and their possible limitations will be presented and discussed.

14:30 Oral

Nanomaterials as seen by Small Angle Scattering

Sigrid Bernstorff

Sincrotrone Trieste, Strada Statale 14, km 163.5, in AREA Science Park, Trieste 34012, Italy

e-mail: bernstorff@elettra.trieste.it

Nanostructured materials are usually not periodically long-range ordered, and are therefore not accessible by conventional methods used on crystalline materials. In fact, many materials of technological importance and their properties are characterized by varying degrees of disorder, and generate diffraction patterns with a pronounced diffuse component and few Bragg peaks. For completely disordered materials such as glasses and liquids a statistical description of the structure is often adopted. Many materials however lack perfect long range order, but have well defined structures on nanometer length-scales. Here the approach of the pair distribution function (PDF), which has its origins in the study of glasses and liquids, can be used to determine their structure from the total scattering including diffuse as well as Bragg scattering.

Small-Angle X-ray Scattering (SAXS) is a well-established and widely used nondestructive technique for the quantitative structural and morphological characterization of non-crystalline or partly ordered materials. The dimensions of the objects which can be investigated range approximately from 1 to some hundreds of nm. SAXS can be applied to a huge variety of systems, such as semiconductors, metal alloys, natural and synthetic polymers, colloids, micelles, micro-emulsions, porous media, liquid crystals, macromolecules in solution or in the solid state, and complex multiphase particulate systems, either isotropically dispersed, or spatially oriented.

Grazing-incidence small-angle X-ray scattering (GISAXS) measurements are sensitive to both the surface morphology and the internal structure of films, and provide information both about lateral and normal ordering at a surface or inside a thin film. Possible applications include thin polymer films, nanoparticles at interfaces or on surfaces, and semiconductor nanostructures. As a result, GISAXS

provides an excellent complement to more conventional nanoscale structural probes such as atomic force microscopy and transmission electron microscopy.

The full potential of these techniques is realized when using a modern third generation synchrotron source (high photon flux, strong beam collimation and choice of wavelength in order to avoid fluorescence or to perform anomalous measurements) and when patterns are recorded with low-noise, fast two-dimensional detectors. Microbeam applications as well as in-situ and real-time studies of e.g. nanoparticle formation and growth in the (sub)millisecond range are possible.

List of Participants

Suzan Abd El All
suzy_a_m@yahoo.com
- Polish Academy of Sciences, Institute of Physics
  Lotnikow 32/46, Warsaw 02-668, Poland
- Center of Research and Radiation Technology
  Nasr City, Cairo 0002, Egypt

Bogusława Adamczyk-Cieślak
badamczyk@inmat.pw.edu.pl
- Warsaw University of Technology, Faculty of Materials Science and Engineering (InMat)
  Wołoska 141, Warszawa 02-507, Poland

Grzegorz Adamski
gadamski@immb.com.pl
- Institute of Glass, Ceramics, Refractory and Construction Materials, Division of Mineral Building Materials (DMBM)
  Cementowa 1, Kraków 31-983, Poland

Ruud Adel den
ruud-den.adel@unilever.com
- Unilever (URDV)
  Olivier van Noortlaan 120, Vlaardingen 3130AC, Netherlands

Osman Adiguzel
oadiguzel@firat.edu.tr
- Firat University
  Department of Physics, Elazig 23169, Turkey

Magdalena Aflori
maflori@icmpp.ro
- Petru Poni Institute of Macromolecular Chemistry of the Romanian Academy
  Aleea Grigore Ghica Voda 41A, Iasi, Romania

Seyed Rouhollah Aghdaee
aghdaee@iust.ac.ir
- Iran university of science and technology (IUST)
  Malekloo Street,Narmak, Tehran 16844, Iran

Jimento G. Aikhuele
jimgreg2@yahoo.com
- University of Benin (JOHN)
  6th Oshifila St, Off Akinremi St, Anifowoshe, Ikeja, Lagos, Lagos 23401, Nigeria

Javier Alarcón
javier.alarcon@uv.es
- University of Valencia (UV)
  Doctor Moliner, Valčncia 46100, Spain

Dmitry V. Albov
albov@struct.chem.msu.ru
- Chemistry Department, Moscow State University
  Leninskie Gory, 1-3, Moscow 119992, Russian Federation

Xavier Alcobe
alcobe@sct.ub.es
- Serveis Cientificotècnics, University of Barcelona (SCT-UB)
  Lluis Sole i Sabaris, 1-3, Barcelona 08028, Spain

Edith Alig
e.alig@chemie.uni-frankfurt.de
- Institut für Anorganische und Analytische Chemie, Johann Wolfgang Goethe-Universität
  Max-von-Laue-Strasse 7, Frankfurt am Main 60438, Germany

Angela Altomare
angela.altomare@ic.cnr.it
- CNR-Istituto di Cristallografia (IC)
  via Amendola 122/O, Bari 70126, Italy

Paul Angerer
paul.angerer@echem.at
- ECHEM Kompetenzzentrum für angewandte Elektrochemie (ECHEM)
  Viktor-Kaplan-Strasse 2, Wiener Neustadt A-2700, Austria

Lorna Anguilano
lorna.anguilano@brunel.ac.uk
- Brunel University
  London, United Kingdom
- University College London (UCL)
  Gordon Street, London WC1HOAJ, United Kingdom

Gilberto Artioli
gilberto.artioli@unipd.it
- Dipartimento di Geoscienze, Università di Padova (UNIPD)
  Via Giotto 1, Padova 35137, Italy

Nathalie Audebrand
nathalie.audebrand@univ-rennes1.fr
- University of Rennes, Sciences Chimiques de Rennes
  Rennes 35042, France

Adekunle O. Ayantunji
dapofm@yahoo.ca
- Gold money nigeria Limited (GML)
59 Awolowo way Ikeja, Lagos 2340, Nigeria

Jan Balcarek
jan.balcarek@precheza.cz
- Precheza a.s.
Nábr. Dr. E. Beneše 24, Přerov 75162, Czech Republic

Levente Balogh
levente@metal.elte.hu
- Eötvös University
Pázmány Péter sétány 1/A, Budapest H-1117, Hungary

Davor Balzar
balzar@du.edu
- University of Denver
2112 E Wesley Ave, Denver 80208, United States

Josep M. Bassas
bassas@sct.ub.es
- Serveis Cientificotècnics, University of Barcelona (SCT-UB)
Lluis Sole i Sabaris, 1-3, Barcelona 08028, Spain

Joaquin Bastida
bastida@uv.es
- Valencia University, Department of Geology
Dr. Moliner, 50, Valencia 46100, Spain

Agnieszka Baszczuk
agnieszka.baszczuk@pwr.wroc.pl
- Wroclaw University of Technology, Institute of Materials Science and Applied Mechanics (PWr - IMMT)
Smoluchowskiego 25, Wrocław 50-370, Poland

Thierry Bataille
thierry.bataille@univ-rennes1.fr
- University of Rennes, Sciences Chimiques de Rennes
Rennes 35042, France

Patricia Bénard-Rocherullé
patricia.benard-rocherulle@univ-rennes1.fr
- University of Rennes, Sciences Chimiques de Rennes
Rennes 35042, France

Jean-Francois Berar
berar@esrf.fr
- CNRS, Institut Néel (NEEL)
25 rue des Martyrs, Grenoble 38042, France

Ciceron A. Berbecaru
berbecaru2ciceron@yahoo.com
- University of Bucharest, Faculty of Physics
Bucharest-Magurele p.o.box mg-11, Bucharest 76900, Romania

Joerg Bergmann
email@jbergmann.de
- Private
Ludwig-Renn-Allee 14, Dresden 01217, Germany

Sigrid Bernstorff
bernstorff@elettra.trieste.it
- Sincrotrone Trieste
Strada Statale 14, km 163.5, in AREA Science Park, Trieste 34012, Italy

Giovanni Berti
g.berti@ing.unipi.it
- University of Pisa, Earth Science Department and C I Material Engineering, Lab for RandD in XRD
Via S. Maria 53, Pisa 56126, Italy
- Consorzio Pisa Ricerche, Diffraction measurement and testing Centre (CPRDMTC)
Corso Italia, Pisa 56100, Italy
- XRD-Tools s.r.l.
Via Giuntini 25, Pisa 56023, Italy

Kenneth R. Beyerlein
beyerle@ing.unitn.it
- Georgia Institute of Technology (GIT)
777 Atlantic Dr., Atlanta, GA 30332-0250, United States
- Department of Material Engineering and Industrial Tecnology, University of Trento (DIMTI)
v. Mesiano 77, Trento 38100, Italy

Petr Bezdicka
petrb@iic.cas.cz
- Institute of Inorganic Chemistry of the ASCR, v.v.i.
c.p. 1001, Rez near Prague 25068, Czech Republic

Marianna Biadene
marianna.biadene@panalytical.com
- PANalytical
Lelyweg 1, Almelo 7600AA, Netherlands

Bożena B. Bierska-Piech
bbierska@us.edu.pl
- University of Silesia, Institute of Materials Science
12, Bankowa Str., Katowice 40-007, Poland

Johannes Birkenstock
jbirken@uni-bremen.de
- University of Bremen, Geosciences
Klagenfurter Str. 2, Bremen 28359, Germany

David L. Bish
bish@indiana.edu
- Indiana University
1001 E. 10th St., Bloomington 47405, United States

Brigitte K. Bitschnau
bitschnau@tugraz.at
- University of Technology, Inst. of Physical and Theoretical Chemistry (TUG)
Rechbauerstraße 12, Graz 8010, Austria

Tom Blanton
thomas.blanton@kodak.com
- Eastman Kodak Company
Research Laboratories B82, Rochester, NY 14650-2106, United States

Raúl E. Bolmaro
bolmaro@ifir.edu.ar
- Instituto de Física Rosario (IFIR)
Bv. 27 de febrero 210 bis, Rosario 2000, Argentina

Volodymyr Y. Bondar
vib@imp.kiev.ua
- G. V. Kurdyumov Institute for Metal Physics of the National Academy of Sciences (IMP)
Vernadsky Blvd. 36, Kiev UA03680, Ukraine

Giulio Borghini
giulio.borghini@unige.it
- Università di Milano, Dipartimento di Scienze della Terra
via Botticelli 23, Milano 20133, Italy

Natalija Borodajenko
ltmtk@inbox.lv
- Riga Biomaterials Innovation and Development Centre
Riga LV-1007, Latvia

Attila Bóta
abota@mail.bme.hu
- Hungarian Academy of Sciences, Chemical Research Centre (CRC/HAS)
Pusztaszeri ut 59-67, Budapest H-1025, Hungary

Hans H. Boysen
boysen@lmu.de
- LMU, Department of Earth and Environmental Sciences, Crystallography
Theresienstr. 41, München 81539, Germany

Łukasz Bratasz
ncbratas@cyf-kr.edu.pl
- Institute of Catalysis and Surface Chemistry, Polish Academy of Sciences (ICSC)
Niezapominajek 8, Kraków 30239, Poland

Lutz Bruegemann
lutz.bruegemann@bruker-axs.de
- Bruker-AXS (BAXS)
Östliche Rheinbrückenstr. 49, Karlsruhe D-76187, Germany

Juergen Bruening
bruening@chemie.uni-frankfurt.de
- Institut für Anorganische und Analytische Chemie, Johann Wolfgang Goethe-Universität
Max-von-Laue-Strasse 7, Frankfurt am Main 60438, Germany

Michela Brunelli
brunelli@esrf.fr
- Europen Synchrotron Radiation Facility (ESRF)
6, Jules Horowitz, Grenoble 38000, France

Christian Buchsbaum
buchsbaum@chemie.uni-frankfurt.de
- Institut für Anorganische und Analytische Chemie, Johann Wolfgang Goethe-Universität
Max-von-Laue-Strasse 7, Frankfurt am Main 60438, Germany

Alexandra Buchsteiner
buchsteiner@hmi.de
- Helmholtz Centre Berlin for Materials and Energy
Glienicker Str. 100, Berlin D-14109, Germany

Olga A. Bulavchenko
isizy@catalysis.ru
- Boreskov Institute of Catalysis (BIC)
pr. akad. Lavrentieva, 5, Novosibirsk 630090, Russian Federation

Maria Cristina Burla
mariacristina.burla@unipg.it
- Università di Perugia, Dip. di Scienze dellla Terra
Perugia 06100, Italy

Victoria A. Burnell
vxb216@bham.ac.uk
- School of Chemistry, University of Birmingham
Edgbaston, Birmingham B152TT, United Kingdom

Aurelio Cabeza
aurelio@uma.es
- Universidad de Malaga (UMA)
Campus Teatinos, Malaga E29071, Spain

Eugenio Casini
eugenio.casini@panalytical.com
- PANalytical
Lissone 20035, Italy

Martin Cernik
mcernik@sk.uss.com
- U.S.Steel Kosice
Vstupny Areal U.S. Steel, Kosice 04454, Slovakia (Slovak Rep.)

Radovan Cerny
Radovan.Cerny@cryst.unige.ch
- University of Geneva
24 quai Ernest-Ansermet, Geneva 1211, Switzerland

Antonio Cervellino
antonio.cervellino@psi.ch
- Swiss Light Source, Paul Scherrer Institute
Villigen PSI 5232, Switzerland

Tabti Charef
tabti_sea2m@yahoo.fr
- University of mostaganem (SEAMM)
University of mostaganem, Mostaganem 27000, Algeria

Dagmara K. Chmielewska
dagach@ichtj.waw.pl
- Institute of Nuclear Chemistry and Technology (IChTJ)
Dorodna 16, Warszawa 03-195, Poland

Anna Crespi Revuelta
acrespi@icmab.es
- Institut de Ciencia de Materials (ICMAB) - CSIC (ICMAB)
Campus de la UAB, Barcelona 080193, Spain

Cyrus Crowder
crowder@icdd.com
- International Centre for Diffraction Data (ICDD)
12 Campus Boulevard, Newtown Square 19073, United States

Maria C. Dalconi
mariachiara.dalconi@unipd.it
- Dipartimento di Geoscienze, Università di Padova (UNIPD)
Via Giotto 1, Padova 35137, Italy

Vitaliy E. Danilchenko
danila@imp.kiev.ua
- G.V. Kurdyumov Institute for Metal Physics National Academy of Sciences (IMP)
Vernadsky Blvd. 36, Kyiv UA03680, Ukraine

Stanislav Danis
danis@mag.mff.cuni.cz
- Charles University, Faculty of Mathematics and Physics, Department of Condensed Matter Physics
Ke Karlovu 5, Prague 12116, Czech Republic

Jolanta Darul
jola@amu.edu.pl
- Adam Mickiewicz University, Faculty of Chemistry
Grunwaldzka 6, Poznań 60-780, Poland

Magdalena Dębicka
magdalena.debicka@up.wroc.pl
- Uniwersytet Przyrodniczy we Wrocławiu, Instytut Nauk o Glebie i Ochrony Środowiska
ul. Grunwaldzka 53, Wrocław 53-357, Poland

Angeles G. De la Torre
mgd@uma.es
- Universidad de Malaga (UMA)
Campus Teatinos, Malaga E29071, Spain

Rob Delhez
r.delhez@tudelft.nl
- Delft University of Technology, Department of Materials Science and Engineering
Mekelweg 2, Delft 2628CD, Netherlands

Ruslan M. Delidon
delrus@bigmir.net
- G. V. Kurdyumov Institute for Metal Physics of the National Academy of Sciences (IMP)
Vernadsky Blvd. 36, Kiev UA03680, Ukraine

Katarina Demsar
katarina.demsar@fkkt.uni-lj.si
- Faculty of Chemistry and Chemical Technology
Askerceva 5, Ljubljana 1000, Slovenia

Ingwer A. Denks
denks@hmi.de
- Hahn-Meitner-Institute (HMI)
Glienicker Str. 100, Berlin D-14109, Germany

Grzegorz Dercz
gdercz@op.pl
- University of Silesia, Institute of Material Science
Bankowa 12, Katowice 40-007, Poland

Ryszard Diduszko
rydidu@op.pl
- Institute of Electronic Materials Technology (ITME)
Wólczyńska 133, Warszawa 01-919, Poland

Robert E. Dinnebier
r.dinnebier@fkf.mpg.de
- Max-Planck-Institut FKF
Heisenbergstr. 1, Stuttgart D70569, Germany

Igor Djerdj
igor.djerdj@mat.ethz.ch
- ETH Zürich (ETHZ)
Wolfgang-Pauli-Strasse 10, Zürich 8093, Switzerland

Wojtek Dmowski
wdmowski@utk.edu
- University of Tennessee (UTK)
Knoxville, TN, United States

Anna Dobrowolska
anilid@poczta.onet.pl
- University of Wrocław, Faculty of Chemistry
Joliot-Curie 14, Wrocław 50-383, Poland

Jennifer A. Doebbler
doebbler@aps.anl.gov
- Argonne National Laboratory (ANL)
9700 South Cass Avenue, Argonne, IL 60439, United States

Eric Dooryhée
eric.dooryhee@grenoble.cnrs.fr
- CNRS, Institut Néel (NEEL)
25 rue des Martyrs, Grenoble 38042, France

Stephen Doyle
doyle@iss.fzk.de
- Forschungszentrum Karlsruhe GmbH, Institut für Synchrotronstrahlung, ANKA (ANKA)
Hermann-von-Helmholtz-Platz 1, Karlsruhe 76344, Germany

Martin Dráb
martin.drab@fjfi.cvut.cz
- Czech Technical University in Prague, The Faculty of Nuclear Sciences and Physical Engineering
Trojanova 13, Prague 2, Prague 12000, Czech Republic

Peter S. Dubinin
Dubinin-2005@yandex.ru
- Siberian Federal University (SFU)
Krasnoyarskii rabochii 95, Krasnoyarsk 660095, Russian Federation

Agata K. Dudek
dudek@mim.pcz.czest.pl
- Częstochowa University of Technology, Institute of Materials Ingineering
Armii Krajowej 19, Częstochowa 42-200, Poland

George Duncan-Jones
g.duncan-jones1@physics.ox.ac.uk
- Oxford University
South Parks Road, Oxford OX1 3QZ, United Kingdom

Yevgeniy M. Dzevin
dzevin@i.ua
- G. V. Kurdyumov Institute for Metal Physics of the National Academy of Sciences (IMP)
Vernadsky Blvd. 36, Kiev UA03680, Ukraine

Kristina Edström
kristina.edstrom@mkem.uu.se
- Uppsala University, Department of Materials Chemistry, Angstrom Laboratory
Uppsala, Sweden

Rachel Eloirdi
eloirdi12@aol.com
- Instute for transuranium elements (ITU)
Postfach 2340, Karlsruhe D-76125, Germany

Ahmad Erfan
ahmad_erfan@hotmail.com
- Sabbah
Safat 1235, Kuwait

Ayhan Erol
aerol@aku.edu.tr
- Afyon Kocatepe Universitesi
  Afyonkarahisar 03200, Turkey

Rachid Essehli
rachid.essehli@uha.fr
- Physics and Chemistry Department of Materials Mulhouse, ICSI (CNRS)
  15, rue Jean Starcky, BP 2488, Mulhouse Cedex 68057, France
- Technische Universität Darmstadt, Institute of Materials Science
  Petersenstr. 23, Darmstadt 64287, Germany

John S. Evans
john.evans@durham.ac.uk
- Department of Chemistry, University of Durham
  Science Labs, South Road, Durham DH1-3LE, United Kingdom

Abdessamad Faik
abdessamad.faik@ehu.es
- Facultad de Ciencia y Tecnología (UPV/EHU)
  P.Box 644, Bilbao 48080, Spain

Christopher L. Farrow
farrowch@msu.edu
- Columbia University
  New York, NY 10027, United States

Tim Fawcett
miller@icdd.com
- International Centre for Diffraction Data (ICDD)
  12 Campus Boulevard, Newtown Square 19073, United States

Yishay Feldman
isai.feldman@weizmann.ac.il
- Weizmann Institute of Science
  Rehovot 76100, Israel

Evgeny Y. Filatov
decan@che.nsk.su
- Institute of Inorganic Chemistry of RAS
  Novosibirsk 630090, Russian Federation

Lothar Fink
fink@chemie.uni-frankfurt.de
- Frankfurt University, Institute of Inorganic and Analytical Chemistry
  Max-von-Laue-Str. 7, Frankfurt am Main 60438, Germany

Andy Fitch
fitch@esrf.fr
- European Synchrotron Radiation Facility (ESRF)
  Grenoble 38043, France

Alastair J. Florence
alastair.florence@strath.ac.uk
- University of Strathclyde, Strathclyde Institute for Pharmacy and Biomedical Sciences
  27 Taylor Street, Glasgow G40NR, United Kingdom

Ulrich Förter-Barth
foe@ict.fhg.de
- Fraunhofer ICT
  Joseph-von-Fraunhofer 7, Pfinztal 76327, Germany

David G. Free
d.g.free@dur.ac.uk
- Department of Chemistry, University of Durham
  Science Labs, South Road, Durham DH1-3LE, United Kingdom

Karen Friese
karen.friese@ehu.es
- Dpto. Física Materia Condensada, Universidad del País Vasco (UPV/EHU)
  Facultad de Ciencia y Tecnología, Apdo. 644, Bilbao 48080, Spain

Hartmut Fuess
hfuess@tu-darmstadt.de
- Technische Universität Darmstadt, Institute of Materials Science
  Petersenstr. 23, Darmstadt 64287, Germany

Elżbieta Gadalińska
elzbieta.gadalinska@ilot.edu.pl
- Instytut Lotnictwa (ILOT)
  Al. Krakowska 110/114, Warsaw 02-256, Poland

Anna B. Gągor
a.gagor@int.pan.wroc.pl
- Institue of Low Temperature and Structure Research, Polish Academy of Sciences (INTIBS-PAN)
  P.Nr 1410, Wrocław 50-950, Poland

FengJu Gao
fengju.gao-inv@univ-cezanne.fr
- Aix-Marseille Université, Institut Matériaux Microélectronique Nanosciences de Provence
  Marseille 13397, France
- CNRS, Faculté des Sciences et Techniques, Campus de St Jérome
  Marseille 13397, France
- Department of Materials Science and Engineering, Beijing Normal University
  Avenue Xinjiekouwai 19, Beijing 100875, China
- Department of Solid State Physics, L. Kossuth University
  Debrecen H-4010, Hungary

Milen Gateshki
Milen.Gateshki@panalytical.com
- PANalytical
  Lelyweg 1, Almelo 7600AA, Netherlands

Bartłomiej A. Gaweł
gawel@chemia.uj.edu.pl
- Jagiellonian University, Faculty of Chemistry
  Ingardena 3, Kraków 30-060, Poland

Juan A. G Carrió
jgcarrio@mackenzie.br
- Presbyterian University Mackenzie (UPM)
  Rua da Consolação 930, Sao Paulo 01302-907, Brazil

Mauro Gemmi
mauro.gemmi@unimi.it
- Università di Milano, Dipartimento di Scienze della Terra
  via Botticelli 23, Milano 20133, Italy

Danila Ghisletti
danila.ghisletti@eni.it
- Eni S.p.A.
  Via Maritano 26, San Donato Milanese 20097, Italy

Carmelo Giacovazzo
carmelo.giacovazzo@ic.cnr.it
- CNR-Istituto di Cristallografia (IC)
  via Amendola 122/O, Bari 70126, Italy

Stanisław Gierlotka
xray@unipress.waw.pl
- Polish Academy of Sciences, Institute of High Pressure Physics (UNIPRESS)
  Sokolowska 29/37, Warszawa 01-142, Poland

Chris J. Gilmore
chris@chem.gla.ac.uk
- University of Glasgow
  University Gardens, Glasgow G12-8QW, United Kingdom

Andrew L. Goodwin
alg44@cam.ac.uk
- University of Cambridge, Department of Earth Sciences
  Downing Street, Cambridge, Cambridge CB23EQ, United Kingdom

Ludwik Górski
l.gorski@cyf.gov.pl
- Institute of Atomic Energy
  Otwock-Świerk 05-400, Poland

Tomasz Goryczka
goryczka@us.edu.pl
- University of Silesia, Institute of Materials Science
  12, Bankowa Str., Katowice 40-007, Poland

Jürgen Göske
juergen.goeske@gmx.de
- ZWL GmbH
  Lauf a d Pegnitz 91207, Germany

Fabia Gozzo
fabia.gozzo@psi.ch
- Swiss Light Source, Paul Scherrer Institute
  Villigen PSI 5232, Switzerland

Thomas Gressmann
t.gressmann@mf.mpg.de
- Max Planck Institute for Metals Research (MPI-MF)
  Heisenbergstrasse 3, Stuttgart 70569, Germany

Anja Griessmeier
anja.griessmeier@bruker-axs.de
- Bruker-AXS (BAXS)
  Östliche Rheinbrückenstr. 49, Karlsruhe D-76187, Germany

Ewa Grzanka
elesk@unipress.waw.pl
- Polish Academy of Sciences, Institute of High Pressure Physics (UNIPRESS)
  Sokolowska 29/37, Warszawa 01-142, Poland

Andrzej Grzechnik
andrzej.grzechnik@ehu.es
- Dpto. Física Materia Condensada, Universidad del País Vasco (UPV/EHU)
  Facultad de Ciencia y Tecnología, Apdo. 644, Bilbao 48080, Spain

Maciej P. Grzywa
grzywa@chemia.uj.edu.pl
- Institute of Catalysis and Surface Chemistry, Polish Academy of Sciences (ICSC)
  Niezapominajek 8, Kraków 30239, Poland

Alessandro F. Gualtieri
alessandro.gualtieri@unimore.it
- Universita di Modena and Reggio Emilia
  Modena, Italy

Nathalie Guillou
nathalie.guillou@uvsq.fr
- Lavoisier Institute, CNRS, University of Versailles (ILV)
  45 av. des Etats-Unis, Versailles 78035, France

Torbjörn Gustafsson
torbjorn.gustafsson@mkem.uu.se
- Uppsala University, Department of Materials Chemistry, Angstrom Laboratory
  Uppsala, Sweden

Abdesslem B. Haj Amara
abdesslem.bamara@fsb.rnu.tn
- Laboratoire de Physique des Matériaux Lamellaires et Nano Matériaux Hybrides (LPMNMH)
  Faculty of science of Bizerte, Bizerte 7021, Tunisia

Zoran Ham
zoran.ham@sandoz.com
- Lek Pharmaceuticals d.d.
  Ljubljana SI-1526, Slovenia

Thomas C. Hansen
hansen@ill.fr
- Institut Laue Langevin (ILL)
  Avenue des martyrs, Grenoble 38042, France

Graeme M. Hansford
gmh14@star.le.ac.uk
- University of Leicester
  University Road, Leicester LE17RH, United Kingdom

Kenneth Harris
HarrisKDM@cardiff.ac.uk
- Cardiff University
  School of Chemistry, Park Place, Cardiff CF103AT, United Kingdom

Thomas Hartmann
hartmann@stoe.com
- Stoe and Cie GmbH
  Hilpertstr. 10, Darmstadt, Darmstadt 64295, Germany

Bernd Hasse
hasse@incoatec.de
- Incoatec GmbH
  Max-Planck-Str. 2, Geesthacht 21502, Germany

David Havlicek
havlicek@natur.cuni.cz
- Charles University, Faculty of Science
  Albertov 6, Prague 12843, Czech Republic

Mikko Heikkilä
mikko.j.heikkila@helsinki.fi
- Department of Chemistry, University of Helsinki
  A. I. Virtasen aukio 1, Helsinki FIN-00014, Finland

Jerry Heng
jerry.heng@imperial.ac.uk
- Imperial College London
  South Kensington, London SW72AZ, United Kingdom

Paul F. Henry
henry@ill.fr
- Institut Laue Langevin (ILL)
  6 Rue Jules Horowitz, Grenoble, France

Akihiro Himeda
himeda@rigaku.co.jp
- Rigaku Co.
  Tokyo 196-8666, Japan

Bernd Hinrichsen
bernd.hinrichsen@bureker-axs.de
- Bruker-AXS (BAXS)
  Östliche Rheinbrückenstr. 49, Karlsruhe D-76187, Germany

Markus Hoelzel
markus.hoelzel@frm2.tum.de
- Technische Universität Darmstadt, Institute of Materials Science
  Petersenstr. 23, Darmstadt 64287, Germany
- Technischen Universität München, Forschungsneutronenquelle FRM-II (FRM2)
  Garching 85747, Germany

Joseph A. Hriljac
j.a.hriljac@bham.ac.uk
- School of Chemistry, University of Birmingham
  Edgbaston, Birmingham B152TT, United Kingdom

Viktor E. Iakovlev
zvik83@mail.ru
- G.V. Kurdyumov Institute for Metal Physics National Academy of Sciences (IMP)
  Vernadsky Blvd. 36, Kyiv UA03680, Ukraine

Margarita Isaenkova
isamarg@mail.ru
- Moscow Engineering Physics Institute (MEPhI)
  Kashirskoe shosse, Moscow 115409, Russian Federation

Toru Ishigaki
toru.ishigaki@j-parc.jp
- Ibaraki University, Frontier Research Center for Applied Nuclear Sciences
  4-12-1 Nakanarisawa, Hitachi 316-8511, Japan

Sonya Ivanova
sonya@svr.igic.bas.bg
- Institute of General and Inorganic Chemistry, Bulgarian Academy of Sciences (IGIC)
  Acad. G. Bonchev Str. bldg. 11, Sofia 1113, Bulgaria

Svetlana N. Ivashevskaya
ivashevskaja@yahoo.com
- Institut für Anorganische und Analytische Chemie, Johann Wolfgang Goethe-Universität
  Max-von-Laue-Strasse 7, Frankfurt am Main 60438, Germany
- Institute of Geology Karelian Research Centre Russian Academy of Sciences
  Pushkinskaya, 11, Petrozavodsk 185910, Russian Federation

Daniel Jansen
djan@geol.uni-erlangen.de
- University Erlangen
  Erlangen 91054, Germany

Anna Jasińska
anna@maius.in.uj.edu.pl
- Jagiellonian University (UJ)
  Kraków, Poland

Jean-christophe Jaud
jcjaud@tu-darmstadt.de
- Technische Universität Darmstadt, Institute of Materials Science
  Petersenstr. 23, Darmstadt 64287, Germany

Roman Jędrzejewski
roman.jedrzejewski@ps.pl
- Szczecin University of Technology (SZUT)
  Pułaskiego 10, Szczecin 70-322, Poland

Dieter Jehnichen
djeh@ipfdd.de
- Leibniz Institute of Polymer Research Dresden
  Dresden 01069, Germany

Rune E. Johnsen
r.e.johnsen@kjemi.uio.no
- University of Oslo, Department of Chemistry
  Oslo N-0315, Norway

Natasa Jovic
natasaj@vin.bg.ac.yu
- VINCA Institute
  POB 522, Belgrade 11001, Serbia

Pavol Juhas
pj2192@columbia.edu
- Columbia University
  New York, NY 10027, United States

James A. Kaduk
James.Kaduk@innovene.com
- INEOS Technologies
  150 W. Warrenville Rd., 600-1008, Naperville IL 60563, United States

Senthil Kumar Kaliappan
senthil.kaliappan@borealisgroup.com
- Borealis Polyolefine GmbH (BOREALIS)
  St.-Peter-Strasse 25, Linz 4021, Austria

Ladislav Kalvoda
ladislav.kalvoda@fjfi.cvut.cz
- Czech Technical University in Prague, The Faculty of Nuclear Sciences and Physical Engineering
  Trojanova 13, Prague 2, Prague 12000, Czech Republic

Tatyana U. Kardash
tanik.kardash@gmail.com
- Boreskov Institute of Catalysis (BIC)
  pr. akad. Lavrentieva, 5, Novosibirsk 630090, Russian Federation

Anna Kario
a.kario@ifw-dresden.de
- Institut fuer Metallische Werkstoffe, IFW
  Dresden, Germany

Małgorzata Karolus
karolus@us.edu.pl
- University of Silesia, Institute of Material Science
  Bankowa 12, Katowice 40-007, Poland

Marta Kasunič
marta.kasunic@fkkt.uni-lj.si
- Faculty of Chemistry and Chemical Technology
  Askerceva 5, Ljubljana 1000, Slovenia

Zbigniew A. Kaszkur
zbig@ichf.edu.pl
- Polish Academy of Sciences, Institute of Physical Chemistry
  Kasprzaka 52/56, Warszawa 01-224, Poland

Irina Kaurova
kaurchik@yandex.ru
- Moscow State Academy of Fine Chemical Tecnology by M. V. Lomonosov
  Vernadskogo pr., 86, Moscow 119571, Russian Federation

David A. Keen
d.a.keen@rl.ac.uk
- Rutherford Appleton Laboratory (RAL)
  Chilton, Didcot, Oxon OX11 0QX, United Kingdom

Lukas Keller
lukas.keller@psi.ch
- Paul Scherrer Institut (PSI)
  Villigen PSI 5232, Switzerland

Arnt A. Kern
arnt.kern@bruker-axs.de
- Bruker-AXS (BAXS)
  Östliche Rheinbrückenstr. 49, Karlsruhe D-76187, Germany

Kyungrae Kim
kr0314@ssu.ac.kr
- Soongsil University, Depr. of Chemistry
  511, Sangdo-dong, Dongjak-ku, Seoul 156-743, Korea, South

Giora Kimmel
kimmel@bgu.ac.il
- Institutes for Applied Research, Ben Gurion University of the Negev
  Beer-Sheva 84105, Israel
- Universitat Rovira i Virgili (URV)
  Av. Països Catalans, 26, Tarragona 43007, Spain

Caroline A. Kirk
c.a.kirk@lboro.ac.uk
- Loughborough University, Department of Chemistry
  Epinal Way, Loughborough LE11 3TU, United Kingdom

Reinhard Kleeberg
kleeberg@mineral.tu-freiberg.de
- Freiberg University of Mining and Technology, Mineralogical Institute
  Brennhausgasse 14, Freiberg 09596, Germany

Marcin Klepka
mklepka@ifpan.edu.pl
- Polish Academy of Sciences, Institute of Physics
  al. Lotników 32/46, Warszawa 02-668, Poland

Andreas Klimera
klimera@isc.fhg.de
- Fraunhofer ISC (ISC)
  Neunerplatz 2, Würzburg 97082, Germany

Michael Knapp
mknapp@cells.es
- CELLS (ALBA)
  Campus UAB, Barcelona 08193, Spain

Thomas Koehler
thomas.koehler@de.bosch.com
- Robert Bosch GmbH
  Postbox 106050, Department CR/ARA, Stuttgart 70049, Germany

Marek A. Kojdecki
m_kojdecki@poczta.onet.pl
- Military University of Technology, Institute of Mathematics and Cryptology (WAT)
  gen S. Kaliskiego 2, Warszawa 00-908, Poland

Takayuki Konya
konya@rigaku.co.jp
- Rigaku Co.
  Tokyo 196-8666, Japan

Huub Kooijman
huub.kooijman@shell.com
- Shell Global Solutions International B.V. (SHELL)
  Badhuisweg 3, Amsterdam 1031CM, Netherlands

Petra Kotnik
petra.kotnik@anton-paar.com
- Anton Paar GmbH
  Anton-Paar-Str. 20, Graz A-8054, Austria

Roman Kozłowski
nckozlows@cyf-kr.edu.pl
- Institute of Catalysis and Surface Chemistry, Polish Academy of Sciences (ICSC)
  Niezapominajek 8, Kraków 30239, Poland

Faton S. Krasniqi
faton.krasniqi@psi.ch
- Swiss Light Source, Paul Scherrer Institute
  Villigen PSI 5232, Switzerland
- Max Planck Institut for Medical Research
  Heidelberg 69120, Germany

Miroslav Krupka
m.krupka@pcs.cz
- PCS s.r.o. (PCS)
  Na Dvorcich 18, Prague 14000, Czech Republic

Tetyana G. Kryshtab
tkrysh@esfm.ipn.mx
- Instituto Politécnico Nacional, Depto. de Ciencia de Materiales, (ESFM)
  Unidad Prof. ALM, Edif. 9, Zacatenco, Zacatenco, México 07338, Mexico

Justyna Krzak-Roś
Justyna.Krzak-Ros@pwr.wroc.pl
- Wroclaw University of Technology, Institute of Materials Science and Applied Mechanics (PWr - IMMT)
  Smoluchowskiego 25, Wrocław 50-370, Poland

Hanna J. Krztoń
hkrzton@imz.pl
- Institute for Ferrous Metallurgy (IMZ)
  Karola Miarki, Gliwice 44-100, Poland

Barbara Kucharska
bratek@mim.pcz.czest.pl
- Częstochowa University of Technology
  Armii Krajowej St., Częstochowa 42-200, Poland

Sumeet Kumar
sumeet.kumar.iitk@gmail.com
- Università degli Studi del Piemonte Orientale (DISTA)
  Via V. Bellini 25/G., Alessandria 15100, Italy

Birgit Kunert
birgit.kunert@tugraz.at
- Institut für Festkörperphysik, TUGraz
  Petersgasse 16, 1. Stock, Graz 8010, Austria

Alexander I. Kurbakov
kurbakov@pnpi.spb.ru
- St.Petersburg Nuclear Physics Institute RAS (PNPI)
  Orlova Roshcha, Gatchina 188300, Russian Federation

Dominik Kurzydłowski
d.kurzydlowski@student.uw.edu.pl
- Uniwersytet Warszawski, Wydział Chemii
  Warszawa, Poland

Radomír Kužel
kuzel@karlov.mff.cuni.cz
- Charles University, Faculty of Mathematics and Physics
  Ke Karlovu 3, Prague 12116, Czech Republic

Bruno Lanson
bruno.lanson@obs.ujf-grenoble.fr
- LGIT, CNRS-UJF
  Grenoble BP53, France

Wieslaw Lasocha
lasocha@chemia.uj.edu.pl
- Jagiellonian University, Faculty of Chemistry
  Ingardena 3, Kraków 30-060, Poland
- Polish Academy of Sciences, Institute of Catalysis and Surface Chemistry
  Niezapominajek 8, Kraków 30-239, Poland

Mika Lastusaari
miklas@utu.fi
- University of Turku, Department of Chemistry
  Turku FI-20014, Finland

Marta Łaszcz
m.laszcz@ifarm.waw.pl
- Pharmaceutical Research Institute, Research and Development Analytical Chem. Dept.
  Rydygiera 8, Warsaw 01-793, Poland

František Laufek
frantisek.laufek@geology.cz
- Czech Geological Survey
  Prague 15200, Czech Republic

Marc J. Ledoux
ledoux@ecpm.u-strasbg.fr
- European Laboratory for Catalysis and Surface Sciences, ELCASS (CNRS-ULP)
  25 rue Becquerel, Strasbourg 67087, France

Andreas Leineweber
a.leineweber@mf.mpg.de
- Max Planck Institute for Metals Research
  Heisenbergstrasse 3, Stuttgart 70569, Germany

Agnieszka Leonarska
aleonars@us.edu.pl
- University of Silesia, August Chełkowski Institute of Physics, Department of Solid State Physics
  Uniwersytecka 4, Katowice 40-007, Poland

Matteo Leoni
Matteo.Leoni@unitn.it
- Department of Material Engineering and Industrial Tecnology, University of Trento (DIMTI)
  v. Mesiano 77, Trento 38100, Italy

Igor N. Leontyev
i.leontiev@rambler.ru
- Southern Federal University (SFU)
  Zorge 5, Rostov-on-Don 344090, Russian Federation

Lyle E. Levine
Lyle.Levine@nist.gov
- National Institute of Standards and Technology, Materials Science and Engineering Laboratory (NIST)
  Bureau Dr. 100, STOP 8553, Gaithersburg, Maryland 20899-8553, United States

Mo Li
mo.li@mse.gatech.edu
- Georgia Institute of Technology (GIT)
  777 Atlantic Dr., Atlanta, GA 30332-0250, United States

Sarah E. Lister
Sarah.Lister@dur.ac.uk
- Department of Chemistry, University of Durham
  Science Labs, South Road, Durham DH1-3LE, United Kingdom

Carine Livage
carine.livage@uvsq.fr
- Lavoisier Institute, CNRS, University of Versailles (ILV)
  45 av. des Etats-Unis, Versailles 78035, France

Gerhard Cox BASF SE Ludwigshafen
gerhard.cox@basf.com
- BASF SE
  Carl Bosch Straße, Ludwigshafen 67056, Germany

Ilze Luse
ilze.luse@llu.lv
- University of Latvia
  Raina Bulvaris 19, Riga LV1009, Latvia

Luca Lutterotti
luca.lutterotti@ing.unitn.it
- Department of Material Engineering and Industrial Tecnology, University of Trento (DIMTI)
  v. Mesiano 77, Trento 38100, Italy

Ian C. Madsen
ian.madsen@csiro.au
- CSIRO Minerals
  Melbourne 3168, Australia

Terry Maguire
maguire@icdd.com
- International Centre for Diffraction Data (ICDD)
12 Campus Boulevard, Newtown Square 19073, United States

Lucia Maini
l.maini@unibo.it
- University of Bologna, Dipartimento di Chimica "G. Ciamician" (UNIBO)
via Selmi 2, Bologna 40126, Italy

Jaroslav Maixner
maixnerj@vscht.cz
- Institute of Chemical Technology (VSCHT)
Technicka 5, Prague 16628, Czech Republic

Juraj Majzlan
Juraj.Majzlan@minpet.uni-freiburg.de
- Univ.Freiburg
Freiburg, Germany

Lorenzo Malavasi
lorenzo.malavasi@unipv.it
- Università di Pavia, Dipartimento di Chimica Fisica
viale Taramelli 16, Pavia 27100, Italy

Małgorzata Małecka
M.Malecka@int.pan.wroc.pl
- Polish Academy of Sciences, Institute of Low Temperature and Structure Research (INTiBS)
Okólna 2, Wrocław 50-422, Poland

Przemyslaw Malinowski
malin77@o2.pl
- Warsaw University, Faculty of Chemistry
Pasteura 1, Warszawa 02-093, Poland

Waldemar Maniukiewicz
wmaniuk@p.lodz.pl
- Technical University of Łódź, Institute of General and Ecological Chemistry
Żwirki 36, Łódź 90-924, Poland

Irene Margiolaki
margiolaki@esrf.fr
- European Synchrotron Radiation Facility (ESRF)
Grenoble 38043, France

Thomas P. Marsh
tpm214@bham.ac.uk
- School of Chemistry, University of Birmingham
Edgbaston, Birmingham B152TT, United Kingdom

Jorge Martinez-Garcia
jorge.martinezgarcia@epfl.ch
- Ecole Polytechnique Federale de Lausanne (EPFL)
Lausanne 1015, Switzerland

Zdenek Matej
matej@karlov.mff.cuni.cz
- Charles University, Faculty of Mathematics and Physics
Ke Karlovu 3, Prague 12116, Czech Republic

Helen M. McDonnell
mcdonnell@icdd.com
- International Centre for Diffraction Data (ICDD)
12 Campus Boulevard, Newtown Square 19073, United States

Marisa Medarde
marisa.medarde@psi.ch
- Laboratory for Developments and Methods, Paul Scherrer Institut
Villigen PSI 5232, Switzerland

Anton Meden
tone.meden@fkkt.uni-lj.si
- Faculty of Chemistry and Chemical Technology
Askerceva 5, Ljubljana 1000, Slovenia

Mahdi Meftah
meftahmahdi@yahoo.fr
- Laboratoire de Physique des Matériaux Lamellaires et Nano Matériaux Hybrides (LPMNMH)
Faculty of science of Bizerte, Bizerte 7021, Tunisia

Tatyana I. Melnikova
melti@list.ru
- Moscow State Academy of Fine Chemical Tecnology by M. V. Lomonosov
Vernadskogo pr., 86, Moscow 119571, Russian Federation

John D. Meneely
j.meneely@qub.ac.uk
- Queens University Belfast
University Road, Belfast BT71NN, United Kingdom

Marco Merlini
merlini@esrf.fr
- European Synchrotron Radiation Facility (ESRF)
  Grenoble 38043, France

Marinela M. Miclau
marinela.miclau@gmail.com
- National Institute for Research and Development in Electrochemistry and Condensed Matter (INCEMC)
  Str. Plautius Andronescu nr. 1, Timisoara 300224, Romania

Witold Z. Mielcarek
mielcar@iel.wroc.pl
- Electrotechnical Institute, Division of Electrotechnology and Materials Science (IEL)
  M. Skłodowskiej-Curie 55/61, Wrocław, Poland

Anna Mikołajska
anna.mikolajska@wp.pl
- Academy of Fine Arts in Cracow, Faculty of Art Conservation, Department of Applied Physics (ASP)
  Lea 29, Kraków 30-052, Poland

Marco Milanesio
marco.milanesio@mfn.unipmn.it
- Università degli Studi del Piemonte Orientale (DISTA)
  Via V. Bellini 25/G., Alessandria 15100, Italy

Nathan P. Miller
miller@icdd.com
- International Centre for Diffraction Data (ICDD)
  12 Campus Boulevard, Newtown Square 19073, United States

Roman Minikayev
minik@ifpan.edu.pl
- Polish Academy of Sciences, Institute of Physics
  al. Lotników 32/46, Warszawa 02-668, Poland

Scott Misture
misture@alfred.edu
- Alfred University
  2 Pine St., Alfred 14802, United States

Anna Moliterni
annagrazia.moliterni@ic.cnr.it
- CNR-Istituto di Cristallografia (IC)
  via Amendola 122/O, Bari 70126, Italy

Asiloé J. Mora
asiloe@ula.ve
- Universidad de Los Andes, Facultad de Ciencias, Laboratorio de Cristalografía
  Merida 5101, Venezuela

Melanie Müller
Melanie.Mueller@fkf.mpg.de
- Max-Planck-Institut FKF
  Heisenbergstr. 1, Stuttgart D70569, Germany

Antonio H. Munhoz Junior
ahmunhoz@yahoo.com
- Presbyterian University Mackenzie (UPM)
  Rua da Consolação 930, Sao Paulo 01302-907, Brazil

Sonia Naamen
naasonia@yahoo.fr
- Faculté des Sciences de Bizerte (FSB)
  Bizerte 7021, Tunisia

Alexander N. Nadeev
nadeev@catalysis.ru
- Boreskov Institute of Catalysis (BIC)
  pr. akad. Lavrentieva, 5, Novosibirsk 630090, Russian Federation

Reinhard B. Neder
reinhard.neder@krist.uni-erlangen.de
- Universität Erlangen, Kristallographie und Strukturphysik
  Staudtst. 3, Erlangen 91058, Germany

Antonia Neels
antonia.neels@csem.ch
- Centre Suisse d'Electronique et de Microtechnique (CSEM)
  Jaquet-Droz 1, Neuchâtel 2002, Switzerland

Andreas Neumann
an.neumann@fz-juelich.de
- Reserch Center of Juelich (FZJ)
  Leo-Brand Strasse 1, Jülich 52425, Germany

Lea Nichtova
nichtova@gmail.com
- Charles University, Faculty of Mathematics and Physics
  Ke Karlovu 3, Prague 12116, Czech Republic

Emmanuel S. Nolot
emmanuel.nolot@cea.fr
- CEA-LETI-MINATEC (MINATEC)
  17 rue des Martyrs, Grenoble 38054, France

Waldemar Nowicki
waldek@amu.edu.pl
- Adam Mickiewicz University, Faculty of Chemistry
  Grunwaldzka 6, Poznań 60-780, Poland

Ryoko Oishi
ryoko.oishi@kek.jp
- High Energy Accelerator Research Organization (KEK)
  1-1, Oho, Tsukuba-city, Ibaraki 3050801, Japan

Antti J. Ojala
antti.ojala@basf.com
- BASF SE
  Carl Bosch Straße, Ludwigshafen 67056, Germany
- University of Jyväskylä
  Survontie 9, Jyvaskyla 40500, Finland

Dmytro I. Oliferuk
vaavandr@i.kiev.ua
- G. V. Kurdyumov Institute for Metal Physics of the National Academy of Sciences (IMP)
  Vernadsky Blvd. 36, Kiev UA03680, Ukraine

Oluwasesan Oluyemi
olusesanyem@gmail.com
- Institute of Biomedical Technologies, Auckland University of Technology (AUT)
  AUT City Campus, Auckland 1142, New Zealand
- National Research Council Canada, Institute for Research in Construction
  1200 Montreal Road, Ottawa K1A0R6, Canada
- Abeokuta North Local Government
  P.O.Box 4399, Ibara, Abeokuta 110001, Nigeria

Detlef Opper
detlef.opper@panalytical.com
- PANalytical GmbH (PAN)
  Nuernberger Strasse 113, Kassel 34123, Germany

Emmanuel A. Osayi
kingsdivine120@yahoo.co.uk
- Royal Institute of Technology, Dept of Materials Science and Engineering, Materials Chemistry Division (KTH)
  Brinellvaegen 23, 2tr., Stockholm SE10044, Sweden

Andrzej Ostrowski
ostry@ch.pw.edu.pl
- Warsaw University of Technology, Faculty of Chemistry
  Noakowskiego 3, Warszawa 00-664, Poland

Marcin Oszajca
marcin@oszajca.pl
- Jagiellonian University, Faculty of Chemistry
  Ingardena 3, Kraków 30-060, Poland

Gábor Oszlányi
go@szfki.hu
- Hungarian Academy of Sciences, Research Institute for Solid State Physics and Optics (SZFKI)
  Konkoly Thege M. út 29-33, Budapest H-1121, Hungary

Walid Oueslati
walsam_tn@yahoo.co.in
- Faculté des Sciences de Bizerte (FSB)
  Bizerte 7021, Tunisia

Tetsuya Ozawa
t-ozawa@rigaku.co.jp
- Rigaku Co.
  Tokyo 196-8666, Japan

Jesús Palacios Gómez
palacios@esfm.ipn.mx
- Instituto Politécnico Nacional, ESFM, Depto. de Ciencia de Materiales, Unidad Prof. ALM (ESFM)
  Edif. 9, Zacatenco, México, Zacatenco, México 07338, Mexico

Lukas Palatinus
palat@fzu.cz
- Ecole Polytechnique Federale de Lausanne (EPFL)
  Ecublens, Lausanne 1015, Switzerland

Luca Palin
lpalin@unipmn.it
- Università degli Studi del Piemonte Orientale (DISTA)
  Via V. Bellini 25/G., Alessandria 15100, Italy

Bogdan F. Palosz
palosz@unipress.waw.pl
- Polish Academy of Sciences, Institute of High Pressure Physics (UNIPRESS)
  Sokolowska 29/37, Warszawa 01-142, Poland

Ewa Pańczyk
epanczyk@ichtj.waw.pl
- Institute of Nuclear Chemistry and Technology (IChTJ)
Dorodna 16, Warszawa 03-195, Poland

Rajiv Paneerselvam
p.rajiv@fkf.mpg.de
- Max-Planck-Institut FKF
Heisenbergstr. 1, Stuttgart D70569, Germany

Karen Pantleon
pantleon@ipl.dtu.dk
- Technical University of Denmark (DTU)
Kemitorvet, b. 204, Lyngby 2800, Denmark

Pablo R. Pardo
pablo.pardo@uv.es
- Valencia University, Department of Geology
Dr. Moliner, 50, Valencia 46100, Spain

Julia E. Parker
julia.parker@diamond.ac.uk
- Diamond Light Source, Science Dept.
Harwell Science and Innovation Campus, Chilton Didcot OX110DE, United Kingdom

Wojciech Paszkowicz
paszk@ifpan.edu.pl
- Polish Academy of Sciences, Institute of Physics
al. Lotników 32/46, Warszawa 02-668, Poland

Krzysztof A. Pawlik
kpawlik@labosoft.com.pl
- LaboSoft
os. Centrum A 2/83, Kraków 31-923, Poland

Julia L. Payne
J.L.Payne@durham.ac.uk
- Department of Chemistry, University of Durham
Science Labs, South Road, Durham DH1-3LE, United Kingdom

Burkhard Peplinski
burkhard_peplinski@web.de
- Federal Institute for Materials Research and Testing (BAM)
Richard-Willstätter-Str. 11, Berlin D-12489, Germany

Inma Peral
iperal@cells.es
- CELLS (ALBA)
Campus UAB, Barcelona 08193, Spain

Yuriy Perlovich
yuperl@mail.ru
- Moscow Engineering Physics Institute (MEPhI)
Kashirskoe shosse, Moscow 115409, Russian Federation

Vaclav Petricek
petricek@fzu.cz
- Czech Academy of Sciences, Institute of Physics
Cukrovarnicka 10, Prague 16253, Czech Republic

Sophia A. Petrova
danaus@mail.ru
- Institute of Metallurgy, Urals Division, Russian Academy of Science (IMETUDRAS)
101 Amundsen, Ekaterinburg 620016, Russian Federation

Rafał M. Petrus
proaktyn@o2.pl
- Wrocław University, Faculty of Chemistry
14 F. Joliot-Curie, Wrocław 50-383, Poland

Roman Pielaszek
roman@pielaszek.net
- Polish Academy of Sciences, Institute of High Pressure Physics (UNIPRESS)
Sokolowska 29/37, Warszawa 01-142, Poland

Adam Andrzej Pietraszko
adam@int.pan.wroc.pl
- Polish Academy of Sciences, Institute of Low Temperature and Structure Research (INTiBS)
Okólna 2, Wrocław 50-422, Poland

Stanisław Pikus
stanpik1@wp.pl
- Faculty of Chemistry, Maria Curie Sklodowska University (UMCS)
pl. Marii Curie Sklodowskiej 3, Lublin 20-031, Poland

Pawel Piszora
pawel@amu.edu.pl
- Adam Mickiewicz University, Faculty of Chemistry
Grunwaldzka 6, Poznań 60-780, Poland

Marco Polito
marco.polito@unibo.it
- University of Bologna, Dipartimento di Chimica "G. Ciamician" (UNIBO)
  via Selmi 2, Bologna 40126, Italy

Stanko Popovic
spopovic@phy.hr
- Faculty of Sciences, Dept. Physics
  Bijenička 32, Zagreb HR-10000, Croatia

Jose M. Posse
josemaria@wm.lc.ehu.es
- Dpto. Física Materia Condensada, Universidad del País Vasco (UPV/EHU)
  Facultad de Ciencia y Tecnología, Apdo. 644, Bilbao 48080, Spain

Thomas Proffen
tproffen@lanl.gov
- Los Alamos National Laboratory (LANL)
  Los Alamos, NM 87545, United States

Stjepan Prugovecki
Stjepan.Prugovecki@panalytical.com
- PANalytical
  Lelyweg 1, Almelo 7600AA, Netherlands

Nadine Rademacher
nrademac@stud.uni-frankfurt.de
- Frankfurt University, Institute of Inorganic and Analytical Chemistry
  Max-von-Laue-Str. 7, Frankfurt am Main 60438, Germany

Ivana Radosavljevic Evans
ivana.radosavljevic@durham.ac.uk
- Department of Chemistry, University of Durham
  Science Labs, South Road, Durham DH1-3LE, United Kingdom

Alicja Rafalska-Łasocha
rafalska@chemia.uj.edu.pl
- Jagiellonian University, Faculty of Chemistry
  Ingardena 3, Kraków 30-060, Poland

Nabil N. Rammo
nabilrammo@yahoo.com
- Materials Research Center
  Baghdad 00964, Iraq

Mark D. Raven
Mark.Raven@csiro.au
- CSIRO Land and Water
  Waite Rd, Adelaide 5064, Australia

Jennifer E. Readman
j.e.readman.1@bham.ac.uk
- School of Chemistry, University of Birmingham
  Edgbaston, Birmingham B152TT, United Kingdom

Hafsia B. Rhaiem
hafsia.rhaiem@fsb.rnu.tn
- Laboratoire de Physique des Matériaux Lamellaires et Nano Matériaux Hybrides (LPMNMH)
  Faculty of science of Bizerte, Bizerte 7021, Tunisia

Daniel P. Riley
DRiley@unimelb.edu.au
- The Univeristy of Melbourne (UNIMELB)
  Grattan Street, Melbourne 3052, Australia

Jordi Rius
jordi.rius@icmab.es
- Institut de Ciencia de Materials (ICMAB) - CSIC (ICMAB)
  Campus de la UAB, Barcelona 080193, Spain

Rosanna Rizzi
rosanna.rizzi@ic.cnr.it
- CNR-Istituto di Cristallografia (IC)
  via Amendola 122/O, Bari 70126, Italy

Juan Rodriguez-Carvajal
rodriguez-carvajal@ill.fr
- Institut Laue Langevin (ILL)
  Avenue des martyrs, Grenoble 38042, France

Jan Rohlicek
rohlicej@vscht.cz
- Institute of Chemical Technology (VSCHT)
  Technicka 5, Prague 16628, Czech Republic

Eli Roijers
eli.roijers@unilever.com
- Unilever (URDV)
  Olivier van Noortlaan 120, Vlaardingen 3130AC, Netherlands

Joanna Ropka
Joanna.Ropka@cryst.unige.ch
- University of Geneva
Geneva 1211, Switzerland

Yuri Rosenberg
yurir@post.tau.ac.il
- Tel Aviv University (TAU)
Ramat Aviv, Tel Aviv 69787, Israel

Matthew R. Rowles
matthew.rowles@csiro.au
- CSIRO Minerals
Melbourne 3168, Australia

Agnieszka Rzepka
Agnieszka.Rzepka@itme.edu.pl
- Institute of Electronic Materials Technology (ITME)
Wólczyńska 133, Warszawa 01-919, Poland

Piotr R. Rzeszotarski
percol@ichf.edu.pl
- Polish Academy of Sciences, Institute of Physical Chemistry
Kasprzaka 44/52, Warszawa 01-224, Poland

Varalak Saengsuwan
varalak.s@student.chula.ac.th
- Department of Physics, Faculty of Science, Chulalongkorn University
6th floor, Mahamakut Build., Payatai rd., Pathumwan, Bangkok 10330, Thailand

István E. Sajó
sajo@chemres.hu
- Hungarian Academy of Sciences, Chemical Research Centre (CRC/HAS)
Pusztaszeri ut 59-67, Budapest H-1025, Hungary

Zsombor Sánta
santa@szfki.hu
- Hungarian Academy of Sciences, Research Institute for Solid State Physics and Optics (SZFKI)
Konkoly Thege M. út 29-33, Budapest H-1121, Hungary

Asya Sattarova
Ciklop1984@yandex.ru
- Moscow State Academy of Fine Chemical Technology
86 Vernadskogo Avenue, Moscow 119571, Russian Federation

Heidi E. Saxell
heidi.saxell@basf.com
- BASF SE
Carl Bosch Straße, Ludwigshafen 67056, Germany

Paolo Scardi
Paolo.Scardi@unitn.it
- Department of Material Engineering and Industrial Tecnology, University of Trento (DIMTI)
v. Mesiano 77, Trento 38100, Italy

Helmut Schaeben
schaeben@geo.tu-freiberg.de
- Technische Universitaet Bergakademie Freiberg, Mathematische Geologie und Geoinformatik
Bernhard-von-Cotta Str. 2, Freiberg D-09599, Germany

Martin U. Schmidt
m.schmidt@chemie.uni-frankfurt.de
- Frankfurt University, Institute of Inorganic and Analytical Chemistry
Max-von-Laue-Str. 7, Frankfurt am Main 60438, Germany

Julius Schneider
julius.schneider@lrz.uni-muenchen.de
- LMU, Department of Earth and Environmental Sciences, Crystallography
Theresienstr. 41, München 81539, Germany

Martin K. Schreyer
mschreyer@ntu.edu.sg
- Nanyang Technological University
Singapore, Singapore

Götz Schuck
goetz.schuck@psi.ch
- Paul Scherrer Institut (PSI)
WLGA, Villigen PSI 5232, Switzerland

Conference Secretariat
secretariat@epdic-11.eu
- Nicolaus Copernicus University, Collegium Medicum , Department of Clinical Biochemistry
ul. Karlowicza 24, Bydgoszcz 85-092, Poland

Luis E. Seijas
seijasluis@ula.ve
- Universidad de Los Andes, Facultad de Ciencias, Laboratorio de Cristalografía
Merida 5101, Venezuela

Anatoliy Senyshyn
senyshyn@gmail.com
- Technische Universität Darmstadt, Institute of Materials Science
Petersenstr. 23, Darmstadt 64287, Germany

Francisco Javier Serrano Esteve
francisco.serrano@uv.es
- Valencia University, Department of Geology
Dr. Moliner, 50, Valencia 46100, Spain

Sebastian Seufert
Sese@geol.uni-erlangen.de
- University Erlangen
Erlangen 91054, Germany

Syed Khalid M. Shah
khalidsyedqau@yahoo.com
- Institute of industrial control system (IICS)
PO.Box 502 Rawalpindi, Rawalpindi 0502, Pakistan

Kenneth Shankland
k.shankland@rl.ac.uk
- Rutherford Appleton Laboratory (RAL)
Chilton, Didcot, Oxon OX11 0QX, United Kingdom

Jianfeng Sheng
sheng@mf.mpg.de
- Max Planck Institute for Metals Research (MPI-MF)
Heisenbergstrasse 3, Stuttgart 70569, Germany

Michael B. Shevchenko
mishevch@yahoo.com
- G. V. Kurdyumov Institute for Metal Physics of the National Academy of Sciences (IMP)
Vernadsky Blvd. 36, Kiev UA03680, Ukraine
- G.V. Kurdyumov Institute for Metal Physics National Academy of Sciences (IMP)
Vernadsky Blvd. 36, Kyiv UA03680, Ukraine

Miłosz Siczek
milosz@eto.wchuwr.pl
- Wrocław University, Faculty of Chemistry
14 F. Joliot-Curie, Wrocław 50-383, Poland

Yulia S. Simakova
yssimakova@geo.komisc.ru
- Institute of Geology of RAS (IG)
Pervomaiskaya st., Syktyvkar 167982, Russian Federation

Eirini Siranidi
esiran@central.ntua.gr
- National Technical University of Athens (NTUA)
Heroon Polytechneiou 9, Athens 157 80, Greece

Leonid I. Skatkov
sf_lskatkov@bezeqint.net
- PCB "Argo"
4/23 Shaul ha-Melekh Street, Beer-Sheva 84797, Israel

Stanisław J. Skrzypek
skrzypek@agh.edu.pl
- AGH, Faculty of Metals Engineering and Industrial Computer Science
30 Mickiewicza Av., Kraków 30-059, Poland

Ľubomír Smrčok
uachsmrk@savba.sk
- Institute Of Inorganic Chemistry, Slovak Academy of Sciences (IIC)
Dubravska cesta 9, Bratislava SK-84536, Slovakia (Slovak Rep.)

Ruben A. Snellings
ruben.snellings@ees.kuleuven.be
- Catholic University of Leuven, Department of Earth and Environmental Sciences (KUL-EES)
Celestijnenlaan 200E, Leuven 3001, Belgium

Joanna Sobczyk
jsobczyk@muz-nar.krakow.pl
- Muzeum Narodowe w Krakowie
3 Maja 1, Kraków 30-062, Poland

Magnus H. Sorby
magnuss@ife.no
- Institute for Energy Technology (IFE)
Institutveien 18, Oslo NO-2027, Norway

Wojciech R. Starosta
w.star@ichtj.waw.pl
- Institute of Nuclear Chemistry and Technology (IChTJ)
Dorodna 16, Warszawa 03-195, Poland

Helen Stoeckli-Evans
helen.stoeckli-evans@unine.ch
- Université de Neuchâtel
Neuchâtel, Switzerland

Tomasz Strachowski
tomasz@unipress.waw.pl
- Polish Academy of Sciences, Institute of High Pressure Physics (UNIPRESS)
  Sokolowska 29/37, Warszawa 01-142, Poland
- Warsaw University of Technology, Faculty of Materials Science and Engineering (InMat)
  Wołoska 141, Warszawa 02-507, Poland

Agnese Stunda
agnese.stunda@rtu.lv
- Riga Biomaterials Innovation and Development Centre
  Pulka Str. 3/3, Riga LV-1007, Latvia

Mark J. Styles
m.styles2@pgrad.unimelb.edu.au
- The University of Melbourne
  Grattan St., Melbourne 3010, Australia

Huawei Su
hs93@le.ac.uk
- University of Leicester
  University Road, Leicester LE17RH, United Kingdom

Silvie Švarcová
svarcova@iic.cas.cz
- Institute of Inorganic Chemistry of the ASCR, v.v.i.
  c.p. 1001, Rez near Prague 25068, Czech Republic

Lech Swinder
lech.swinder@polpharma-group.com
- Pharmaceutical Works Polpharma, Research and Development Department
  19 Pelpińska Str., Starogard Gdański 83-200, Poland

Maciej J. Szczerba
maciekszczerba@interia.pl
- Polish Academy of Sciences, Institute of Metallurgy and Materials Sciences (IMIM PAN)
  Reymonta 25, Kraków 30-059, Poland

Andrey Tamonov
tamonov@nf.jinr.ru
- Joint Institute for Nuclear Research
  Dubna, Russian Federation

Chiu C. Tang
c.c.tang@diamond.ac.uk
- Diamond Light Source, Science Dept.
  Harwell Science and Innovation Campus, Chilton Didcot OX110DE, United Kingdom

Nadezda V. Tarakina
tarakina@ihim.uran.ru
- Russian Academy of Sciences, Ural Division, Institute of Solid State Chemistry (ISSC)
  Pervomaiyskay, 91, Ekaterinburg 620219, Russian Federation

David J. Taylor
djt35@btopenworld.com
- ICDD
  Wigan WN5-7QJ, United Kingdom

Test Test
samaramaboss@poczta.onet.pl
- Waters
  Lektykarska 25 m. 21, Warszawa 01-687, Poland

Olivier Thomas
olivier.thomas@univ-cezanne.fr
- Aix-Marseille Université, Institut Matériaux Microélectronique Nanosciences de Provence
  Marseille 13397, France

Stephen P. Thompson
stephen.thompson@diamond.ac.uk
- Diamond Light Source, Science Dept.
  Harwell Science and Innovation Campus, Chilton Didcot OX110DE, United Kingdom

Saara K. Tiittanen
saara.tiittanen@orionpharma.com
- Orion Corporation Orion Pharma (ORION)
  Orionintie 1, Espoo 02101, Finland

Korede M. Tolonisede
tolonisede@yahoo.com
- Lynq Communications Limited
  49, Bode Thomas Street, Surulere, Lagos, Lagos 23401, Nigeria

Paweł E. Tomaszewski
p.tomaszewski@int.pan.wroc.pl
- Institute of Low Temperature and Structure Research, Polish Academy of Sciences
  P.Nr 1410, Wrocław 50-950, Poland

Hideo Toraya
toraya@rigaku.co.jp
- Rigaku Co.
  Tokyo 196-8666, Japan

Maryjane Tremayne
m.tremayne@bham.ac.uk
- School of Chemistry, University of Birmingham
  Edgbaston, Birmingham B152TT, United Kingdom

Martin Tremblay
martin.tremblay@panalytical.com
- PANalytical
  Lelyweg 1, Almelo 7600AA, Netherlands
- Université de Montréal, Département de physique, Regroupement Québécois sur les Matériaux de Pointe (RQMP)
  C.P. 6128 succ. centre-ville, Montréal, Québec, Montreal H3C 3J7, Canada

Dmytro M. Trots
dmytro.trots@desy.de
- Hamburger Synchrotronstrahlungslabor HASYLAB (HASYLAB)
  Notkestrasse 85, Hamburg D-22603, Germany
- Technische Universität Darmstadt, Institute of Materials Science
  Petersenstr. 23, Darmstadt 64287, Germany

Elena A. Tyunina
tyunina_elena@mail.ru
- Moscow State Academy of Fine Chemical Technology
  86 Vernadskogo Avenue, Moscow 119571, Russian Federation

Kristian Ufer
kristian.ufer@bgr.de
- Freiberg University of Mining and Technology, Mineralogical Institute
  Brennhausgasse 14, Freiberg 09596, Germany

Tamás Ungár
ungar@ludens.elte.hu
- Eötvös University
  Pázmány Péter sétány 1/A, Budapest H-1117, Hungary

Geert Vanhoyland
geert.vanhoyland@bruker-axs.de
- Bruker-AXS (BAXS)
  Östliche Rheinbrückenstr. 49, Karlsruhe D-76187, Germany

Jan B. Van Mechelen
mecheljb@xs4all.nl
- University of Amsterdam, HIMS, crystallography (UVA)
  Valckenierstraat 65, Amsterdam 1018XE, Netherlands

Sergey G. Vasilovskiy
vassg@nf.jinr.ru
- Joint Institute for Nuclear Research
  Dubna, Russian Federation

Gavin Vaughan
vaughan@esrf.fr
- European Synchrotron Radiation Facility (ESRF)
  Grenoble 38043, France

Andrew M. Venter
amventer@necsa.co.za
- Necsa Limited (NECSA)
  Church Street West Extension, Pretoria 0001, South Africa

Arnold C. Vermeulen
arnold.vermeulen@panalytical.com
- PANalytical
  Lelyweg 1, Almelo 7600AA, Netherlands

Robert Von Dreele
vondreele@anl.gov
- Argonne National Laboratory (ANL)
  9700 South Cass Avenue, Argonne, IL 60439, United States

Stanislav Vratislav
stanislav.vratislav@fjfi.cvut.cz
- Czech Technical University in Prague, The Faculty of Nuclear Sciences and Physical Engineering
  Trojanova 13, Prague 2, Prague 12000, Czech Republic

Wiktor Walerczyk
w.walerczyk@int.pan.wroc.pl
- Institue of Low Temperature and Structure Research, Polish Academy of Sciences (INTIBS-PAN)
  P.Nr 1410, Wrocław 50-950, Poland

Kia S. Wallwork
kia.wallwork@synchrotron.org.au
- Australian Synchrotron
  800 Blackburn Road, Melbourne 3168, Australia

Haixia Wang
saliencas@hotmail.com
- Technische Universität Darmstadt, Institute of Materials Science
Petersenstr. 23, Darmstadt 64287, Germany

Joanna B. Warycha
a.warycha@iel.wroc.pl
- Electrotechnical Institute (IEL)
Skłodowskiej-Curie 55/61, Wrocław 50-369, Poland

Yves Watier
watier@esrf.fr
- European Synchrotron Radiation Facility (ESRF)
Grenoble 38043, France

Dariusz Wegrzynek
d.wegrzynek@iaea.org
- International Atomic Energy Agency (IAEA)
Wagrame Strasse, Wien A-1400, Austria
- AGH University of Science and Technology, Faculty of Physics and Applied Computer Science (AGH)
Mickiewicza 30, Kraków 30-059, Poland

Władysław Weker
wweker@poczta.onet.pl
- Państwowe Muzeum Archeologiczne (PMA)
Długa 52, Warszawa 00-241, Poland

Udo S. Welzel
u.welzel@mf.mpg.de
- Max Planck Institute for Metals Research (MPI-MF)
Heisenbergstrasse 3, Stuttgart 70569, Germany

Ewa Werner-Malento
ewerner@ifpan.edu.pl
- Polish Academy of Sciences, Institute of Physics
al. Lotników 32/46, Warszawa 02-668, Poland

Pamela S. Whitfield
pamela.whitfield@nrc.gc.ca
- Institute for Chemical Process and Environmental Technology National Research Council of Canada
Ottawa ONK1A06, Canada

Lutz Wilde
lutz.wilde@cnt.fraunhofer.de
- Fraunhofer Center Nanoelektronische Technologien
Dresden 01099, Germany

Laura M. Williams-Vestal
LauraVestal@chevron.com
- Chevron Corporation
3901 Briarpark Drive, Houston, TX 77042-5301, United States

Andrew S. Wills
a.s.wills@ucl.ac.uk
- University College London, Department of Chemistry (UCL)
Gordon Street, London WC1HOAJ, United Kingdom

Lyn Wilson
lyn.wilson@scotland.gsi.gov.uk
- Historic Scotland
7 South Gyle Crescent, Edinburgh, Edinburgh EH129EB, United Kingdom

Marcin Wójtowicz
mwojt@eto.wchuwr.pl
- Wrocław University, Faculty of Chemistry
14 F. Joliot-Curie, Wrocław 50-383, Poland

Marek Wołcyrz
m.wolcyrz@int.pan.wroc.pl
- Polish Academy of Sciences, Institute of Low Temperature and Structure Research (INTiBS)
Okólna 2, Wrocław 50-422, Poland

Harm Wulff
wulff@chemie.uni-greifswald.de
- Universität Greifswald
Felix-Hausdorffstr. 4, Greifswald 17487, Germany

Ewa Wytrykowska
ksieg@unipress.waw.pl
- Polish Academy of Sciences, Institute of High Pressure Physics (UNIPRESS)
Sokolowska 29/37, Warszawa 01-142, Poland

Hongliang Xu
xu@hwi.buffalo.edu
- Hauptman-Woodward Institute (HWI)
700 Ellicott Street, Buffalo 14203, United States

Igor S. Yakimov
I-S-Yakimov@yandex.ru
- Siberian Federal University (SFU)
Krasnoyarskii rabochii 95, Krasnoyarsk 660095, Russian Federation

Yaroslav I. Yakimov
yar_yakimov@mail.ru
- Siberian Federal University (SFU)
Krasnoyarskii rabochii 95, Krasnoyarsk 660095, Russian Federation

Nao Yamada
nao.yamada@bruker-axs.jp
- BRUKER AXS K.K
3-9-A, Moriya-cho, Kanagawa-ku, Yokohama-shi, Kanagawa 221-0022, Japan

Meglena Yoncheva
meglena@svr.igic.bas.bg
- Institute of General and Inorganic Chemistry, Bulgarian Academy of Sciences (IGIC)
Acad. G. Bonchev Str. bldg. 11, Sofia 1113, Bulgaria

Ahmet Yönetken
yonetken68@hotmail.com
- Afyon Kocatepe Universitesi
Afyonkarahisar 03200, Turkey

Kirill V. Yusenko
yusenko@che.nsk.su
- Institute of Inorganic Chemistry of RAS
Novosibirsk 630090, Russian Federation

Stefano Zanardi
stefano.zanardi@eni.it
- Eni S.p.A.
Via Maritano 26, San Donato Milanese 20097, Italy

Teresa Zaremba
teresa.zaremba@polsl.pl
- Silesian University of Technology, Department of Inorganic Chemistry and Technology
ul. Krzywoustego 6, Gliwice 44-100, Poland

Oleksandra V. Zarytska
zarickaya@rambler.ru
- Physical Engineering Centre, National Academy of Sciences of Ukraine (FTC)
Vernadskiy's blvd., 36, Kiev 03680, Ukraine

Joanna Zdunek
jzdunek@inmat.pw.edu.pl
- Warsaw University of Technology, Faculty of Materials Science and Engineering (InMat)
Wołoska 141, Warszawa 02-507, Poland

Zhongfu Zhou
zhouz5@cardiff.ac.uk
- Cardiff University
School of Chemistry, Park Place, Cardiff CF103AT, United Kingdom

Andrzej Zieba
zieba@novell.ftj.agh.edu.pl
- AGH University of Science and Technology (AGH)
al. Mickiewicza 30, Kraków 30-059, Poland

Index

D

E

F

G

H

I

J

K

L

M

N

O

P

Q

R

S

T

U

V

W

X

Y

Z